# Google

This is a digital copy of a book that was preserved for generations on library shelves before it was carefully scanned by Google as part of a project to make the world's books discoverable online.

It has survived long enough for the copyright to expire and the book to enter the public domain. A public domain book is one that was never subject to copyright or whose legal copyright term has expired. Whether a book is in the public domain may vary country to country. Public domain books are our gateways to the past, representing a wealth of history, culture and knowledge that's often difficult to discover.

Marks, notations and other marginalia present in the original volume will appear in this file - a reminder of this book's long journey from the publisher to a library and finally to you.
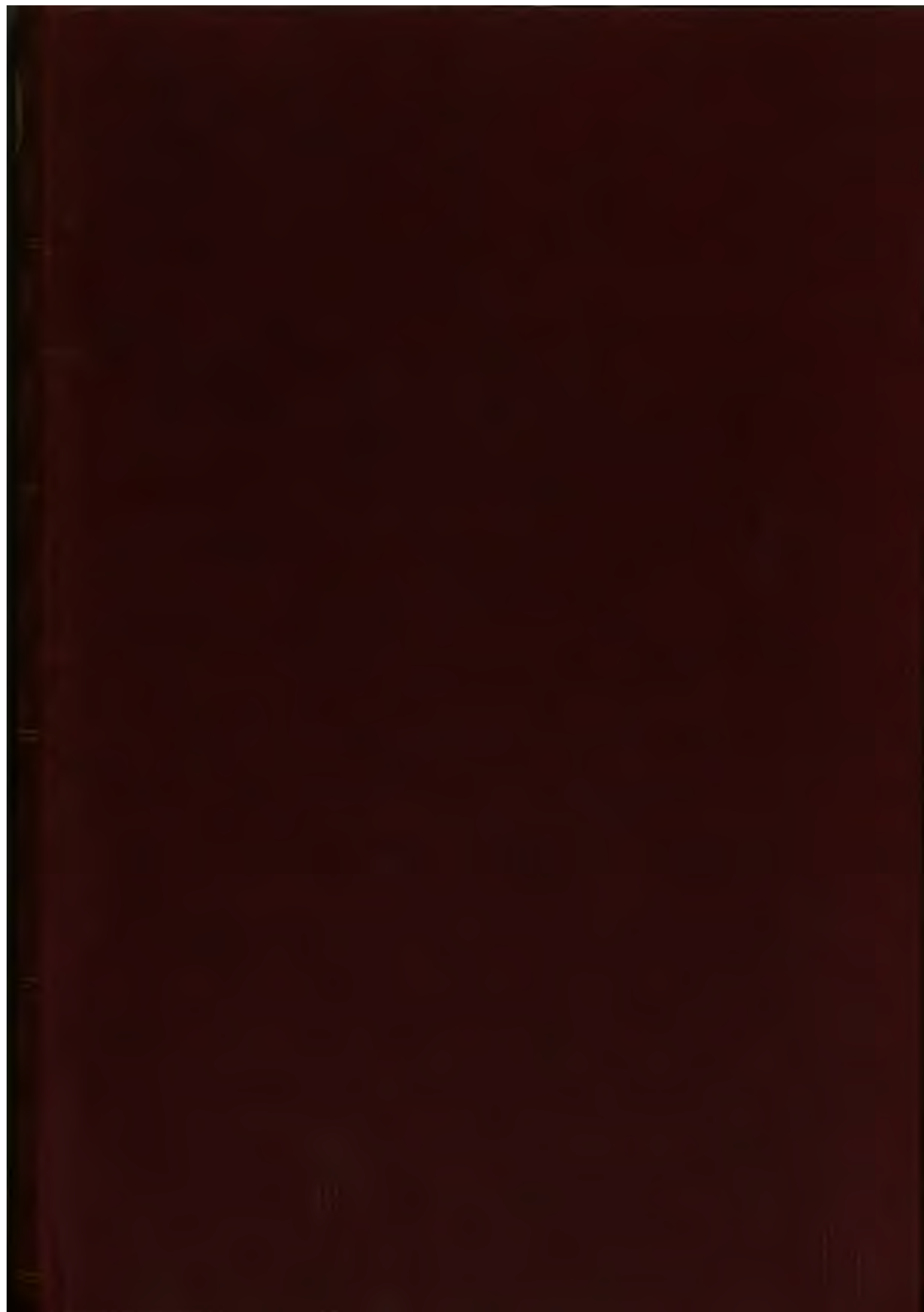
## Usage guidelines

Google is proud to partner with libraries to digitize public domain materials and make them widely accessible. Public domain books belong to the public and we are merely their custodians. Nevertheless, this work is expensive, so in order to keep providing this resource, we have taken steps to prevent abuse by commercial parties, including placing technical restrictions on automated querying.
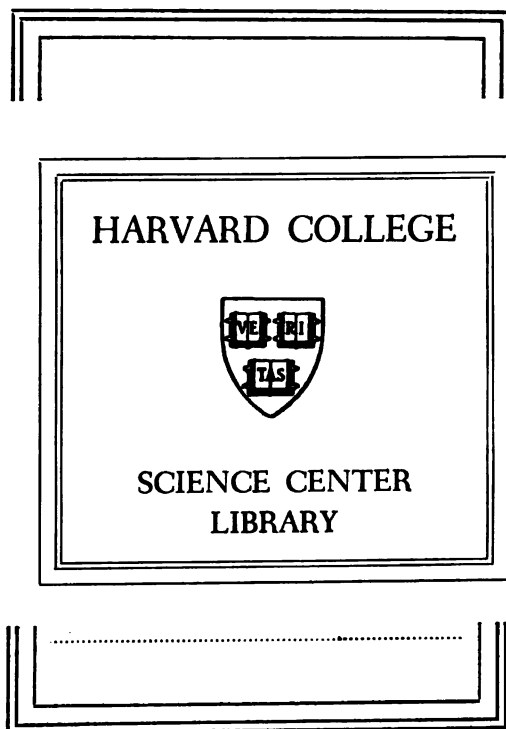
We also ask that you:

+ *Make non-commercial use of the files* We designed Google Book Search for use by individuals, and we request that you use these files for personal, non-commercial purposes.

+ *Refrain from automated querying* Do not send automated queries of any sort to Google's system: If you are conducting research on machine translation, optical character recognition or other areas where access to a large amount of text is helpful, please contact us. We encourage the use of public domain materials for these purposes and may be able to help.

+ *Maintain attribution* The Google "watermark" you see on each file is essential for informing people about this project and helping them find additional materials through Google Book Search. Please do not remove it.

+ *Keep it legal* Whatever your use, remember that you are responsible for ensuring that what you are doing is legal. Do not assume that just because we believe a book is in the public domain for users in the United States, that the work is also in the public domain for users in other countries. Whether a book is still in copyright varies from country to country, and we can't offer guidance on whether any specific use of any specific book is allowed. Please do not assume that a book's appearance in Google Book Search means it can be used in any manner anywhere in the world. Copyright infringement liability can be quite severe.

## About Google Book Search

Google's mission is to organize the world's information and to make it universally accessible and useful. Google Book Search helps readers discover the world's books while helping authors and publishers reach new audiences. You can search through the full text of this book on the web at `http://books.google.com/`

# THE INTERFEROMETRY OF REVERSED AND NON-REVERSED SPECTRA

By CARL BARUS

*Hazard Professor of Physics and Dean of the Graduate Department
in Brown University*

# THE INTERFEROMETRY OF REVERSED AND NON-REVERSED SPECTRA

By CARL BARUS

*Hazard Professor of Physics and Dean of the Graduate Department
in Brown University*

CARNEGIE INSTITUTION OF WASHINGTON

PUBLICATION No. 249

# CONTENTS.

# CONTENTS.

# PREFACE.

The following account of my experiments has been given chronologically. Although many of the anomalous features, in which the interferences of superposed coördinated spectra first presented themselves, were largely removed in the later work, yet the methods used in the several papers, early and later, are throughout different. It therefore seemed justifiable to record them, together with the inferences they at first suggested. The pursuit of the subject as a whole was made both easier and more difficult by the unavoidable tremors of the laboratory in which I am working; for it is possibly easier to detect an elusive phenomenon if it is in motion among other similar stationary phenomena. But it is certainly difficult, thereafter, to describe it when found.

It will be convenient to refer to the cases in which one of the two coincident spectra from the same source is rotated 180° with reference to the other on a transverse axis (*i.e.*, an axis parallel to the Fraunhofer lines), under the term *reversed spectra;* while the term *inverted spectra* is at hand for those cases in which one of the paired spectra is turned 180° relative to the other on a longitudinal axis (*i.e.*, an axis parallel to the *r–v* length of the spectrum). In this book the latter are merely touched upon, briefly, in Chapter I, but they are now being investigated in detail and give promise of many interesting results. The chapter contains a full account of what may be seen with a single grating—the linear phenomenon, as I have called it, and which, if it stood alone, would be difficult to interpret.

In Chapter II, therefore, the interferences of reversed spectra are treated by the aid of two gratings, in virtue of which a multitude of variations are inevitably introduced. The phenomena are thus exhibited in a way leading much more smoothly to their identification.

This endeavor is given greater promise in Chapter III, which contains a comparison of the interferences of reversed and non-reversed spectra, the latter produced in a way quite different from those in my earlier work. Naturally these in their entirety are even more bewilderingly varied, and become particularly so when, as in Chapter IV, an intermediate reflection of one spectrum is admitted. But with this I was on more familiar ground, as I have hitherto, in these publications, given such investigations particular attention.

The flexibility of the new methods is well shown in Chapter V, where separated component beams can with equal facility be made to run in parallel, or across each other at any angle, and perhaps both, with the double result visible in the field of the telescope. In case of crossed rays a remarkable phenomenon is shown, in which very small differences in wave-length imply a remarkably large difference in rotational phase (virtually resolving power) of the two interesting groups of interference fringes due to each wave-length.

Spectra obtained with two, or at times even with one grating, are often annoyingly furrowed with large transverse fringes. These are investigated in Chapter VI, and referred to diffractions resulting from residual errors in the rulings. In Chapter VII, finally, several examples of new methods of investigation are given. They show the important bearing of the diffraction at the slit of the collimator on all these experiments. The cleavage of a field of diffracted rays as an essential preliminary is here put in direct evidence.

In Chapters VIII to XIII I have returned to my older experiments with the displacement interferometer. The subjects adduced, like the dispersion of air at low and high temperatures, the adiabatic expansion of air, etc., are pursued less with the object of reaching results of precision than of testing the limits of the displacement method and developing it.

My thanks are due to Miss Abbie L. Caldwell for very efficient assistance in preparing the manuscript and drawings for the press.

CARL BARUS.

BROWN UNIVERSITY, *Providence, Rhode Island*.

# CHAPTER I.

## THE INTERFERENCES OF CROSSED SPECTRA.

**1. Introductory.**—If two component spectra from the same source coincide throughout their extent the elliptic interferences will be spread over the whole surface, provided, of course, the respective glass and air-path differences of the two component rays are not so great as to throw the phenomenon beyond the range of visibility. In the usual method of producing these interferences, where the corresponding reflections and transmissions of the two component rays take place at the same points of the same plane surface, the interference pattern is automatically centered, or nearly so. This is not the case when, as in the following experiments, the interfering beams are separated in some other way; and the problem of centering is often one of the chief difficulties involved; and if the beams are to be treated independently, it is difficult to obviate this annoyance.

Suppose, now, that one of the spectra is rotated around an axis normal to both, by a small angle. Will the interferences at once vanish, or is there a limiting angle below which this is not the case? In other words, how far can one trench with light-waves upon the case of musical beats, or of interferences not quite of the same wave-length?

Instead of approaching the question in this form, in which it would be exceedingly difficult, experimentally, I have divided it into two component parts. Let one of the spectra be rotated 180° around a *longitudinal* axis, parallel to the red-violet length of the spectrum and normal to the Fraunhofer lines. In such a case, interference should be possible only along the infinitely thin longitudinal axis of rotation to which both spectra are symmetrical, one being the mirror image of the other. One would not expect these interferences to be visible. It is rather surprising, however, that this phenomenon (as I have found) may actually be observed, along a definite longitudinal band in the spectrum, about twice the angular width of the distance between the sodium lines and symmetrical with respect to the axis of rotation. It is independent of the width of the slit, provided this is narrow enough to show the Fraunhofer lines to best advantage.

Again, let one spectrum be rotated 180° about a given Fraunhofer line (transverse axis), the nickel or mean $D$ line, for instance. The two coplanar spectra are now mutually reversed, showing the succession red-violet and violet-red, respectively. Interference should take place only along the mean $D$ line and be again inappreciable. Experimentally, I was not at first able to find any interferences for this case in the manner shown below, but this may have been due to inadequacies in the experimental means employed, for the dispersion was insufficient and the reflecting edge of the paired mirrors too rough. Improving the apparatus, I eventually found the phenomenon,

7

but appearing as a single line, vividly colored above the brightness of the spectrum; or, again, more jet-black than the Fraunhofer lines and located in the position of the coincident wave-lengths of the two superimposed spectra.

It is possible, however, as will be shown in § 4, to obtain two spectra in such a way that if their longitudinal axes coincide the Fraunhofer lines intersect at a small angle, and *vice versa*. In such a case, for coincident Fraunhofer lines, interference occurs in a band around these lines and is absent in the rest of the spectrum; whereas, if the longitudinal axes are coincident, the interferences are arranged with reference to these axes. These results seem to bear on the question, but it is difficult to clearly resolve them.

The methods used in this paper consist chiefly in bringing the two first-order spectra of a grating, or the second-order spectra or their equivalents, to interfere. In this respect they contain an additional method of interferometry which may be useful, if for any reason it is necessary that the two component beams are not to retrace their paths.
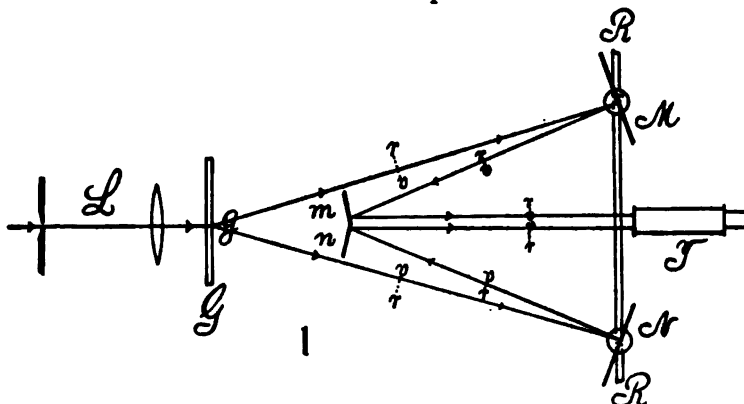


**2. Coincident spectra with one reversed on a given Fraunhofer line.**—In figure 1, L is a narrow vertical sheet (subsequently broadened by the diffraction of the slit) of white sunlight or arc light from a collimator, G the transparent grating ruled on the side g, from which the first or second order of spectra gM and gN originate. M and N are opaque mirrors mounted adjustably on a firm rail, RR, each of them with three adjustment screws relative to horizontal and vertical axes. M is provided with a slide micrometer (not shown). From M and N the beams pass to the smaller paired mirrors, *m* and *n*, which should meet in a fine vertical line at a very obtuse angle. A silvered biprism would here be far preferable, but none having the required angle was available. From *n*, *m*, the beams pass into the telescope T. As the spectra are each divergent after issuing from g, they can be made to overlap on leaving *n*, *m*, by aid of the adjustment screws on M and N. Moreover, as the spectra are mirror images of each other, as suggested in figure 1, any spectrum lines (as, for instance, the D) may be put in coincidence on using one of the adjustment screws specified. It is necessary that the telescope T be sufficiently near M in order that the micrometer may be manipulated.

The $D$ lines placed in coincidence are obviously opposites, each line being paired with the mate of the other. A fine wire must be drawn across the slit of the collimator, in order that the vertical coincidence may be tested. One should expect the interferences to appear between the $D$ lines on gradually moving the micrometer mirror $M$, parallel to itself, into the required position. As stated above, I did not at first succeed in finding the interferences, but the experiment is a delicate one. In a repetition with first-order spectra, it would be advisable to replace the plane mirrors $m$, $n$, by slightly concave mirrors, about 2 meters in focal distance, and to replace the telescope $T$ by a strong eyepiece. This is the method used in the next paragraph, and it was more easily successful.

Later I returned to the experiment with the same adjustment, except that the plane mirrors $m$, $n$, were placed *beyond* the grating, with the object of using the equivalent of second-order spectra to get more dispersion. This plan did not fail, and, having once obtained the interferences, the reproduction seemed quite easy, as they remained visible while the micrometer $M$ was moved over about 5 mm. or more, a very important observation. Their appearance with a *small* telescope was that of a single fine line, alternately flaming yellow (very bright on the yellow background of the surrounding part of the spectrum) and jet black as compared with the $D$ lines, between which the interferential line was situated, and on an enhanced yellow ground. The flicker is referable to the tremor of the laboratory, which makes it impossible to keep these interferences quiet. Shutting off the light from either mirror, $M$ or $N$, naturally quenches the interferences, but leaves the yellow part of the spectrum behind.

Obviously, coincidence of the longitudinal axes of the spectra alone is needed. Therefore, upon moving the two double $D$ lines apart, by aid of the adjustment screws on the mirror $M$ and $N$, symmetrically to the ends of the yellow field in the telescope, the interferences were isolated and located midway between the $D$ doublets of each spectrum, *i.e.*, in the center of the field of the telescope. They could now be observed to better advantage. In the small telescope there is apparently but one dark line. If stationary, its ultimate character, when centered, would be surmised to be given by the intersection of a vertical diameter with a series of confocal ellipses, successively bright and dark, as indicated in figure 2. The light and dark parts alternate or flicker. On moving the micrometer, the vertical intersector $A$ takes a more and more lateral position like $B$, so that the trembling interferences would soon be invisible, as they rapidly become finer and hair-like (not shown).

On using higher magnification (larger telescope), two black lines bordering
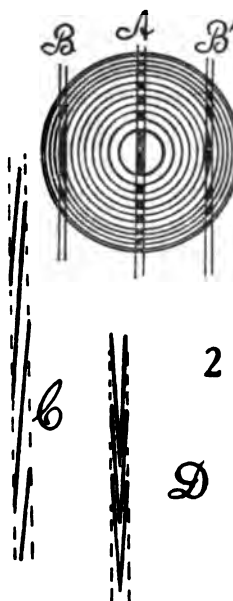
a bright line, or a black line between two bright lines, seemed to be visible; but the interferences would have to be stationary to be definitively described, since the width of the pattern is not more than one-third to one-half of the distance between the sodium lines.[1] The interferences, moreover, did not now readily conform to the design B, figure 2, anticipated, but were more of the type C, with long, dark lines slightly oblique to the vertical, and vibrating within a vividly yellow band. Sometimes these were heavier, with two or three faint lines on one side.

Further experiment showed that the phenomenon is not influenced by the width of the slit, except that it is clearest and sharpest with the narrowest slit possible and vanishes when the slit is made so wide that the Fraunhofer lines disappear. It may easily be produced by the modified method following, in any wave-length red, yellow, green, etc., with no essential difference except in size. It is present, moreover, in all focal planes, *i.e.*, the ocular of the telescope may be inserted or pulled out to any distance, yet the same phenomena persist on the vague, colored background. A number of observations were made to detect the change of the pattern of the interference, between its entrance into the field and its eventual evanescence, in case of the continuous displacement of the mirror M over 5 mm. In figure 2 this would be equivalent to a passage of B into B' through A, and the fringes for a distant center should therefore rotate, as they actually do in the experiments of the next paragraph. But in the present case the type C *persists;* the lines may become longer or all but coalesce and their inclination may change somewhat. They nevertheless remain fine and nearly vertical, until they vanish completely and there is no rotation. Nor could the phenomenon be found again within the length of the given micrometer screw. Hence it is improbable that these interferences conform at once to the ordinary elliptic type for which figure 2 applies, even if the ellipse is considered exceptionally eccentric. The use of two slits, one following the other, does not change the pattern.
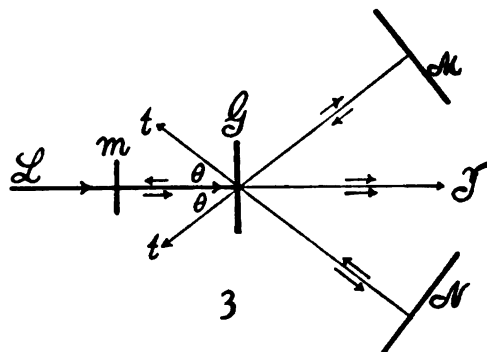


The modified method of experiment was one of double diffraction. In figure 3, L is the blade of light from the collimator, which passing *under* the plane mirror, *m*, penetrates the grating G, whence the diffracted first-order beams reach the opaque mirrors M and N. These return the beams, nearly normally but with an *upward* slant, so that the color selected intersects the

---

[1] The use of the $D_1$ $D_2$ distance of the sodium lines for the measurement of the breadth of the interference phenomenon is a mere matter of convenience in describing it. It will be shown in the next report that the breadth of the strip carrying interference fringes is quite independent of the dispersion of the optic system.

grating at a higher level than $L$. A second diffraction takes place at about the same angle, $\theta$, to the direct ray $t$, and the coincident rays now impinge on the mirror $m$. They are thence reflected into the telescope at $T$. This method admits of easier adjustment, as everything is controlled by the adjustment screws on $M$ and $N$. Plane mirrors $M$, $N$, and $m$ only are needed, the latter being on a horizontal axis to accommodate $T$. The direct (white) beam is screened off after transmission through the grating, if necessary. But it rarely enters the telescope.

**3. The same. Further experiments.**—In place of the plane mirror, $m$, a slightly concave mirror (2 meters in focal distance, say) may be used with advantage and the telescope $T$ replaced by a strong eyepiece. In this way I obtained the best results.

It is to be noticed that the apparatus (fig. 3) may serve as a spectrometer, provided the wave-length $\lambda$ of one line and the grating space $D$ are known, and the mirror, $M$, is measurably revolvable about a vertical axis. In this case any unknown wave-length, $\lambda'$, is obtained by rotating $M$ until $\lambda'$ is in coincidence with $\lambda$. Supposing the $\lambda$'s of the two spectra to have been originally in coincidence and that $\theta$ is the angle of $M$ which now puts $\lambda'$ in coincidence with $\lambda$, it is easily shown that

$$\lambda'-\lambda = \lambda \,(2\sin^2 \theta/2 + \sqrt{D^2/\lambda^2 - 1}\,\sin\theta)$$

Angles must in such a case be accurately measurable, $i.e.$, to about 0.1 minute of arc per Ångström unit, if the grating space $D = 351 \times 10^{-6}$, as above. Counter-rotation of the mirror $N$ till the $\lambda$'s coincide would double the accuracy. The usual grating, however, has greater dispersion and would require less precision in $\theta$.

Finally, a still simpler and probably more efficient device consists in combining the mirror $m$ and the plane grating $G$, or of proceeding, in other words, on the plan of Rowland's method for concave reflecting gratings. In such a case the light would enter in the direction $TG$, figure 3, be reflected along $GM$, back along $MG$, and then return along $GT$ at a slightly higher or lower level than on entering. The equation just given would still apply, and many interesting modifications are suggested. Experiments of this kind are to be tested. Moreover, in case of the plane-transmitting grating and plane mirror, as above shown, the same simplification is possible if the lens is replaced by the telescope at $T$. But in this case the spectra are intersected by strong, stationary interferences due to reflections from front and rear faces and consequently not conveniently available. A reflecting grating and telescope would not encounter this annoyance. In general, however, as in the disposition adopted in figure 3, the light enters opposite the observer, and, as the light directly transmitted can be screened off, this is a practical convenience in favor of the transparent grating. The reflected spectra used may be placed at any level by rotating the mirror $m$ on a horizontal axis.

On further repeating the work by the use of the concave mirror $m$, a strong eyepiece at $T$, figure 3, and using a compensator, I eventually succeeded in

*erecting* the interference design *C*, figure 2. It then took the form given at *D*, and this seems to furnish the final clue to the subject. In other words, the design consists of a new type of extremely eccentric ellipses, with their long axes parallel to the Fraunhofer lines, each end having the outline of a needle-point, possibly even concave outward. Only one end of the long, closed curves is obtainable. These jet-black lines dance on the highly colored background of less than half the width between the two sodium lines. The interference design would, therefore, be the same (apart from color) as that which would be obtained if the spectrum containing ordinary elliptic interferences were to shrink longitudinally from red to violet, till it occupied less than half the space between the two *D* lines. In fact, I have at other times obtained just such patterns, with all the colors present, but *not in the pure yellow*, as in the present case. Vertically, the path-difference is always due to more or less obliquity of the rays passing through the plate of the grating. Horizontally, however, the equivalent path-difference is complicated, in the present case, by the fact that one wave-length of a pair has increased, whereas the other has diminished, while both may pass through the same thickness of glass and air.

**4. Coincident spectra with one reversed on a given longitudinal axis.**—For this experiment it is necessary to reflect the first-order spectra issuing at the grating *G*, figure 4, from the ruled face *g* (a narrow, preferably horizontal, blade of white light is here furnished by the collimator *L* with a horizontal slit, and the rulings of the grating are also horizontal and parallel to it), twice in succession and preferably from mirrors *M* and *N* and *m* and *n*, reflecting normally to each other and inclined at an angle of, roughly, 45°. Each of the mirrors *M* and *N* must be revolvable about a horizontal axis parallel to the slit and furnished with three adjustment screws relatively to axes normal to each other, one of which is horizontal. The mirrors *m*, *n* are the silvered faces of a prism right-angled at the edge. It is, moreover, to be placed on the slide of a Fraunhofer micrometer so that the prism may be moved, gradually up and down, for the adjustment of distances.

On leaving the mirror *m*, *n*, the two spectra are carried by nearly horizontal and parallel sheets of divergent rays, which pass outward from the diagram. But it will be seen that one of the two spectra reaching the observer is reversed on the longitudinal axis relatively to the other; *i.e.*, if one is in the position

$$\text{red} \left\{ \begin{matrix} \text{top} \\ \text{bottom} \end{matrix} \right\} \text{violet, the other will be red} \left\{ \begin{matrix} \text{bottom} \\ \text{top} \end{matrix} \right\} \text{violet.}$$

The subsequent passage of the rays is shown in figure 5, which is the side elevation and therefore at right angles to the preceding figure. The rays from *m* and *n* impinge on a distant, slightly concave mirror *K* (about 1.74 meters in focal distance), placed somewhat obliquely, so that when the rays come to a focus at *F* near the micrometer they may just avoid it. The partially overlapping spectra at *F* are viewed by a strong eyepiece, *E*. The observer at *E* can then control the Fraunhofer micrometer by which *m*, *n* is raised and lowered, and the three adjustment screws of *M*.

The adjustment consists in first roughly placing all parts in symmetry with sunlight, until the two spectra appear at $E$. The lens may be removed. There should be a bright, narrow spectrum band on each side of and near the edge of the prism *mn;* for it is clear that after passing the lens $E$, corresponding rays from $M$ and $N$ must both enter the pupil of the eye to be seen together. To make the spectrum parallel, the mirror *mn* is rotated, as a whole, around a vertical axis. The three screws on the mirrors $M$ and $N$ then assist in completing the adjustment; the rotation around the horizontal axis brings



4.

5
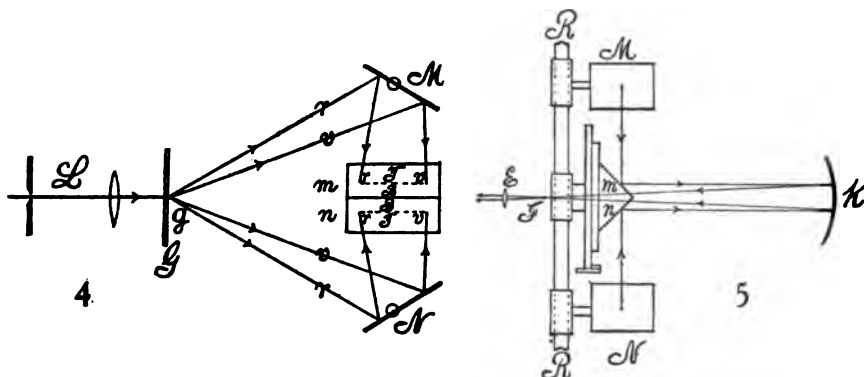
the sodium lines in coincidence (both must be clearly seen and sharp and at an appreciable distance apart); that around the oblique axis gives rise to more or less overlapping, as required. The need of a sharp coincidence of the sodium lines is very *essential* in all these experiments.

After proper vertical position of *mn* has been found by slowly moving the micrometer screw up and down, the fringes appear. They are usually very fine lines, possibly indicating distant centers of the ellipses to which they belong. The appearance is roughly suggested in figure 6. They are thus totally different from the preceding set, § 3. They pass from the type $a$ through $b$



6

(contraction toward the violet end was not noticed) into the type $c$, when the mirrors *mn* move in a given direction. The center of the ellipses is in the vertical through the field of view for the adjustment $b$, in which case the lines pass from end to end of the spectrum as a narrow band near the longitudinal axis of actual coincidence of spectra, symmetrically.

The height or breadth of the longitudinal interference band, $d$ in figure 6, is not greater than 1.5 to 2 times the distance apart of the sodium lines at right angles to the band. From this the angular divergence of the breadth of the band may be found, since $\lambda = D \sin \theta$, where $\lambda$ is the wave-length of light, $D$ the grating space, and $\theta$ the angle of diffraction. Hence for the two sodium lines

$$\Delta\theta = \Delta\lambda / D \cos \theta$$

Since $D = 351 \times 10^{-6}$, cos $\theta = .986$, and $\Delta\lambda = 6 \times 10^{-8}$; therefore $\Delta\theta = 1.7 \times 10^{-4}$ radians. Since the width of the band is about twice this, it will be 68 seconds of arc, or, roughly, about a minute in breadth. Within the strip, when the fringes are horizontal, I counted about five of them, so that their distance apart would be about 14 seconds of arc.

It appears, therefore, that rays of a given color, say of the wave-length at $D$, which leave the grating at a given point and at an angle of about one minute in the plane of the $D$ line, are still in a condition to interfere; whereas one would anticipate that only those rays which lie in the common longitudinal axis of rotation of the two coincident spectra, symmetrical to this, should be in this condition. Such interference should not be appreciable, since the white rays are independent and apparently come from two different points of the slit. If we consider the angular deviation of pencils of parallel rays crossing the grating to be equivalent to the divergence of their respective optical axes at the collimating lens (about 45 cm. in focal distance), the distance apart of two points of the slit, the rays of which are still able to produce interference, is

$$x = 45 \times \Delta\theta = 45 \times 1.7 \times 10^{-4} = 7.6 \times 10^{-3} \text{ cm.}$$

or nearly 0.1 mm. Hence points of white light in the slit about 0.1 mm. apart along its length are included in the band of interferences in question, extending in colored light from red to violet. This seemingly anomalous result will be fully interpreted at another opportunity.

**5. Interference of the corresponding first-order spectra of the grating, in the absence of rotation.**—This apparatus seemed to be of special interest, since the rays used do not retrace their path and are thus available for experi-



ments in which rays traveling in one direction only, are needed.[*] I have tried both the adjustments given in figures 7 and 8, the latter, since the rays are more nearly normally reflected at the mirrors $M$ and $N$, having some advantages; but the other succeeds nearly as well. The difficulty encountered is a curious one of adjustment, which was not anticipated. In other words, if the longitudinal axes of two identical spectra are in coincidence, the Fraunhofer lines are likely to be at a small angle to each other and complete inter-
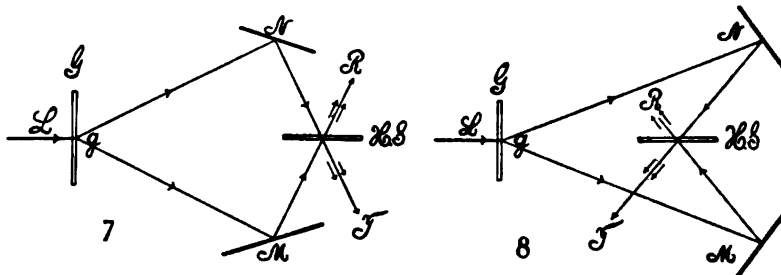
---

[*] Cf. Am. Journal of Sci., xxxiv, p. 101, 1912, on the interferometry of an air column carrying electrical current.

ference is therefore impossible.  Again, if the spectrum lines are in coincidence, the longitudinal axes usually diverge by a small angle.  Furthermore, the interferences are almost always eccentric and the lines hair-like, indicating distant centers.   I have not succeeded in making a perfect adjustment, systematically; but the discrepancies indicated are themselves interesting in their bearing on the subject of this paper.

In figures 7 and 8, $L$ is a vertical blade of white light from a collimator with fine slit, and $G$ is the grating.  The two first-order spectra leaving the ruled face at the line $g$ strike the opaque mirrors $M$ and $N$, the former on a micrometer moving the mirror parallel to itself.  From $M$ and $N$ the rays reach the half-silvered plate of glass $HS$, where one is transmitted and the other reflected into the telescope $T$.  The coincident rays $R$ are superfluous.

After placing the parts and roughly adjusting them for symmetry with sunlight, the finer adjustment may be undertaken.  It may be noticed that the two systems $M$ and $N$, and $G$ as well as $HS$, can be used for further adjustment separately.  All are provided with adjustment screws relatively to rectangular axes.  To put the mirrors $M$ and $N$ in parallel and in the vertical plane with the grating $G$, the half-silvered plate should be removed
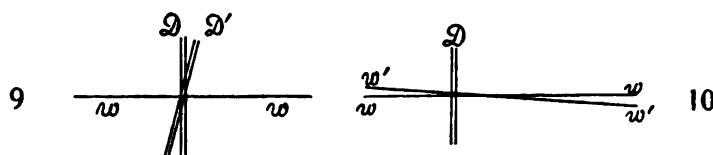


and replaced by a small white vertical screen of cardboard, placed at right angles to the direction of $HS$ in figure 7 and receiving both spectra.  A fine wire is drawn across the slit to locate the longitudinal axis, and an extra lens may be added to the collimator and properly spaced until the doublet insures sharp focussing.  Both mirrors, $M$ and $N$, are now rotated on horizontal axes, until the longitudinal black lines in their spectra cease to diverge and coincide accurately.  $G$, $M$, $N$, may now be considered in adjustment.  On returning the half-silvered plate, $HS$, it in turn is to be carefully rotated around horizontal and vertical axes, until the horizontal black line in the spectrum and the sodium line (always incidentally present in the arc lamp) both coincide.  But, as a rule, it will be found that if the longitudinal axes, $ww$, figure 9, coincide, the $D$ lines cross each other at a small angle, exaggerated in the figure.  The interferences, when found by moving the micrometer at $M$, are usually coarse, irregular lines, indicating a center not very distant and located on the level of a band where the $D$ lines cross.

On the other hand, if the $D$ lines are brought to coincidence by moving the adjustment screws on $M$ and $N$ (which throws them out of parallel), the longitudinal axes $ww$, $w'w'$, figure 10, diverge at a small angle and the interferences are found in a vertical band where the lines $ww$ and $w'w'$ cross.  This band is relatively wide, however, as compared with the cases in paragraphs 2 and 3.  Nevertheless, I have looked upon these results as additional proof

of the possibility of interference; for in neither case ought they to occur if the spectra are not quite coincident horizontally and vertically. If they do occur, it would at first sight seem that a certain small latitude of wave-length adjustment is permitted even with light-waves.

I was at first inclined to refer the cause of this lack of simultaneous parallelism to the grating itself, as it occurred with an Ames grating ruled on glass, with a Michelson reflecting grating, and with a film grating, in about the same measure. But subsequently, on adopting the method of figure 8, the divergence was largely removed and the interferences were now visible throughout the whole of the spectrum. The discrepancy is probably due to insufficient normality of the plate of the grating to the incident white ray, since one of the rays is twice reflected. In any case the adjustment of the coincident sodium lines must be very accurate if the fringes are to be sharp; certainly as little as half their distance apart will obscure the phenomenon.

Though the spectra are bright, the interferences are not as good as with the usual method (paragraph 1); *i.e.*, the dark lines are not black. Neither have I found an available or systematic method for centering the fringes, so that the lines obtained are usually delicate. Again, the position of the collimator, both as regards slit and lens, is here of very serious importance. Any micrometeric horizontal motion of either, in its own plane, will throw the fringes out. Finally, the whole spectrum travels with the motion of the micrometer mirror $M$. The apparatus is thus too difficult to adjust for use, to be of practical interest when simpler methods are at hand. The effect of tremors acting prejudicially on so many parts is exaggerated.

**6. Conclusion.**—The phenomena of paragraphs 2, 3, and 4, showing definite and characteristic interference in case of two coincident spectra crossed either on a longitudinal or transverse axis, represent the chief import of the present chapter. These results can not be directly due to the diffraction of a slit (regarding the line of coincidence as such), owing to their relatively small magnitudes and their independence of the breadth of the slit. Since there is in each case but a single line of points or axis, the disturbance of which comes from identical sources, we might regard the image of this line in the telescope to be modified by the diffraction of its objective. But if the interferences originated in this way, the Fraunhofer lines of the spectrum should show similar characteristics and the diffraction pattern should differ from those observed. Thus the conclusion is apparently justified that distinct and independent points of the narrow slit whose distance apart on its length is not greater than 0.1 mm. contribute rays to the field of interference in each of the colors of the spectrum (longitudinal axes coinciding).

The phenomenon of inversion is virtually one of homogeneous light, the same type of interference occurring in each color from red to violet. When the fringes are horizontal, homogeneous light and a correspondingly broad slit would replace the spectrum. They belong, moreover, to the elliptic category, being of the same nature, apart from their limitations, as those

used in displacement interferometry. With the exception of the points lying on the longitudinal axis of rotation or of coincidence, all the pairs of points of the two coincident spectra owe the major part of their light to different sources; *i.e.*, the points of the superposed spectra are not colored images of one and the same point in the slit.

Again, in case of rotation of one of the coincident spectra around a transverse axis (Fraunhofer line), colors which differ in wave-length by about half the distance apart of the two sodium lines seem also to admit of interference. This permissible difference of wave-length is thus relatively about

$$\frac{\Delta\lambda}{\lambda} = \frac{\cdot5\times6\times10^{-8}}{59\times10^{-6}} = 5\times10^{-4}$$

or less than 0.1 per cent. The character of these interferences is distinctive. They are not of the regular elliptic type, but arise and vanish in a succession of nearly vertical (parallel to slit), regularly broken lines. Later observation, however, revealed as their true form a succession of long spindles or needle-shaped designs. The chief peculiarity observed is their almost scintillating mobility, which in the above text has been referred to the inevitable tremors of the laboratory. It is, however, interesting to inquire into the conditions of the possibility of observable beating light-waves. For two waves, very close together, of frequency $n$ and $n'$ and wave-lengths $\lambda$ and $\lambda'$, if $V$ is the velocity of light, the number of beats per second would be

$$n'-n = V\left(\frac{1}{\lambda'}-\frac{1}{\lambda}\right) = V\frac{\Delta\lambda}{\lambda^2}$$

Therefore in case of the two sodium lines, for instance,

$$n'-n = 3\times10^{10}\times6\times10^{-8}/3480\times10^{-12} = 5\times10^{11}$$

*i.e.*, about $5\times10^{10}$ beats per 0.1 second, the physiological interval of flickering. Naturally this seems to be out of all question, even if one is confronting a source which is an approach to a mathematical line. The endeavor will have to be made to produce these interferences under absolutely quiet surroundings. Their appearance is altogether singular and not like the case of paragraph 4, where there is also perceptible tremor, or with the general case of trembling interference patches, with which I am, unfortunately, all too familiar.

In this place, however, it is my sole purpose to present, at its face value, an observation which is spatial, independent of time consideration; and the laterally cramped character of the new interference, with its long, hair-like lines thrust into a strip less than half the distance apart of the sodium lines, is the only evidence submitted. If the coincident path of two rays of slightly different wave-lengths, $\lambda$ and $\lambda'$, which interfere, is $x$, then there are $x/\lambda$ and $x/\lambda'$, complete waves in the given path, and, in case of original identity in phase, instantaneous reënforcement will occur when

$$x\,(1/\lambda - 1/\lambda') = 1, 2, 3,\ldots\ldots n$$

In other words, at the $n$th reënforcement

$$\Delta\lambda = n\lambda^2/x$$

Hence, since $\lambda^2$ is very small and $x$ relatively very large, the small value of $\Delta\lambda$ (*i.e.*, the very thin strip of spectrum within which the phenomenon occurs) is apparent. In the above experiments the estimates, in round numbers, were $\Delta\lambda = 2.4\times10^{-8}$, $\lambda^2 = 36\times10^{-10}$. Hence if $n = 1$,

$$x = 36\times10^{-10}/2.4\times10^{-8} = .15 \text{ cm.}$$

so that one reënforcement would have to occur about at each 1.5 mm. along the rays. Nevertheless, the formidable difficulty remains to be investigated, viz, why these nominally beating wave-trains, with an infinitesimal group period ($10^{-11}$ sec.), could be recognized at all.

The characteristic feature of the new phenomenon is this, that apart from intensity it *persists, without variation, through a path-difference of over 5 millimeters; i.e.*, through 15,000 or 20,000 wave-lengths. It follows, since the optical paths grating-mirror-grating are alone significant, that two individual light-waves of the same ray over 15,000 wave-lengths apart are still appreciably identical. Beyond that the waves under consideration no longer correspond in orientation and can not interfere in a way to produce alternations of accentuated brightness and darkness.

# CHAPTER II.

FURTHER STUDY OF THE INTERFERENCE OF REVERSED SPECTRA.

**7. Apparatus with one grating.**—The different methods suggested in paragraph 3 were each tried in succession, but none of them were found equally convenient or efficient in comparison with the method finally used in the preceding paper. To begin with the annoyances encountered in the use of a reflecting grating, it was found that the impinging light from the collimator and the reflected doubly diffracted beam from the grating lie too close together, even if all precautions are taken, to make this method of practical value. The use of Rowland's concave grating without a collimator is out of the question, since the spectra formed on the circular locus of condensation, if reflected back, will again converge into a white image of the slit, colored if part of the spectrum is reflected. The plane-reflecting grating, though not subject to this law, requires a collimator, and, since marked obliquity of rays is excluded, it will hardly be probable that the elusive phenomena can be obtained in this way. A compromise method, in which both the reflecting and the transmitting grating are used, will be described in paragraph 10. Though apparently the best adapted of all the methods used, it has only after difficult and prolonged research led to results. These, however, proved very fruitful in their bearing on the phenomena.

For first-order spectra, where there is abundance of light (it is often difficult to exclude all the whitish glare in the field of the telescope completely), the method of figure 11, which shows normal rays only, is still preferable. Here the impinging collimated beam $L$ passes below the opaque mirror $m$ and through the lower half of the grating $G$. The diffracted pencil is reflected nearly normally but slightly upward, by the mirrors $M$ and $N$ (the former carried on a micrometer slide), to be again diffracted at the grating and therefore to impinge as definitely colored light on the lower edge of the concave mirror $m$ (about 1.5 to 2 meters in focal distance), whence it is brought to a focus at $F$ and viewed by the strong eyepiece $E$. Considerable dispersion and magnification is obtained in this way; indeed, the two $D$ lines stand far apart and the nickel line is distinctly visible between them. There must be a fine hair wire across the slit so that the longitudinal axes of the spectra may be accurately adjusted. The mirror $m$ above the impinging beam must be capable of rotation about a vertical and a horizontal axis in order that the focus $F$ may be appropriately placed between $M$ and $N$. With $G$ at 1 meter and $m$ at 2 meters from $F$, the disposition is good. The micrometer $M$ is easily at hand. Though the direct beam may be screened off, the glare reflected back from the grating and the glare from the objective of the collimator are not excluded, as stated. In fact, it was eventually found necessary

19

to carry this pencil in an opaque tube reaching from the objective of the collimator, as far as the grating.

With first-order spectra this method always succeeded satisfactorily, and in case of a ruled grating the phenomenon is exhibited brilliantly, if the paths GM and GN are optically nearly equal. After some experience it is fairly easy to find it. I have not, however, been able to obtain it with a film grating, even after using a variety of excellent samples. This is not remarkable, for the film grating is hardly sufficiently plane to produce clear regular reflection, and the corresponding paths GM and GN would not, therefore, be definite.

Second-order spectra are too faint and can not be seen, unless the glare is excluded in the manner stated. All modifications of the method seemed without avail, until finally the light was led from the collimator objective C, figure 11, to the grating G, in a cylindrical tube, whereupon both the glare from the objective and the rearward reflection from the grating were effectively screened off. This tube must, of course, lie below the returning pencil, i.e., it must not (in section) cover more than the lower half of the grating. In this case the second-order spectra, though faint, were seen clearly; but
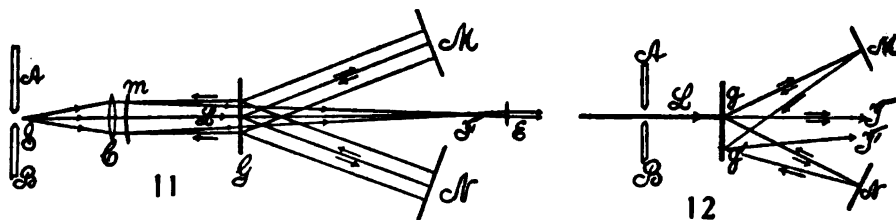


the scintillating interferences could not be observed until the very weak eyepiece, E, was used with the concave mirror m; or a weak telescope with a plane mirror. It was then detected, but showed no essential difference from the case of first-order spectra. The larger dispersion, in other words, was unavailable. The phenomenon was seen most distinctly by drawing out the eyepiece of the telescope, as the light is thereby concentrated, although the Fraunhofer lines vanish. Second-order spectra are therefore not necessarily advantageous. The phenomenon is very hard to find, and the experiments were persisted in only to obtain the result under different conditions.

The tube-like light conductor referred to above is, of course, advantageous in case of first-order spectra. If the concave mirror is used, the phenomenon may even be seen brilliantly with the naked eye.

An alternative method of half-silvering the ruled face of the grating and then using it as a reflector was tried with success. The beam of parallel rays from the collimator L, figure 12, is transmitted by the grating (ruled, half-silvered face, g toward the mirrors M and N) and the two diffracted beams then returned by the opaque mirrors M and N, to be in turn diffracted by reflection into the telescope T. In fact, this method succeeds with the unsilvered grating; for the rays diffracted, by reflection, from the ruled face (toward the telescope), but not very well. The reflection from the rear face

of the grating is so cut up by the strong, stationary interferences that it is unavailable. The grating plate must, of course, be slightly wedge-shaped, otherwise all the spectra would be superposed. In case the ruled face is half-silvered, however, the stationary interferences are practically absent, while two strong spectra are reflected from the silvered side. The phenomenon may then be produced at all distances of $G$ from $M$ and $N$ (2 meters and less), but best at distances within 1 meter. It is, however, frequently hard to find unless different distances apart of the mean $D$ lines are tested. This may be due to the fact that the silver film is not quite equally thick.

Besides the symmetrical position, $gT$, figure 12, the two corresponding unsymmetrical positions $g'T'$ were tested with success; and it appeared that while in the case $gT$ the phenomenon is virtually linear, dark or bright, like a Fraunhofer line, a succession of dark lines inclined to the vertical may appear for the unsymmetrical position $g'T'$. Dark lines are apt to be broadened.

Questions relative to the effect of oblique incidence were also tested by aid of the concave-mirror method shown in figure 11, the white light from $C$ to $G$ being conducted in an inch tube of pasteboard, immediately under the concave mirror, $m$. Figure 13, $a$, shows the general disposition of apparatus.
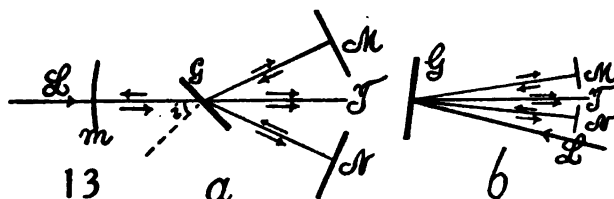


The angle of incidence $i$ is gradually increased, until the return rays from $N$ meet the grating at nearly grazing incidence. No essential difference in the phenomenon was observed, however, except that it was apt to be broader in the non-symmetrical positions and to suggest fine new lines in parallel with the old. In a return to the symmetrical position, sharp lines were especially distinct, usually showing one dark and two bright lines, while two dark and one bright occurred less frequently. It could be seen quite vividly with the naked eye. When the telescope was used and the ocular drawn far forward, the multilinear form was often suggested. On broadening the slit the black lines vanish first and a flickering band remains after the Fraunhofer lines are gone. Finally, the phenomenon could be seen even when the longitudinal axes of the spectra were not quite coincident, but it rapidly became fainter in intensity.

Figure 13, $b$, suggests a method of using a reflecting grating, either plane or (possibly, if the incident light is parallel) concave, for the production of the phenomenon. $G$ is the grating, receiving the collimated white light, $L$, which is diffracted toward $M$ and $N$, thence reflected (at a different elevation) back to $G$, to be again diffracted towards $T$, above or below the direct beam, where it is observed. I have not, however, been able to obtain results with these methods owing to subsidiary difficulties.

**8. Observations and experiments with a single grating.**—On considering figure 11, it will be seen that the doubly reflected, doubly diffracted rays are also in a condition to interfere. Thus the rays *GMGNG* and *GNGMG* have identical path-length, or at least path-difference; but it is improbable that superimposed on the strong spectra this effect could be seen, for the reflection from the ruled face of the grating is very slight and the divergent spectra have weakened seriously. The scintillating interferences, on the other hand, are much brighter than the superposed spectra. Such interferences, also, should be independent of the play of the micrometer *M*, since the path-difference of these beams is not changed thereby, each being identically lengthened or shortened. Furthermore, the interposition of a thick plate-glass compensator in *GM* should have no effect. Neither of these inferences applies for the phenomenon in question, which persists for a definite displacement of *M*, only, and the introduction of a compensator requires the usual equivalent displacement of *M*, within the range of the phenomenon. Finally, the interferences relatively to a phenomenon produced by double diffraction would not be modified.

Many experiments were made to ascertain the path-difference within which the phenomenon is visible. This can not be accurately determined, since it is a question of stating when an observation, which is becoming rapidly less distinct, has actually vanished. Moreover, any imperfection of the micrometer throws out the coincidence of longitudinal spectrum axes, while a readjustment breaks the continuity of the micrometer displacement, or reading. Results were obtained as follows, for example, $\Delta N$ being the displacement of the mirror *M*:

With telescope............................ $\Delta N = 0.34, 0.45, 0.41$ cm.
With concave mirror and lens.............. $0.45, 0.35, 0.41$ cm.
With concave mirror and adjustment....... $0.50$ to $0.60$ cm.

The low readings are due to the micrometric wabbling of the micrometer slide. Since $\Delta N$ is the double path-difference, the number of wave-lengths in question may be put

$$\frac{2 \times .45}{60 \times 10^{-6}} = 1.5 \times 10^4$$

*i.e.*, the distances along the ray are 15,000 to 20,000 wave-lengths apart, about as estimated in the above paper. This is the characteristic feature of the phenomenon.

Between its extreme ranges of visibility the appearance of the phenomenon scarcely changes. It ceases to be visible rather suddenly; and this is to be expected, since we are dealing directly with two wave-trains displaced relatively to each other. It is visible for a wide slit even after the Fraunhofer lines vanish. It disappears by decreasing in width, when the slit is closed. If the ocular of the telescope is drawn out, the phenomenon may even be observed after the Fraunhofer lines have vanished, in the dark, stringy spectrum of an extremely fine slit. When the longitudinal axis of the spectrum is indicated by a fine wire across the slit, the adjustment consists in bringing

the black longitudinal lines of the two spectra together. The question thus arises how close this coincidence is to be. When the phenomenon is sharp, it has been found possible to displace the two black lines so that a fine, bright strip of spectrum may just be seen between, without quite destroying the interferences. Naturally they are then much weaker. This result is in harmony with the observations made on rotating one spectrum, on a longitudinal axis, 180° with reference to the other.

Since the phenomenon was originally produced with sunlight, it might be supposed that the edges of the Fraunhofer line, under conditions of tremor, would interfere with each other as indicated in figure 14, where $A$ is one and $B$ the other of the two superposed spectra. The change of wave-length is suggested by the slant of lines on the diagram. In such a case, whereas the conditions $a$ and $c$ would show bright overlapping spectra, the dark line would appear under condition $b$. But even in this case, lines of slightly different wave-length would have to interfere with each other. The crucial test was made by using an arc-lamp spectrum, and it was then found that the phenomenon appeared as well as with sunlight.
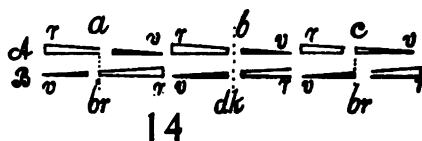


A further question at issue is the breadth of spectrum needed to produce the phenomenon; for the observed breadth would be influenced by the quiver of the apparatus. With this end in view, different lines of the spectrum were placed in full coincidence, and it was found that for none of the secondary lines in the orange-yellow spectrum was it extinguished or even modified. If, however, the corresponding $D$ lines of the spectra $(D_1D_1'; D_2 D_2')$ were superposed, the phenomenon in these experiments played like a wavy strip at their edges only. Sometimes a bright line flashed through the middle of the coincident lines. One would conclude, therefore, that the part of the spectrum used in producing these interferences is not much broader than either the $D_1$ or $D_2$ lines, while the other marked lines in the orange-yellow are too narrow to appreciably influence it. These results will be greatly amplified in the work done with two gratings below.

A corresponding experiment was now made with *sodium light*. To obtain a sufficiently intense source, solid caustic soda was volatilized between the carbons of the electric arc, $A$ and $B$, figure 12, or the corresponding case in figure 11. On drawing the carbons apart, strong $D$ lines were seen, in the entire absence of an arc spectrum, at first so broad as to be self-reversing. Gradually they became finer and eventually reached the normal appearance of the $D_1$, $D_2$ lines. In order to facilitate adjustment and with the object of obtaining cases correlative with the results for the dark-line spectrum, a beam of sunlight (as at $L$, figure 12) was introduced between the carbons and the phenomenon established faultlessly in the usual way. The pencil of sunlight was then screened off and the arc light substituted, or the two were used together.

These observations seemed to show that when the normal $D_1$ or $D_2$ lines were placed in coincidence, the thread-like phenomenon fails to appear with

all the characteristics visible in the case of sunlight. When the slit is broadened an alternation of brightness, or flicker of light, may be detected vaguely. With a slit of proper width to show the Fraunhofer lines all this seemed to vanish. The actual phenomenon was therefore apparently not reproduced or improved either by homogeneous light or by widening the slit. Such experiments alternating with sunlight were made at considerable length, but the adaptation of methods for two gratings discussed in paragraph 10 will nevertheless throw out this conclusion.

If the narrow sodium line is broadened by adding fresh sodium at the carbon, so that the yellow spectrum is again self-reversed, the phenomenon plays with extreme vividness around either of the reversed and coincident $D_1$ or $D_2$ lines, or even within the black line in question, if narrow. But here the light is no longer homogeneous. Sometimes when the solar spectrum is used, a black line preponderates; in other adjustments a flashing bright line is in place; but the reason for this can not be detected by the present method.

**9. Inferences.**—If the wave-length of the two spectra is laid off in terms of the angle of diffraction, $\theta$, measured in the same direction in both cases, the graph will show two loci as in figure 15, $a$, intersecting in the single point of coincident wave-lengths $\lambda_0$. It appears, however, as if the wave-lengths at $\varphi_1$ and $\varphi_3$, $\varphi_2$ and $\varphi_4$, are still in a condition to interfere. The phases $\varphi_1$ and $\varphi_3$, $\varphi_2$ and $\varphi_4$, differ because of path-difference introduced for instance at the micrometer, the phases $\varphi_1$ $\varphi_2$, $\varphi_3$ $\varphi_4$ differ because of color differences, having passed through refracting media of glass and air. Probably the phase-difference $\varphi_1 - \varphi_3 = \varphi_2 - \varphi_4$, these having the same color-difference; and $\varphi_1 - \varphi_2 = \varphi_3 - \varphi_4$, having the same path-difference. At $\lambda_0$, $\theta_0$, the two phases $\varphi_0$ are due to path-difference only.

To allude again to the *question of beats*: if ten beats per second are discernible, the beating wave-trains in the case of the given grating would be only $6 \times 10^{-10}$ second of arc apart in the spectrum. If the phenomenon has a breadth of $3 \times 10^{-8}$ cm. in wave-length, as observed, then the number of beats in question will be $2.5 \times 10^{11}$ per second. All this is out of the question, so far as the phenomenon appreciable to the eye is concerned. If beats were due to a difference of *velocity* resulting from the dispersion of air, and if $T$ is the period of the beats, $\lambda$ the mean wave-length, $\delta\frac{1}{\mu}$ the difference of the reciprocal indices of refraction, we may write

$$T_1 = \frac{\lambda}{v\delta(1/\mu)}$$

If, furthermore, $\mu = A - B/\lambda^2$, where $B = 1.34 \times 10^{-14}$, $\delta\lambda = 2.4 \times 10^{-8}$,

$$T_1 = \frac{\lambda^4}{2vBd\lambda} = \frac{1.3 \times 10^{-17}}{2 \times 3 \times 10^{10} \times 1.34 \times 10^{-14} \times 2.4 \times 10^{-8}} = .7 \times 10^{-6} \text{ sec.}$$

or
$$N_1 = 1.4 \times 10^6 \text{ beats per sec.}$$

which would also be inappreciable.

If both the difference of wave-length and wave-velocity are considered, we should have for the first spectrum $v$ and $n$, and for the second spectrum $v$ and $n'$. The conditions would be left unchanged, if the second velocity is taken equal to the first and the frequency $n'(v'/v)$ replaced by $n'$. From this it follows that the number of beats $N$ is nearly

$$N = v\left(\frac{1}{\mu\lambda} - \frac{1}{\mu'\lambda'}\right) = -v\left(\frac{\delta\lambda}{\mu\lambda^2} + \frac{\delta\mu}{\lambda\mu^2}\right)$$

If $\delta\lambda$ is considered negative, if $\mu = A - B/\lambda^2$ and the multipliers $\mu$ and $\mu^2$ be neglected,

$$N = v\delta\lambda\left(\frac{1}{\lambda^2} - \frac{2B}{\lambda^4}\right)$$

which is the difference of the two cases above computed. As the first is very large compared with the second, the visibility of the phenomenon is not changed.

The theory of group waves usually introduces a factor 2. Thus if $\lambda_1$, $v_1$, $n_1$, be the group wave-length, velocity, and frequency,

$$\lambda_1 = 2\lambda^2/\delta\lambda \qquad v_1 = v\,\delta(\mu\lambda)/(\mu^2\delta\lambda) \qquad n_1 = v\delta(\mu\lambda)/(2\mu^2\lambda^2)$$

or,

$$n_1 = \frac{v\delta\lambda}{2}\left(\frac{1}{\mu\lambda^2} - \frac{2B}{\lambda^4}\right)$$

or with the above data

$$n_1 = \tfrac{1}{2}\,(2.0\times10^{11} - 1.4\times10^{6})$$

results otherwise like the above and without bearing here. There is a possible question whether differences of wave-length due to velocity and not to period can be treated as dispersion.

The occurrence of *forced vibrations* has also been looked to as an explanation. Though here again, even if the spectra are almost always of unequal intensity, the reason for the preponderance of one would have to be stated. True, equal mean strength is not equivalent to equal instantaneous strength. In the case of forced vibrations, however, if the harmonic forces of one spectrum are $F = A \cos pt$ (forced, $T = 2\pi/p$), of the other $F = A' \cos qt$, (free, $T = 2\pi/q$) and there is no friction, the resulting harmonic motion will be given by

$$y = \frac{A}{q^2 - p^2}\cos pt$$

Now if we regard the case of figure 15, on one side of the line of coincidence $\lambda_0$, $q^2 > p^2$; on the other side, $p^2 > q^2$. Hence, whenever a brilliant line flashes out due to coincident phases, there should also be a black line due to opposition; and, in fact, when the phenomenon is produced under conditions of perfect symmetry of the component beams, this seems to be its character; *i.e.*, the enhanced line cuts vertically across the breadth of the spectrum. The case $q^2 = p^2$, being of infinitely small breadth, would not be visible. It is not to be overlooked, however, that in certain adjustments, particularly in

the non-symmetrical case of figure 13, more than two black lines frequently occur. (Cf. § 15.) These accessory lines are ordinarily very thin and crowded on one side of the phenomenon only. It is thus merely the prevalent occurrence of paired dark and bright lines that are here brought to mind. Again, the suggestion of many oblique lines has occurred in some of the observations. These would be quite unaccounted for.

Finally, many attempts were made to find whether the phenomenon would occur again beyond its normal range of about $2 \times 0.5$ cm. of displacement. But, though the micrometer screw actuating the mirror $M$ was effectively $2 \times 3$ cm. long, no recurrence could be found. At the ends of its range the phenomenon drops off rather abruptly.

None of the inferences put forward adequately account for the phenomenon as seen with a single grating, as a whole. In this dilemma I even went so far as to suppose that a new property of light might be in evidence. One feature, it is true, has been left without comment, and that is the width of the slit-image. If $ab$, figure 15 $b$, is the angular width $(d\theta)$ of this image, the case of figure 15 $a$ should be additionally treated in terms of figure 15 $b$.

But within the limits of the present method of experiment, with but one grating, this circumstance seems to offer no clue. If, for instance, the spectra actually coincide in color throughout their extent, as in ordinary interferences, the interference patterns should be *enormous*, for the path-difference



15
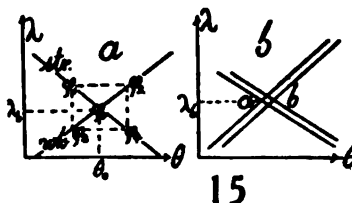
may be zero. The invariability of the present phenomena as to size within its long range of presence, the occurrence of intensely sharp and bright or dark single lines, with a distance $(d\theta)$ much less than the distance apart of the $D_1, D_2$ lines, is in no way suggested by the width of slit-image. Moreover, in spite of its persistence, the interference phenomenon of reversed spectra has the sensitiveness of all interferences. Slight tapping on the massive table throws it out altogether. Clearly, therefore, a modification of method is essential if new light is to be thrown on the phenomenon, and from this viewpoint a *separation* of the two diffractions seems most promising.

**10. Apparatus with two gratings.**—All the varied experiments described in the preceding paragraph failed to show any essential modification of the linear interference pattern obtained. In a measure this was to be anticipated, inasmuch as both diffractions take place at the same grating. It therefore seemed promising to modify this limitation of the experiments, although the difficulty of finding the phenomena would obviously be greatly increased. The separation of the two diffractions, however, seemed to be alone capable of resolving the phenomenon into intelligible parts.

In the present method the glass grating $G$, figure 16, receives the white beam $L$ from the collimator, which is then diffracted to the opaque mirror $M$

(on a micrometer slide) and $N$, thence to be reflected to the reflecting grating $G'$, plane or curved. Here the two beams of the identically colored light selected are again diffracted to the telescope or lens at $T$. Since the gratings $G$, $G'$, rarely have the same grating constant, their proper position must be found by computation and trial. In my work the distances to the line of mirrors $NM$ were 165 cm. for $G$ and 90 cm. for $G'$. This method automatically excludes the direct beam $a$ and all glare, and gives excellent spectra both in the first and second orders. The use of two gratings, however, introduces the difficulties of adjustment specified, as the two $D$ doublets corresponding to $N$ and $M$ will not, as a rule, be parallel and normal to the longitudinal axes of the spectrum, unless all cardinal features, like the rulings and their planes, are quite parallel. If the grating is not normal to the impinging beam, the axis of the corresponding spectrum is a curved line. The spectra are, moreover, likely to be unequally intense, a condition not infrequent even in the preceding method. It is possible that this may be due to the grating itself, but probably unequal parts of the corresponding beams are



16
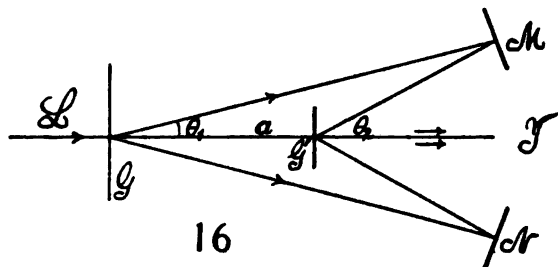
used in the two cases, or the mirrors are unequally good. As a result, in my earlier work I was not able to produce the phenomena with two gratings, after many trials, in spite of the clearness of the overlapping spectra; but the same serious difficulties are encountered whenever interferences are produced from two independent surfaces.

Later, having added a number of improvements to facilitate adjustments, I returned to the search again and eventually succeeded. There are essentially four operations here in question, supposing the grating $G$ approximately in adjustment. By aid of the three adjustment screws on each of the mirrors $M$ and $N$, figure 16, the fine wire drawn across the slit may be focussed on the grating, if an extra lens is added to the collimator and the black horizontal shadows of that wire, across the corresponding spectra, placed in coincidence. The grating $G'$ is then to be moved slowly fore and aft, normal to itself, on the slide, so that the position in which the sodium lines are nearly in coincidence to an eye placed at the telescope, $T$, may be found. The grating $G'$ is next to be slowly rotated on a line (parallel to $LT$) normal to its surface, to the effect that the black axes of both spectra (i.e., the spectra as a whole) may coincide. This must be done *accurately*, and the last small adjustments may be made at the screws controlling $M$ and $N$. Finally, the micrometer

slide carrying $M$ is to be moved fore and aft until the interferences appear. These operations are difficult even to an experienced observer. The fringes are very susceptible to tremors, and only under quiet surroundings do they appear sharply. At other times they move, as a whole, up and down and intermittently vanish.

The fringes so obtained, figure 17, were totally different from the preceding and consisted of short, black, equidistant, nearly horizontal lines across the active yellow strip of spectrum, at the axis of coincidence. The strip was about of the same width as above. Thus the pattern presented the general appearance of a barber's pole in black and yellow, the width being less than the sodium interval, $D_1$, $D_2$, and the distance apart of fringes usually smaller. They were visually in motion up and down, rarely quiet, no doubt owing to tremor. Since the fringes were nearly horizontal or less than 30 degrees in inclination, it was possible to enlarge the width of the slit without destroying them, as in case of the hair-like vertical fringes in paragraph 2 above. In this way a breadth of strip greater than the distance $D_1$, $D_2$, could be obtained with sunlight or arc light, though a moderately fine slit was still desirable.



17
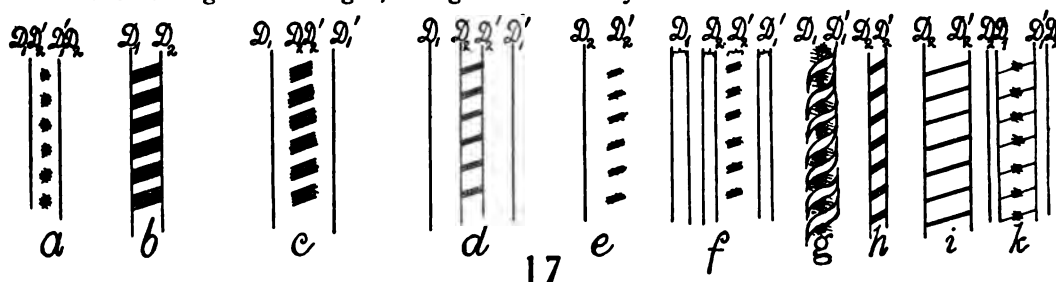
In general, the characteristics noted above were again observed. Thus on moving the micrometer screw controlling $M$, the interferences appeared rather abruptly. They vanished in a similar manner, after about 0.4 cm. or more of the micrometer screw had been passed over. In other words, the fringes remain identical for a path-difference of about $2 \times 0.4$ cm., or nearly 15,000 wave-lengths.

If we call the four $D$ lines available in the two solar spectra $D_1$, $D_2$, $D'_1$, $D'_2$, respectively, a number of curious results were obtained on placing them variously in approximate coincidence. Thus figure 17 $a$, when each $D$ line of one spectrum coincides with the mate of the other $(D_1, D'_2; D'_1, D_2)$, equidistant dots, surrounded apparently by yellow luminous circles, appeared between the two doublets. On widening the slit the dots changed to a grating of nearly horizontal lines covering the strip $D_1$, $D_2$, figure 17 $b$. The lines in one part of the slit seemed to slope upward and in another to slope downward. With a large telescope the phenomenon was more dim and quiet, apparently. The fringes often lie in more definite focal planes and cease to be visible when the ocular of the telescope is far outward, differing from the case above.

The phenomenon of chief interest, however, was observed (figure 17 $c$) in placing two identical $D$ lines in coincidence $(D_1; D_2 D'_2; D'_1)$. The fringes

were then seen across the coincident lines, now no longer visible, quite independent of the absence of light. This would seem to mean that the otherwise quiet ether within the black line is stimulated into vibration by the identical harmonic motions of the bright fields at and beyond the edges of the line (diffraction). The question will presently be broached again in a different way. Here I may note that in the above cases of transverse lines (§ 8) it is often possible to observe a very fine parallel yellow line within the coincident $D_2$, $D'_2$, or $D_1$, $D'_1$, doublets, excited, therefore, in the dark space and splitting the line.

The experiments were now repeated with the sodium arc, and these also gave some striking results. Thus in the case of figure 17 $d$ the lines were separated, but the yellow striations seemed to show across the dark space between $D_2$ and $D'_2$. When the yellow light was too weak, cross-hatchings were seen only across $D'_2$, as in figure 17 $e$. Frequently the phenomenon figure 17 $f$ occurred on broadening the slit, in which $D_2$ and $D'_2$ interfered, but only $D'_2$ was marked. Screening off $D_2$ (left mirror) at once removed the fringes. I have interpreted this observation as the result of parallax, due to the fact that the lines and the interferences are seen in different focal planes.
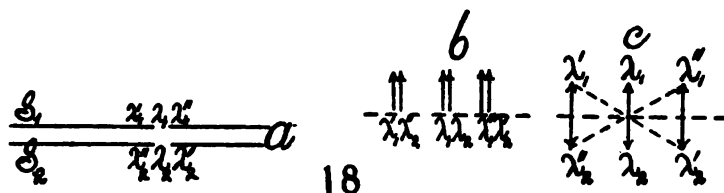


On the basis of these results one might with some plausibility adduce the following remarks in explanation of the phenomenon: In figure 18 $a$, let $S_1$ and $S_2$ be the overlapping reversed spectra and let the line of symmetry be at $\lambda_1$, $\lambda_2$. Then if identical ether vibrations can react on each other across a narrow ether gap, rays as far as $\lambda'_1$, $\lambda'_2$ and $\lambda''_1$, $\lambda''_2$ being of identical source and wave-length, respectively, are still in a condition to interfere. There would then be three groups of interferences, $\lambda_1 \lambda_2$, $\lambda'_1 \lambda'_2$, $\lambda''_1 \lambda''_2$. If, figure 18 $b$, all are in phase, we should have a brilliant line; if all are in opposite phases, a dark line on the principle of figure 18 $c$. Naturally, if wave-trains react on each other across an ether gap, small as compared with the $D_1$, $D_2$ interval, the assumption made above relative to interference of different wave-lengths is superfluous. My misgiving in the matter arises from the misfortune of having taken down the original apparatus, for modification, and having since been unable to reproduce them with anything like the decisiveness with which they were at first apparently observed. I can not now be certain whether what occurred was actually what I seemed to see, or whether the broad illumination of the sodium flash (broad individual lines, $D_1$ to $D_2$, virtually a continuous spectrum) may not have misled me. The experiments were continued, as follows.

**11. Experiments continued. New interferometer.**—At the outset it was necessary to ascertain the reason for the difference of the phenomena, as obtained with one grating in paragraph 8 and with two gratings in paragraph 10. As the probable cause is a lack of parallelism of the rulings in the latter case, it was necessary to remount the second grating $G'$ in the manner shown in figure 19. Here $AA$ is a baseboard, capable of sliding right or left and of rotating on a horizontal axis parallel to the grating. The latter (in a suitable frame) is held at the bottom by the axle, $e$, normal to the grating and by the two set-screws $a$ and $b$ carried by the standards $c$ and $d$. Thus the grating could be rotated around an axis normal to its plane. At first a Michelson plane-reflecting grating $G'$ and a telescope were used, as in figure 16; but it was found preferable (fig. 20) to use a Rowland concave reflecting grating $G'$, with the strong lens at $T$, the grating receiving a beam of parallel rays of light for each color from the collimator and first grating $G$. In this case, with sufficiently high dispersion, a large, strong field was obtained, in which even the very fine lines of the solar spectrum were quite sharp. Rotating grating $G'$ around a parallel horizontal axis, like $AA$, figure 19, made little
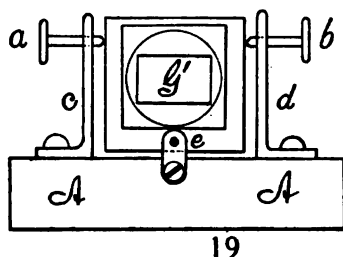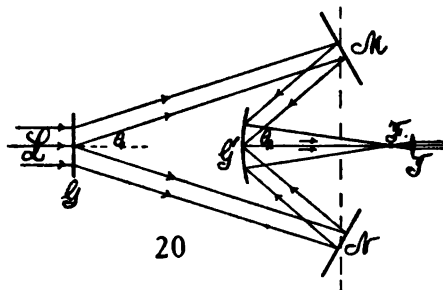


19                    20

difference, relatively speaking; but rotation around the axis $e$, normal to its plane, carried out by actuating $a$ and $b$ in opposite directions, made fundamental differences in the appearance of the phenomenon and eventually suggested a new interferometer for homogeneous light.

The adjustments are the same as in case of figure 16, $G$ being the transparent grating, except that $G'$ is now a concave grating and $T$ a strong eyepiece. The distances $G'T$ and $GT$ were of the order of 1 and 2 meters.

On rotating the grating $G'$ on an axis normal to its face, from a position of slight inclination of the rulings toward the left, through the vertical position, to slight inclination to the right, the fringes passed through a great variety of forms, to be described in detail in § 13 below. Difference of focal planes between the Fraunhofer lines and the interferences were common, so that effects of parallax were apt to occur. Thus when $D_2$ and $D'_2$ coincide, the ladder-like phenomenon may lie between $D'_2$ and $D'_1$; or the ladder may pass obliquely between the $D_2 D_1$ and $D'_1 D'_2$ doublets. The first experiment with the new and powerful apparatus (plane transparent grating $G$, grating space $351 \times 10^{-6}$ cm., and the concave reflecting grating $G'$, grating space $173 \times 10^{-6}$ cm., fig. 20) was made with the object of verifying, if possible, the

reaction of parallel ether wave-trains on each other across a very narrow ether gap. The sodium arc lamp was used as a source of light. The results as a whole were negative, or at least conflicting. Usually when strong interferences were observed for coincident positions of $D_2$, $D'_2$, for instance, there was no passage of fringes across the dark space when $D_2$ and $D'_2$ were slightly separated. At the beginning of the work (possibly as the result of lines broadened by a flash of sodium light) the stretch of interference fringes across the dark space was certain; but such evidence is not quite trustworthy, for a continuous spectrum (i.e., lines broadened by the flash) would necessarily produce the striations. With a very fine slit the coincident $D_1$, $D'_1$ or $D_2$, $D'_2$ was frequently much broadened by a sort of burr of fringed interferences. When the lines are self-reversed, superposition of $D_1$, $D'_1$, etc., frequently showed vivid interferences across the intensely black middle line. This and the passage of the bright and dark lines across the superposed $D_1$, $D'_1$ lines of the solar spectrum are thus the only evidence of the reaction of separated light-rays on each other across an ether gap observed in the new experiments, and the above results could not be repeated.

On introducing a refined mechanism to establish the sharpest possible coincidence of the $D_1$, $D'_1$ or $D_2$, $D'_2$ lines, it seemed as if these lines could at times be brought to overlap with precision, without the simultaneous appearance of the interferences around then; but on drawing out the ocular of the telescope or the lens the cross-hatching invariably appears. If the coincidence is not quite sharp, the phenomenon is usually very strong in the isolated bright strip. Horizontal fringes are best for the test.

An additional series of experiments was made some time later by *screening* off parts of the concave grating $G'$, in order to locate the seat of the phenomenon at the grating. Screening the transmitting grating $G$ was without consequence; but on reducing the area $G'$ to all but the middle vertical strip about 5 mm. wide, a very marked intensification of the phenomenon followed. Although the spectrum as a whole was darker, the interferences stood out from it, relatively much sharper, stronger, and broader than before. The Fraunhofer lines were still quite clear. Thus the pattern, g, figure 17, was now very common, both with sunlight and with sodium light. For a given slit the phenomenon began with a strong burr c, figure 17, completely obliterating and widening the superposed $D_2$, $D'_2$ lines. When these lines were moved apart, the striations followed them, as in figure 17, h and i, to a limit depending on the width of the slit. A still more interesting pattern is shown in figure 17 k, in which the interferences proper are strong and marked between the two $D_1$ $D'_1$ doublets, but much fainter striations are also evident, reaching obliquely across and obviously with the same period.

With this improvement I again tested the ether-gap phenomenon, using the sodium arc, and to my surprise again succeeded. $D_1$ $D'_1$ lines of half the breadth of the doublets apart induced strong fringes between them, and the experiments were continued with the same results for a long time. Several days after, however, with another adjustment, it in turn failed. Clearly

there is some variable element involved that escaped me, and it will hardly be worth while to pursue the question further with the given end in view, without a radical change of method.

Screening middle parts of the grating (in relation to § 15) did not lead to noteworthy results here, but such experiments will become of critical importance below.

A word may be added in relation to Fresnellian interferences in the present work. These would be liable to occur if the observations had been made *outside* of the principal focus, with the sodium lines blurred. In all the experiments on the excitation of a narrow ether gap, however, the $D$ lines were clearly in sight and sharp, so that the phenomena of non-reversed spectra and homogeneous light (in the next section) are not here in question. True, such interferences may often be found in the case of reversed spectra, when the sodium lines are purposely blurred, by pushing the ocular toward the front or to the rear.

**12. Experiments continued. Homogeneous light.**—To turn to a second class of experiments: very important results were obtained with homogeneous light (sodium arc) on placing the $D_1D'_1$ or $D_2D'_2$ lines in coincidence and then broadening the slit indefinitely or even removing it altogether. A new type of interferences was discovered, linear and parallel in character and intersecting the whole yellow field. These lines could (as above) be made to pass from a grid of very fine, hair-like, nearly horizontal lines to relatively broad, vertical lines, on changing the orientation of the grating $G'$, figure 16. Small changes of position of the grating produced a relatively large rotation and enlargement of the lines of the interference pattern. The fringes, when vertical and large, are specially interesting. The distances between successive fringes obtained were about the same (accidentally) as the $D_1D_2$ distance of the sodium lines. They are quiet in the absence of tremor. If $D_1D'_1$ or $D_2D'_2$ were only present, the field would be an alternation of yellow and black striations; but as both doublets are present, the interferences overlap the flat (non-interfering) yellow field of the lines not in coincidence. The fringes are nevertheless quite distinct. A single homogeneous line (like the green mercury line) would give better results. It is necessary that the line selected (say $D_1D'_1$) should coincide horizontally and vertically before the slit is broadened. Otherwise no fringes appear in the yellow ground, or at least not in the principal focal plane. On using a thin mica compensator, it is easy to make these fringes move while the mica film is rotated; and they pass from right to left and then back again from left to right, as the mica vane passes through the normal position of minimum effective thickness. Thus this is a new form of interferometer with homogeneous light. The fringes remain identical in size, from their inception till they vanish, while the micrometer $M$, figure 16, passes (as above) over about 15,000 wave-lengths. In this respect the new interferometer differs from all other types, the two air-paths, $GMG'$ and $GNG'$, alone being in question. The condition of occurrence will be investigated in paragraph 13.

**13. Experiments continued. Contrast of methods.**—As these fringes were produced with a concave reflecting grating, the question may be put whether they would also appear in case of the plane reflecting grating, $G'$, in the adjustment of figure 16. The experiment was therefore repeated with a wide slit, or with no slit at all, and there was no essential difference in the two classes of results.

On the contrary, when the method of but one grating and sodium light was used (fig. 11), the interferometer fringes, in case of a very wide slit or the absence of a slit, could not be produced over the yellow field, as a whole. There appeared, however, an obviously pulsating flicker in parts of the field, on reducing the width of the slit till the sodium lines were each about the width of a $D_1D_2$ space, with either $D_1D'_1$ or $D_2D'_2$ superposed. The sharply outlined slit showed an irregular, rhythmic brightening and darkening over certain parts of its length. These broad pulsations were very violent, very much in character with the linear phenomenon above. This behavior is very peculiar, recalling the appearance of a bright yellow ribbon undulating, or flapping fore and aft, so as to darken parts of its length rhythmically. The pulsations, moreover, were quite as active if seen at night, when the tremors of the laboratory were certainly reduced to minimum. Nevertheless, I am now convinced that such tremor only is in question.

Regarding the phenomenon as a whole, one may argue that in case of the wide slit and single grating, in which the lines for both diffractions are therefore rigorously parallel, the interference fringes are on so large a scale as to cover the whole field of view and thus to escape detection; *i.e.*, that a single vague, quivering shadow of a flickering field is all that may be looked for, in the limited field of view of the eyepiece.

Returning to the case of two gratings and the wide vertical interference fringes and, in turn, all but closing the slit (vertical interferences and sodium arc light), the pulsating phenomenon simply narrowed in width. The two or three sharp vibrating lines, alternating in black and yellow of the original phenomenon (Chapter I), did not appear. The cause of this is now to be investigated.

**14. Experiments continued. Rotation, etc., of grating.**—The method of two gratings (fig. 16 or 20, plane transmitting and concave reflecting) was first further improved by perfecting the fore-and-aft motion of the grating $G'$ ($G'$ movable in the direction $G'T$ on a slide), as well as the precision of the independent rotation of $G'$ normal to its face; *i.e.*, around $G'T$. These adjustments led to further elucidation of the phenomenon. To begin with the fore-and-aft motion of the concave grating $G'$ (*i.e.*, displacements in the directions $G'T$, fig. 20), it was found that the fringes, figure 21, *a, b, c, d, e*, in any good adjustment, pass from extremely fine, sharp, vertical striations, which gradually thicken and incline to relatively coarse, horizontal lines, finally with further inclination in the same direction into fine vertical lines again, while $G'$ continually moves (through about 5 cm.) on the slide normal to the face

of the grating. It was not at all difficult to follow the continuous tilt of these lines through the horizontal, occurring on careful and continuous front-and-rear motions of the grating $G'$ through the limiting positions. The fringes usually vanish vertically merely because of their smallness.

Again, on rotating the grating $G'$ around an axis normal to its face, the fringes merely vary in size, without changing their inclination. Thus if the horizontal fringes (which were here always closer than the inclined set) are in view, these will pass from extremely small-sized, fine, hair-like striations, through a maximum (which is a mere shadow, as a single fringe probably fills the field) back into the fine lines again. Only a few degrees of rotation of the grating suffice for the complete transformation. The maximum is frequently discernible only in consequence of a flickering field. An oblique set of fringes is equally available, remaining oblique as they grow continually coarser and in turn finer with the continuous rotation of the grating.

When the very large horizontal fringes are produced by this method, the change into vertical fringes by fore-and-aft motion of $G'$ is very rapid, so that relatively wide, nearly vertical forms may be obtained. All these effects may be produced by solar or by arc light, around the line of symmetry of the overlapping spectra; or with sodium light when either $D_1D'_1$ or $D_2D'_2$ 21 coincide.

The fine vertical or inclined lines appear as such when the slit is widened, either in case of white or of sodium light. These are the inter- 22 ferometer fringes seen above (§ 6), coarse or fine. With sodium light any width of slit, or no slit at all, is equally admissible. The same is true for the narrow maxima. Lines nearly horizontal were sometimes obtained, pointing, as a whole, toward a center.



$a$  $b$  $c$  $d$  $e$

Finally (and this is the important result) the extremely large horizontal maxima, when a single fringe fills the field, can not be seen apart from pulsations, in the case of a wide slit. With a very narrow slit, such as is suited for the Fraunhofer lines, these horizontal fringes appear as intensely bright or very dark images of the slit. In other words, the normal phenomenon of overlapping symmetrical spectra as described in Chapter I is merely the vertical strip of an enormous horizontal interference fringe, made sharp and differentiated by its narrowness. This case occurs at once when the rulings of the two gratings $G$ and $G'$ are all but parallel, and hence it is the regular phenomenon when but a single grating is used for the two diffractions, as in figures 11 and 12.

In later experiments on the effect of the rotation of the grating, $G'$, around a normal axis, the above results were found to be incomplete. If the rotation is sufficient in amount (a few degrees, always very small), it appears that, after enlarging, the fringes also rotate. But the rotation in this case corresponds to a *vertical* maximum, as indicated in figure 22, the vertical set being
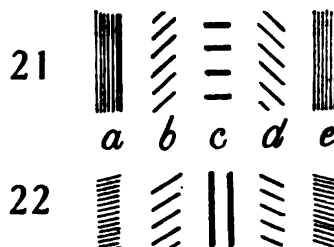
the coarsest possible for a given fore-and-aft position of the grating $G'$. In the figure, the sequence $a$, $b$, $c$, $d$, $e$ is obtained for a continuous rotation of the grating (in one direction around a normal axis).

It now became interesting to ascertain how the vertical set $c$, figure 22, would behave with the fore-and-aft motion. The experiments showed that there was no further rotation, but that, while $G'$ passes normally to itself over about 1.5 cm. on the slide, the vertical fringes pass from extreme fineness at the limit of visibility, through an infinite vertical maximum (a single vague shadow pulsating in the field), back to extreme fineness again, without any rotation. If the edges of the corresponding yellow strips (superposed $D_1$, $D'_1$ lines) did not quite coincide, the fringes were seen outside of the principal focal plane, as usual. Probably the vertical and horizontal maxima are identical in occurrence and appear in case of parallelism in the rulings of the two gratings $G$ and $G'$, and the absence of path-difference. Hence if a single grating is used, as in the original method, the interferometer fringes are not obtainable. This is an important and apparently final result, remembering that fore-and-aft motion is probably equivalent to a rotation around a vertical axis, parallel to the grating.

With regard to the rotation in case of fore-and-aft motion of $G'$, it is well to remark that in approaching the position $c$, figure 24, it is apt to be very rapid as compared with the displacement, precisely as in the case of the picket-fence analogy.

Hence the original phenomenon, consisting of single lines, can not be manifolded by increasing the width of slit. It vanishes for a wide slit into an indiscernible shadow. The phenomenon is a strip cut across an enormous black or bright horizontal fringe, by the occurrence of a narrow slit. Moreover, the scintillations variously interpreted above are now seen to be due to tremors, however different from such an effect they at first appear; *i.e.*, the enormously broad, horizontal fringe changes from dark to bright, *as a whole*, by any half wave-length displacement of any part of the apparatus. It is thus peculiarly sensitive to tremors. On the other hand, oblique or fine vertical fringes are always recognizable for any size of slit. The inquiry is finally pertinent as to why the phenomenon is so remarkably sharpened by a narrow slit; but this must be left to the following experiments.

To be quite sure that the concave grating $G'$ had no fundamental bearing on the phenomenon, I again replaced it by the Michelson plane reflecting grating (fig. 16, $G$ transmitting, $G'$ reflecting). In the same way I was able to rotate the fringes, continuously, through a horizontal maximum of size by fore-and-aft motion of $G'$. Rotation of $G'$ in its own plane increased or decreased the breadth and distance apart of the fringes through a maximum, coinciding with the parallelism of the rulings of the two gratings. Here I also showed decisively that as the rungs of the interference ladder (fig. 21 $c$) thickened and receded from each other, the design passed, in the transitional case, through the original phenomenon of the single vertical line dark or brilliant yellow, for a slit showing the Fraunhofer lines clearly. The phenome-

non vanishes with the spectrum lines as the slit is widened, but, on the other hand, persists as far as the interference of light for a narrow slit. Finally, the apparent occurrence of more than one line is referable to the presence of more than one *nearly* horizontal wide band in the field of the telescope. Thus, for instance, cases between $b$ and $c$ near $c$ and between $c$ and $d$ near $c$, figure 24, are the ones most liable to occur when both diffractions take place at a single grating. This result will be used in paragraph 15.

**15. Tentative equations.**—In the first place, the actual paths (apart from the theory of diffraction) of the two component rays, on the right and left sides of the line of symmetry, $II'Z$, figure 23, will be of interest. The computation may be made for the method of two gratings at once, as the result (if the distance apart of the gratings is $C=0$) includes the method with one grating; *i.e.*, the more complicated figure 23, where $G$ is the transmitting and $G'$ the reflecting grating, resolves itself into a case of figure 24, with but one grating, $G$. $M$ and $M'$ are the two opaque mirrors, $I$ the normally incident homogeneous ray. Supposing, for simplicity, that the grating planes $G$ and $G'$ are parallel and symmetrically placed relatively to the mirrors $M$ and $M'$, as in the figure, the ray $Y$ diffracted at the angle $\theta_1$ is reflected into $X$ at an angle $\theta_2 - \theta_1$ and diffracted into $Z$ normally, at an angle $\theta_2$, on both sides. Under the condition of symmetry assumed $X + Y - (X' + Y') = 0$, or without path-difference. Let $N$ be the normal from $I$ to $M$, and $n$ the normal from $I'$ to $M$, with a similar notation on the other side. Hence if $I$ be given an inclination, $di$, $\theta_1$ is incremented by $d\theta_1$, $Y + X$ passes into $y_1 + y + x$, $Y' + X'$ into $y'_1 + y' + x'$, decremented at an angle $d\theta'_1$, while both are diffracted into $Z'$. Since generally

$$\sin \theta_1 - \sin i = \lambda/D \qquad \cos \theta_1 d\theta_1 = \cos \theta'_1 \, d\theta'_1$$

for homogeneous light and the same $di$. Hence $d\theta_1 = d\theta'_1 = d\theta$, say. If $\delta = \theta_2 - \theta_1$, and $\sigma = \theta_2 + \theta_1$, the auxiliary equations

$$X + Y = C \frac{\sin \theta_1 + \sin \theta_2}{\sin \delta} \qquad C = \frac{N - n}{\cos (\sigma/2)}$$

are useful. From a consideration of the $yC$ and $yx$ triangles, moreover, the relations follow:

$$y + y_1 = \frac{N}{\cos (\delta/2 - d\theta)} \qquad y_1 = \frac{N - n}{\cos (\sigma/2) \cos (\theta_1 + d\theta)} \qquad x = y \frac{\cos (\theta_1 + d\theta)}{\cos (\theta_2 - d\theta)}$$

and from the $y'_1 C$ and $y'x$ triangles, similarly,

$$y' + y'_1 = \frac{N}{\cos (\delta/2 + d\theta)} \qquad y'_1 = \frac{N - n}{\cos (\sigma/2) \cos (\theta_1 - d\theta)} \qquad x' = y' \frac{\cos (\theta_1 - d\theta)}{\cos (\theta_2 + d\theta)}$$

Hence, after some reduction, the path on one side is

$$x + y + y_1 = \frac{2N \cos (\sigma/2)}{\cos (\theta_2 - d\theta)} - \frac{N - n}{\cos (\sigma/2) \cos (\theta_2 - d\theta)}$$

which may be further simplified to

$$x+y+y_1 = \frac{N\cos\sigma + n}{\cos(\theta_2 - d\theta)\cos(\sigma/2)}$$

From this the path on the other side will be

$$x'+y'+y'_1 = \frac{N\cos\sigma + n}{\cos(\theta_2 + d\theta)\cos(\sigma/2)}$$

The path-difference, $\Delta P$, thus becomes, nearly,

$$\Delta P = N\frac{\cos\sigma + n}{\cos(\sigma/2)}\left(\frac{1}{\cos(\theta_2 + d\theta)} - \frac{1}{\cos(\theta_2 - d\theta)}\right) = \frac{N\cos\sigma + n}{\cos(\sigma/2)}\frac{2\sin\theta_2}{\cos^2\theta_2}d\theta$$

This is perhaps the simplest form attainable. If, apart from diffraction, this should result in interference, the angular breadth of an interference fringe would be ($\Delta P = \lambda$)

$$d\theta = \frac{\lambda\cos^2\theta_2}{2\sin\theta_2}\frac{\cos(\sigma/2)}{N\cos\sigma + n}$$

and if $D$ is the grating space and $\sin\theta = \lambda/D'$,

$$d\theta = \frac{(D'^2 - \lambda^2)\cos(\sigma/2)}{2D'(N\cos\sigma + n)}$$
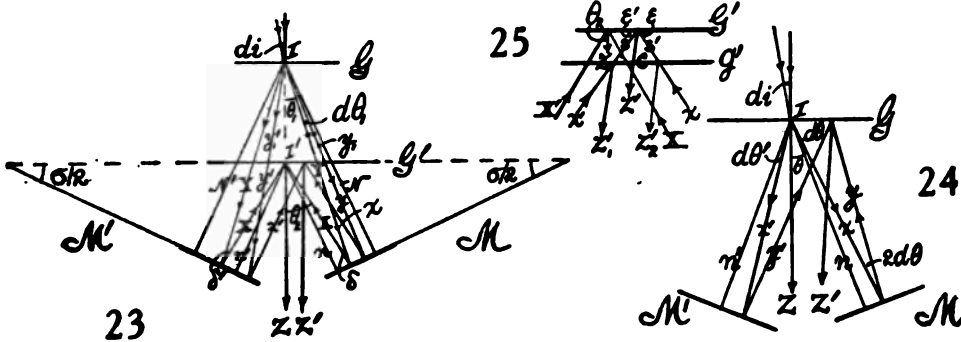


In case of a single grating

$$\sigma/2 = \theta_2 = \theta \qquad N = n \qquad \cos\sigma = 2\cos^2\theta - 1$$

or

$$\Delta P = \frac{2N\cos^2\theta}{\cos\theta}\frac{2\sin\theta}{\cos^2\theta}d\theta = 4N\tan\theta d\theta$$

a result which may be reduced more easily from figure 24. Hence, the angular distance apart of the fringes would be ($\Delta P = \lambda$)

$$d\theta = \frac{\lambda}{4N\tan\theta} = \frac{D\cos\theta}{4N} = \frac{\sqrt{D^2 - \lambda^2}}{4N}$$

if $D$ is the grating space. To find the part of the spectrum ($d\lambda$) occupied by a fringe in the case postulated, since $\sin\theta = \lambda/D$,

$$\frac{d\theta}{\cos\theta} = \frac{d\lambda}{D\cos^2\theta} = \frac{D}{4N}$$

and from the preceding equations, finally,

$$d\lambda = \frac{D^2 - \lambda^2}{4N}$$

where $d\lambda$ would be the wave-length breadth of the fringe, remembering that the fringes themselves are homogeneous light.

In the grating used

$$D = 351 \times 10^{-4} \text{ cm.} \qquad \lambda = 60 \times 10^{-4} \text{ cm.} \qquad n = 100 \text{ cm.}$$

or

$$d\lambda = \frac{1200}{400} 10^{-10} = 3 \times 10^{-10} \text{ cm.}$$

This is but 1/200 of the distance, $d\lambda = 6 \times 10^{-4}$ cm., between the $D$ lines. Hence such fringes would be *invisible*. Moreover, $d\theta \propto 1/N$; the fringes, therefore, should grow markedly in size as $N$ is made smaller. Experiments were carried out with this consideration in view, by the single-grating and concave-mirror method, $N$ being reduced from nearly 2 meters to 20 cm., without any observable change in the breadth or character of the phenomenon. It showed the same alternation of one black and one or two bright linear fringes, or the reverse, throughout. Hence, it seems improbable that the phenomenon, *i.e.*, the interference fringes, are referable to such a plan of interference as is given in figure 24.

Similarly, for the case of two gratings, figure 23,

$$d\theta = \frac{\cos(\sigma/2)\ (D'^2 - \lambda^2)}{2D'(N \cos \sigma + n)}$$

where, if we insert the data $\theta_1 = 9°40'$ and $\theta_2 = 19°55'$

$$D' = 173 \times 10^{-4} \text{ cm.} \qquad N = 162 \text{ cm.} \qquad n = 82 \text{ cm.} \qquad \lambda = 58.9 \times 10^{-4} \text{ cm.}$$

then

$$d\theta = \frac{.967 \times 10^{-10} \times 263}{10^{-4} \times 346 \times (162 \times .87 + 82)} = .33 \times 10^{-4} \text{ radians.}$$

Thus $d\theta$ is about of the same small order of values as above, *i.e.*, less than one-tenth second of arc or 1/1000 of the $D_1D_2$ space, and thus quite inappreciable. Some other source, or at least some compensation, must therefore be found for the interferometer interferences seen with homogeneous light.

The full discussion of the effective path-difference in terms of the diffractions occurring will be given in § 27, in order not to interrupt the progress of the experimental work here. It will then be obvious that the mere effect of changing the obliquity of the incident homogeneous rays, $I$, introduces no path-difference, or that the fringes observed are varied by the displacements and rotations of the grating, $G'$, and the mirrors $M$ and $N$.

**16. Experiments continued. Analogies.**—With this possible case disposed of, it now becomes necessary to inquire into the other causes of the phenomenon, as described in paragraph 13. This is conveniently done with reference to figure 26, where $n$ and $n'$ are the axes of the pencil of yellow light, reflected from the opaque mirrors $M$ and $N$, after arrival from the transmitting grating

*G.* It is necessary to consider the three positions of the reflecting grating $G'$; viz, $G'$, $G'_1$, and $G'_2$. In the symmetrical position $G'$, the pencils whose axes are $n$ and $n'$ meet at $a$ and are both diffracted along $r$. In the position $G'$, they are separately diffracted at $b$ and $b'$ in the direction $r_1$ and $r'_1$, and they would not interfere but for the objective of the telescope, or, in the other case, of the concave mirror of the grating. In the position $G'_2$, finally, the pencils $n$ and $n'$ are separately diffracted at $c$ and $c'$ into $r_2$ and $r'_2$ and again brought to interference by the lens or concave mirror, as specified.

Now it is true that the rays $na$ and $n'a$ (position $G'$), though parallel in a horizontal plane, are not quite collimated in a vertical plane. The pencils are symmetrically oblique to a central horizontal ray in the vertical plane, and their optical paths should therefore differ. But fringes, if producible in this way here, have nothing to do with the rotation of the grating in its own plane and may here be disregarded, to be considered later.



26        27
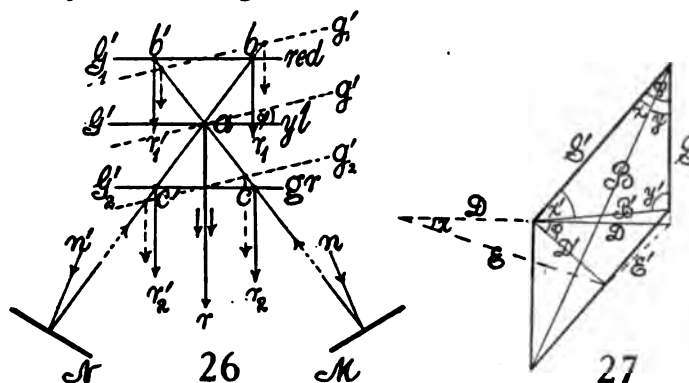
To take the rotation of the fringes first, it is interesting to note in passing that the interferences obtained by rotation around a normal axis recall the common phenomenon observed when two picket fences cross each other at a small angle $\varphi$. It may therefore be worth while to briefly examine the relations here involved (fig. 27) where $S'$ and $S$ are two corresponding pickets of the grating at an angle $\varphi$ and the normals $D'$ and $D$ are the respective grating spaces. The intersections of the groups of lines $S'$ and $S$ make the representative parallelogram of the figure ($S$ taken vertical), of which $B$ is the large and $B'$ the small diagonal. The angles indicated in the figure are $x+y=\varphi$ and $x'+y'+\varphi=180°$. As the bright band in these interferences is the locus of the corners in the successive parallelograms, $B$ is the distance between two bright bands, while $B'$, making an angle $y'$ with $S$, is the direction of these parallel interference bands relative to the vertical. Let the free ends of $D$ and $D'$ be joined by the line $E'$; and if $D$ is prolonged to the left and the intercept is $D$ in length, let this be joined with the end of $D'$ by $E$. Then the triangle $DED'$ and $S'BS$, $DE'D'$ and $S'B'S$, may be shown to be similar by aid of the following equations:

$$SD = S'D' \qquad D' \sin \varphi = E \sin x \qquad S' \sin \varphi = B \sin y \qquad \frac{D'}{S'} = \frac{E}{B} \frac{\sin x}{\sin y}$$

If $E$ is expressed in terms of $D$ and $D'$, and $B$ in terms of $S$ and $S'$, and the first equation is used, then

$$\frac{S}{S'} = \frac{\sin x}{\sin y} = \frac{D'}{D}$$

from which, in the fourth equation,

$$B = \frac{E}{\sin \varphi} = \frac{\sqrt{D^2 + D'^2 + 2DD' \cos \varphi}}{\sin \varphi}$$

Similarly,

$$B' = \frac{E'}{\sin \varphi} = \frac{\sqrt{D^2 + D'^2 - 2DD' \cos \varphi}}{\sin \varphi}$$

Again, the angle $y'$ is given from

$$\frac{\sin(180 - (\varphi + y'))}{\sin y'} = \frac{D'}{D}$$

or on reduction

$$\tan y' = \frac{D \sin \varphi}{D' - D \cos \varphi}$$

If $D = D'$, or $S = S'$, then

$$B_0 = \frac{D}{\sin(\varphi/2)} \qquad B'_0 = \frac{D}{\cos(\varphi/2)}$$

$$\tan y' = \frac{\sin \varphi}{\sin(\varphi/2)} = \cos(\varphi/2)/\sin(\varphi/2), \text{ or } \tan y' \tan \varphi/2 = 1$$

Thus if $\varphi = 0$, $\tan y' = \infty$, $y' = 90°$, or the fringes are horizontal and $B = 2S$. If $y'$ is nearly zero

$$\tan y' = \varphi/(\varphi^2/2) = 2/\varphi$$

changing very rapidly with $\varphi$.

If one grating of a pair, with identical grating spaces $D$, is moved parallel to itself, in front of the other, the effect to an eye at a finite distance is to make the grating spaces $D$ virtually unequal; or

$$B = B_0 \frac{\sqrt{1 + (D'/D)^2 + 2(D'/D) \cos \varphi}}{2 \cos(\varphi/2)}$$

so that for an acute angle $\varphi$, the fringe breadth is increased. Thus $B_0$ is a minimum in case of coincident gratings.

The analogy is thus curiously as follows: The fringes just treated rotate with the rotation of either grating in its own plane and pass through a minimum size with fore-and-aft motion; whereas in the above results the optical grating showed a passage through a maximum of size with the rotation of either grating in its own plane and a rotation of fringes with fore-and-aft motion of the grating.

Returning from this digression to figure 26, if the grating $G'$ is not quite symmetrical, but makes a small angle $\varphi$ with the symmetrical position as at $g'$, the fore-and-aft motion will change the condition of path-excess on the right (position $g'_2$, $M$ path larger) to the condition of path-excess on the left

(position $g'_1$, $N$ path larger); and if the motion is continuous in one direction, $g'_2$, $g'$, $g'_1$, the path-difference will pass through zero. No doubt the angle $\varphi$ is rarely quite zero, so that this variable should be entered as an essential part of the problem. The resulting conditions are complicated, as there are now two angles of incidence and diffraction and it will therefore be considered later (§ 28). It is obvious, however, that if for a stationary grating $G'$, figure 26, the angle $\varphi$ is changed from negative to positive values, through zero, the effect must be about the same as results from fore-and-aft motion. In both cases excess of optical path is converted into deficiency, and *vice versa*. Hence, as has been already stated, the effects both of the fore-and-aft motion and of the rotation of the grating $G'$ around a vertical axis parallel to its face conform to the interference fringes of figure 21, a to e.

It is common, moreover, if a concave grating is used (with parallel rays) at $G'$, to find the two sodium doublets due to reflection from $M$ and $N$ approaching and receding from each other in the field of view of the ocular when the grating $G'$ is subjected to fore-and-aft motion. This means that although the axes of incident rays are parallel in two positions, whenever $i$ varies (as it must for a concave grating and fore-and-aft motion), the diffracted rays from $M$ and $N$ do not converge in the same focus in which they originally converged, but converge in distinct foci. For if $\sin i - \sin \theta = \lambda/D$ or $\cos i\, di = \cos \theta\, d\theta$, suppose that for a given $i$, $\theta = 0$; then $\cos i\, di = d\theta$. But the deviation, $\delta$, of the diffracted ray from its original direction is now $di + d\theta$, or

$$\delta = di(1 + \cos i) = 2di \cos^2 i/2$$

Similarly, the principal focal distance $\rho'$, for varying $i$, is not quite constant. From Rowland's equation, if parallel rays impinge at an angle $i$ and are diffracted at an angle $\theta = 0$,

$$\rho' = \frac{R}{1 + \cos i} = \frac{R}{2 \cos^2 i/2}$$

If $i = 20°$, then $\cos^2 i/2 = .976$, and $\rho' = R/2$, nearly but not quite.

I have not examined into the case further, as both the sodium doublets are distinctly seen if the ocular follows them (fore and aft), and the lateral displacement of doublets is of minor interest.

With the plane reflecting grating this discrepancy can not enter, since for parallel rays the angles of incidence remain the same throughout the fore-and-aft motion, and therefore the angles of diffraction would also be identical.

Two outstanding difficulties of adjustment have still to be mentioned, though their effect will be discussed more fully in the next chapter. These refer to the rotation of the grating $G'$, around a vertical axis and around a horizontal axis, in its own plane or parallel to it. The rotation around the vertical axis was taken up in a restricted way above, in figure 13, Chapter II. The effect (rotation of $G'$) is to change the inclination of the fringes passing from inclination to the left through zero to inclination towards the right. The effect is thus similar to the fore-and-aft motion, as shown in figure 21.

It was here, with the ocular thrown much to the right (near $M$), that I again encountered the arrow-shaped fringes of figure 2, $D$, Chapter I. Though they are rarely quiet, the observation can not be an illusion. As seen with white light and a fine slit they are merely an indication of fringes which, when viewed with a broad slit and homogeneous light, will be horizontal.

Rotation around a horizontal axis parallel to the face of the grating must also destroy the parallelism of the rulings. The usual effect was to change the size of fringes (distance apart, etc.); but I was not able to get any consistent results on rotating $G'$, owing to subsidiary difficulties. On rotating the grating $G$, however, a case in which fine rotation around a horizontal axis was more fully guaranteed, the fringes passed with continuous rotation through a vertical maximum, as in figure 22.

In figure 26, the central region $a$ of the grating $G'$ is found, on inspection, to be yellow in the position $G'$, red in the position $G'_1$, and green in the position $G'_2$. The slit in this case must be very fine. For a wide slit and homogeneous light, the continuous change in the obliquity of pencils is equivalent to the continuous change of wave-length in the former case. It is therefore interesting to make an estimate of the results to be expected, if the vertical fringes for the cases $bb'$ or $cc'$ were Fresnellian interferences, superposed on whatever phase-difference arrives at these points. In the usual notation, if $c$ is the effective width at the concave grating, $F$ its principal focal distance, $x$ the deviation per fringe, $d\theta$ the corresponding angle of deviation, $\lambda$ the wave-length of light,

$$x = \lambda F/c \text{ or } d\theta = \lambda/c$$

If $c = 1.6$ cm., $\lambda = 6 \times 10^{-5}$ cm., then $d\theta = 3.7 \times 10^{-5}$, or about $7''$ of arc.

The corresponding deviation $d\theta D$ equivalent to $d\lambda D$ of the $D_1 D_2$ lines would be (if the grating space is $D = 173 \times 10^{-6}$ cm., $\theta = 20°$, nearly, the normal deviations for yellow light),

$$d\theta_D = \frac{d\lambda_D}{D \cos \theta} = \frac{6 \times 10^{-8}}{173 \times 10^{-6} \times \cos 20°} = 3.7 \times 10^{-4}$$

Thus $\dfrac{d\theta}{d\theta_D} = 0.1$, or, in this special case, there would be ten hair lines to the $D_1 D_2$ space. As $c$ is smaller or larger, there would be more or less lines. This is about the actual state of the case as observed. Finally, if $c$ is very small, the fringes are large, since

$$\frac{d\theta}{d\theta_D} = \frac{\lambda D \cos \theta}{c d\lambda_D}$$

Thus conditions for practical interferometry would actually appear, the fringes being of $D_1 D_2$ width for $c = 0.17$ cm., provided a wide slit and homogeneous light of at least $D_1$ or $D_2$ grade is used. Such an interferometer seems to differ from other forms, inasmuch as the fringes remain of the same size and distribution, from their entrance into the field to their exit; or for a motion of the opaque mirror $M$ of about 6 mm.

To resume the evidence thus far obtained, we may therefore assert that in the case of homogeneous light and a wide slit, or the absence of a slit, the field would either be bright or dark, as a whole. There is a single enormous horizontal fringe in the field. Hence the pronounced flickering with half wave-length displacements of any part of the apparatus. With the slit narrowed until the Fraunhofer lines are seen sharply, the linear phenomenon in question (Chapter I) appears. This may become ladder-like, but it always remains very narrow ($\frac{1}{2} D_1 D_2$) when the rulings of the two gratings are not quite parallel.

**17. Subsidiary diffractions.**—The behavior of the linear phenomena sometimes suggests probable relations to the Fresnellian interferences, produced, however, not within the telescope, as in §§ 27, 28, Chapter III (for the interferences are seen together with the Fraunhofer lines in the principal focal plane), but outside of it, at the grating, as suggested by figure 26. If the concave grating $G'$ is screened off, until a width of strip parallel to the rulings and not more than 5 mm. wide is used, the linear phenomenon is much enhanced, being both broader and stronger, without losing its general character. Here the $D$ lines are still visible. The ladder-like patterns show an equally pronounced coarsening. So far as these phenomena go, it is obvious that the resolving power of the grating must be in question, seeing that the total number of rulings has been greatly reduced. The use of screens with narrower slits carries the process farther; but after the opening is less than 2 mm. in width the available light is insufficient for further observation. If a small lens is used, the phenomena can still be seen over 2 meters beyond the principal focus of the grating.

A screen was now made as in figure 28 a, with two slits about 2 mm. wide and 2 mm. apart (b), and placed over the effective part of the grating. The result, after careful trial as to position, was noteworthy. Oblique fringes were widened to many times the $D_1 D_2$ space and coarsened, showing a definite grid-like design, as in figure 28 b, whereas, on removing the screen, the original pattern of a regular succession of brilliant dots (fig. 28 c) again appeared.

It was with the linear fringes, however, that the evidence obtained was most striking; for these now showed all the Fresnellian interferences (fig. 28 d). On removing the screen, the brilliant linear phenomenon (fig. 28 e), which in all the experiments made had thus far resisted manifolding, appeared at once. The pattern, d, moreover, when viewed with a small lens, within a meter in the direction of the rays, showed very definite enlargement with distance. Though a fine slit was needed, the resolving power of the grating was now too small to show any Fraunhofer lines. Similar results were obtained for a wire 1 or 2 mm. in diameter. With the screen, figure 28 a, and a bar, b, 1 mm. wide, the fine interference grid due to the bar, and the coarse grid due to the spaces (the fine lines being about twice as narrow as the coarse, but all of the same inclination) were often obtained together (fig. 28 f). A space 1 cm. wide intersected by a bar 2 mm. wide gave similar results, fine grids or

thick lines, according as one or both spaces were used. If *either* mirror, $M$ or $N$, is screened, the whole phenomenon vanishes.

It follows, then, if $rv$ and $v'r'$, figure 29, represent the two reversed, overlapping spectra at the grating, $b$ the focus and $aa'b$ the direction of the homogeneous diffracted rays condensed at $b$, that about 0.5 cm. of the spectrum, $d'a'$ and $ad$ on either side of $a$, is chiefly active in modifying the resulting diffraction pattern. Within this the homogeneous rays, $cc'$ and $dd'$, are capable of interference. Although the wave-fronts entering $b$ are slightly spherical, their radius is about $r = 1$ meter, and they may therefore be regarded plane. In such a case the angular width $dx$ of the illuminated strip at $b$, for a width of screen $dd' = 1$ cm., between two extinctions, may be written

$$d\theta = \frac{dx}{r} = \frac{\lambda}{dd'} = \frac{60 \times 10^{-6}}{1} = 6 \times 10^{-5}$$

whereas the angular breadth of the $D_1D_2$ doublets is about $37 \times 10^{-5}$; *i. e.*, the rays from $d$ and $d'$, if in phase, should cease to illuminate $b$ at a breadth of about one-sixth the distance between the sodium lines. The rays within
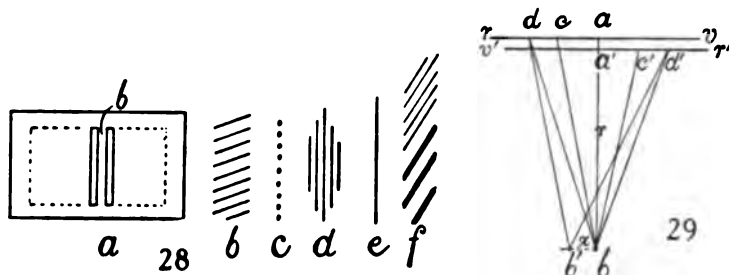


$dd'$ would correspond to greater widths; those from $cc'$, for instance, 0.5 millimeter apart, would illuminate twice the estimated width, so that a strip at $b$, with a breadth of one-third the interval $D_1D_2$, is a reasonable average. All rays, however, would produce illumination at $b$. As the screens are narrower, not only would the fringe be broader, but more lines would appear, because there is less overlapping. All this is in accord with observation. Excepting the occurrence of independent half wave-fronts, the phenomena do not differ from the ordinary diffraction.

With regard to waves of slightly different lengths, focussed at $b'$, each is there superposed on a wave of different length from its own, and appreciable interference ceases for this reason. If the slit is widened, the phenomenon (with white light) also vanishes by overlapping. The case of the screen with two spaces has already been treated in relation to figure 26. In general, these are cases of the diffraction of a rod, or of a slit, which are possible only if the colors, $\lambda$, are symmetrically distributed to the right and to the left of it. Thus they require *both* spectra and can not appear if single spectrum only is present. To reveal the nature of the phenomenon, a wide slit and homogeneous light must be resorted to, as has been done in the present paper, even if white light and the fine slit totally change the aspect of the fringes.

**18. Conclusion.**—To return, finally, to the original inference, it appears that beating wave-trains have not been observed, but that the striking scintillations are due to an exceptional susceptibility of the apparatus to laboratory tremors, when exhibiting the phenomenon in question. Of this I further assured myself by observations made at night and on Sunday, though there is some doubt in my mind. What has certainly been observed is the interference of a $D_1$ or $D_2$ line with a reversed $D'_1$ or $D'_2$ line, both having the same source and longitudinal axis. One can only assert, therefore, that light of the wave-length interval of the breadth of these lines is capable of interference, when the line is reversed.

The phenomena, as a whole, are to be treated as diffractions of symmetrical *half wave-fronts*, each of which may be separately controlled by the corresponding micrometer.

# CHAPTER III.

---

**19. Introduction. Method.**—The chief purpose of the present paper is the search for phenomena similar to those of Chapter II, but in which the two spectra brought to interference are not inverted relatively to each other. Incidentally the strong interferences may have a value on their own account. It has been shown that the totality of the phenomena with spectra reversed on a transverse or a longitudinal axis are quite complicated, and a series of companion researches in which similar results are aimed at, in the absence of inversion, is thus very desirable.

The apparatus (fig. 30) is a modification of that shown in figure 50, in the next section, $MM$ being the base of the Fraunhofer micrometer, $SS$ the slide, $E$ the micrometer screw. The brass capsules $A$ and $B$ are securely mounted on the slide $S$, free from the base $M$, and on the base $M$ free from the slide



30

31
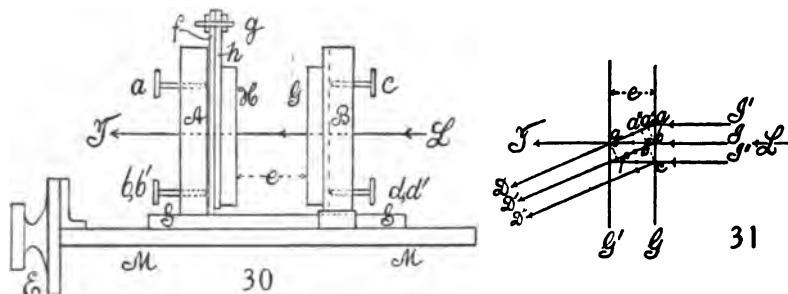
$S$, respectively. Each capsule is provided with three adjustment screws relative to horizontal and vertical axes $a$, $b$, $b'$, and $c,d,d'$, together with strong rearward-acting springs, by which the gratings $G$ and $H$ at a distance $e$ apart may each be rotated slightly around a vertical or a horizontal axis (plane dot slot mechanism). The two gratings $G$ and $H$ must be identical, or very nearly so, as to the number of lines per inch, and with their ruled faces toward each other. These faces, as well as the ruled lines, are to be nearly in parallel. To secure the latter adjustment a bolt, $g$, normal to the face of the grating $H$, serves as an axis, and an available tangent screw and spring (not shown) is at hand for fine adjustment. This device is of great importance in bringing the longitudinal axes of the two spectra due to $G$ and $H$ into coincidence, and a fine wire must be drawn across the slit of the collimator to serve as a guiding-line through the spectrum. Any lack of parallelism in slit and rulings rotates the fringes.

46

The beam of light, $L$, either white or homogeneous, as the experiment may require, is furnished by a collimator (not shown), which, with the telescope at $T$ (placed in plan, in figure 31, at $T$ or $D$), are the usual parts of a spectroscope. The collimator with slit is always necessary for adjustment. It may then be removed if the phenomenon is to be studied in the absence of the slit. The telescope is frequently replaced to advantage by a lens. White light is to be furnished by the arc lamp (without a condenser), by sunlight, or by an ordinary Welsbach burner. Both spectra are naturally very intense. A sodium flame suffices for the work with homogeneous rays.

The adjustments in case of white light are simple and the interferences usually very pronounced, large, and striking. Brilliant spectra, channeled with vertical narrow black lines, are easily obtained when the longitudinal axes are placed accurately in coincidence by rotating the plate $h$ carrying the grating $H$, on the plate $f$, around the axis $g$. If the gratings are quite identical the sodium lines will also be in coincidence. Otherwise the two doublets, $D_1D_2$ and $D'_1D'_2$, of the two spectra (nearly identical in all their parts and in the same direction) are placed in coincidence by rotating either grating around a vertical axis. Thereupon the strong fringes will usually appear for all distances, $e$, less than 2 cm. These fringes are nearly equidistant and vertical and intersect the whole spectrum transversely. They are not complicated with other fringes, as in the experiments of the next section. They increase in size till a single shadow fills the field of view, in proportion as the distance $e$ is made smaller and smaller to the limit of complete contact. With the two adjustments carefully made, finally, by aid of the fringes themselves, further trials for parallelism are not necessary. Two film gratings, or even films, give very good fringes. During manipulations great care must be taken to keep the angle of incidence, $i$, rigorously constant; *i.e.*, to avoid rotating both gratings together or the apparatus as a whole, as this displaces the sodium doublets relative to each other and seriously modifies the equations.

**20. White light. Colored fringes.**—The two sodium doublets seen in the arc spectrum are usually equally brilliant, and but one set of strong fringes is present in the field of the telescope. Relatively faint fringes may sometimes occur, due, no doubt, to reflection, as investigated in the next section.

If both gratings are rotated, changing the angle of incidence from $0°$ to $i°$, the fringes disappear from the principal focal plane, but reappear strongly in another focal plane (ocular forward or rearward). In such a case the $D$ lines are no longer superposed. To be specific, let $i$ and $i'$, $\theta$ and $\theta'$, be the angles of incidence and diffraction at the two gratings in question, the angle between their ruled faces being $i-i'$. Let $D$ and $D'$ be the two grating constants, and nearly equal. Then for a given color, $\lambda$, in relation to the individual normals of the two gratings,

$$\sin \theta - \sin i = \lambda/D \qquad \sin \theta' - \sin i' = \lambda/D'$$

Now if $\theta'$ is referred to the original normal it becomes $\theta'' = \theta' + i - i'$,

or $$\sin (\theta'' - i + i') - \sin i = \lambda/D'$$

If the sodium lines are to coincide, $\theta = \theta''$, or approximately

$$\sin (\theta - (i - i')) - \sin i' = \sin \theta - \cos \theta \cdot (i - i') - \sin i' = \lambda/D'$$

or on eliminating $\sin \theta$

$$\sin i - \sin i' - (i - i') \cos \theta = \frac{\lambda}{D} - \frac{\lambda}{D'}$$

which is nearly

(1) $$\frac{i - i'}{D - D'} = \frac{\lambda}{D^2(1 - \cos \theta)}$$

In case of the Wallace grating below

$$D = 1.75 \times 10^{-4} \qquad \lambda = 58.93 \times 10^{-6} \qquad i - i' = 10^4 \times 3.29 \, (D - D')$$

Thus if the inclosed angle $i - i'$ between the plates is 1 degree, or 0.0175 radian, $D - D' = 5.3 \times 10^{-7}$, about 0.3 per cent of $D$ and equivalent to about 43 lines to the inch. With adequate facilities for measuring $i$, this method may be useful for comparing gratings, not too different, in terms of a normal or standard, practically, since the finite equations may also be expanded. In a similar way the slight adjustments of the longitudinal axes of the two spectra may be made by rotating one grating around a horizontal axis; but this correction is less easily specified. Finally, one should bear in mind that with film gratings there is liable to be an angle $i$-$i'$ between the adjusted plates. Fortunately this has very little bearing on the method below.

The range of displacement of grating within which the fringes may be used with an ordinary small telescope extends from contact of the two gratings to a distance of $e = 2$ to 3 cm. beyond.

In figure 31, which is a plan of the essential planes of the apparatus, $G$, $G'$ being the ruled faces of the gratings in parallel, $I$, $I'$, $I''$, three impinging rays of white light diffracted into $D$, $D'$, the points $a, b, c, a', a'', b$ are in the same phase, so that the path-difference of the rays from $b$ at $g$ and $f$ is easily computed. If the single ray $I$ is diffracted into $D$ and $D'$ or $I$ and $I'$ into $D$, $I$ and $I''$ into $D'$, $I'$ and $I''$ into $D$ and $D'$, the equations for these fringes should be (if $\Delta P$ is the path-difference),

$$\Delta P = e(1 - \cos \theta) = e(1 - \sqrt{1 - \lambda^2/D^2})$$

where $D$ is the grating space, $e$ the distance apart, and $\lambda$ the wave-length. Thus the micrometer value of a fringe for a color $\lambda$ should be, under normal incidence,

(2) $$\delta e = \frac{\lambda}{1 - \cos \theta} = \frac{\lambda}{1 - \sqrt{1 - \lambda^2/D^2}}$$

For two colors $\lambda$ and $\lambda'$

$$n\lambda = e(1 - \cos \theta) = eM \qquad (n + n')\lambda' = e(1 - \cos \theta') = eM'$$

if $n'$ is the number of fringes between $\lambda$ and $\lambda'$. Thus

(3)
$$n' = e\frac{M'\lambda - M\lambda'}{\lambda\lambda'}$$

or the number of fringes increases as $e$ is greater.

Equation (2) does not, as a rule, reproduce the phenomenon very well. Since the grating space $D$ of the two gratings is rarely quite the same, the air-plate inclosed, in case of apparent coincidence of the sodium lines, is slightly wedge-shaped, as in figure 32. Hence the two diffractions take place at incidences $0°$ and $\alpha°$, respectively, and the corresponding angles of diffraction will be $\theta$ and $\theta'$. If we consider the two corresponding rays $I$ and $I''$, diffracted at the first and second face, respectively, and coinciding at $c$ in the latter, the points $a$, $b$, and $a'$ ($ba'$ normal to $ac$), are in the same phase, and we may compute the phase-difference at the coincident points at $c$. Since the distance $bc$ is

$$e' = e\frac{\cos\alpha\cos\theta}{\cos{\frown}(\theta - \alpha)}$$



32    33    34
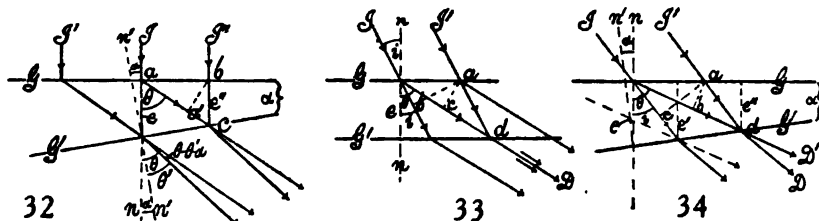
the path-difference is

$$n\lambda = \frac{e\cos\alpha\cos\theta}{\cos(\theta - \alpha)}(1 - \cos\theta)$$

whence

(4)
$$\delta e = \frac{\lambda\cos(\theta - \alpha)}{\cos\theta\cos\alpha\cdot(1 - \cos\theta)}$$

which changes into equation (2) when $\alpha = 0$ and $n = 1$. Fortunately this correction is, as a rule, small. In case of the Wallace gratings ($D = 1.75 \times 10^{-4}$ cm.), for instance, if $\lambda = 58.93 \times 10^{-6}$, then $\theta = 19°\ 40'$ or $\delta e = 1.01 \times 10^{-3}$; whereas if $\alpha = 5°$, then $\delta e = 1.04 \times 10^{-3}$; if $\alpha = 10°$, then $\delta e = 1.07 \times 10^{-3}$, etc.

If the incidence is at an angle $i$ and the plates are parallel, figure 33, the inquiry leads in the same way to an equation of more serious import. If the gratings $G$ and $G'$ are at a distance $e$ apart and the incident rays are $I$ and $I'$, the points $a$, $b$, $c$ are in the same phase. Hence the two rays leaving $d$ and diffracted along $D$ correspond to a path-difference

(5)
$$\frac{e}{\cos i}(1 - \cos(\theta - i))$$

whence

$$\delta e = \frac{\lambda\cos i}{1 - \cos(\theta - i)}$$

Table 1 and fig. 35 show the variation of fringes with the angle of incidence $i$, equation (5). Hence if the angle of incidence is changed from $-5°$ to $+5°$, $\delta e$ increases to nearly 3 times its first value. This, therefore, accounts for the large discrepancies of $\delta e$ found in the successive data below. To secure increased sensitiveness and to make the apparatus less sensitive to slight changes of $i$, this angle should be about $25°$, in which case $\delta e$ is about three wave-lengths per fringe. But normal incidence is frequently more convenient.

Finally, in figure 34, if the angle of incidence is $i$ and the two faces $G$ and $G'$ make an angle $\alpha$ with each other and are initially at a distance $e$ apart, changing successively to $e'$ and $e''$, the points $a$, $b$, $c$, being in the same phase, the two rays $D$ and $D'$ leaving at $d$, at an angle $\theta-i$, will have a path-difference at $d$ equal to

$$e\frac{\cos\theta\cos\alpha}{\cos i\cos(\theta-\alpha)}(1-\cos(\theta-i))$$

whence

(6) $$\delta e = \frac{\lambda\cos i\cos(\theta-\alpha)}{\cos\alpha\cos\theta(1-\cos(\theta-i))}$$



35

TABLE I.—Wallace gratings. $D=10^{-4}\times1.75$. $\lambda=10^{-5}\times58.93$.

| $i$ | $10^3\times\delta e$ | $i$ | $10^3\times\delta e$ |
|---|---|---|---|
| $+19°40'$ | $\infty$ | $-5°$ | 0.643 |
| $+15°$ | 16.740 | $-10°$ | 0.443 |
| $+10°$ | 4.090 | $-15°$ | 0.321 |
| $+5°$ | 1.840 | $-20°$ | 0.240 |
| $\pm0°$ | 1.012 | $-25°$ | 0.185 |

This equation reproduces the preceding equation (5) if $\alpha=0$ and the original equation (2) if $\alpha=i=0$. It shows that a discrepancy or angle between the plates is of minor importance. Hence the change of this angle may be used to bring the sodium lines in coincidence when the gratings differ slightly in their grating constants $D$. On the other hand, changes of incidence $i$ are of extreme importance.

Experiments made with the film grating showed that equation (2) not only fits very badly, but that $\delta e$ per fringe is a fluctuating quantity. Table 2 gives some results obtained by measuring the successive values obtained for $\delta e\times10^3$, corresponding to 10 fringes. Fringes were distinctly seen within 3 cm. of displacement by an ordinary telescope.

TABLE 2.

Gratings 15,050 lines to inch; computed values $10^3\delta e=0.94$ cm. per fringe.

First sample:    Second sample:
$10^3\delta e=1.22$ cm.   $10^3\delta e=0.98$ cm. } (normal incidence)
1.07           1.21
1.16

1.06 } (oblique incidence)
1.11
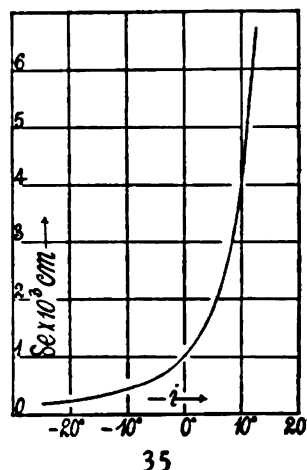
TABLE 2.—*Continued*

Wallace gratings 14,050 lines to inch; computed value $10^3 \delta e = 1.01$ cm. per fringe.

$10^3 \delta e = 1.22$ cm. (large fringes); $10^3 \delta e = 1.35$ (different $i$)

| | |
|---|---|
| 1.24 | 1.32 |
| 1.25 | 1.30 |
| 1.23 | 1.35 |
| 1.23   (small fringes) | 1.33 |
| 1.23 | 1.33 |
| | 1.32 |
| | 1.34 |

The reason for lack of accord is given in equations (5) and (6) and table 1. Any wedge effect of the glass plate is probably negligible. To show that the irregularity of the above results is to be sought in the accidental variations of the angle of incidence $i$ at both gratings, the rough experiments in table 3 suffice.

TABLE 3.

| | |
|---|---|
| $i$, negative (less than 10°),<br>Ocular drawn in,<br>focus changing. } | $\delta e \times 10^3 = 0.77$ cm.<br>.78<br>.74 |
| $i = 0$; ocular set for<br>principal focal plane.  Na lines<br>in field and coincident, } | $\delta e \times 10^3 = 1.18$ cm.<br><br>1.12 |
| $i$, positive (less than 10°),<br>ocular drawn out, } | $\delta e \times 10^3 = 1.69$ cm.<br>1.66 |

Thus, as equation (6) implies, small variations of $i$ produce relatively large variations of $\delta e$, and if $i$ passes continuously through zero, from negative to positive incidence, $\delta e$ increases continually and may easily be more than doubled. If the phenomenon is in focal planes in front of the principal plane (ocular in), $\delta e$ is small, and *vice versa*. Moreover, this enormous discrepancy is quite as marked for thin glass (2 mm.) as for thick glass plates (8 mm). Again, the rather stiff screw of the micrometer, which twisted the whole apparatus slightly, was sufficient to introduce irregularity. Placing the telescope close to the grating or far off made no difference. Hence the position of the optical center of the objective does not affect the result.

An additional result was obtained by placing a plate of glass between the two gratings $G$ and $G'$. The effect was an unexpected *enlargement* of fringes, increasing with the thickness of the glass plate (0.6 cm. or more). The reason for this is given by equation (3), in paragraph 2, for the number of fringes $n'$ between two colors $\lambda$ and $\lambda'$,

$$n' = \frac{e(M'\lambda - M\lambda')}{\lambda\lambda'}$$

where $M = 1 - \cos\theta$, $M' = 1 - \cos\theta'$. Since $n'$ is a number, the glass plate can be effective only in changing $\theta$ and $\theta'$. As both are diminished by refraction, the cosines are increased and $1 - \cos\theta$, $1 - \cos\theta'$ are both decreased. Hence $n'$ is decreased or the number of fringes is decreased, and their distance apart is thus larger.

It is obvious that when the sodium lines are not superposed the fringes can not lie at infinity, but are found in a special focal plane, depending on

the character of coincidence; *i.e.*, whether the rays are convergent or divergent. Finally, a slight rotation of the slit around the axis of the collimator rotates the fringes in the opposite direction to the sodium lines, and it is rather surprising that so much rotation of slit (10° or 20°) is permissible without fatally blurring the image. The slightest rotation of one grating relatively to the other destroys the fringes.

Naturally, the colored fringes vanish when the slit is widened or when it is removed. To give them sharpness, moreover, the beam passing through the grating must be narrow laterally. It is possible to see these colored fringes with the naked eye; but the transverse and longitudinal axes must in this case be slightly thrown out of adjustment, so that the fringes are no longer visible in the telescope. To the eye they form a somewhat fan-shaped set of colored fringes; *i.e.*, narrower below than above. Neither are the lines quite straight. If the collimating lens is removed, a slit about 0.1 cm. wide across a white flame will also show (to the telescope or to the eye) fine, strong lines rotating in opposite direction to the slit, according as the transverse and longitudinal axes are differently placed. As has been already stated, it is with the latter condition that the focal plane in which the fringes lie varies enormously.

Finally, when the sodium lines are superposed but the longitudinal axis of the spectra not quite so, a second class of fringes appear, which, however, are always more or less blurred. They rotate with great rapidity over 180° when one grating rotates over a small angle relatively to the other and the angle between the longitudinal axes of spectra passes through zero. In the latter position the regular fringes appear in full strength in the principal focus. To see the secondary interferences, the ocular must be drawn inward (toward the grating), and these fringes increase in size with the displacement of the ocular away from its position when regarding the principal focal plane. This secondary set of fringes is always accompanied by another very faint set, nearly normal to them and apparently quivering. The quiver may be due to parallax and the motion of the eye. These are probably the vestiges of the regular set of fringes, out of adjustment.

**21. Homogeneous light. Wide slit. Transverse axes coincident.**—If there is no color-difference, fringes of the same kind will nevertheless be seen in the telescope, on widening the slit indefinitely. Path-difference is here due to differences of obliquity in the interfering rays. As in the preceding case, accurate adjustments of the longitudinal and transverse axes (in case of sodium, $D_1$ and $D'_1$ or $D_2$ and $D'_2$ coincide horizontally and vertically) of the homogeneous color-field are essential if strong fringes are to appear in the principal focus. These fringes are, as a rule, well marked, and widening the slit merely increases the width of the channeled, homogeneous field of view. If, owing to slight differences of grating space, the sodium lines are not quite superposed automatically, this may be corrected by rotating either grating, or else the apparatus as a whole, until the fringes are strongest. The

fringes may be made to vanish under inverse conditions. Table 4 shows their close relation to the preceding colored set, so far as motion of the micrometer is concerned.

TABLE 4.

Ives grating. 15,050 lines to inch, computed $\delta e = 10^{-3} \times 0.94$ cm. per fringe.

$10^{3}\delta e = 0.72$ cm. (large fringes)   $10^{3}\delta e = 0.83$ cm. (small fringes)
.80                                            .80
.77

Wallace grating. Wide slit. Coincident Na lines. Fringes in principal focus, very clear and strong.

$10^{3}\delta e = 1.16$ cm.        $10^{3}\delta e = 1.06$ cm.

small   $\begin{cases} 1.16 \\ 1.16 \\ 1.17 \end{cases}$    1.08
fringes                                                      1.16

Wallace grating. Wide slit. Non-coincident Na lines.

$10^{3}\delta e = 1.34$ cm.        $10^{3}\delta e = 1.38$ cm.
(small fringes) 1.28               (large fringes)1.35

The fringes decrease in size as $e$ increases and exhibit the same irregularity of $\delta e$ values, due, no doubt, to the same causes (equation 6). Moreover, $\delta e$ is here below the normally computed value, supposing the angle $i$ to be negligible. In fact, figure 36 shows the optical center of the collimator $C$; so that
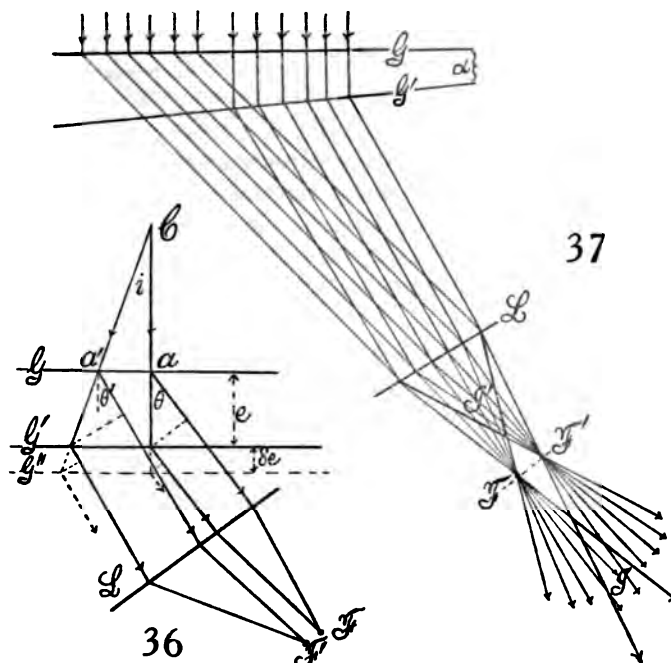


$Ca$ and $Ca'$ are the axes of parallel pencils, diffracted by the gratings $G$ and $G'$ at the angles $\theta$ for $Ca$ and $\theta'$ for $Ca'$. The rays are subsequently condensed at $F$, the focus of the telescope, $L$ being the principal plane of the objective. The general path-difference is thus, by equation (5), $e(1 - \cos (\theta' + i))/\cos i$, which distributes the fringes from right to left with variation of $i$.

If the grating $G'$ is displaced $\delta e$ parallel to itself, however, the path-difference will again be increased by $\lambda$ whenever

$$\delta e = \frac{\lambda \cos i}{1 - \cos (\theta' + i)}$$

Since $i$ is small, this equation will not differ appreciably from equation (2), with which it coincides for the central fringes.

If the sodium lines are not superposed, these fringes may still be seen, but they are not in the principal focal plane and the new focal plane changes continually, as the fringes grow in size. Examples are given in table 4. The large values of $\delta e$ show that $i$ was not actually negligible. Experiments similar to the above, bearing on the reason for the discrepancy (equation 6), were tried with the thin Wallace gratings, and the results are given in table 5.

TABLE 5.—Thin Wallace grating.

| $i$ negative (within 10°) | $\delta e \times 10^3 = 2.60$ cm. | $\delta e \times 10^3 = 2.40$ cm. | |
|---|---|---|---|
| Ocular in, | 2.34 | 2.45 | |
| | 2.57 | | |
| $i = \div 0$, normal incidence, | $\delta e \times 10^3 = 1.48$ cm. | $\delta e \times 10^3 = 1.37$ cm. | (small |
| Ocular set for principal | 1.50 | 1.37 | fringes) |
| focal plane, | 1.37 | 1.32 | (large |
| | | 1.19 | fringes) |
| $i$ positive (within 10°) | $\delta e \times 10^3 = 0.86$ cm | $\delta e \times 10^3 = 0.96$ | (small |
| Ocular out, | .88 | .86 cm. | fringes) |
| | | .85 | |
| | | .87 | (large |
| | | .96 | fringes) |

As before, the effect of $i$ passing from negative (through zero) to positive values is enormous, $\delta e$ increasing nearly threefold for a change of $i$ estimated as within 20.° Here, however, the drawn-out ocular (towards the observer) corresponds to the small values of $\delta e$, whereas above the reverse was the case. This depends upon which of the spaces $D$ or $D'$ is the greater.

**22. Homogeneous light. Fine slit. Transverse axes not coincident.**—To obtain this group of interferences, the two sodium lines from a very fine slit are thrown slightly out of coincidence; i.e., by not more than the $D_1 D_2$ distance. In the principal focal plane, therefore, these doublets are seen sharply, while if the ocular is drawn sufficiently forward or rearward, an interesting class of fringes soon appears which resemble Fresnel's fringes for two virtual slits. These fringes may be seen, however, on both sides of the focal plane and increase in size with the distance of the plane of observation (focus of ocular) in front or behind the principal focal plane. In figure 37 the two gratings, $G$ and $G'$, are struck by parallel pencils from the collimator at different angles of incidence (0° and $i$°). The two diffracted pencils of parallel rays are caught by the objective $L$ of the telescope and condensed at the principal foci, $F$ and $F'$, appearing as two bright yellow lines. In front and behind the plane $FF'$, therefore, are two regions of interference, $I$ and $I'$, throughout which the Fresnellian phenomenon may be seen in any plane parallel to $FF'$, observed by the ocular. When the electric arc is used with a very fine

slit, these sodium fringes often appear at the same time as the colored fringes, and, though they are usually of different sizes, their lateral displacement with a change of distance apart of the gratings, $\delta e$, is the same. The fringes in question appear alone when the sodium burner is used. They may then (at times) be observed with the naked eye, with or without a lens, and they fail to appear in the telescope unless the objective is strengthened by an additional lens. They are always vertical, but finer in proportion as the $D_1D_2$ and $D'_1D'_2$ doublets are moved farther apart. They become infinite in size, but still strong, when the doublets all but coincide, showing a tendency to become sinuous or possibly horizontal. Rotation of either grating $G$ around an axis normal to itself and relative to the other produces greatly enhanced rotation of the fringes, as in all the above cases, but they soon become blurred.

Only in the case when the horizontal axes of the field coincide (parallel rulings, etc.) do they appear strong. When the angle of incidence (or non-coincidence) is increased for both gratings, the size of the fringes increases; but when the $e$ distance is increased by the micrometer, the fringes are apparently constant as to size. However, after displacement of 4 mm. they are liable to become irregular and stringy, though still moving. A fine slit is not essential, particularly when $e$ is small. They vanish gradually when the slit is too wide. If a telescope with a strong objective is used, these fringes may be seen, retaining their constant size long after those of the next paragraph vanish. Examples of data are given in table 6, and $\delta e$ is too low in value as compared with the computed datum for $i = 0°$. With the Wallace gratings, these fringes were best produced by the aid of the sodium lines, in the ordinary electric arc, simultaneously with the colored fringes and for the case of a very fine slit.    They were apparent both with an ocular drawn out or drawn in.    In the former case several successive groups were observed.    Beginning with the sharp sodium lines in principal focus ($D_2$ and $D'_2$ coincident), a slight displacement of the ocular outward showed the first group, this resembling a grid of very fine striations. Further displacement outward produced a second set, equally clear but larger. A third displacement of the ocular outward showed the third set, and these now coincided with, and moved at, the same rate as the colored fringes in the same field. Other groups could not be found. No doubt, for these four successive steps the interference grids of $D_1$ and $D'_1$, $D_2$ and $D'_2$ are coincident and superposed, until they finally find their place in the colored phenomenon.

TABLE 6.—Ives grating. Homogeneous light. Fine slit. Sodium lines not coincident.

$$\delta e \times 10^3 = 0.87 \text{ cm.}$$
$$\begin{matrix} .77 \\ \underline{\phantom{.}} \\ .83 \end{matrix}$$

**23. Homogeneous light. Slit and collimator removed.**—Fringes similar to those seen with the wide slit above may be observed to better advantage by removing the slit altogether. The sodium flame is then visible as a whole; and if the adjustments are perfected it is intersected with strong, vertical black

lines, visible to the naked eye or through a lens or a suitably strengthened telescope. They decrease rapidly with increase in $e$, but vanish to the eye before the preceding set in paragraph 22. The sodium lines need not be in adjustment, but the longitudinal axes of the field must be, as usual. If diffuse white light is present, faint colored fringes may be seen at the same time. If the collimator only partly fills the field of view, these diffuse light fringes and the preceding set may occur together. Both rotate markedly for slight rotation of either grating in its own plane. There seems to be a double periodicity in the yellow field, but it is too vague to be discerned. When magnified with a lens, they admit of a play of $e$ within about 0.6 cm. from contact. When the sodium lines are not coincident, the focal plane continually changes with $e$. Otherwise it remains fixed.

Some data are given in table 7.

TABLE 7.—Ives grating. Homogeneous light. Collimator and slit removed. Focus continually changing.

| | |
|---|---|
| Large fringes; ocular out; lens on $\left\{\begin{array}{l}\\ \\ \\ \end{array}\right.$ | $\delta e \times 10^3 = 0.95$ cm. |
| | 1.01 |
| | 1.04 |
| Ocular in, lens on | 1.02 |
| Very small fringes, lens off $\left\{\begin{array}{l}\\ \\ \end{array}\right.$ | 0.96 |
| | 1.01 |
| Wallace grating. Sodium lines coincident. | |
| Principal focal plane | $\delta e \times 10^3 = 1.08$ cm. |
| | 1.18 |
| | 1.20 |

These data are similar to the above and subject to the same discrepancy whenever slight variation of the angle of incidence accidentally occurs. In figure 38 the case of three rays from a given flame-point $F$ is shown corresponding to the equation

$$\delta e = \frac{\lambda \cos i}{1 - \cos (\theta + i)}$$



38

when $i$ passes from positive to negative values. If either of the gratings is displaced and if they are parallel, the focal plane will not change; but if $G$ and $G'$ are not parallel, the focal plane differs from the principal plane and now moves with the grating.
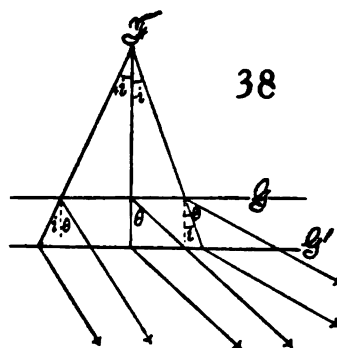
24. Inferences.—The above data show that the equation underlying all the interferences observed is the same. The interferences themselves may result from different causes, but their variation in consequence of the motion of the grating, $\delta e$, is due to one and the same cause. This is best seen by producing them simultaneously in pairs. As a means of finding an accurate comparison of the number of lines per centimeter on any grating, in comparison with those on the given grating, the method used in paragraph 20 deserves consideration.

If the fringes are to be used for practical purposes, great care must be taken to keep the angle of incidence of the impinging light constant. This was not done in the present paper, where the purpose is merely an identification of the phenomena. Moreover, a micrometer with the screw running easily is essential, as otherwise the frame is liable to show appreciable twist (change of incidence) during displacement of the fringes.

The fringes are not of the sensitive type, but they admit of a large range of displacement and are therefore adapted to special purposes.

With regard to their bearing on the behavior of reversed spectra, for the interpretation of which the present experiments were undertaken, it is obvious that the interferences with homogeneous light and a wide slit (paragraph 21), or in the absence of a slit (paragraph 23), are of analogous origin in both cases. It makes no difference, therefore, whether one of the spectra is reversed or not, except, perhaps, that in the former case (inversion), the coincidence of longitudinal and transverse axes is a more insistent condition. The colored fringes of paragraph 20 obviously can not be produced with reversed spectra. There remain the fringes with the fine slit and homogeneous light (paragraph 22); in other words, the occurrence of a sort of generalized Fresnellian interferences, within the telescope, modified by causes which lie outside of it. Thus $D_1$ and $D'_1$ or $D_2$ and $D'_2$ may be placed sufficiently close together to produce a region of interference before and behind the principal plane in which the sodium lines are in focus. If the $D_1D'_1$ lines are 0.01 cm. apart and the fringes seen likewise at 0.01 cm. apart, their position, measured from the principal plane, will be at

$$ R = \frac{XC}{\lambda} = \frac{10^{-4}}{6 \times 10^{-5}} = \frac{5}{3} \text{ cm.} $$

or less than 2 cm. The ocular would then have to be displaced forward or rearward by this amount. But there are two sodium doublets, each pair of which is to interfere. Suppose that $D_2$ and $D'_1$ are in coincidence so that the
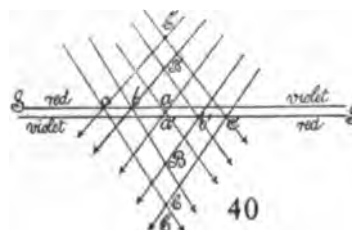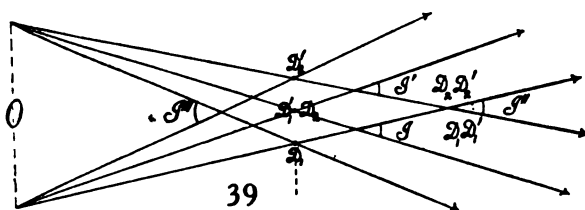


scheme is $D_1: D_2D'_1: D'_2$, as in figure 39, where $o$ is the principal plane of the objective and $D_1$ to $D'_2$ the principal focal plane. We should then have the separate regions of interference $I$ and $I'$ and the combined regions $I''$ and $J'''$. When the breadth of the latter is the whole number of fringes, the two patterns clearly merge into a single pattern. The experiments show several of these stages, terminating outermost in the focal plane of the colored fringes under the given conditions. Since the fringes lie on hyperbolic loci the problem

itself is beyond the present purposes; but it appears that the colored fringes will not appear until the corresponding $D_1$ and $D_2$ lines are shared by the whole of the two continuous spectra.

The final question at issue is the bearing of the present Fresnel phenomenon on the reversed spectra. If in figure 40, $s$ and $s'$ represent the traces of two reversed spectra in the principal focal plane, superposed throughout their extent (*i.e.*, in longitudinal coincidence), the rays $a_1a'_1B$, through the line of symmetry $a$, $a'$, are at once in a condition to interfere with a given difference of phase; but so are all the symmetrically placed pairs of colors, $c$, $c'$, $b$, $b'$, of the two spectra (the distances $cc'$, $bb'$, being arbitrary), provided the corresponding rays meet. As they do not meet in the principal focus, they can interfere only outside of this—$b$ and $b'$ at $B$, $c$ and $c'$ at $C$, etc. Similar conditions must hold at $B'$ and $C'$ within the principal focal plane. The linear interference is thus successively transferred to different pairs of wave-lengths. The phenomena of this paper can not, therefore, be detected in case of reversed spectra, because in the principal focal plane *different* wave-lengths are everywhere superposed, except at the narrow strip $aa'$, which experiment shows to be about one-third of the width of the sodium doublet, in apparent size. Beyond the principal focus the corresponding conditions in turn hold for the rays at $B$, $C$, etc., $B'$, $C'$, etc. Hence there can not be any Fresnellian interferences (paragraph 22), for there are not two virtual slits, but only a single one, as it were, and the interferences are laid off in *depth* along the normal $C'C$. The phenomenon may, in fact, be detected along this normal for 2 or 3 meters.

**25. Rotation of colored fringes. Non-reversed spectra.**—When the slit is oblique, it effectively reproduces the wide slit, locally, and therefore does not destroy the colored fringes. At every elevation in the field the slit is necessarily linear, though not vertical. In figure 41, let the heavy lines, $H$, denote the colored fringes for a fine vertical slit and white light, showing nearly the same distance apart, throughout. Let the light lines, $L$, denote the fringes for a wide vertical slit and homogeneous light, $\lambda$. These fringes are due to the successively increased or decreased obliquity of the rays in the horizontal plane. Now let $acb$ be the image of the oblique slit in homogeneous light. It is thus merely an oblique strip, cut from the area of light lines or striations, as it were, and consists of an alternation of black and bright dot-like vertical elements in correspondence with the original striated field. We may suppose $ab$ to have rotated around $c$, so that the vertical through $c$ is its position on the colored field (white light and fine vertical slit).

A color, $\lambda'$ (near the one $\lambda$), corresponding to the field of the lines $L$ in case of a wide slit and homogeneous light $\lambda'$, will supply nearly the same grid, so far as the distance apart of fringes is concerned. But the grid is displaced laterally, in consequence of the different angle of diffraction, $\theta$. This is shown by the dotted lines $D$ in figure 41, the effect being as if the slit had been displaced laterally. If the wide slit for homogeneous light $\lambda'$ is now narrowed and

inclined as before, an alternation of bright and dark elements will appear in the image of the slit *ed*, corresponding to $\lambda'$. If we suppose that for white light and the fine vertical slit the position of the fringe ($\lambda'$) was at $c'$, we may again regard $c'$ as an axis of rotation. To find the fringes such as *ff*, it is then only necessary to connect corresponding black elements on *ab* and *ed*. Their inclination is thus opposite to *ab* and *ed*, or they have rotated in a direction opposite to that of the slit. If, for instance, the slit image *ab* or *ed* is gradually moved back to the vertical, the points *g* and *h* will move with great rapidity and in both directions toward infinity and the fringes *ff* and *f'f'* become vertical lines through *c* and *c'*, respectively.

It is interesting to inquire into the frequency of fringes, *n*, when the angle of diffraction, $\theta$, is changed. From the original equation $e = n\lambda/(1-\cos\theta)$, since $d\lambda/d\theta = D\cos\theta$, the rate of change

$$\frac{dn}{d\theta} = \frac{e}{D}\,\frac{1}{1+\cos\theta} = \frac{e}{D+\sqrt{D^2-\lambda^2}}$$

where *e* is the distance apart of films and *D* the grating space. Since $\cos\theta$ varies but slowly with $\theta$ and is additionally augmented by 1, $dn/d\theta$ is nearly constant and about equal to $e/2D$.
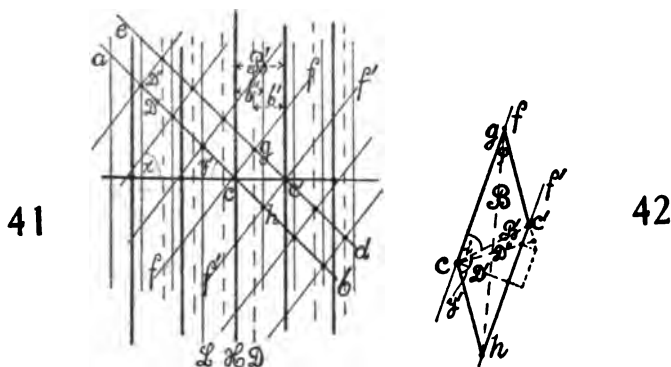


The fringes and slit images are thus given by the two sides of the parallelogram *cgc'h* for the two colors $\lambda$ and $\lambda'$. The diagonal *cc'* represents $d\theta$; the diagonal *gh* has no signification. On the other hand, the normal distances apart, $D'$ and $D''$, of *ff* and *f'f'* and *ab* and *ed* are both important.

If $D'$ and $D''$ are the normal distances apart of the fringes and the slit images, respectively, $B$ and $B'$, the two diagonals of the rectangle *cgc'h*, modified for convenience in figure 42,

$$D' = D''(\cos\varphi + \sqrt{B'^2/D''^2 - 1}\,\sin\varphi)$$

which may be obtained from the two small triangles below $c'$. If $B = D''$, $D' = D''\cos\varphi$; and if $\varphi = 0$, $D' = D'' = d\theta$, remembering that *c* and *c'* lie on two consecutive colored fringes obtained with white light and a fine slit. If the slit images and fringes are symmetrical, each is at an internal angle, $90-\varphi/2$, to the longitudinal axis of the spectrum.

But these equations, though useful elsewhere, have very little immediate value here, because the experimental variables, figure 41, are $B'$, the distance between two consecutive colored fringes and $b''$ and $b'$ the corresponding distance between the fringes in case of homogeneous light in each case $\lambda$, $\lambda'$; and the angle $y'$, which indicates the inclination of the slit. Thus $B'b'b''$ are given by computation and $y'$ is specified at pleasure. Obviously, if parallelograms are to be obtained, figure 41, $b' = b''$, appreciably. This is the case in experiment. Hence if we evaluate the height in the triangle $cgc'$ for each angle it follows easily that

$$\sin x' = \frac{\tan y'}{\sqrt{(B'/b' - 1) + \tan^2 y'}}$$

If $B' = b'$, $x' = 90°$ for all values of $y'$; i.e., the fringes remain vertical. If $B'$ is equal to $2b$, $x' = y'$, the fringes and slit are symmetrically equiangular with the longitudinal axis of the spectrum. This is nearly the case in figure 41 and frequently occurs in experiment. If $b'$ differs from $b''$, the fringes would not be straight. This also occurs, particularly when the thickness $e$ of the air-film is very small.

**26. Final treatment of reversed spectra. Hypothetical case.**—To obtain an insight into the cause of the interferometer fringes as obtained with reversed spectra and two gratings, it is convenient to represent both gratings, figure 43, $GG$ and $G''G'$, as transmitting, and suppose both diffracted beams, $ID'$ and $ID''$, subsequently combined in view of the principal plane $PP$ of an objective or a lens. It is clear that this simplified device can apply only for homogeneous light. In the case of white light, the opaque mirrors $M$ and $N$ (of the interferometer, above) return a divergent colored beam or spectrum, so that only for a single color can the second incidence be the same as the first. Again, if the constants of the two gratings are different, it is the function of these mirrors to change the incidence at the second grating correspondingly, so that for homogeneous light the rays issue in parallel. Finally, no reference to the lateral displacement $OG''$ and $OG'$ of rays need be made because, as more fully shown in the next paragraph, this is eliminated by the theory of diffraction.



The motion of the opaque mirrors $M$ and $N$ (above), on a micrometer, merely shortens the air-paths $GG'$ or $GG''$ in its own direction, and consequently the same fringe reappears for an effective displacement of half a wavelength, as in all interferometers.
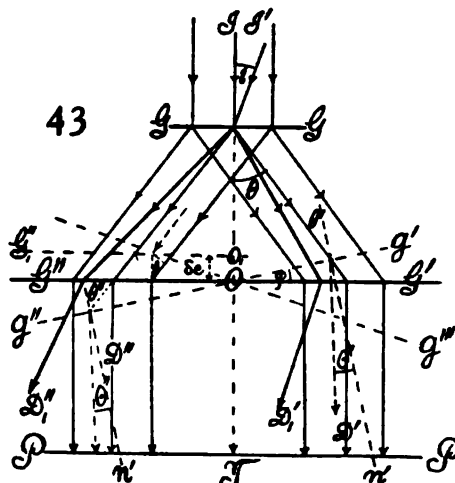
The case of a single grating, moreover, is given if the planes of the grating $GG$ and $G'G''$ and their lines are rigorously parallel, the planes $OG'$ and $G''O$ being coplanar. To represent the interferences of the two independent gratings and with homogeneous light for the case of oblique incidence, it is necessary to suppose the grating $G'G''$ cut in two halves at $O$, parallel to the rulings, and to displace the parts $OG'$ or $OG''$ separately, normally to themselves. Figure 43 shows that for normal incidence $i = 0$, the displacement per fringe, $\delta e$, would be

$$\delta e = \frac{\lambda}{1 - \cos \theta}$$

or the fringes are similar to the coarse set of the present chapter.

If the rays impinge at an angle $i$, figures 43 and 46, they will be parallel after the two diffractions are completed; for it is obvious that the corresponding angles of incidence and diffraction are merely exchanged at the two gratings. Hence the homogeneous rays $I'$, impinging at an angle $i$, leave the grating at $D'_1$ and $D''_1$ in parallel, at an angle of diffraction $i$, and the rays unite into a bright image of the slit. If, however, $OG'$ be displaced to $O_1G'_1$, parallel to itself, as in figure 44, the paths intercepted are

$$\frac{e}{\cos i}, \text{ and } \frac{e}{\cos i}.\cos (\theta - i)$$

and the path-difference per fringe, therefore,

$$\delta e = \frac{\lambda \cos i}{1 - \cos (\theta - i)}$$

which reduces to the preceding equation if $i = 0$. Hence a series of interference fringes of the color $\lambda$ must appear in the principal focus of the telescope or lens, on either side of $i = 0$. The theory of diffraction again annuls the apparent path-difference between $GG$ and $G'G''$.

**44**          **45**          **46**
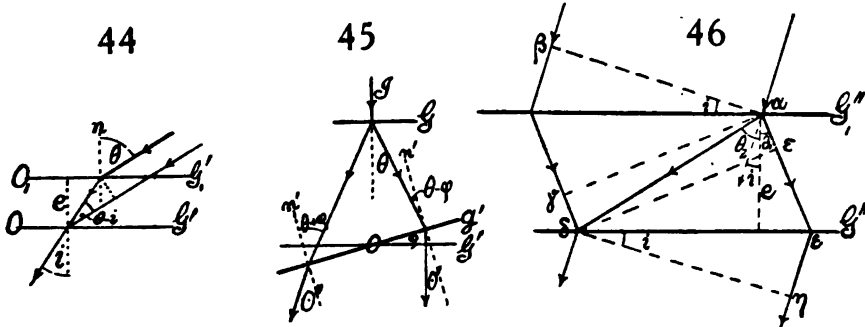


As to the number of fringes, $n$, between any two angles of incidence $i$ and $i'$, it appears that for homogeneous light of wave-length $\lambda$,

$$n = \frac{e}{\lambda}\left(\frac{1 - \cos (\theta - i)}{\cos i} - \frac{1 - \cos (\theta' - i')}{\cos i}\right)$$

where $e$ is the distance apart of the two parallel halves of the grating $G''O$, $OG'$. Hence $n$ vanishes with $e$, or the fringes become infinitely large. Lateral displacements are here without signification, as stated above.

If the grating $G'$ is rotated over an angle $\varphi$, figure 43, and $e = b\varphi$ where $2b$ is half the virtual distance apart at the grating $G'$ of the two corresponding rays impinging upon it (Chapter II, fig. 26), the rotation of the grating per fringe is thus

$$\delta\varphi = \frac{\lambda}{b}\frac{\cos i}{1 - \cos(\theta - i)}$$

or $n$ (above) passes through zero as $\varphi$ or $b$ decreases from positive to negative values. If $b$ is considered variable there is a wedge-effect superposed on the interferences.

It is this passage of $n$ through zero that is accompanied by the rotation of the fringes, as above observed.

In case of two independent gratings, $GG$ and $G'G''$ ($G'G''$ to be treated as consisting of identical halves, $OG'$ and $G''O$), nearly in parallel, fringes may be modified by rotating $G'G''$ around the three cardinal axes passing through the point of symmetry $O$. The rotation of $G'G''$ around an axis $O$ normal to the diagram is equivalent to the fore-and-aft motion of $G'G''$ when mirrors are used (fig. 26, Chap. II). The rotation around $OT$ in the diagram and normal to the face of the grating requires adjustment at the mirrors around a horizontal axis to bring the spectra again into coincidence. This is equivalent to rotation around $G''OG'$. Both produce enlargement, and rotation of fringes is already explained.

Let the grating $G'G''$ be rotated over an angle $\varphi$ into the position $g'g''$, figure 45. Then the angle of incidence at the second grating, $\theta$, on one side is increased to $\theta'' = \theta + \varphi$ and on the other decreased to $\theta' = \theta - \varphi$. In such a case the diffracted rays are no longer parallel. If $\theta'$ and $\theta''$ are two angles of diffraction on the right and on the left,

$$\sin\theta' + \sin(\theta - \varphi) = \sin(\theta + \varphi) - \sin\theta'' = \lambda/D$$

whence

$$\sin\theta'' + \sin\theta' = 2\sin\varphi\cos\theta$$

or if $\theta$ is the mean value of $\theta'$ and $\theta''$

$$\theta = \varphi\cos\theta, \text{ nearly.}$$

Similarly, since $\sin\theta = \lambda/D$, for $i = 0$,

$$\sin\theta' - \sin\theta'' = 2\lambda(1 - \cos\varphi)/D$$

Hence only so long as $\varphi$ is very small, are the rays appreciably parallel on rotating $G'G''$ around $O$ normal to the diagram; but this is usually the case, as $\varphi = 0$ is aimed at, and fringes are thus seen in the principal focus.

To the same degree of approximation is it clear that on rotating the grating into a position such as $og''$ the rays emerge parallel to $IT$, figure 43.

The next question at issue is the rotation of fringes with fore-and-aft motion, or rotation around an axis $O$ normal to the diagram, as shown in figure 26,

Chapter II. In other words, when $e$, the virtual distance apart, is zero, since $n \propto e/\lambda$, the fringes are infinitely large horizontally. The collimator, however, furnishes a pencil of rays which are parallel in a horizontal sectional plane only. They are not collimated or parallel in the vertical plane (parallel to the length of the slit). Hence when the fringes are reduced to a single one of infinite size horizontally, this is not the case vertically; *i.e.*, from top to bottom of the spectrum the path-difference still regularly varies. The adjustment around an axis through $O$, $G'OG''$, normal to the rulings, is still outstanding. It does not seem worth while to enter the subject further because much of the rotational phenomenon will depend upon whether the axes used are, in fact, truly vertical or parallel to the slit. In my apparatus this was not quite guaranteed, and the quantitative results obtained may therefore be due to mixed causes. Also, a rotation around an axis normal to $O$ always requires an adjustment for superposition of the longitudinal axes of the spectra, and this introduces path-difference.

Finally, the case of figure 21, Chapter II, or the rotation around an axis parallel to $IT$ in the present figure 43, is to be considered. This has already been given in terms of colored fringes (white light), but it occurs here for homogeneous light, in which case the above explanation is not applicable. Seen in the principal focal plane with telescope and wide slit, the *non-reversed* spectra would require careful adjustment of longitudinal and transverse axes; otherwise they vanish. Nothing will rotate them.

Figure 43 shows that if $G'G''$ is rotated about $IT$, the effect is merely to destroy the fringes, since the coincidence of the longitudinal axes of the spectra is here destroyed. No effect is produced so far as path-difference is concerned. To restore the fringes, therefore, either of the opaque mirrors $M$ or $N$ of the apparatus must be rotated on a horizontal axis until the two spectra are again longitudinally superposed. It is this motion that modifies the path-difference of rays in a vertical plane. In other words, when the fringes corresponding to any virtual distance apart, $e = b\ \varphi$, of the halves of the grating $G'G''$, have been installed, the rays *as a whole* may still be rotated at pleasure around a horizontal axis. In this way a change in the number of fringes intersected by a vertical line through the spectrum is produced. The number of intersections will clearly depend on the obliquity of the rays (axes of vertical pencils), and will be a minimum when the center of the field of view corresponds to an axis of rays normal to the grating $G'G''$. In other words, the vertical maximum in figure 22 occurs under conditions of complete symmetry of rays in the vertical plane. If, therefore, $e$ or the virtual distance apart of the half gratings, $G''O$ and $OG'$, is also zero, the field will show the same illumination throughout.

In conclusion, therefore, to completely represent the behavior of fringes, it will be sufficient and necessary to consider that either grating, $G'G''$ for instance, is capable of rotation, not only around a vertical axis through $O$, but also through a horizontal axis through $O$ parallel to the grating. The last case has been directly tested above, Chapter II, § 16. But a rotation

around these two axes is equivalent to a rotation around a single oblique axis, and the fringes will therefore in general be arranged obliquely and parallel to the oblique axis.

Thus if $\varphi_v$ and $\varphi_h$ are the angles of rotation of the grating (always small) around a vertical and a horizontal axis, respectively, and if $x'$ is the angle of the interference fringes with the horizontal edge or axis of the spectrum

$$\tan x' = \frac{\varphi_v}{\varphi_h}$$

so that if $\varphi_v = 0$, $x' = 0$; if $\varphi_h = 0$, $x' = 90°$. This recalls the result obtained above for the interferences of two coarse grids. In other words, for a rotation of grating around a vertical axis (parallel to slit) the fringes of maximum size will be horizontal (Chapter II, fig. 21), because the adjustment around the horizontal axis remains outstanding and the residual fringes (large or small) are therefore parallel to it. For a rotation of grating around a horizontal axis, the fringes of maximum size will be vertical (Chapter II, fig. 22), for the vertical adjustment is left incomplete. When both adjustments are made, a single fringe fills the whole infinite field, and this result follows automatically if but a single grating is used to produce the fringes, as in the original method (Chapter I).

To deduce equations it is convenient to regard both gratings as transmitting and to suppose one of them to be cut into independent but parallel halves, either by a plane through its middle point and parallel to the rulings (vertical axis of rotation), or by a plane through the same point and normal to the rulings (horizontal axis of rotation). The parallel halves of the grating are then displaced along the normal, $e$, to both.

### 27. Case of reflecting grating. Homogeneous light.—The results exhibited in figure 43 for transmitting gratings are shown in figures 47 and 48 for the combination of one transmitting grating $G$ and one reflecting grating $G'$ (the adjustment used in Chapter II), for which the direct path-lengths of rays were computed (cf. figs. 23 and 24, Chapter II). The path-differences obtained were inadmissible. It is now necessary to completely modify the demonstration.

In figure 47 the rays are shown for the case of complete symmetry of all parts, gratings at $G$ and $G'$ vertical and parallel, opaque mirrors at $M_1$ and $N_1$, telescope or lens at $T$. The incident ray $I$ at normal incidence is diffracted and reflected into $Y$, $X$, $T$, and $Y'$, $X'$, $T$, respectively; the incident ray $I'$ at an angle of incidence $di$ into $Y_1$, $X_1$, etc., and $Y'_1$, $X'_1$, etc., respectively; both at a mean angle of diffraction $d\theta$ (nearly) to the right, corresponding to $di$.

The angles of diffraction ($di = 0$) are $\theta_1$, and $\theta_2$; the double angles of reflection, therefore, $\delta = \theta_2 - \theta_1$, on both sides; the double angles of the grating $G'$ with the mirrors $M_1$ and $N_1$, symmetrically, $\sigma = \theta_1 + \theta_2$.

The normal from the point of incidence at $G$ and at $G'$, $N$, and $n$ makes angles $\delta/2$ with $Y$ and $X$, respectively, on both sides. The method of treat-

ment will consist in reflecting $G'$ in $M_1$ and $N_1$, producing the planes $G'_1$ and $G'_2$ (virtual images), and then rotating $M_1$ and $G'_1$ 180° around $IT$ (axis of symmetry) into coincidence with $N_1$ and $G'_2$ (interference). Then the rays prolonged into $\alpha$ and $\beta$ coincide with the rays prolonged into $\alpha'$ and $\delta'$ and the (virtual) diffracted rays $T_1$ and $T_2$ become $T'_1$ and $T'_2$. The ray on the left, prolonged into $\epsilon$, is diffracted into $T_2$. Then the interferences will all be given by discussing the left half of this diagram, which is amplified in figure 48.
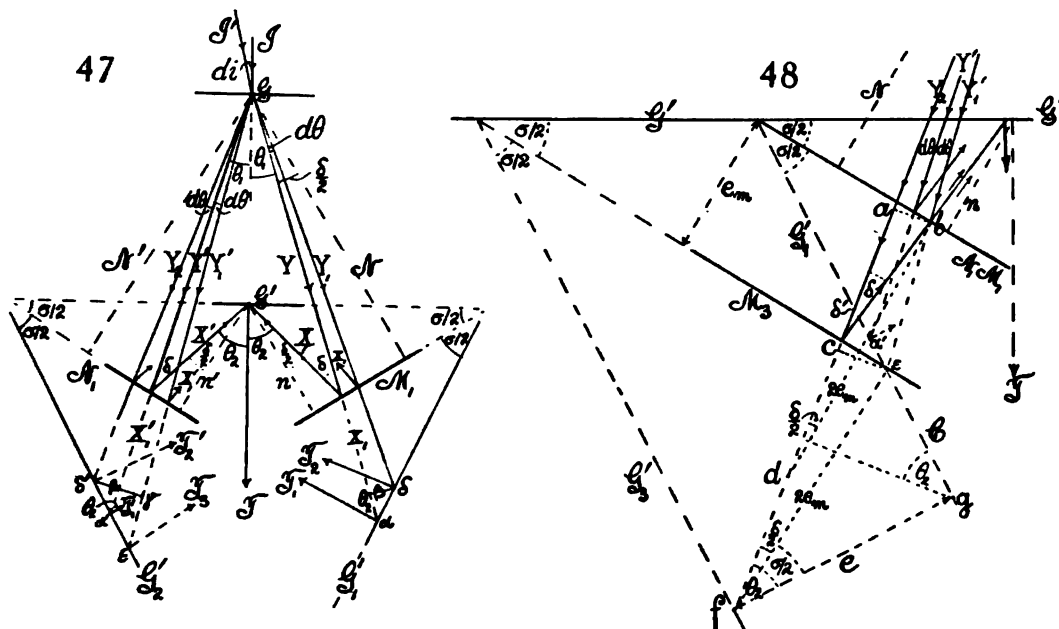


Since the distance $GG'$, figure 47, is very large, the rays are nearly parallel. Thus the arc $\delta'\gamma$, with its center at $G$, is practically a plane wave-front, perpendicular to the rays in $\delta'$, $\beta'$, $\gamma$, and the diffracted rays $T'$, $T'_2$, and $T'_3$ are also practically parallel. Hence in the case of symmetry and coincidence of $M_1$ and $N_1$ the points $\delta'$, $\beta'$, $\gamma$, $\delta'$, $\alpha'$, and $\epsilon$ are in the same phase (diffraction). In other words, there is no path-difference between $Y+X$ and $Y'+X'$, whether the angle of incidence is zero or not ($Y_1+X_1$ and $Y'_1+X'_1$). The whole field in the telescope must therefore show the same illumination (homogeneous light, wide slit) between the maximum brightness and complete darkness. Interference fringes can occur only when the opaque mirror, $M_1$, is displaced parallel to itself out of the symmetrical position. If $M_1$ and $N_1$ are symmetrical, as in figure 47, the displacement of $G'$, fore and aft, parallel to itself, is without influence.

This reduces the whole discussion to the normal displacements of the system $G'$, $M_1$, $N_1$, given in figure 48. Let the mirror $M_1$ be displaced over a normal distance $\epsilon_m$ to the position $M_2$, $N_1$ remaining in place. Then the image of $G'$ will be at $G'_2$, at a perpendicular distance, $\epsilon$, from its original posi-

tion $G'_1$. The path-difference so introduced, since $a$ and $b$ ($ab$ normal to the ray $Y_2$ impinging on $M_2$ at $c$ and reflected to $b$) are in the same phase, is

$$2\epsilon_m \cos \delta/2$$

and the displacement per fringe[1] will be

$$\delta\epsilon_m = \frac{\lambda}{2 \cos \delta/2}$$

which is nearly equal to $\lambda/2$, as in most interferometers, remembering that $\epsilon_m$ and $\delta\epsilon_m$ refer to the displacement of the mirror $M_1$. Two interfering rays will be coincident at $b$.

In the next place $\epsilon$ and $\delta\epsilon$ may be reduced from the corresponding displacements $\epsilon_m$ and $\delta\epsilon_m$ of the mirror $M_1$. In figure 48 the figure $fdb\epsilon$ is approximately a parallelogram with the acute angles $\delta/2$. Hence, since $\theta_2 = (\delta + \sigma)/2$

$$2\epsilon_m \cos \sigma/2 = \epsilon$$

as is also otherwise evident. Thus per fringe, if the length $\epsilon g = c$

$$\lambda = \delta\epsilon \cos \theta_2 + \delta c \sin \theta_2$$

since $\delta c = 2\delta\epsilon_m \sin \sigma/2$.

If $G'$ is displaced parallel to itself, $\delta\epsilon$ will not be modified, since each virtual image $G'_1$ and $G'_2$ moves in parallel, in the same direction, by the same amount. If then the grating $G'$ is rotated around an axis at $G'$, perpendicular to the diagram, figure 47, over a small angle, $\varphi$, the result (apart from the superposed rotational effect) is equivalent to a displacement of the mirrors $M_1$ and $N_1$ in opposite directions, producing a virtual distance apart $\epsilon$ and the corresponding interference fringes. In other words, the rotational effects may be explained here in the same way as in the preceding paragraph.

The angle $2d\theta$, within which the interference rays lie, per fringe, is subtended by $\delta\epsilon_m$, and this may be put roughly ($N = 162$ cm., normal distance)

$$2d\theta = (2\delta\epsilon_m \sin \delta/2)/N = (\lambda \tan \delta/2)/N$$

This angle is very small, scarcely $10^{-8} \times 3.2$ radians, or less than 0.01 second of arc. Hence all pencils consist of practically parallel rays.

An important result is the angular size of the fringes; i.e., if $\epsilon_m$ and $\lambda$ are given

$$-\frac{d\theta_2}{dn} = \frac{\lambda}{\epsilon_m \sin \delta/2} = \frac{D_2 \sin \theta_2}{\epsilon_m \sin \delta/2}$$

$D_2$ being the grating space.

Thus they become infinitely large when $\epsilon_m$ passes through zero. The angular size is independent of the distance between the gratings. It ought, therefore, to be easy to obtain large interference fringes, which is not the case. The reason probably lies in this: that the two opaque mirrors are not quite

[1] The differential symbol $\delta$ is unfortunately also used to designate the double angle of reflection $\delta$. But it is improbable that this will lead to confusion.

symmetrical, so that in figure 47, on rotation of $M_1$ 18⌣° on $GG'$, the trace of $M_1$ crosses $N_1$ at an angle. If $d\theta/dn = 3.7 \times 10^{-4}$, the distance apart of the sodium lines, and $D_2 = 173 \times 10^{-4}$ cm.,

$$e = 1.8 \text{ cm., about}$$

*i.e.*, path-lengths on the two sides should differ by about 2 centimeters, if the mirrors were quite symmetrical.

**28. Non-symmetrical positions. Fore-and-aft motion.**—It remains to account for the marked effect produced on displacing the grating $G'$ in a direction nearly normal to itself. If the displacement is symmetrical, or even if the grating and mirrors are reciprocally non-symmetrical (*i.e.*, the former at an angle $\varphi$ to the transverse line of symmetry $gg'$, the latter inclosing an angle $\alpha$, fig. 49), no effect results from the displacement of $G'$, if the mirrors $M_1$ and $N_1$ are so placed that the virtual images $G_m$ and $G_n$ are parallel and the diffracted rays, therefore, also parallel. In such a case $G_m$ and $G_n$ are dis-



49

placed by the same amount, normally, their distance apart is constant, and the intercepts of rays equal.
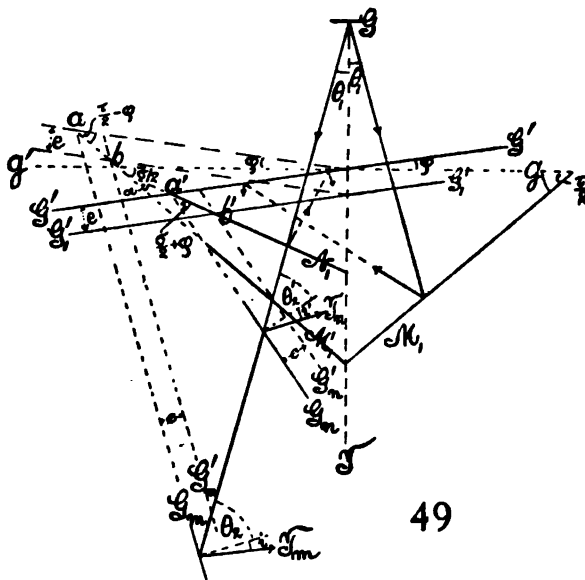
If, however, this compensation does not occur; if the grating $G'$, the mirrors $N_1$ and $M_1$ make angles $\varphi, \sigma/2, \tau/2$, respectively $(2\alpha = \tau - \sigma)$, with the transverse line of symmetry $gg'$, the fore-and-aft motion of $G'$ is more effective as the angle $\alpha - \varphi$ is greater. The diffracted rays are then no longer parallel, but make angles of incidence at the second grating, $\theta'_2$ for the $N_1$ side and $\theta_2$ for the $M_1$ side, and of diffraction $i'$ and $i$, respectively, as shown in figure 49, at $T_n$ and $T_m$. The following relations between the angles are apparent:

$$\sigma = \theta'_1 + \theta'_2 - \varphi \qquad \tau = \theta_1 + \theta_2 + \varphi$$

If at the first grating $\theta_1 = \theta'_1$ and $\alpha$ is the angle between the mirrors,

$$2\alpha = \tau - \sigma = \theta_2 - \theta'_2 + 2\varphi$$

The images are at an angle $\beta$, where

$$\beta = 2(\alpha - \varphi) = \theta_2 - \theta'_2$$

If $G'G'$ is displaced to $G'_1G'_1$ over a normal distance $e$, or $e/\cos \varphi$ along the line of symmetry $GT$, the virtual images $G_m$ and $G_n$ will be displaced to $G'_m$ and $G'_n$ over the same normal distance $e$. This is obvious, since the quadrilaterals $ab$ and $a'b'$ are rhombuses by the law of reflection, and hence the perpendicular distances $e$ between the (equal) sides all identical.

If $D_2$ is the grating space of $G'$,

(1)        $\sin \theta_2 + \sin i = \lambda/D_2$        $\sin \theta'_2 + \sin i' = \lambda/D_2$

or if $i$ and $i'$ are very nearly equal and both small, as in the experiment,

(2)        $$\cos \theta_2 d\theta = -\cos i\, di$$

Again, in case of the displacement $e$ of $G'$, the paths are shortened at $G_m$ by $e/\cos \theta_2$, at $G_n$ by $e/\cos \theta'_2$, resulting in the path-difference $\Delta P$, or

(3)        $$\Delta P = e(\sec \theta_2 - \sec \theta'_2)$$

Since $\theta_2$ and $\theta'_2$ are nearly the same, this may be adequately simplified by differentiation. Putting

(4)        $d\theta = \theta_2 - \theta'_2 = 2(\alpha - \varphi)$        $\Delta P = 2(\alpha - \varphi)e \tan \theta_2 \sec \theta_2$

Hence per fringe, apart from sign,

(5)        $$\delta e = \frac{\lambda \cos^2 \theta_2}{2(\alpha - \varphi) \sin \theta_2}$$

Thus, if

$\lambda = 6 \times 10^{-5}$        $\alpha - \varphi = 1° = 0.0175$        $\theta_2 = 20°$

then

$$\delta e = \frac{6 \times 10^{-5} \times 0.88}{2 \times 0.0175 \times 0.342} = 0.004,4 \text{ cm}.$$

per fringe for each degree of arc of non-symmetry, $\alpha - \varphi$.

The effectiveness of the fore-and-aft motion, according to this equation, is evidence of a residual angle, $\alpha - \varphi$, of non-symmetry. This is not improbable, as my apparatus was an improvised construction, lacking mechanical refinement. Further, the wedge effect due to $\alpha$, which makes $e_m$ variable, would be superposed on the interferences, and hence these could not be increased in size above a certain maximum. This is also quite in accord with observation.

If $\alpha = \varphi$, $\beta = 2(\alpha - \varphi) = 0$ and $\theta_2 = \theta'_2$; i.e., the virtual images $G_m$ and $G_n$ and the diffracted rays are parallel and $\delta e = \infty$. In other words, the fore-and-aft motion has no effect. If $\alpha = 0$, $\beta = 2\varphi$; or if $\varphi = 0$, $\beta = 2\alpha$. In either case $\delta e$ is finite, and fore-and-aft motion is effective. If the mirrors and grating were rotated in counter-direction so that $\varphi$ is negative, $\delta e$ will depend on $\alpha + \varphi$, and the fore-and-aft effect will be correspondingly marked. Moreover, the interference will not in general appear in the principal focus, but usually sufficiently near it for adjustment.

If $\delta e_0$ is the actual displacement of the grating $G'$ in the line of symmetry, $\delta e_0 = \delta e/\cos \varphi$, so that the angle $\varphi$ enters equation (5) again, but only to a small extent.

# CHAPTER IV.

## THE DISTANCE BETWEEN TWO PARALLEL TRANSPARENT PLATES.

**29. Introductory.**—The problem of finding the distance separating two parallel glass disks, as well as their degree of parallelism, is frequently one of practical importance. Thus, in my work on the repulsion of two such disks, it would enter fundamentally, and it has long been my intention to repeat that work with two half-silvered glass disks, for comparison with the case of metallic disks. It has since occurred to me that the method devised by my son, Mr. Maxwell Barus, and myself* would probably be ideal for the purpose, both for very small distances (within 0.1 mm.) as well as for distances ten or more times larger. This method admits of use of the film grating, and there are three types of interferences of successive orders of fineness, the first virtually involving the colors of thin plates (resolved spectroscopically), the other two being dependent on diffraction. To measure the thickness of the air-space it would be necessary to count the number of fringes between two definite Fraunhofer lines only, supposing the constants of the grating to be given.

**30. Apparatus.**—The apparatus has been designed for transmitted light, in preference, though the case of reflection is also available.
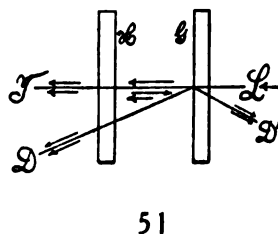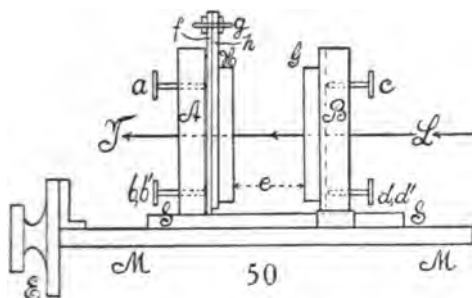


*MM*, figure 50, is the base of a Fraunhofer micrometer, firmly attached below to a massive tripod (not shown). *SS* is its raised slide, and *E* the head of the micrometer screw, reading to $10^{-4}$ cm. The open case *A* is screwed to the slide *SS* and contains the glass plate *H* half-silvered on the right. *H* is attached to a plate of brass, on the plane-dot-slot principle, and may therefore be rotated around the vertical and horizontal axis by aid of a rearward spring mechanism (not shown) and the adjustment screws *a, b, b′* (the last not visible). The grating *G*, with a ruled face on the left, is similarly carried by the open rectangular case *B*, screwed down to the base *M* of the micrometer. Thus *B* is stationary, while *A* moves. Three adjustment screws, *c, d, d′* (*d′* not shown), and a spring pulling to the right suffice to rotate *G* around the

* C. Barus and M. Barus, Carnegie Inst. Wash. Pub., No. 149, Part I, Chapters II and III. 1911.

vertical and horizontal axis. The thickness of the efficient air-film is thus *e-* and *H* and *G* may be brought to touch or to recede from each other several centimeters. *L* is the collimator (slit and lens), furnishing intense white sun, light or arc light, and the beam, after traversing the system, is viewed by the telescope *T* (direct beams, fig. 51), or *D* (diffracted beams).

The plate *H* is half-silvered, but the grating *G* is left clear. In this case, however, only the fine fringes are seen strongly on transmission. The others appear on reflection at *G*, preferably in the second order of spectra. Fine fringes are not well reflected, but the medium and coarse fringes are very strong and clear, and the first observations were made by means of them.

Thereafter the ruled face of the grating was half-silvered. This largely destroys the reflected field, *D'*, except the fine fringes, but the transmitted field *D* is now strong, particularly in the second order of spectra, for all the three sets of fringes in question. Mr. Ives's direct-vision prism grating shows the fine fringes well in the direct beam *T*. The lines are always rigorously straight, so far as they can be observed; *i.e.*, it is impossible to bring *H* and *G* rigorously in contact, not only because of dust, but since the grating (at least) is not optical plate. The fine fringes may always be found in the principal plane of a telescope, but the medium and coarse fringes usually lie in other focal planes differing from each other. By placing the ocular it is thus possible to eliminate any of the interferences or to show a single set in the field only.

To find the fringes, the direct white-slit images are made to coincide throughout their extent, and the same may be done with a pair of spectrum lines in the superposed spectra. The proper *e* is then to be sought. Owing to imperfect plane parallel plates, it may be necessary to correct this by the adjustment screws on the mirror until sharp, strong fringes are seen in the corresponding focal plane.

**31. Equations.**—The equations for the three useful interferences in question are for $r < \theta_m$ and a similar group for $r > \theta_m$

(1)                     $n\lambda = 2e\mu \cos r$

(2)                     $n\lambda = 2e\mu \cos \theta'_m$

(3)                     $n\lambda = 2e\mu(\cos r - \cos \theta'_m)$

where $\lambda$ is the wave-length of the color used, $n$ the order of the interference, $e$ the thickness of the sheet to be measured, and $\mu$ index of refraction, if $i$ is the angle of incidence of the white light on the grating, $r$ the angle of refraction in the plate ($\mu$), and $\theta'_m$ the angle of diffraction of the $m$th order of spectra therein. If the sheet is an air-space, these equations become simplified, since $\mu = 1$ and $r$ is replaced by $i$, $\theta'_m$ by $\theta_m$, the angle of diffraction in air. Thus, since positive values are in question,

(4)                     $n\lambda = 2e \cos i$

(5)                     $n\lambda = 2e \cos \theta_m$

(6)                     $n\lambda = 2e(\cos i - \cos \theta_m)$

In the present apparatus I have made $i=r=0$, a more convenient plan of testing the method, though not necessary and, in fact, often inconvenient in practice. The equations are, finally,

(7)        $n\lambda = 2e$

(8)        $n\lambda = 2e \cos \theta_m = 2e\sqrt{1-(m\lambda/D)^2}$

(9)        $n\lambda = 2e(1-\cos \theta_m) = 2e(1-\sqrt{1-(m\lambda/D)^2})$

if $D$ is the grating space, and the interference in question is due to the grating spectrum of the $m$th order.

The meaning of the equations (7), (8), and (9) is given in figure 52. The case of equation (7) may be seen in the direct white ray, figure 52 $a$, provided the light of the focussed slit-image is resolved by direct-vision spectroscope. For this purpose Mr. Ives's grating with attached direct grating prism may conveniently be placed in front of the telescope $T$, figure 50, focussed on the slit. After adjustment these fringes appear strong. Of course, $H$ and $G$



52        53
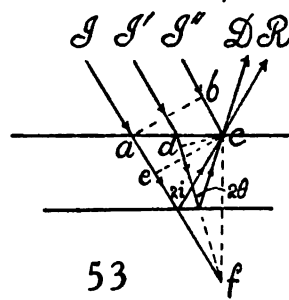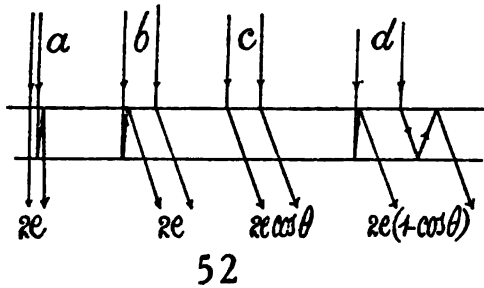
must be parallel and all but touch. Under the same conditions the fringes may be seen laterally in any order of spectrum, as in figure 52 $b$. Figure 52 $c$ illustrates equation (8) and figure 52 $b$ equation (9). Figure 53, finally, illustrates the general case of incidence, $i$.

The first and second orders of spectra are alone intense enough to produce marked effects. In case of $i=0$, a double diffraction of the first order, $\theta'$ reinforces a single diffraction of the second order, $\theta_2$, since

$$\lambda/D = (\sin \theta' - \sin \theta) = \sin \theta_2/2,$$
$$(\sin \theta' - \lambda/D) = (2\lambda/D)/2 \text{ or } \sin \theta' = 2\lambda/D$$

Probably for this reason they are visible. The general case, equations (4), (5), and (6), is illustrated in figure 53, the rays $I$, $I'$, and $I''$ being incident, $R$ reflected, and $D$ diffracted. The retardations are $ef$ and $df$, respectively. If the diffractions differ by a whole number of wave-lengths the total diffraction is obtained. One would be tempted to resolve the case by aid of a wavefront $ab$, in which case the equations would be different; but they do not reproduce the phenomenon.

**32. Method.**—Suppose, now, two Fraunhofer lines, $\lambda$ and $\lambda'$ of the spectrum, are selected as the rays between which interference fringes are to be counted. Then, in case of equation (7), if $n'$ is the number of interference rings between $\lambda$ and $\lambda'$,

(10)          $$n\lambda = (n+n')\lambda' = 2e$$
(11)          $$n = n'\lambda'/(\lambda-\lambda')$$
(12)          $$2e = n'\lambda\lambda'/(\lambda-\lambda') = Cn'$$

In order to measure $e$, therefore, it is necessary to count the number of fringes $n'$ between $\lambda$ and $\lambda'$, and $e$ varies directly as $n'$.

If the mean $D$ and magnesium $b$ lines be taken as limiting the range, $10^6\lambda = 58.93$ cm., $10^6\lambda' = 51.75$ cm., $C_1 = 10^{-4} \times 4.25$; then

| | |
|---|---|
| $n' = 1$ | $10^5 e = 0.21$ cm. |
| $= 10$ | $= 2.1$ |
| $= 100$ | $= 21$    etc. |

As it will not be convenient to count more than 100 lines ordinarily, the method is thus limited to air-spaces below 0.2 mm. and becomes more available as the film is thinner. Of course, in case of plates which contain specks of dust or lint, or are not optically flat on their surfaces, it is extremely difficult to get $e$ down below 0.002 cm., so that ten fringes between $D$ and $b$ would require very careful preparation.

If equation (8) is taken, $\lambda$ is to be increased to

$$L = \lambda/\cos\theta_m = \lambda/\sqrt{1-(m\lambda/D)^2}$$

where $m$ is the order of the grating spectrum, whose rays interfere. Thus equations (11) and (12) now become, since $nL = (n+n')L' = 2e$

(13)          $$n = n'L/(L-L')$$
(14)          $$2e = n'LL'/(L-L') = C_2 n'$$

If first order of diffractions are in question, $m = 1$, $10^6 L = 59.11$, $10^6 L' = 52.33$, $C'_2 = 10^{-4} \times 4.20$. Thus for

| | |
|---|---|
| $n = 1$ | $10^5 e = 0.21$ cm. |
| 10 | 02.1 |
| 100 | 021. |

scarcely differing from the preceding case, so that one would not know in which series one is working.

If the diffractions occur in the second order, $m = 2$,

$$10^6 L_2 = 62.56 \qquad 10^6 L'_2 = 54.15 \qquad C''_2 = 10^{-4} \times 4.03$$

thus again differing but slightly from the above.

If we inquire into the condition of coincidence and opposition of these fringes, the following results appear: Let the spectrum distance between the $G$ and $b$ line be taken as unity, and let there be $n_1$ and $n_2$ first-order fringes in this distance. Then in $\dfrac{1}{n_1}-\dfrac{1}{n_2}$ is the difference of distance per fringe. Let

$x$ be the number of long fringes, to restore the original coincident phase; *i.e.*, let $x$ longer fringes gain one long fringe on the $x$ shorter fringes. Then

$$x(1/n_1 - 1/n_2) = 1/n_1 \qquad x = C_1/(C_1 - C_2)$$

that is, $x$ fringes constitute a new period. From the above data

$$x = 4.25 \times 10^{-4}/4.4 \times 10^{-6} = 96.5$$

It follows that the length of coincident strips is subject to

$$e = C_1(n_1 - 1) = C_2 n_2 = C n_2/x \text{ or } C = \frac{C_1 C_2}{C_1 - C_2}$$

where $C$ is the new constant. This would place the fringes beyond the coarse group below, but naturally $C$ is enormously dependent on small errors in $C_1$ and $C_2$.

Finally, if equation (9) be taken, the $\lambda$ is to be increased to

$$M = \lambda/(1 - \cos \theta_m) = \lambda/(1 - \sqrt{1 - (m\lambda/D)^2}$$

in order that equations similar to the above may apply. Thus

$$n = \frac{n'M}{M' - M} \qquad 2e = \frac{MM'}{M' - M} = C_3 n'$$

In the diffractions of the first order of spectra $m = 1$ and $10^8 M = 4.150$,

$$10^8 M' = 4.747 \qquad C'_3 = 0.0330$$

These are the coarse order of fringes, so that

| $n =$ | 1 | $2e = 0.033$ |
|---|---|---|
| | 10 | 0.33 |
| | 100 | 3.3 , etc. |

Fringes are thus still strongly available, even if the distance apart of the plates is over 2 cm.

If the diffractions are of a second order of spectra, $m = 2$,

$$10^8 M = 1.016 \qquad 10^8 M' = 1.165 \qquad C'''_3 = 10^{-3} \times 7.85$$

These fringes are therefore of intermediate order, since

| $n =$ | 1 | $2e = 0.0078$ cm. |
|---|---|---|
| | 10 | 0.0785 |
| | 100 | 0.785 |

They would be enhanced, since they coöperate with the double diffractions of the first order.

### 33. Observations and corrections. Preliminary work.—The following work was done merely with a view to testing the equations and with no attempt at accuracy. The grating was left unsilvered, so that the ruled sur-

faces confronted the half-silvered surface on ordinary plate glass. Consequently, the fine fringes were observed by transmitted light behind, and the medium and coarse fringes by reflected light in front. The micrometer was a good instrument for general purposes, but hardly equal to the present work, where the slightest rocking of the slide introduces annoyances.

To count the number of fringes between $D$ and $b$, since the fringes were not generally seen in the principal focal plane of the telescope, it was considered sufficient to rotate the cross-hair into an oblique position, until its ends terminated in the $D$ and $b$ lines, respectively, and then to count the number of fringes on running the eye down the wire from end to end. When there are many fringes, 25 to 50, the eye is apt to tire before reaching its destination, so that several counts must be made and the mean taken.



54
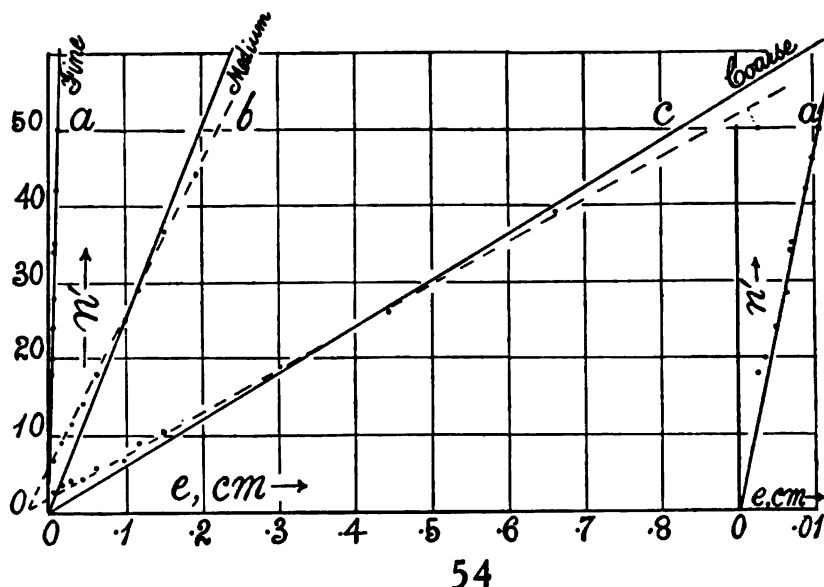
The results are given as a whole in figure 54, where the distance between plates, measured in centimeters on the micrometer, beginning at an approximate zero, is laid off horizontally and the number of fringes vertically, in case of each of the three series. The computed line $e = Cn'/2$ is drawn in full and the observations laid off with regard to it. The zeros do not quite correspond, as very small distances here are significant. With the fine fringes I did not spend much time, as they are virtually colors of thin plates seen by diffraction. The chief difficulty with these small distances is that the plates touch and a complete readjustment is necessary. After touching, the micrometer acts like a forcing screw and its reading is too low. This is the meaning of the data in the curves $a$ and $a'$, the latter with its horizontal scale magnified ten times. The object of this series is chiefly to locate the position of the line in relation to the other lines.

The observations for medium and fine fringes were made together, so that a single micrometer reading suffices. Beginning with very small distances apart, called zero, this was rapidly increased to nearly 1 cm. The fine fringes soon vanished, later the medium fringes vanished, finally (when $e$ is several centimeters) the coarse fringes also vanish. The three together, therefore, cover with accuracy a relatively enormous range of displacement for measurements of this kind.

The curves $b$ and $c$ show that the observations are not completely reproduced by the line. Mean lines drawn through the observations indicate that the zeros do not correspond sufficiently for the two lines $b$ and $c$ to locate the common zero. This is inevitable, since the micrometer begins to count at a small distance as specified, which is otherwise arbitrary. In fact, it should be noticed, as an accessory property of this interferometry, that the two lines for finding the zero determine the absolute reading of the micrometer, mutually, and these readings are here 0.22 mm. too large. But even if the zeros were horizontally to coincide, the observations would not adequately conform to the computed lines. All that can be affirmed is that the angle between the observed and computed loci is about the same.

The main reason for the divergence is referable to the fact that the air-space is not quite plane parallel, but slightly wedge-shaped, so that the effect of the angle of the wedge is superposed on the interferences. Any slight unsteadiness of the micrometer slide, for instance, would already introduce the wedge discrepancy, without necessarily interfering with the sharpness of visibility, while any attempt to readjust would destroy the continuity of measurement. There will also be many secondary reasons for divergence, as, for instance, the three separate focal planes in which the fringes lie and the fact that the glass plates which limit the air-space are themselves wedge-shaped; other, but fainter, fringes are marching through the spectrum, such cases as coincidence and opposition, for instance, as were pointed out above, etc. But the adequate reason for the discrepancies in this paper is the incidental change of the angle of incidence, $i$.



If the film is wedge-shaped, very little disturbance results; but the correction to the second order of small quantities is unfortunately somewhat cumbersome. Let the edge of the wedge of air be vertical and subtend a small angle, $\varphi$, figure 55, between the two faces $A$ and $B$. Let $I$ and $I'$ be the two corresponding rays incident at the angle $i$ at the first face and at the angle $i+\varphi$ at the second face, $n$ and $n'$ being the normals. Let $e$ and $e'$ be the consecutive thicknesses of the air-plate, taken normal to $B$ for convenience. Then the $I$ rays $R'$ will issue at the $A$ face, after reflection, at an angle $i+2\varphi$, and will interfere with the $I'$ rays $R$, if the objective of the telescope is sufficiently
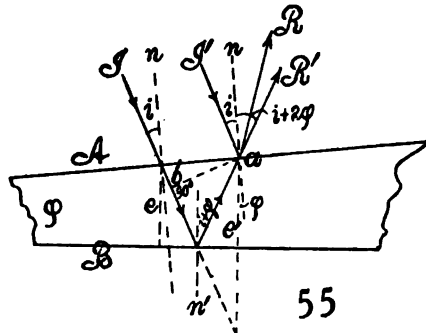
large to converge both to the same point of the image, spectroscopically resolved. If the wave-front $ab$ is drawn and $e'$ prolonged, it follows at once that

$$n\lambda = 2e \cos (i+\varphi) \qquad e' = e\left(1 + 2\frac{\sin (i+\varphi) \sin \varphi}{\cos i}\right)$$

Hence

$$n\lambda = 2e\left(\cos (i+\varphi) + \frac{\sin (i+\varphi) \sin \varphi}{\cos i}\right)$$

If $i = 0$ and $\varphi$ very small, this becomes

$$n\lambda = 2e\left(1 - \frac{\varphi^2}{2} + 2\varphi^2\right) = 2e\left(1 + \frac{3}{2}\varphi^2\right)$$

If in the first equation $i$ is replaced by the angle of diffraction $\theta$, the equation for the diffracted fringes, as far as $\varphi^2$, may be reduced to

$$n\lambda = 2e\left[\cos \theta + \varphi \sin \theta - \frac{\varphi^2}{2}\left(\frac{4}{\cos \theta} - 7 \cos \theta\right)\right]$$

so that $\varphi \sin \theta$ is the chief correction.

Finally, the equation for the coarse fringes becomes

$$n\lambda = 2e\left[1 - \cos \theta - \varphi \sin \theta + \frac{\varphi^2}{2}\left(3 + \frac{4}{\cos \theta} - 7 \cos \theta\right)\right]$$

with a similar equation for the medium fringes.

If we neglect the second order of small quantities ($\varphi^2$), the last equation for the medium fringes may be put in another form, since

$$2\lambda/D = \sin \theta \text{ and } \lambda/L = 1 - \cos \theta \qquad \sin \theta = \frac{2L}{D}(1 - \cos \theta)$$

whence

$$2e = \frac{nL}{1 - 2\varphi L/D} = \frac{(n+n')L'}{1 - 2\varphi L'/D}$$

$D$ being the grating space and $\lambda$ the wave-length. Hence if $n$ be eliminated,

$$2e = n'\frac{LL'}{L - L' - (2\varphi/D)(LL' - LL')} = n'\frac{LL'}{L - L'}$$

In other words, if $\varphi$ is small so that $\varphi^2$ may be neglected, the relation of $e$ and $n'$ is independent of $\varphi$; or a slightly wedge-shaped air-film will show the same result as a plane-parallel film. Experiments made by turning the adjustment screws seem to bear this out, provided the mean thickness remains unchanged.

To give the whole subject further study, I have since half-silvered the grating as specified, so that all the fringes may be seen by transmitted light, preferably in the second order, since there is an abundance of light available. The apparatus in such a case takes a good shape and is convenient for manipulation. But these details will have to be given at some other time, and it is the chief purpose of this paper to exhibit the phenomenon as a whole.

In conclusion, I may recall that if we regard 100 fringes between the $D$ and $b$ lines as still available for counting under proper facilities, the successive ranges of measurements will be roughly as follows:

|  | $e=0.021$ cm. | $e=0.392$ cm. | $e=1.65$ cm. |
|---|---|---|---|
| Fine fringes.......... | $n'=100$ | ........ | ...... |
| Medium fringes....... | $n'=54$ | $n'=100$ | ...... |
| Coarse fringes....... | $n'=1.3$ | $n'=23.8$ | $n'=100$ |

The transition from fine fringes to medium is a little abrupt. Otherwise, in cases where manual interference is not permissible, all thickness of air-films, from a fraction of a wave-length of light to nearly 2 cm., may be adequately measured in this way to advantage. It is probable, moreover, that it would be advisable to observe the fine fringes by transmitted light, but to leave the grating (which may be a film grating) clear, and to observe the medium and coarse fringes by reflected light. A concave mirror and lens (reflecting telescope) should be used for this purpose, as this will put the observer behind the plates in all cases.

# CHAPTER V.

**34. Introduction. Methods.**—To exchange the component beams of the interferometer, to mutually replace the two pencils which interfere, is not an unusual desideratum, for instance, in the famous experiment of Michelson and Morley. To replace two pencils of component rays, traveling more or less parallel to each other, by pencils moving more or less normal to each other, or to be able to operate upon pencils of corresponding rays (from the same source, crossing each other at any angle) at their point of intersection, may be of interest in a variety of operations to which the interferometer lends itself, or may even suggest novel experiments. The facility with which this may be done, or at least partially done, with the above types of spectrum interferometers, particularly when homogeneous light is used, has tempted me to investigate a number of cases.

Let us begin with the above diagrammatic method, using two transmitting gratings, G and G', figure 56, with the same (or in general with different) grating constants. Let L be the incident beam of collimated homogeneous light, m, n, m', n', four opaque mirrors on vertical and horizontal axes parallel to their faces. The ruled faces of the gratings are to be toward each other. Then the beams Gm and Gn may be reflected either *across* each other, as shown at mn' and nm', thence along n'G' and m'G', and, after a second diffraction at G', unite to enter the telescope at T; or they may be reflected along m, m', and



56

n, n', parallel to each other, and thereafter take the same course. In the first case homogeneous light is apparently not necessary. It will be seen that the path of the rays is the same, except for the branches mn' and nm', and mm' and nn', respectively normal and parallel to each other; moreover, that the rays are exchanged, a and b left and right combining at G' in one case, b and a left and right in the other. The rays cross at c in free space and are available there for experiments. Direct light is to be screened off. The question is whether the mirrors m and n, m' and n', can be adjusted mechanically to move symmetrically toward each other on a vertical axis with sufficient precision to guarantee replacement. This is a matter of trial, though a successful issue is, of course, problematical. It would be advantageous to arrange the experiment so that only one pair of mirrors—*e.g.*, m and n—need

78
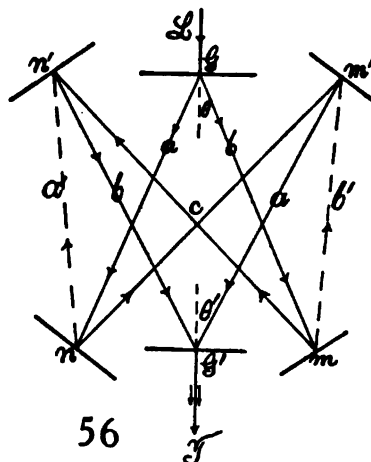
be moved, whereas the others, $m'$ and $n'$, are ends of the same rigid plate. Gratings of different constants may advantageously contribute to this end. Beyond this, the paths $mn'$ and $nm'$ and $mm'$ and $nn'$ may be increased to any length, either directly or by multiple reflections from a special system. Many other modifications are suggested. If white light is used, the phenomenon is confined to a narrow strip of spectrum and the fringes must be horizontal.

As I did not have two ruled transmitting gratings and as film gratings seemed unpromising for work of this kind, the method of figure 57 represents a simple disposition of reflecting gratings, of which several were available. The ruled faces of the gratings $G'$ and $G$ face away from each other.



57                                        58
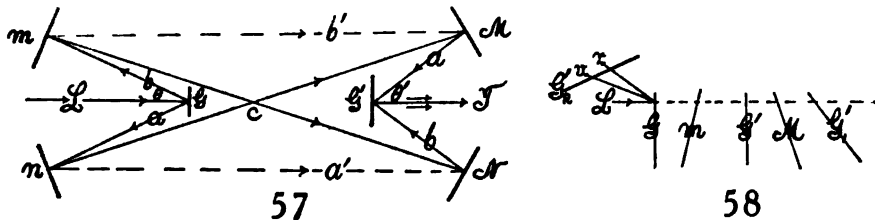
The former receives the collimated pencil of homogeneous light, $L$, and after diffraction the partial beams pass to the pair of opaque mirrors $m$ and $n$ (symmetrically placed), and thence by reflection to a similar pair of mirrors, $M$ and $N$. From here the pencils reach the second grating, $G'$, where each is again diffracted into the common ray $G'T$, entering the telescope $T$. The grating $G'$ may be concave with the lens at $T$ beyond the principal focus. If the mirrors $M$ and $N$ are symmetrically rotated, the parallel component pencils $Nn$ and $Mm$ may be replaced by the pencils $Mn$ and $Nm$, crossed at any angle. Homogeneous light is preferable. Simultaneously the rays are exchanged. The pencils, $Mm$, etc., may be of any length, and in general the remarks in the preceding paragraph apply.

A more flexible design also suggests itself, with four fixed mirrors, $m$, $n$, $m'$, $n'$, four movable mirrors, $M$, $N$, $M'$, $N'$, rotating symmetrically around vertical axes parallel to the faces of the gratings $G$ and $G'$, these being parallel to each other, as in figure 57. On rotating $M$, $N$, $M'$, $N'$, the rays may be exchanged. Here $M$ . . . . $N'$ should be a near system, $m$ . . . . $n'$ a fixed and far system of mirrors. Other methods will presently be described.

**35. Experiments. Reflecting gratings. Parallel rays.**—The experiments were begun with the apparatus as in figure 57, $G$ being a Michelson grating and $G'$ a Rowland grating, each with somewhat less than 15,000 lines to the inch. The distance of $G$ from the mirrors $m$ and $n$ was about 22 cm., of $G$ from $G'$ about 60 cm., and of $G'$ to the focal point just ahead of the lens (or the line of mirrors $M$ and $N$) about 90 cm. The latter were about 50 cm. apart. In the absence of sunlight, the arc lamp was used, and the fringes for reversed spectra were found without great difficulty. It was also easy to

erect them by rotating $G'$ on an axis normal to its face. A difficulty, however, existed in retaining the fringes with a flickering arc. It will be seen that in this case the line $LG$ moves over a small angle in all directions with the bright spot on the positive carbon, so that the angle of incidence is varied, and with it the angle of diffraction $\theta$ at $G$. All this is magnified by reflection from the mirrors. Moreover, unless the collimator lens is very near $G$, the illuminated part or bright line on $G$ is displaced right and left. Path-difference between $GnNG'$ and $GmMG'$ is thus modified. If the faces of the mirrors are not all quite in a vertical plane or parallel to the same plane, the up-and-down play of the arc will mar the longitudinal coincidence of the two superposed spectra, and hence the interferences will vanish. Thus they appear and disappear periodically, depending on the accidental position of the bright spot of the arc; and if this annoyance is to be avoided, sunlight or a steady light must be used. The phenomenon and the spectra were not nearly so bright as when observed with the transmitting grating, a result probably due both to the additional reflections (particularly those at the grating) and to the high dispersion.

In other respects the behavior was the same as that described in Chapters I and II, though the strip of fringes for reversed spectra seemed to be somewhat broader, probably owing to the increased dispersion and hence the greater breadth of adequately homogeneous spectrum light. The linear phenomenon, moreover, consisted of two or more black lines alternating with bright, whereas a single black line was the characteristic feature above. When different strips of the grating $G$ are used (the illumination should not be more then 0.5 cm. wide), considerable fore-and-aft displacement at the mirror $M$ is necessary.

The adjustment for crossed rays $Mn$ and $Nm$, figure 57, is subject to new conditions. In case of white light and a narrow slit, the dispersion produced by $G$ is at least partially annulled by $G'$ instead of being incremented; for the change of the angle of incidence here compensates the changes of the angle of diffraction. Thus if $\sin i_v - \sin \theta_v = \lambda_v/D$ for violet and $\sin i_r - \sin \theta_r = \lambda_r/D$ for red, and if $\sin i_v = \lambda_v/D$ and $\sin i_r = \lambda_r/D$, then $\sin \theta = \sin \theta_r = 0$.

A sharp, white image of the slit may thus be seen for the reflection from each mirror $M$ and $N$, or the images may be colored if but a part of the spectrum is reflected from $M$ and $N$. The system of two gratings, $G$ and $G'$, tends to become achromatic. It would seem to follow, therefore, that in general homogeneous light and a wide slit would have to be used, but this introduces additional annoyances, inasmuch as the transverse axes of the spectra (sodium lines), which are to coincide, are not visible, but must be replaced inadequately by the edges of the slit. The experiment is thus (particularly in view of the faint illumination seen in the telescope) difficult, and in a laboratory not free from agitation, or in the absence of a good mercury lamp of intense homogeneous light, it did not seem worth while to spend much time on it. Moreover, a similar investigation will presently be made with a transmitting grating.

In other words, in case of the rays $nM$, the violet is incident at a larger angle at $G'$ than the red, and but one color (yellow) can be diffracted along $G'T$, whereas in case of the rays $mN$ violet is incident at $G'$ at a smaller angle than red, and $G'$ may thus be so placed that all rays are diffracted along $G'T$, supposing the two gratings to be nearly identical as to dispersion. Figure 58, presently to be described, suggests the inclination of the successive vertical planes in figure 57.

One curious result deserves special mention. Each separate spectrum ($a$ or $b$, fig. 57, without superposition) shows very definite coarse stationary interferences; i.e., the usual appearance of channeled spectra. The cause of this long remained obscure to me, but will be explained in Chapter VI. The gratings being of the reflecting type and the mirrors silvered on the *front* face, there is no discernible cause for interferences. No film or set of parallel plates enters into the experiments. If in figure 57 the grating $G'$ is reflected at $M$ into $G'_1$, and this image reflected in $m$ into $G'_2$, the phenomenon may be treated as if the gratings were transmitting in a manner shown in figure 58. Here the direction of the traces of the grating $G$ and $G'$, the mirrors $m$ and $M$ only are given, together with the direction of the reflected images of $G'$ in $M$ ($G'_1$), and in $m$ ($G'_2$). Then the violet ($v$) and red ($r$) rays from $G$ impinge on $G'_2$ virtually with a greater angle for $v$ and a smaller one for $r$, as already suggested. An enhanced spectrum must be produced beyond $G'_2$. This second spectrum is channeled.

**36. Experiments. Transmitting grating. Parallel rays.**—The chief difficulty in the preceding experiments was the absence of sufficiently intense homogeneous light. This may be obviated by using the transmitting grating. But as two samples were not available (as in fig. 56), the simplified method of figure 59 was tested, where but a single grating $G$ is used. Here the light $L$ from collimator and slit impinges on the grating $G$ and is diffracted to the opaque mirrors $M$ and $N$. From here it is reflected to the corresponding opaque mirrors $m$ and $n$, to be again reflected to the grating $G$, and finally diffracted along the line $GT$. The interferences are observed by the telescope at $T$. In order that the undeviated white beam may not enter the telescope annoyingly, the diffraction $LG$ takes place in the lower half of the grating and the mirrors are slightly inclined upward, so that the second diffraction $GT$ may occur in the upper half of the grating. To obviate glare in the field, the beam $LG$ is carried to the grating in an opaque tube and all undeviated light is suitably screened off. The distances $mn$ to $G$ and $G$ to $MN$ were about a meter each.

The interferences were easily found. They are usually at an angle to the vertical, but may be erected by rotating the grating on an axis normal to its face. They were linear and exactly like the cases of Chapter I, probably in consequence of the low dispersion of the grating used. Considerable magnification at the telescope is thus admissible.

The horizontal fringes traveling up or down are available for interferometry,

and the independent and separated component beams *Mm* and *Nn* are conveniently accessible.

The experiments with homogeneous light (sodium arc) gave perfectly regular striations covering the whole of the wide slit image, *uniformly*. With glass compensators o.6 to o.1 cm. or more thick on both sides, the striations became somewhat smaller, as was to be anticipated. Fringes could be erected and enlarged by rotating the grating on an axis normal to its face and by other corresponding rotations. The fringes, as a whole, were large and splendid and suitable for general purposes in interferometry.

### 37. Experiments. Transmitting grating. Crossed rays.

—The second position of this apparatus was now tested, the rays passing along the diagonal of the rectangle (fig. 59) and crossing at *G* in the grating. The interfering pencils were thus *GNGmG* and *GMGnG*. The slit should be quite wide. Seen in the telescope at *T*, therefore, the dispersion is reduced in virtue of double diffraction, the tendency being toward white slit images, as already explained. A variety of very interesting results were obtained after the interferences had been found. The outgoing and returning paths are coincident, and both component rays pass through the grating two times, the ruled face being towards the telescope.
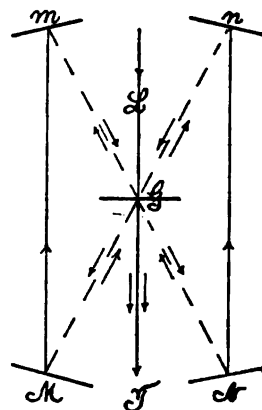


59

The adjustment is at first somewhat difficult. Having made a rough setting of the mirrors as to distance, etc., by the aid of sunlight or arc light, so that the spectra may be seen, two wide slit images will appear in the telescope *T*, but they will usually be differently colored. The mirrors *m* and *n* are then to be rotated around vertical axes (fine-screw motion) until both slit images are identically colored and coincide. After this, homogeneous light (sodium arc) must be used and the rotation of mirrors on the vertical and horizontal axes repeated until both fields are identically yellow on coincidence. The sharply focussed edges of the wide slit are now the vertical and horizontal guide-lines for adjustment. All corresponding lines must coincide if the phenomenon is to be obtainable. Thereafter the micrometer at *M*, actuating the mirror fore-and-aft parallel to itself, is manipulated till the fringes appear.

Two types of interference may be observed. The first are variations of nearly equidistant fringe patterns, obtained with homogeneous light only and covering the whole wide slit image on good adjustment. They would appear equally well in the absence of the slit. The second type is obtained in the presence of white light, or of the mixture of white light with the homogeneous light. It is a linear phenomenon, identical in appearance with the one described in Chapter I, though occurring here in the case of a *wide slit*. Both are very vivid, and the latter particularly, when at its best, in violent tremor.

It is convenient to describe the homogeneous fringes first. White light must be absent, the wide field full yellow, and the longitudinal and side edges of the two slit images sharply superposed. When the fringes appear they will usually be oblique; but they may be made vertical by rotating the grating on an axis normal to its face. If the grating is in the symmetrical position of figure 59, the size of fringes is an intermediate minimum. To enlarge them, curiously enough, the grating must be slightly rotated, either way, on a *vertical* axis. The fringes then pass through a maximum of size at a definite angle on either side of the minimum. In such a case they also appear rapidly to become irregular and their perturbation is naturally enhanced. They contain a double periodicity, which will presently be carefully examined.

Fore-and-aft motion of the grating has no effect. In displacing the mirror at $M$ on the micrometer, the fringes remain visible for an excursion of at least 0.7 cm. In fact, in case of a strong telescope and wide slit they were not lost for a micrometer displacement of over 1 cm., *i.e.*, much over 30,000 wavelengths of path-difference. As a rule, the fringes are strong only in part of the yellow field, and in such a case the center of intensity moves with the displacement of $M$ across the slit image, to disappear at the edges, as in the usual cases of displacement interferometry. Slight non-coincidence of the horizontal edges of the slit images slightly rotates the fringes, but they soon vanish completely. Slight rotation of the grating around the vertical axis distributes the fringes more evenly over the field, the proper setting being determined by trial. Displacement by aid of a compensator of glass gave the usual results.

Later I returned to the experiments with sodium light and with the grating rotated around a vertical axis to the right or left and out of the symmetrical position of figure 59. In each case the fringes passed through maximum size at an angle of asymmetry of about 5° or 10° from a normal position. Beyond or below this they diminish in size. Naturally, to bring the fringes to the center of the field, the micrometer screw at $M$ or $N$ had to be adjusted for path-difference, as in displacement interferometry generally.

The details of the interference patterns obtained were in astonishing variety. Suppose that by rotating the grating around an axis normal to its face the fringes are made nearly but not quite *vertical* at the beginning. Then on rotating the grating around a vertical axis into the position for maximum size just specified, the standard type of large fringes seen are of the appearance shown in figure 60a. In other words, they look and behave like independent, thick, twisted cords, hung side by side. The evolution of these independent parallel striations of fringes may be detected on rotating the mirror $M$ or $N$ around a vertical axis, thus moving one slit image in definite amounts, micrometrically, over the other, horizontal edges remaining superposed. As the one slit image passes in this way across the other, the original type, figure 60b, apparently continuous, breaks up and enlarges into the type c by the rotation of its parts. Thus the successive lengths of the continuous fringe b behave like a series of magnetic needles, each rotating on its own pivot. These may

again correspond and appear as a single striated field; but more frequently the form figure 60a is in evidence, though sometimes quite irregular. In fact, there are many variations of this design. Families of curves, intersecting each other nearly orthogonally, may even appear.

If the fringes are originally quite vertical, there seems to be no rotation, but two sets of vertical fringes apparently pass through each other as the mirror $M$ is rotated micrometrically on a vertical axis. These fringes at intervals again unite into an apparently simple striation. One slit image may be broader than the other. Fringes of different sizes then appear, so long as the smaller is within the larger, and are most intense when the vertical edges meet. In general, therefore, the interference patterns of originally nearly vertical fringes consist of a succession of *strands*, nearly in parallel, which behave alike but independently.
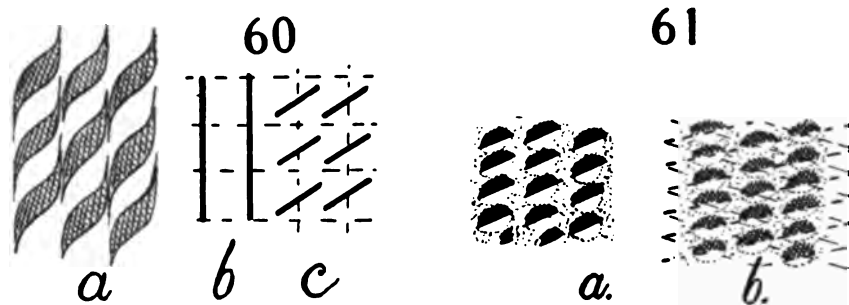


If the grating is rotated on an axis normal to its face until the fringes are nearly horizontal, a correlative series of interesting phenomena may be observed. When the grating is normal to the incident pencil, the fringes are usually arranged in parallel strands. They are equidistant in each strand; but these strands are separated by a narrow band of even color, so that the phenomenon looks as if thick, twisted, yellow cords were hanging apart, side by side. Usually the central or the two central cords are more intense, and there may be four to six in all, filling the whole of the wide-slit image. On rotating the mirror, $M$ or $N$, micrometrically, on a vertical axis, the fringes of the strand may be made to correspond, so as to fill the field with uniform striations and without apparent vertical separation. This is particularly the case when the fringes are very fine.

On rotating the grating to the right or to the left about 20°, on the vertical axis from the symmetrical position of figure 58, the fringes reach a maximum of size, after which (on further rotation to about 30°) they diminish indefinitely. These maximum cases are shown in figure 61, a and b, and their appearance is now that of a string of elongated beads, hung vertically and equidistant. On rotating $N$ about a vertical axis, slightly, the nodules become quite horizontal. They are continually in motion, up and down, and quiver about the horizontal position like small disturbed magnetic needles. At times the field appears reticulated (indicated in the figure), as if two sets of nearly horizontal fringes intersected at a small angle. It is now difficult to obtain

continuous striations on rotating $N$, but the whole field may easily be filled with nodules. The occurrence of two maxima is probably an incidental result, as in other adjustments but a single one appeared. Naturally the rotation of the grating or of the mirrors $M$ and $N$ changes the path-difference of the pencils crossing within it, so that the micrometer screw at the mirror $M$ must be moved in compensation. Thus this is another method of displacement interferometry and the usual equation suffices.

The following rough experiments were made: Placing the strong fringes in the center of the field (slit image), the reading of the micrometer was taken. Then a thick glass plate, $e = 0.71$ cm., was inserted in one beam, nearly normally, and the micrometer displacement, $\Delta N$, was found when the fringes were brought back to the center of the field again. The results were (for instance)

$$\Delta N = 0.375 \qquad 0.393 \text{ cm.}$$

The displacement equation is ($\mu$ being the index of refraction of the plate)

$$\mu = 1 + \Delta N/e - 2B/\lambda^2$$

where the correction for dispersion may be put $2B/\lambda^2 = 0.026$. Hence $\mu = 1.50$, $1.52$, as was anticipated. On using white light, where there is but a single strand, a cross-hair, and greater care as to the normality of the plate compensator, etc., there is no reason why results of precision should not be obtained.

**38. The same. The linear phenomenon.**—The occurrence of the linear phenomenon reciprocally with the fringes for homogeneous light is interesting. It usually appears when there is a flash of the arc lamp, $i.e.$, a displacement of the crater, introducing white light into the sodium arc. It is thus undoubtedly due to the reversed spectra for white light and may, in fact, be produced by using the white arc or sunlight in place of the sodium arc. When the mirror $M$ is displaced on the micrometer parallel to itself, the linear pattern moves through the wide-slit image from right to left; or the reverse. It does so also when either mirror, $M$ or $N$, is slightly rotated on a vertical axis. The change in appearance during this transfer is very striking. In the middle, between the extreme right and left positions, the linear phenomenon is exceptionally strong and fairly tumbling in its mobility. Toward the right or left from the center it becomes gradually less intense, and on one side merges into the homogeneous striations which then appear. On the other side it seems merely to vanish. Doubtless the linear phenomenon is found, as usual, at the line of symmetry of two reversed spectra; but, as both spectra are shrunk to very small lateral dimensions, many colors probably adequately coincide. In an achromatic reproduction of the slit all colors will coincide.

It is thus not necessary that the edges of the slit images should be superposed to produce the linear phenomenon. What is still more curious is the

result that not even the longitudinal axes of the spectra need be quite in coincidence, though, of course, the phenomenon appears most intensely for the case of precise superposition. The angle of admissible separation of longitudinal axes is, however, much larger here than in the usual cases above, so that one of the longitudinal guide-lines of the two spectra may be appreciably above the other.

The last result and the fact that the linear phenomenon appears here with an indefinitely wide slit are new features. The cause of the latter has just been referred to the exceptionally reduced width of spectrum resulting from the double diffraction. If the dispersion were quite reduced to zero, all colors in a definite narrow, transverse strip of the white slit image would be in a condition to interfere. This strip contains the superposed images of an indefinitely fine slit. The slit in any other position, right or left, would have two non-coincident images. Hence, when one wide-slit image moves over the other, there is also a shift of the linear phenomena.

To produce the linear phenomenon with sunlight is difficult. The interferences should first be produced with the sodium arc, strongly, and the arc thereafter replaced with sunlight entering the slit at the same angle. Furthermore, the pencil leaving the collimator should be a narrow, vertical blade of light, and at the mirrors, $M$ and $N$, red and green light should be screened off, retaining only a narrow strip of yellow light for each. Finally, to avoid glare, the slit is not to be too broad nor too narrow to cut off the yellow field of the telescope.

Under these circumstances of completed adjustment, the linear phenomenon usually appears strongly. Its form may be greatly modified by rotation of either mirror, $M$ or $N$, micrometrically, around the vertical axis, as already suggested. The types are given in figure 62, quite fine, nearly vertical lines, $q$, changing to moving, coarser forms, $m$, and these into the tumbling variety, $t$, very coarse and nearly horizontal. The latter change by rotation and diminution into $m'$ and $q'$, while $N$ is being continually rotated over a very small angle, sliding one slit image continuously over the other. In the condition $t$, the fringes rotate with astonishing rapidity, and this rotation is nearly $180°$; i.e., if the angle between $m$ and $m'$ is $\alpha$, the angle of rotation has been $180° - \alpha$, so that between $q$ and $q'$ there is about $180°$ of rotation. At the stage $t$, with fine micrometric adjustment, the fringes may be made quite horizontal, and they are then relatively large and square, or at times shaped like blunt arrowheads. This rapid rotation of fringes near $t$ accounts for their turbulence, since tremors have the effect not merely of raising and lowering them, but also of producing the rotary motion in question. They may also be rotated, of course, on slightly tilting the grating about an axis normal to its face. Rotating the latter on an axis parallel to its face places the phenomenon in different parts of the superposed yellow field.

Since a preponderance of yellow homogeneous light is present in the whole of the superposed wide-slit images in the telescope, it is not difficult to suggest the cause for the variations of the interference pattern when one image passes

horizontally over the other. The forms, *t*, correspond to minimum path-difference, remembering that in accordance with figure 59 all rays pass the plate of the grating twice.

Further experiments were made with sunlight to detect the changes which befall the phenomena in different focal planes. The ocular of the telescope was gradually drawn out from an inner extreme position to an outer extreme position, through the normal position for principal focal plane. In this case a variation of form corresponding closely to figure 62 was also observed. The characteristic feature, however, was the prevalence of arrow-head or caret-shaped lines, both in the case of the extremely fine striations and of the coarser nodules. In the former case these roof-like designs were closely packed from end to end of the phenomenon and usually pointed upward. They recall the top edges of extremely eccentric ellipses in displacement interferometry, and in view of their lateral motion with the micrometer *M* and the decreased dispersion due to double diffraction, their origin may be similar.

**39. The same. Inferences.**—When the pencils, *Mm* and *Nn*, figure 59, are parallel and sodium light is used, the whole field is uniformly striated, whether the striations are made fine or coarse. I have found it impossible, on placing plate compensators (0.5 to 1.5 cm.) in both beams and rotating these to any degree whatever, to produce any suggestion of a secondary periodicity in the field. The fringes for a thick compensator, slightly wedge-shaped, merely become a little finer. Films of mica are liable to blur the field. In general, moreover, reflections would be relatively weak and thus inappreciable. They would require a separate adjustment for coincidence and not appear with the principal phenomenon. Hence the strands of interferences obtained in case of crossed rays are in a measure unique. The second periodicity is not stationary, but a part of the phenomenon. The glass plate of the grating produces an effect in virtue of its thickness, precisely as in the case of the displacement interferometry of my earlier papers.

Experiments made with polarized light proved to be entirely negative. The phenomenon appears between a polarizer and an analyzer so long as sufficient light is present to exhibit it. Observation with a nicol, in the absence of the polarizer, showed nothing but the obvious effect of reflection.

The occurrence of these parallel strands for crossed rays and homogeneous light is thus difficult to explain. I have tried a great variety of methods of superposing special interferences, etc., to produce the nodules with parallel rays, *mM* and *nN*, or to break them with crossed rays, *mN* and *nM*, without avail. There is no focal plane effect, nor any polarization effect. It is therefore necessary to confront the case at its face value, as in figure 63. Here *S*
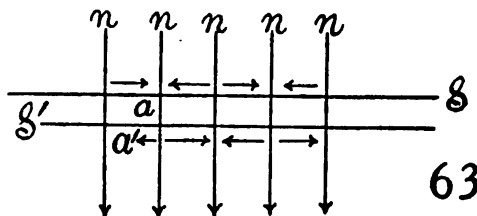
and $S'$ are the traces of two longitudinally coincident reversed spectra, drawn apart for distinction, the region of the $D$ lines only being used. The light is homogeneous to this extent and the slit wide, so that there is oblique incidence. Then every point of $S$ should (on adjustment) interfere with every point of $S'$, the result showing a uniformly striated field in the telescope. This is emphatically the case for the parallel rays, $mM$, $nN$; but with the crossed rays, $mN$, $nM$, the interference is confined to the rays in the equidistant positions, $n$, in figure 63, and midway between them the field is a neutral yellow. In other words, between the rays $n$ the rays are displaced, as shown by the arrows, recalling the arrangement of nodes in acoustics.

Corresponding rays $a$ and $a'$ (for instance) do not coincide and hence can not interfere, the region $aa'$ remaining neutral. In figure 64 the rays crossing at $c$ (fig. 57) have been shown for three nodes and the transverse arrows indicate the directions in which the rays have been urged laterally. Naturally, I am merely stating the case as immediately suggested by the results. One may argue that there may be a secondary periodicity in the grating. But why
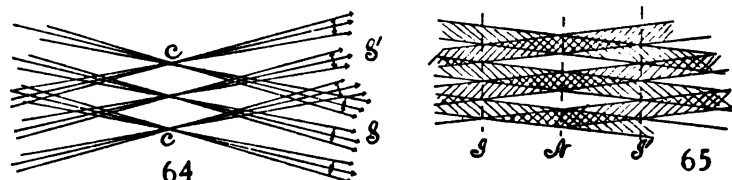


does it not appear at all in the case of parallel pencils, when it is so obtrusive in the case of crossed pencils of rays? Again, the interferences are unquestionably due to $D_1$ and $D_2$ light, simultaneously. If the grids for these two wavelengths should be at a slightly different angle to each other, their superposition would give something like the observed phenomenon, apart from details. Thus in figure 65 the two grids due to $D_1$ and $D_2$, intersecting at a small angle, may be interpreted as appearing strand or cord like at $N$, and neutral at $I$ and $I'$. With white light the linear phenomenon would eventually become achromatic.

But, again, why should lines so close together as $D_1$ and $D_2$ show any appreciable difference of angle or rotational phase-difference in their interference pattern? Intersecting grids, moreover, can be produced by other methods and nearly always betray their origin. The final inference is that suggested by figures 63 and 64, that homogeneous rays on crossing (here in a medium of plate glass) may exert a lateral influence on each other, to the effect that identical rays emerging from the crossing are arranged in equidistant nodal planes according to figure 63.

**40. Experiments. Reflecting grating. Crossed rays.**—In the preceding experiments the remarkable phenomenon of double interferences was obtained with glass-plate apparatus. It is improbable that any secondary interference can have been produced by the presence of reflected light, since the reflected pencils will be weak as compared with the primary pencils and

differently situated. It is nevertheless necessary to forestall all misgivings by avoiding glass plates altogether and adapting the methods of figure 57, where reflecting surfaces (front faces) only are present, to the experiment for crossed rays $mN$ and $nM$.

In the apparatus as finally perfected, $G$, figure 57, was a Michelson plate grating and $G'$ a Rowland concave grating, each with about the same grating constant. A strong lens was placed at $T$ for observation at the focus of the concave mirror of $G'$. The latter was capable of fore-and-aft motion, of rotation about a vertical axis in its own plane and about an axis normal to that plane; $G$ was capable of rotation about a horizontal axis parallel to its plane. Thus the possibility of fore-and-aft motion and the three cardinal rotations for the gratings, together with a micrometric fore-and-aft motion of $M$, was at hand, as well as the rotation of $M$ and $N$ about horizontal and vertical axes.

The interferences were found after establishing the coincidence of the yellow homogeneous fields, in the manner described in the preceding paragraph. The fringes were at first small and apparently single, but they could be enlarged at pleasure and the two definite systems separated by fore-and-aft motion of $G'$. They occupied only a part of the wide yellow slit image, the sodium arc being used. On actuating the micrometer at $M$ there was displacement of the interference pattern as a whole, so that the conditions of displacement interferometry are here also implied, though the equations are liable to be different. On rotating $M$, micrometrically, about a vertical axis, the structure of the interference reticulations changed and was at times reduced to a single set.

Whenever the arc flashed, or when white light was used, the linear phenomenon appeared alone, either cross-hatched or longitudinal, depending upon the character of the reticulated pattern for homogeneous light. With sunlight, even after narrowing the blade from the collimator and screening off red and green light, the phenomenon was faint and hard to find, unless it was produced alternately with sodium arc.

With the arc freshly charged with sodium, but a single set of interferences or else the linear phenomenon appears, since the broadened sodium lines are equivalent to a continuous spectrum in this region. Not until the excess of sodium has all been evaporated and the sodium lines are normal does the true reticulation show itself. It is interesting to describe two cases of this double-interference pattern, obtained by gradual and successive fore-and-aft motion of the grating $G'$, between limits, while the edges of the two wide-slit images, respectively horizontal and vertical, are kept in contact throughout.

Suppose the original fine fringes to be nearly vertical; then the apparently simple fringes, $a$, figure 66 (their appearance, however, would lead one to suspect their simplicity), change to the cord-like strands $b$, appearing like helices of a very large pitch. Both interference fringes are still nearly parallel, and they cover the whole wide-slit image uniformly. These eventually pass into the square or rectangular reticulation, $c$, with both systems equally strong. Probably intermediate forms have here been skipped. The system, $e$, occurs

very soon afterward, in which the difference in size of fringes has become enormous. Following *e*, the procession is reversed in *g*, *h*.

Both systems (*α* and *β* systems, say) have passed through maxima, but not at the same time, or not for the same fore-and-aft adjustment. Both systems have rotated, the rotation being very rapid near the maximum. The reticulations quiver and look precisely like capillary waves in a rectangular trough of mercury, except that they are usually at an angle to the bounding edges of the superposed slit images.
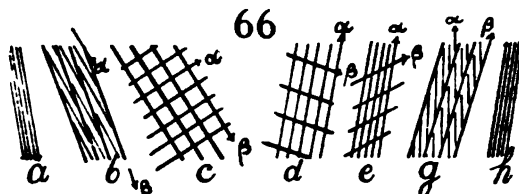


In this quivering system of two identically strong fringes it is difficult to make out the rotations, but after considerable revision the sequence in figure 67 was definitely ascertained. Beginning with the extreme fore-and-aft position of *G'*, and moving it successively forward in steps of 1 or 2 millimeters, the apparently single grid, 1 changes to 2, where the two systems *α* and *β* can be disentangled, *α* expanding and rotating more rapidly, so that 3 and 4 follow. Here *α* is horizontal and probably of maximum size, *β* is still nearly vertical and but slightly expanded. Therefore, while the *α*-effect wanes the *β*-effect waxes, and the squared or orthogonal type, 5, is produced. The lines are here equally strong and it is the symmetrical figure of the series. Thereafter in 5, 6, 7, 8, and 9 the chief expansion and rotation is transferred to the *β* system, with which the *α* system has changed functions. Hence both systems rotate nearly 180° in the same direction and pass through maximum size; but the maximum is retarded in rotational phase for one as compared with the other. Rotation and growth are accelerated near the maximum. The total displacement of the grating *G'* between the cases 1 and 9 (fig. 67) was about 2 cm.; but this depends upon the obliquity of the grating and incidental conditions, as explained above.
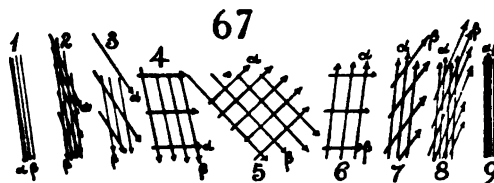
Suppose, in the second place, that the original fringes, 1, figure 67, were nearly horizontal; in such a case the evolution is much the same, but the symmetrical form number 5 becomes smaller and more and more flatly rhomboidal horizontally. Probably the scheme of rotation is the same, but is much harder to ascertain in view of the flat forms. On the other hand, the field now abounds in vertical strands of interferences, like those of the preceding paragraph, and nodules are often in evidence, as before.

If the original lines are quite vertical, they do not seem to rotate with fore-and-aft motion of *G'*, but form intersecting, vertical, apparently simple systems throughout the motion. Slight departure from the vertical produces rhomboids very long vertically and often very coarse.

**41. The same. Compensators.**—A compensator of ordinary plate glass, at the intersection $c$, figure 57, produces no effect, if symmetrical to both beams. If not symmetrical, the interferences are displaced to right or left in the field of the telescope, as in any case of displacement interferometry, depending on which component beam receives the longer glass-path. Thus this adjustment corresponds to the grating in the preceding paragraph, the difference being that in the latter case the same ruling is used for both diffractions. Hence the interference figures obtained are simpler, showing vertical strands only. In the present case strands occur in all directions. The maxima for oblique positions of the glass plate were not found with reflecting gratings.

If the compensator is within 1 inch in thickness, its introduction occasions no difficulty. The interference pattern may be changed, but it remains the same during the rotation of the compensator; but if the latter is thicker than 2 inches, the figure is usually so small as to be found with difficulty, unless the grating $G'$ is brought forward, to allow for the mutually inward refraction of the rays. If this is done, the same figure may be reproduced. On advancing the grating, plate compensators much over 3 inches thick were tested without the slightest annoyance. Lenticular compensators require special adjustment and are very difficult of use.

The effects of rotating the grating about the three cardinal axes have all been considered above. In the present instance two sets of fringes are symmetrically rotated, subject to the same conditions. Rotation of $G'$ around a horizontal axis requires an elevation or depression of the arc lamp, if the fringes are to remain in the field. Rotation around a vertical axis separates the slit images, and a readjustment for superposition is necessary. Results so obtained are therefore complicated and were not studied.

**42. Miscellaneous experiments. Fringes with mercury light.**—A few random experiments made with the sodium arc, in the presence and absence of the magnetic field, showed no results; nor was this to be expected, as a reasonably strong field would blow out the arc. Again, the insertion of a glass compensator, 0.7 cm. thick, in one of the component beams, developed no maximum on rotating the compensator about a vertical axis. Thus with reflecting gratings the peculiar behavior of the transmitting grating, showing a maximum on either side of a symmetrical minimum (§36, 37), is not reproduced.

The effect of rotating the first reflecting grating $G$ on a vertical axis is only to throw the sodium light out of one side or the other of the (superposed) slit images. No available means of enlarging the fringes indefinitely was found. It is probable that this would require fine adjustment for symmetry. The field of interference, as a whole, is within a spot-like area which may be moved up and down, or right and left, by the vertical and horizontal adjustment screws on the mirror $M$. Coincidence at the two sides of the slit favor different interferences. The case is always as if, at a single point of the field only, there were actual coincidence, and that the interference pattern is grouped closely around it.

With the use of an ordinary glass mercury lamp (27 storage cells, 5 ampères) the fringes are found with difficulty when the beam at the first grating is wide. On using a vertical blade of light the definition was improved. The fringes are faint, very susceptible to motion, and at times even absent. They occur, however, as a *single* set, as was anticipated, showing that the above duplicated fringes are actually due to the two sodium lines. The mercury fringes are easily rotated and pass through a horizontal maximum with fore-and-aft motion. Rotating G about a normal axis may further increase this maximum size to a limit at which the fringes appear irregular or sinuous. A displacement of the mirror M over 0.7 cm. was easily permissible, without destroying the fringes. They occur, as above stated, within a certain adjusted spot area of the field of view. An attempt was again made to detect a Zeeman effect by placing the poles of an electromagnet on the two sides of the lamp; but here again no difference was discernible on opening and closing the electric circuit. The field, however, for incidental reasons, could not be made strong enough for a critical experiment.

**43. Inferences.**—After these experiments (made with the apparatus figure 57, free from glass plates and depending on reflections only) the cause of the phenomenon is no longer obscure. Obviously one of the paired grids in figure 66 or 67 belongs to each sodium line. The retardation of one phenomenon, rotationally, as compared with the other, is due to the difference in wave-length between $D_1$ and $D_2$. The phase-difference between numbers 4 and 6 (fig. 67) is thus equivalent to 6 Ångström units. If the displacement of $G'$ is about 0.3 cm., there should be about 0.5 mm. displacement, fore and aft, for 1 Ångström unit. If the grating, $G'$, is on a micrometer, this should be a fairly sensitive method of detecting small differences of wave-length, or give evidence of doublets lying close together. The sensitiveness clearly increases with the length of path of the component rays and may thus be increased.

With this definite understanding of the phenomenon, it is desirable to deduce the equations, which in the occurrence of parallel rays would not differ essentially from those of Chapter II or III. It is useful, however, to treat the new case of crossed rays. In figure 69 the angles of diffraction are $\theta_1$ and $\theta_2$, if the incidence of light, $L$, is normal at $G$ and at an angle $i_2$ at $G'$, $G$ and $G'$ being parallel. The mirrors are set symmetrically at angles $\sigma_1$ and $\sigma_2$ to the normal in question, and the diffracted rays are reflected at angles $\alpha_1/2$ and $\alpha_2/2$, respectively. The reflected rays cross the normal at an angle $\beta$. Then

$$\sin \theta_1 = \lambda/D_1 \qquad \sin \theta_2 = \lambda/D_2 - \sin i_2$$

where $D_1$ and $D_2$ are the grating constants. From the figure

$$\alpha_1/2 = \theta_1 + \sigma_1 - 90° \qquad \alpha_2/2 = \theta_2 + \sigma_2 - 90° \qquad \theta_1 = \alpha_1 + \beta \qquad \theta_2 = \alpha_2 + \beta$$

From these equations,

$$D_2 \sin i = D_2 \sin (2\theta_2 + 2\sigma_2 + \beta) - D_1 \sin (\dots)$$

If $D_1 = D_2$, then $\theta_1 = \theta_2$, $\sigma_1 = \sigma_2$, and therefore $i_2 = 0$.

Thus the relations are quite complicated, but if $D_1 = D_2$, or the gratings have the same constant, rays of all wave-lengths should, after double diffraction, issue normally to the grating $G'$, and the arrangement is therefore achromatic. If $D_1$ is not quite the same as $D_2$, but nearly so, an adjustment of $\sigma$ would probably meet the case approximately. If the original incidence is at an angle $i_1$, $D_1 \sin i_1$ would have to be subtracted from the first member, but the diffractions would now differ on the two sides of the apparatus.

The relations of the rotations of the striations of $D_1$ and $D_2$ light to the fore-and-aft motion is next to be considered. It will be convenient to make use of figure 68 for this purpose, the notation being the same as in figure 69. The two rays, 1 and 2 ($D_1$ and $D_2$), have both been introduced, and the position of $G'$ is such that the $D_2$ rays intersect in its face and are diffracted into $T_2$. In such a case the combined pencil is divergent, $D_1$ rays will undergo an earlier intersection, and consequently be separately diffracted into $T_1$ and



$T'_1$. Hence $D_1$ and $D_2$ are differently circumstanced in relation to the fore-and-aft motion, and the rotation produced will thus be advanced in one case, as compared with the other, for the reason discussed in Chapter III, paragraph 26. It is also clear that the difference of phase in the two rotations will be greater, as the total path of rays between $G$ and $G'$ is greater, so that the large distances used in the present experiments (nearly 3 meters) account for the astonishing sensitiveness of the phase of rotation to the wave-length difference. In fact, $D_2$ will be in the same phase as $D_1$, if the grating is moved forward from $G'$ to $g'$, figure 68, since in both cases the rays intersect in the normal. Hence if $R$ is the total path $GmNG'$, and if the angle of dispersion between $D_1$ and $D_2$ is $d\theta$, $\theta_2$ the angle of diffraction at $G'$, and $h$ the displacement from $G'$ to $g'$, $D$ the grating space,

$$Rd\theta = h \sin \theta_2$$

or

$$d\theta = \frac{h\lambda}{DR}$$

and the resolving power

$$\frac{d\lambda}{\lambda} = \frac{h}{R \cos \theta_2} = \frac{Dh}{R\sqrt{D^2 - \lambda^2}}$$

In the given adjustment, roughly,

$$d\theta = 3.7 \times 10^{-4} \qquad R = 300 \text{ cm.} \qquad \theta_2 = 20°$$

whence

$$h = \frac{3 \times 10^2 \times 3.7 \times 10^{-4}}{0.34} = 0.3 \text{ cm.}$$
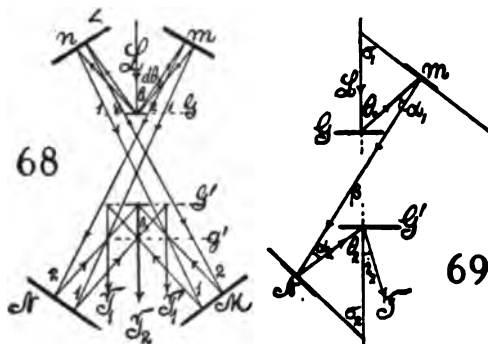
As the resolving power is, roughly, $h/R$, and if $h = 0.003$ cm. is still appreciable,

$$d\lambda/\lambda = \frac{3 \times 10^{-3}}{3 \times 10^{2}} = 10^{-5}$$

*i.e.*, lines 1/100 of the distance apart of the sodium lines should be rotationally separated.

Again, the displacement, fore and aft, between like rotational phases of $D_1$ and $D_2$ should be about 3 mm., and this agrees fairly well with the order of values found.

The case of the transmitting grating (fig. 59) is thus also elucidated, though it is not clear to me why the duplication of fringes is so efficiently concealed in the nodular forms observed. The reason for the minimum of size, for the symmetrical position $i = 0$, and the two maxima for oblique positions of the grating ($i = \pm 20°$ about), suggests an explanation similar to that given in Chapter II. In other words, in the oblique position the short path-length is compensated by the increased thickness resulting from the greater obliquity of grating, whereas the long path-rays traverse the plate of the grating more nearly normally. In this way the path-difference is reduced as compared with the symmetrical position, and the fringes are therefore larger. The oblique grating acts as a compensator in both of the component beams, and the fringes may be visible, even if in the original position (fig. 59) they are all but invisible. If, however, the apparatus (fig. 57) is used with a plate-glass compensator symmetrical at $c$, there are no maxima or minima for any obliquity. Hence the tentative explanation for the case of figure 59 is not warranted.

The fore-and-aft motion of the plate grating (fig. 59) produces no effect, since the rays are reflected back so as to retrace their paths. They are also reflected between parallel mirrors $N$, $m$ and $n$, $M$. Thus the path-difference is not modified. The result is merely a decrease of the distance $M$, $N$, and a corresponding increase of $m$, $n$, and *vice versa*.

The marked effects produced by rotating the transmitting grating around a normal axis, finally, follow the explanations given for the rotation of fringes of non-reversed spectra in Chapter III, paragraphs 25 and 26.

In conclusion, an interesting application of the apparatus (fig. 56) or the other similar types may be suggested. By half-silvering the mirrors and providing a similar opaque set *beyond* them, there should be no difficulty (in the case of homogeneous light) of bringing the interferences due to crossed rays, $c$, and to parallel rays, $a'b'$, into the field of the telescope *together*. Strictly homogeneous light (mercury arc) would be needed to obviate the duplication of the sodium arc. In such a case, therefore, the parallel fringes could be used after the manner of a vernier on the crossed fringes, with a view to a repetition of the experiment of Michelson and Morley, if this experiment had not been so thoroughly carried out by the original investigators. However, the plan would be to rotate the apparatus, as a whole, so that the two crossed rays would be alternately in and at right angles to the earth's motion, whereas the two parallel rays would preserve the same relation to that motion. Naturally, the parallel and crossed paths would in such a case have to be lengthened by multiple reflections.

# CHAPTER VI.

## CHANNELED SPECTRA OCCURRING IN CONNECTION WITH THE DIFFRACTIONS OF REFLECTING GRATINGS.

**44. Introductory.**—Throughout the preceding work I had noticed that the spectrum due to either of the component beams, after successive reflection from two reflecting gratings, was often regularly furrowed by transverse black bands, before the two spectra were brought to interfere. As these fringes are stationary, they do not modify the phenomenon investigated; but questions now arise as to whence these reflected fringes of a *single beam* come. They are not strong, as a rule, and I was therefore inclined to attribute them to some imperfection of the silvering of the opaque mirrors, but this proved not to be the case, so that it seemed worth while to examine them by special experiments.

**45. Apparatus.**—The apparatus for this purpose, as one beam only is wanted, is quite simple. In figure 70, L is a vertical blade of parallel rays of white light from a collimator and slit. These rays impinge on the plane grating G, whence the orders 1, 2, 3, etc., of spectra are reflected. Either of these pencils may be received by the second grating G', plane or concave, from which spectra of any order are available. If o denotes the reflected pencils, the groups from two gratings may be distinguished as (3, 1), (3, 0), (3, −1), (3, −2), etc., as in the figure. Any of these two different pencils is to be examined at T by a lens or telescope, for instance, and the latter (with strengthened objective where needed) is more convenient, even when the concave grating is used. A wide slit S, revolvable about G, is often useful for screening off spectra or parts of spectra. In some experiments the grating G' may be replaced by an opaque mirror.
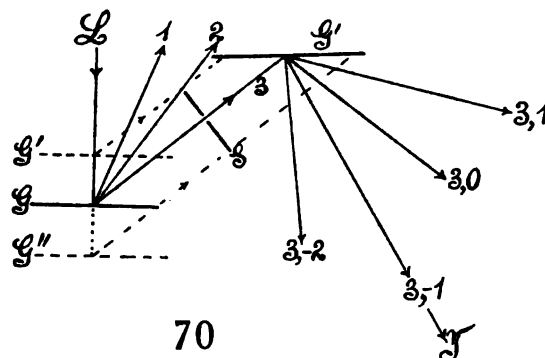
The gratings are provided with the usual adjustments for parallelism of rulings and slit. G' and T must be capable of considerable right-and-left motion, and G, in particular, of controllable fore-and-aft motion.



70

**46. Scattering.**—An interesting result of this work is the evidence and spectroscopic quality of scattered rays, incidentally encountered. For instance in figure 70, if the slit S is narrow, it cuts off all the rays but the orange yellow of the third order, and the reflected spectra (3, 1), (3, −1), etc., will largely

consist of orange-yellow light. Associated with each of these reddish-yellow patches, however, are vividly violet-blue patches, each separated from the reddish yellow by an almost total absence of green, relatively speaking. If the light is very intense, the connecting part of the spectrum also appears, but it is always far less vivid than the ends of the spectrum in question.

Inasmuch as all violet radiation proper has been screened off at $S$, it is obvious that violet light must have been scattered in all directions from $G$, a part of which, therefore, passes the slit and is resolved by the second grating $G'$. Moreover, as the scattering lines of the grating are equidistant, the scattered light has a regular wave-front. (Cf. Carn. Inst. Wash. Pub. No. 229, 1915, pp. 100—102.)

The correlative experiment of detecting the reddish light transmitted after scattering was also tested. For this purpose the reflecting grating $G$ may be replaced by a transmitting grating, slit $S$ placed beyond, and the light then analyzed by a second grating $G'$ behind the slit and diffracting toward it on one side. But no results of value were obtained.

**47. Fringes with white light.**—The experiments with the apparatus (fig. 70) were commenced with sunlight and (what is essential) a fine slit. Fringes are found in all combinations of doubly diffracted pencils (3, +1), (3, −1), (3, −2), etc.; (2, 1), (2, −1), etc.; (1, −1), (1, 1), etc., but none in the reflected pencils (3, o), (2, o), (1, o), etc., as a rule. Whether the grating $G'$ be concave or plane, it is best to use a telescope at $T$, because (when provided at the objective with an auxiliary concave or a convex lens) it more easily offers a wide range of observation along its axis than an ocular. The latter must be wide and has to be shifted bodily; but both methods were used. A concave grating at $G$ and plane grating at $G'$ gave no results. The concave grating is usually more free from channeled spectra.

Of the great variety of fringes obtained, I shall give only two typical examples. The second order of spectra for $G$ (plane) was separated from the others by the slit $S$ and diffracted into $G'$ (fig. 70). The successive fringes appear as the ocular is drawn *outward* from the principal focus.

Combination $G2$, $G'$o: Only a good sodium doublet, which became washed on drawing out the ocular of $T$, was obtained; no fringes appeared.

Combination $G2$, $G'−1$: Just outward from the principal focus a large, coarse, irregular set of fringes appeared; next (ocular farther out) a large regular set, somewhat diffuse, possibly double and superposed; then a finer, half-size, very regular set, possibly decreasing. After this the mottled surfaces of the gratings were successively in focus. A weak spectacle lens was now added to the objective of $T$, whereupon very large regular fringes were seen when the ocular was far out.

Combination $G2$, $G−2$: The ocular moving outward from the principal focus, the fringes seen in succession were as follows: large, regular, vague; half-size sharp; surfaces vertically striated; (lens on) fine regular set in red; doubled regular set in green.

Combination $G_2$, $G-3$: Fine set just before the surfaces appeared, which were delicately striated; fine regular set; coarse set, both close to surface; (with lens on) fine regular set; doubled, strong regular set.

Different distances between $G$ and $G'$ had very little influence on the size of the phenomena. A few examples may be given, which are observed when the ocular is moved outward.

$G_3$, $G_1$: Distance 10 cm.—Fringes, faint regular; strong irregular; faint regular; flat field; surfaces visible; faint regular.

Distance 25 cm.—Strong irregular; faint regular; small regular; large (double) irregular; lines slit into fine fringes; large faint regular.

Distance 46 cm.—Large strong, with two absorption bands; fine regular; double-sized faint; surfaces with fine striations; alternations of fine and coarse lines; faint, regular, large, etc.

Fringes of different color are often in different focal planes. When a lens is used with the concave grating, observations must sometimes be made 2 meters off to get the large regular fringes. Red fringes may be narrower than the corresponding violet set.

If the grating $G$ is moved fore and aft, parallel to itself, the fringes are shifted across the stationary sodium line, as in displacement interferometry.

Whereas in the positive combination (3, 1), (3, 2), etc., the spectra widen, they tend to close up for the negative combinations (3, —1), (3, —2), etc. With two identical plate gratings they may image the white slit. But this seems to have little effect on the fringes seen as a whole when the ocular is out of focus.

When *white* light is used and the grating $G'$ replaced by an opaque mirror, or in case of combinations which involve direct reflection (2, 0; 3, 0; etc.) at $G'$, there seem to be no fringes.

**48. Fringes with sodium light.**—While there is some difficulty in obtaining the fringes with white light, fringes with homogeneous light are obtained at once, provided the light is sufficiently intense. A sodium arc lamp, or a mercury lamp, with a fine slit, must therefore be used. In this case, moreover, the grating $G'$ may often be replaced by an opaque mirror, or the fringes of the order $G_2G_0$, $G_2G_0$, etc., may be produced with entire success. On moving $G$ fore and aft, they again travel across the sodium line. Often, in fact, two sets of fringes seem to be shifted. A few examples again may be given of the great variety in this display while the ocular is being drawn out:

$G_1$, $G'-2$: Sodium lines $D_1D_2$ single size; large strong fringes, lines split.

$G_1$, $G'-1$: Closed spectrum; striations continuous.

$G_1$, $G'_0$: Reflection; $D_1D_2$ single size; surfaces of gratings finely striated.

$G_1$, $G'_1$: $D_1D_2$ double size; strong grid seen very near the surface of $G'$.

$G_1$, $G'_2$: $D_1D_2$ treble size, out of reach.

$G_2$, $G'_0$: Reflection; no fringes.

$G_2$, $G'-1$:  Distance 12 cm.—Coarse irregular; with lens fine regular
set, near and beyond the surfaces.

$G_2$, $G'-1$:  Distance 45 cm.—Surfaces with doubled fine striations;
with lens finally strong and regular.

$G_2$, $G'-1$:  Distance 60 cm.—Regular faint; irregular double, very
strong; surfaces striated; with lens strong double irregular;
finally regular small.

$G_3$, $G'1$:  Regular; regular line split; irregular coarse; surfaces finely
striated, $G$ coarser; fringes grow continually larger without
vanishing.

On moving $G$ fore and aft, two grids seem to travel through each other in
opposite directions.  This probably accounts for the occurrence of irregular
fringes.  The size of fringes seems to be a minimum for a conjugate focus
near the surfaces.  The whole phenomenon is continuous.  Irregular fringes,
probably superpositions, become regular in other focal planes.

$G_3$, $G'2$:  About the same; minimum size at the surfaces, increasing
about three times as the ocular is drawn either way.

$G_3$, $G'0$; also $G_3$, mirror:  About the same results, only brighter and
better.  Hence in case of large dispersion two gratings are not
needed.  The two sodium lines, when the ocular is drawn out
of focus, multiply themselves at regular intervals, so that the
grids are sometimes distinct, sometimes partially superposed.
Thus the classic diffraction phenomena of a slit suggest them-
selves as the starting-point for an explanation of the present
phenomena as a whole.

$G_3$, $G'0$, produced alternately with sodium light and sunlight, showed
the same sequence of fringes (the large ones with a tendency
to split) in the former case, while nothing appeared in the case
of white light.

**49. Grating on a spectrometer.**—It seemed necessary, therefore, to con-
sider the diffraction of a fine slit, when seen in the telescope, somewhat in
detail.  In Chapter III the production of beautiful Fresnellian interferences
from two identical slit images and homogeneous light was demonstrated; but
an equally clear manifestation of the diffraction of a slit image, when the
ocular is out of focus, does not seem to occur.  The broad image of the slit
out of focus shows a stringy structure only, but no separation is easily obtain-
able.  Fringes, as such, are quite absent when the ocular is drawn out.

The light of the sodium arc was now passed through a very fine slit and
collimator and reflected from a plate grating.  The above intermittently
regular and irregular fringes were strikingly obtained with the ocular out of
focus.  As this is successively more and more drawn out, fine lines become
coarser, and then seem to subdivide, giving the structure a fluted appear-
ance, frequently regular.  There is, in other words, a double periodicity.  In

the case of highly diffracting grating ($D = 10^{-6} \times 175$), the results appear best in the second order.

The same beautifully duplicated fringes were obtained with a transmitting film grating of about the same dispersion, particularly well in the first order.

The sodium flame gives too little light for the present purposes, but the phenomenon is seen.

Believing that some irregularity might be introduced by the double-sodium line, I installed a mercury lamp for comparison. In the first experiment a film grating ($D = 173 \times 10^{-6}$) was used, the ocular traveling outward from the principal focus. Both the green and the double yellow mercury lines enlarged and showed fringes of increasing size and number together. The green field had a darker band, the yellow a bright band in the middle. As the fringes enlarged, each split up into secondary fringes, 4 or 5 eventually, and this again occurred for both green and yellow fields.

Rotating the grating around a vertical axis seemed to shift the primary fringes laterally over the stationary secondary fringes. A concave lens for positions anterior to the principal focus and a convex lens for posterior positions (toward the eye) were successively added to increase the range of observation. On both sides of the principal focal plane (fig. 71) fringes occur, which enlarge with the distance $x$ from that plane. As they enlarge, each fringe splits up into secondary fringes, which in turn enlarge.



Sometimes the arrangement is irregular. Green and yellow fields may overlap, but they do not do so conformably.
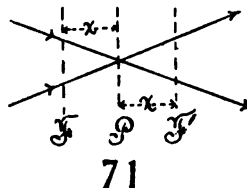
The undeviated ray, however fine the slit may be, merely shows a stringy field, sometimes suggesting structure, but never showing clear-cut fringes.

The same kind of results were obtained with a reflecting grating of about the same dispersive power. In the second order the fringes were particularly clear and regular. Primary fringes, finally, carried three to four secondary fringes each.

Next, a ruled transmitting grating of less dispersive power (grating constant $352 \times 10^{-6}$ cm.) was adjusted for mercury light. Here in the undeviated ray and in the first order no clearly separated fringes were obtained. In the second and third orders, however, they were very perfect, and followed the above rules, showing sharp secondary fringes.

It follows, therefore, that a certain degree of dispersion is needed to resolve the fringes, which is inadequate in amount in the order zero, in this case, and scarcely so in the first order. In the higher orders the conditions are met. Using a very fine slit, however, I later just succeeded in separating the fringes in the first order.

Finally, I returned to the endeavor of detecting diffraction fringes in the undeviated image, using a micrometer slit, a good achromatic lens (or no lens), and a distant (2 meters), moderately strong telescope. In this case separated and distinct diffraction fringes, white throughout, were undoubtedly obtained. They moved with the eye so as rarely to be stationary and in the same direc-

tion if the ocular is drawn out, or the reverse if it is thrust in. On close examination two sets, in different focal planes, seemed to be present, one stationary and the other moving as described, and accounting for the observed pronounced parallax. Suggestions of movable fringes accompanying the stationary are also present when the latter are produced by the grating. In this case the stationary fringes are strong; in the case of simple diffraction the movable fringes are more prominent.

**50. Inferences.**—There can be no doubt that the great variety of channeled spectra obtained, when white light is successively diffracted by two gratings, is referable to the fringes obtained in the diffraction of homogeneous light, observed outside the principal focal plane, on a spectrometer. In other words, if light of a given pure color (sodium, mercury) is used, a single grating suffices. Each line of the spectrum is resolved into well-defined groups of fringes, if it is observed either in front of or behind the principal focal plane. The arrangement of fringes varies in marked degree with the distance of the plane observed from the latter ($x$, fig. 71). If reflecting gratings are used, there is no other possible source of interferences; but reflecting and transmitting gratings show the phenomenon equally well.

After finding how easily the Fresnellian interferences of two virtual slits could be reproduced in the telescope (Chapter III) and observed on either side of (before or behind) the sharp images, it seemed reasonable to suppose that the diffraction of a slit could also be produced and exhibited in this way; but the availability of this anticipation is attended with much greater difficulty. The image of a very distant slit does indeed show separated diffraction fringes on either side of the principal focal plane in the observing telescope. But they move right and left with the eye, in the same direction if the ocular is drawn outward from the principal focal plane, and in the direction opposite to the eye if the ocular is thrust in. Hence, in this respect, the fringes do not at once recall the phenomena under consideration. Usually the blurred image, out of focus, is stringy, without definite structure. It is resolved in a single focal plane only.

To obtain sharp stationary fringes from an image of the slit, this image must be produced by the diffraction of a grating having a dispersing power above a certain minimum. Thus in a grating of about 7,000 lines to the inch the undeviated slit image and the image of the first order are not clearly resolved, unless the slit is very fine. In the second and higher orders, however, the resolution is very pronounced and the fringes stationary.

The resolution of fringes is equally manifest in front of or behind the principal focal plane, so that if a weak convex lens is added to the objective of the telescope, the succession of fringes is found with an outgoing ocular; if a weak concave lens is added to the objective, the succession is found with an ingoing ocular, starting in each case near the principal focus. As the fringes increase in size they in turn subdivide, sometimes irregularly, as if each fringe were a new slit image, capable of undergoing secondary diffraction. Beyond these secondary fringes no further resolution was detected.

Returning to the work with two successive gratings and white light, the channeled spectra obtained are too complicated for concise description. A very interesting result, however, is the passage of the fringes across the stationary sodium line, when the first grating $G$ is moved fore and aft in a direction normal to its plane. The region of the $D$ line is thus alternately dark and bright. The direction of these rays remains unaltered while the illumined strip is shifted horizontally across the ruled space (fig. 70) of the second grating. Usually it is difficult to see the $D$ line in the focal plane of the fringes. When homogeneous light is used this fiducial mark is necessarily absent and the cross-hairs of the ocular must be supposed to replace it. The shift of the fringes is then equally obvious, and sometimes (sodium light) different groups seem to travel in opposite directions while the grating $G$ moves in one direction. In case of homogeneous light and two gratings, moreover, the fringes seem to be of minimum size in the conjugate focal plane of the gratings. They increase in size and in turn split up in focal planes before and behind this.

An insight into these occurrences was finally obtained in observation with homogeneous light in the spectrometer by shifting the grating (transmitting) in its own plane, right and left. The fringes in such a case move *bodily* across the field of the telescope, new groups entering on one side for those which leave on the other. These fringes, even if quite distinct, are differently arranged in coarse and fine series and are frequently accompanied by dark or bright bands. This probably also accounts for the effect of the fore-and-aft motion of the grating, mentioned above. Moreover, it would be interesting to search for repetitions of given groups of fringes while the grating is being shifted parallel to itself, from end to end, as this might indicate the residual imperfections of the screw with which the grating was ruled. If the ocular is drawn and set outward from the principal focal plane (at which the slit image is quite sharp) into a different position, the fringes move in a direction opposite to the grating. If the ocular is set inward from the principal focal plane, they move in the same direction as the grating. This would not be unexpected; but secondary fringes or something else in the field seem to remain stationary. Successive fields may be quite different as to arrangement of fine and coarse lines, but all plane gratings exhibit the same phenomena. Thus it is obvious that the fringes of the present paper result from a residual irregularity in the rulings of the grating. Micrometrically, the successive strips of a slit image, however fine, are of unequal intensity. Between these there is diffraction, as may be tested by examining the clear glass at the edge of the ruled space.

To attempt a theory of these phenomena seems premature; but it is obvious that in the otherwise indistinguishable images of a slit in homogeneous light, however sharp or however narrow, the nature of its origin still persists and may be detected by observations outside of the principal focal plane. A fine slit is in all cases presupposed, and all the phenomena vanish for a wide slit. On the other hand, the width of the pencils of parallel rays may be far greater than is necessary to show the strong Fraunhofer lines, if indeed there is any limitation to this width.

# CHAPTER VII.

**51. Purpose.**—It is preliminarily the object of the present paper to examine a variety of new methods for the production of interferences with spectra, with a view to the selection of as simple a design as possible for practical purposes. Some interesting differences appear in the results, so that the simplicity of construction does not necessarily recommend the apparatus for use.

In the second place, the endeavor will be made to assemble appurtenances in such a way that the extremely mobile phenomena may be under control, even in a moderately agitated laboratory. In case of the early interferometer experiments, the interferences disappeared on merely touching the apparatus, and are rarely or never at rest; whereas it is, of course, necessary that they should remain visible while the micrometer is being moved. These experiments are now nearly completed, but will preferably be described in a succeeding report.

**52. Methods and apparatus.**—Some prismatic methods were tested in the earlier volume, but not developed; for the plan of using a transmitting grating twice, or two gratings in succession, seemed to contain greater promise. The prism method is, however, more simple than any of the others and therefore deserving of special study.

In figure 72 the large right-angled prism $P$, with its faces silvered, receives the pencil of parallel white rays, $L$, on its orthogonal faces and reflects them to the plane opaque mirrors $n$ and $m$. From here the rays are further reflected, either nearly in parallel, as in the figure, or crossed, as at $c$, $c'$, to the remote opaque mirrors $N$ and $M$, which in turn reflect them to the plane or concave grating $G$. If the rays converge at the appropriate angle of diffraction, $\theta$, a selected color will be diffracted in the direction of the normal to $G$ in each case. If the two paths are nearly equal, these rays will therefore interfere in the axis $GT$ and the results may be observed by a telescope or a lens at $T$. In my apparatus the distances $mM$ and $nN$ were of the order of 2 meters. In consequence of the three successive reflections, it is somewhat difficult to
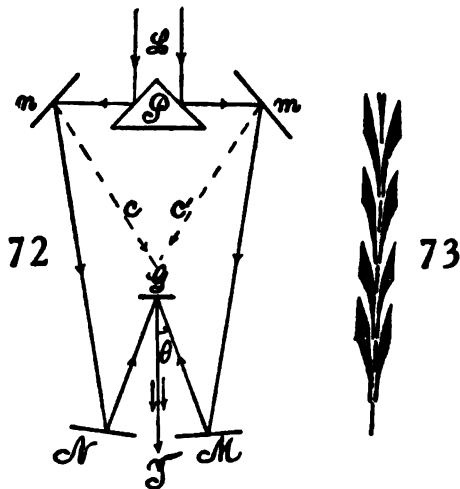
obtain spectrum lines normal to the axis of the spectrum, so that if the latter are superposed the lines will be at an angle. But if this is small, it does not seriously interfere with the occurrence of fringes, as they extend from top to bottom of the spectrum.

The appearance in general is of the linear character heretofore described. They pass symmetrically from extreme fineness, through a maximum size, to fineness again, with the fore-and-aft motion of the grating $G$, and they usually rotate near the maximum.

If the mirror $M$ is displaced nearly in a direction normal to itself, on a micrometer, the fringes undergo the same evolution, and in this respect differ from the case where the primary differentiator, $P$, was also a grating. In this case the displacement of $M$ showed no discernible modifications of the size or character of the fringe pattern. The fringes merely moved. In figure 72 the effect of moving $G$ or $M$ fore and aft is similar, since it throws the point of convergence of the rays $NG$ and $MG$ in front of or behind the grating. The result is therefore different when white light impinges on $G$ from what it is when the light is already nearly homogeneous.

The limit of visibility is also inferior to the double-grating method heretofore used, for the fringes passed between the limits of visibility through the maximum size, for a displacement of $M$ of only about 3 mm. Smaller ranges may occur. On limiting the incident beam at $L$ to a breadth of about 0.5 cm., the fringes became much broader and relatively intense.

There is, of course, an abundance of light, so that the screening of the incident beam is not disadvantageous. In this case, when the fore-and-aft position (illuminated strips on the grating coincide, as in figure 72) and the position of the grating relative to its normal axis were carefully adjusted, large arrow-headed fringes, as in figure 73, were obtained, usually less closely packed vertically. Apart from tremors, these move slowly up and down (breathing), as a result, no doubt, of changes of temperature in the air-paths. A mica film inserted into one beam and slowly rotated produced similar motion, besides introducing its own grid of vertical and parallel fringes. The reason for the occurrence of these arrows is not quite clear to me, though they are associated with horizontal fringes and homogeneous light, the doubly inflected forms belonging to inclined fringes and homogeneous light.

In the endeavor to reproduce these fringes with the sodium arc, I failed after long trials. The reason may be sought in the flicker of the arc, whereby the beam passes from one side to the other of the edge of the prism $P$, but it is probably due to the inadmissibility of a wide slit.

**53. The same. Crossed rays.**—The present method, using four mirrors, has, nevertheless, the advantage of admitting the use of either parallel or crossed rays. Inasmuch as these rays are white until they leave the grating, the method is interesting. On being tested it showed the same peculiarities as the preceding. The crossed rays ($cc'$, figure 72) are more nearly normal to the mirrors $M$ and $N$; nevertheless the range within which the interfer-

ences are visible is not above 2 mm. of displacement of $M$. The fringes may, as usual, be made as large as possible, by first superposing the two illuminated strips on the grating $G$ (by fore-and-aft motion) and then rotating the grating on an axis normal to its face until the best conditions appear. Both spectra are very bright, but liable to be in different focal planes from inadequate planeness of the reflecting system. If work of precision is aimed at, this condition is of foremost importance.

**54. Another method.**—If the opportunity of using crossed pencils of white light is to be dispensed with, the prism method may be simplified, as shown in figure 74. Here $P$ is a prism with silvered sides and a prism angle of less than $30°$. It receives horizontal white rays $L$ from a collimator, which, after reflection from the opaque mirrors $M$ and $N$, impinge on the grating $G$, plane or concave, and are observed at $T$ by a telescope or lens.

If $\varphi$ is the prism angle and $\theta$ the angle of diffraction, it is easily seen that the angle between the rays reflected at $M$ or $N$ is

$$\delta = \theta - \varphi$$

Hence, if $P$ is a $30°$ prism, the observations can be made only in the second-order spectra. If observations in the first order are desired because of the greater illumination, $\varphi$ must be less than $20°$, as a rule, for a grating of about 15,000 lines to the inch. The mirrors $M$ and $N$ make an angle of $\sigma/2 = (\varphi+\theta)/2$ with the line $MN$.



The first experiments were made with a $30°$ prism and second-order spectra from a concave grating ($D = 177 \times 10^{-4}$ cm.). Sunlight was used. The two superposed spectra were magnificent, with abundance of light and high dispersion; but the spectra were of unequal intensity and in different focal planes, so much so that the images of the guiding horizontal thread of the spectra could scarcely be seen together. This made the adjustment for coincident longitudinal axes very difficult, and the interferences were not found until after long trial. The reason for this is the probable concavity or convexity of one or more of the reflecting surfaces. Another difficulty was the distance apart of the mirrors $M$ and $N$ (roughly, 150 cm. for a distance of about 2 meters from $P$ to $T$), so that it was inconvenient to observe and actuate the mirror micrometer at $M$. Further attempt at improvement was therefore abandoned.

This prism was now replaced by one of less angle than $\varphi = 20°$, also well silvered. In the first experiments the adjustment did not admit of a coincidence of light, except near the $C$ line of the red; but $M$ and $N$ were now less than 90 cm. apart, while the distance between $G$ and $T$ was about 110 cm., and
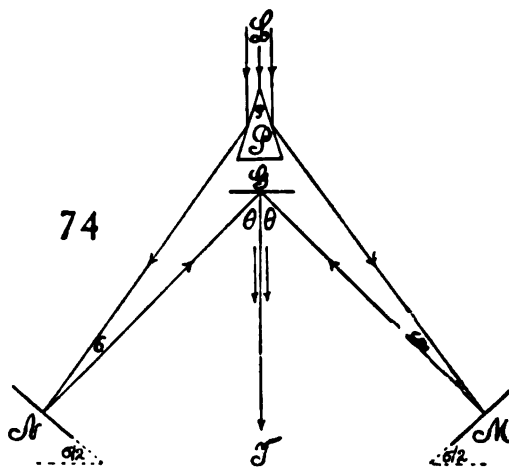
between $G$ and $P$ about 10 cm. In this case the focal planes were nearly identical and the interferences easily found in the red region between the two $C$ lines. They appeared as small red pearls, very vivid on limiting the lateral extent of the pencil $L$ to about 5 mm., but, to my astonishment, they very soon vanished on displacing $M$ in a direction normal to itself 1 or 2 mm.

**55. Methods using prismatic dispersion.**—The small range of displacement available in the prismatic reflection methods induced me to devise corresponding refraction methods, to see whether these would show any advantage in this respect. Accordingly the interferometer (fig. 75) was installed and the fringes found without much difficulty. Here $P$ is the symmetrical prism, receiving the collimated beam of incident white light on the faces meeting at the obtuse edge and refracting them in relation to the smaller prism angle $\varphi$. This must be less than 45°, for convenience in observation, as otherwise the dispersed beams meeting the opaque mirrors $M$ and $N$ will



75          76
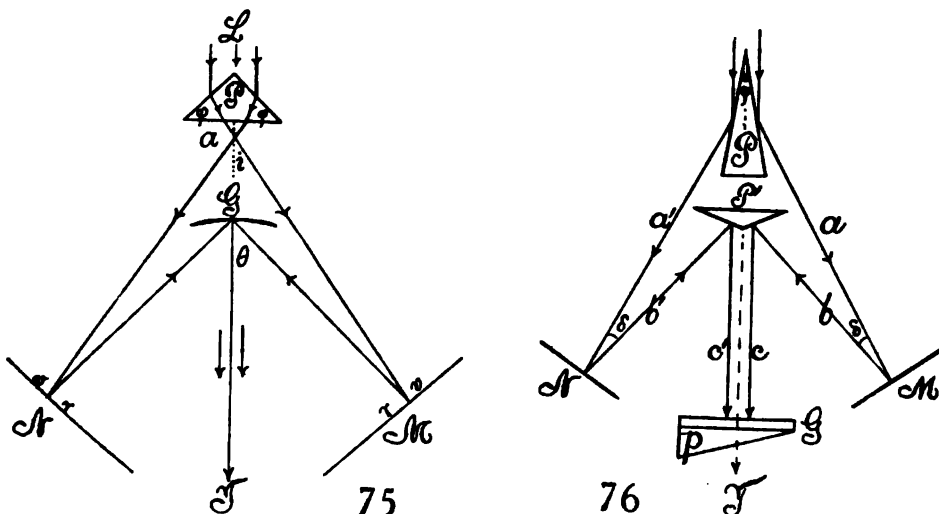
be too far apart for manipulation, supposing, of course, that the distance $PM$ and $PN$ are over a meter. I used an equilateral 90° prism for want of a better. The spectra reflected from $M$ and $N$ respectively impinge on the grating $G$, concave or plane, and are viewed at $T$ with a lens or telescope. In consequence of the large angle $\theta$, second-order spectra were used, without apparent disadvantage. The dispersion of $P$ and $G$ being summational, the total is very large.

To return to the angles again, if $\phi$ denotes the obtuse prism angle, and $r$ the angle of refraction, the angle of incidence is $90° - \phi/2$, or

(1)                              $\cos \phi/2 = \mu \sin r$

Again,

(2)                              $\sin i' = \mu \cos (\phi/2 + r)$

when $i'$ is the angle of emergence. Hence

$$\sin i' = \cos \phi/2 (\sqrt{\mu^2 - \cos^2 \phi/2} - \sin \phi/2)$$

If $\phi = 90°$, then $\sin i = (1/2)(\sqrt{2\mu^2 - 1} - 1)$. Thus if $\mu = 1.55$, then $\sin i' = 0.475$, and $i' = 28.4°$. Now, since $i + \delta = \theta$, the angle $\theta$ will obviously have to be in the second order of the spectra of the grating $G$.

Although the two spectra obtained in this way were highly dispersed and very brilliant, the interference phenomenon itself was not much superior to the case where reflection from the (silvered) faces of the prism was employed. The fringes disappeared, in fact, for a displacement of 1 or 2 mm. of the mirror $M$, showing the usual inflation of form just before vanishing. The details also were of the same nature, the large arrow-shaped forms being obtained when illuminated strips on the grating were superposed and the latter slightly rotated until the maximal conditions appeared.

To increase the range, the angle $\delta$ must be reduced, as far as practicable. This is possible in the present method, since the points of intersection at $a$ and $G$ may be made to all but coincide. Reflection from the mirrors $M$ and $N$ would then be normal. To attain this end it will be necessary either to have the grating constant or the prism angle $\phi$ predetermined, or to use rays of suitable divergence at $L$.

**56. Methods with paired prisms.**—White light (fig. 76, $L$) from a collimator is reflected in turn from the silvered sides of the sharp prism $P$, from the opaque mirrors $M$ and $N$, and from the silvered blunt prism $P'$, as shown by the component beams $abc$ and $a'b'c'$. Thereafter the white beams are diffracted by an Ives film grating $G$, with attached prism $p$, and observed in a telescope at $T$. Interference, therefore, takes place in the focal plane of the telescope and would not (for the case in fig. 76) occur in its absence. Very interesting results were obtained with this apparatus. The spectra are non-reversed or else (if slit and grating are rotated 90°) inverted. The work, however, is still in progress and will be described elsewhere. I will merely add, in this place, that the work with prisms is important, inasmuch as it shows the essential part played by the diffraction of the slit of the collimator, in its bearing on the phenomena of the present report. It is the function of the prism $P$ to cleave the diffracted field which leaves the collimator. For this reason pencils identical in source are found on both sides of $P$. The experiments thus furnish the final link in the theory of the phenomena.

Furthermore, as the above results already show, the range of displacement of either opaque mirror ($M$, $N$) within which interference fringes are visible, increases in marked degree with the dispersion to which the white ray is subjected on separation and before the resulting partial rays reach their final recombination. These ranges increase from a fraction of a millimeter to almost a centimeter, while the width of the strip of spectrum carrying the interference fringes, *caet. par.*, remains the same. This also has a fundamental bearing on the phenomenon and is under investigation. The question at issue is whether increase of range of displacement results simply from the geometry of the optic system, or whether wave-trains are actually uniform throughout greater lengths, in proportion as they have been more highly dispersed.

# CHAPTER VIII.

## THE LINEAR TYPE OF DISPLACEMENT INTERFEROMETERS.

**57. Introductory.**—This apparatus will be referred to in various places in this book and presents certain interesting features. The incidence of the grating is normal $(I = R = o)$, and both component rays in their vertical projection lie strictly in the same plane. To make the horizontal projection also collinear is not quite possible in practice, because the direct or unreflected rays and the corresponding spectra would overlap with the spectra of the interferometer. As the former are much more intense, the interference patterns would scarcely be visible in the combination. To avoid this, the rays diverge slightly (a few degrees, depending on the distance between grating and opaque mirrors) in a vertical plane. But this is of no consequence, as the horizontal projections only are used in the measurements. One may note, in passing, that this avoidance of coincidence with undesirable spectra secured by tilting the grating and the corresponding opaque mirror in the same direction is, in general, one of the essentials of the adjustments.

The advantage of the linear displacement interferometer is this: that it can be built on a rail and mounted along a wall or a pier. If the rail is tubular, a current of water may be passed through it from the middle toward both ends, to insure constancy of temperature.

**58. Apparatus.**—The apparatus was constructed as follows and gave good results at once, showing strong interferences. The ellipses were, in fact, oblate in the red, circular in the yellow, and prolate in the blues, but clear throughout.
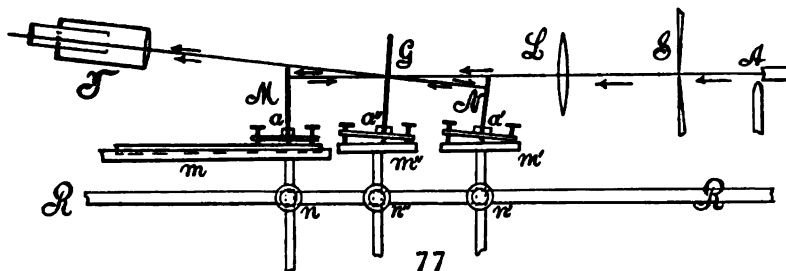


Light enters from an arc lamp, $A$, or Nernst burner, or the sun, at the slit $S$, and is collimated by the lens $L$. Then the parallel rays pass the grating $G$ with its ruled side toward $L$. From the grating the reflected beam returns to the opaque mirror $N$, and is then reflected into the auxiliary or adjustment telescope, $T$. The component beam transmitted at $G$ is reflected from the opaque mirror $M$, returned to the ruled side of $G$, and thus also reflected into $T$ coincidently with the other beam.

Figure 77 shows that the entering undivided beam *LG* passes just above the mirror *M*, and is reflected just below this from the top of *N*. Similarly, the reunited beam *GT* passes just above *M*, but is reflected from the top of *M*, the object being to make the vertical angle at *G* as small as possible.

The mirrors *M* and *N* and the grating *G* are on adjustable bases, *a*, *a'*, *a"*, each controlled by three leveling screws on a plane-dot-slot arrangement in the tablets *m*, *m'*, *m"*, the axis of rotation being horizontal and normal to the diagram. The tablets, furthermore, may be revolved and raised or lowered by the rods *n*, *n'*, *n"*, which are attached by ordinary clamps to the large, tubular, horizontal rail, *RR*, in question, admitting of a circuit of water. The latter is secured to the pier.

The angles of inclination of the figure are much exaggerated, since the distance $MG = GN$ (nearly) is from one-half to several meters in extent.

The mirror *M* is on a Fraunhofer micrometer suggested at *m*. The bases, *a*, *a'*, *a"*, are drawn to the tablets, *m*, *m'*, *m"*, by firm springs, preferably running into the tubes below them.

The axis of the adjustment telescope, *T*, lies in the plane of the figure and serves the purpose of bringing the direct slit images into horizontal and vertical coincidence. When this is done it may be removed, if desirable, as the ray *GT* is not thereafter used. *T* should not be attached to the rail, but placed on an independent table, or standard, so as not to be an integrant part of the interferometer. The telescope, *T* (not shown), for the observation of the interferences, should be independently mounted on the same table. This telescope lies outside of the diagram, to the right or the left of it, to catch either of the two diffraction spectra selected. It will be seen that these lie quite above the direct diffraction spectra of the ray *LGM*. Otherwise, as this is much more intense, it would completely wipe out the interference spectra and their combination. The latter, when seen alone, are very brilliant, black and colored patterns, running through the spectrum when the micrometer, *m*, is manipulated. If the distance *GN* is large and the grating *G*, as usual, slightly wedge-shaped, the superfluous rear reflection from *G* may be blotted out at *N* by a small screen. It is easily recognized, as it is brown from scattered light.

The installation is simple. The parts being adjusted nearly symmetrically, the undivided ray from a wide slit is brought to the top of *M* by raising or lowering the lamp. This should first be done roughly with the lens and slit removed. *N* has at the same time been placed just below the beam, and this passes through the middle part of *G*. The latter is then inclined by the adjustment screws until the component beam *GN* strikes the top of *N*, symmetrically. Next *N* is inclined and rotated (vertical axis) until the reflected beam enters the telescope, *T*. Finally, *M* is inclined and rotated (vertical axis) until the reflected rays *MG* and *GT* also enter the telescope, the final sharp adjustment being made with a narrow slit and the eye at the telescope. The mirror *M* must also have a fine vertical adjustment (not shown). If the

distances $NG$ (face toward the light) and $MG$ are equal, the interferences are then easily found by moving the mirror $M$ on the micrometer toward the grating.

As compared with the other non-linear interferometers used under like conditions, the present instrument, even when mounted on a ¼-inch gas-pipe, $RR$, showed itself remarkably steady, so that rings could be observed in spite of the tremors of the hill on which the laboratory is built.

### 59. Film-grating adjustment. Michelson's interferometer.

—If the grating $G$ is a film grating, like those in the market, with 14,000 lines to the inch, it should be mounted smoothly on the unruled side, on a *thick* glass plate, with Canada balsam, and without a cover plate for the ruled side. It is to be adjusted with the glass side toward the source of light, so that the reflection taken may be from this side only (see $r$, fig. 78). In the telescope, $T$, directed toward the reflected beams, two slits (one for each component beam) only appear, as the glass plate does not reflect on the side covered by the grating ($g$ in fig. 78). The slits placed in coincidence will then show the elliptic inter-



80          78          79
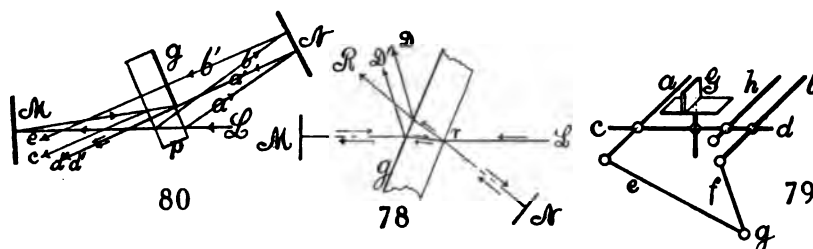
ferences in the diffracted beam $D$ at the proper distances. With so large a dispersion as the above, the ellipses are usually too large. They should then be reduced in size by a compensator placed in the beam on the ruled side of the grating; or, preferably, the grating may be mounted on a plate of glass fully 1 cm. (or more) thick, as in figure 78. This thick plate has the additional advantage of eliminating the stationary interferences due to the front and rear faces of the grating. In case of thin glass plates (2 or 3 mm.), these stationary interferences are very strong, coarse, vertical lines and exceedingly annoying.

If the film grating is carefully mounted in this way, it is nearly as good as a ruled grating. There is, however, one insuperable objection, inasmuch as the ruled face, though it does not reflect sharply, does diffract, and this more strongly than the other. Thus there are always 3 superposed spectra in the telescope, the third coming from the film side only, whereas the other two are produced by the rays coming coincidently from $r$ on the unruled side of the grating. Hence the velvety blackness of the interferences in case of the ruled gratings can not be reproduced by the film grating, since the interferences are spread out on a colored ground. They are, however, quite strong enough for all practical purposes, and the lines are sharply and symmetrically

traced. A vertical wire 2 or 3 mm. thick, placed symmetrically in front of the objective of the telescope, makes the interference relatively strong and sharp, by blotting out the third spectrum partially; but it at the same time diminishes the light available. A wide slit in front of the objective subserves the same purposes better.

If the distance apart of the mirrors $M$ and $N$ and the grating $G$ is large, it is best to *dispense with the rail RR* altogether, and to mount the mirrors and grating *directly on the pier or wall*. This has the additional advantage of a large free space between $M$ and $G$ or $G$ and $N$, so that spacious apparatus like a fog-chamber may be independently mounted there. This was the case in the optic experiments on the thermal coefficients of the refraction of air, etc., below, where the distance between $MG$ and $GN$ was nearly 2 meters. In such a case, moreover, in addition to the usual three adjustment screws of the mirror $M$ at the micrometer, it is desirable to have two others bearing on the rigid parts of the support, so that the final adjustment may be made elastically. By devising a tetrahedral plan of bracing $M$, $G$, $N$, independent of each other, using short rods and clamping all parts on relatively short stems, I eventually obtained a mounting which was almost free from tremors, even amid the disturbances of the surrounding laboratory. In figure 79 one of these mountings is suggested: $a$ and $b$ are ¼-inch gas-pipes (about a foot long), sunk into the wall of the pier at their rear ends; $cd$ is a cross-rod of same size and material, clamped in place, and supporting the grating (or a micrometer) $G$. The screw $h$ abutting against the wall gives the horizontal elastic adjustment. The braces $e$ and $f$, which may be adjusted by rotation (screw) abutting in $g$ at the wall, give the grating vertical elastic adjustment. Thus $h$, $e$, and $f$, rotate $G$ around vertical and horizontal axes, respectively.

**60. Michelson's interferences.**—If the collimator, $SL$, is removed and replaced by a strong sodium flame provided with a condenser, Michelson's interferences will appear at $T$ when the instrument is in adjustment. It is rather surprising that, even in case of a film grating adjusted as above, they are well-defined circles covering the whole field of the telescope. If the collimator $SL$ is retained and the sodium light introduced from the side by aid of a reflecting mirror, placed between the grating $G$ and the collimating lens $L$, both interferences may be observed at the same time in corresponding telescopes. The mirror introducing the homogeneous light should in such a case be provided with a clear space (silver removed), through which the white beam, $SL$, may pass without obstruction. In a vertical plane the interferences have the same size and character at the sodium line. Horizontally the spectrum interferences vary with the dispersion.

If an apparatus constructed of gas-pipe is employed, however, it is far too frail for the practical use of the Michelson interferences. Vibrations within the apparatus are excited on merely touching it. For the purpose of displacement interferometry, however, such an apparatus is quite adequate; for the measurements are taken when the tremors have vanished.

**61. Film grating. Another adjustment.**—The supernumerary spectra may be gotten rid of altogether by using the method shown in figure 80. Here the impinging vertical sheet of white light, $L$, from the collimator, falls upon the clear or unruled part $p$ of the plate of the grating, the film extending out as far as shown at $G$. If $M$ and $N$ are the opaque mirrors, the reflected rays $a$ and $b$ passing $G$ are additionally reflected into $a'$ and $b'$, and thence, after leaving the grating, into $c$ and $d$. As both of the latter pass through the film, both produce spectra; but $b'$ and $e$ may be blotted out by a screen at the mirror $N$. This leaves only $d$ beyond the grating. Again, the transmitted ray from $L$, after reflection at $M$, is again reflected into $c$ and $d'$, which is made coincident with $d$. But $c$, being reflected from the unruled side, has no spectrum. Thus the spectra due to the two rays $d$ alone interfere.

Had the grating been reversed, *cæt. par.*, then the ray $c$ would have produced the strongest spectrum, and superposed on the other two it would have greatly diminished the clearness.

In the telescope, whereas the ray $a'$ prolonged is white, the ray $d'$ from $M$ and reflected from the film is strongly azure blue, due to regularly scattered light. This blue image is apt to be less sharp, unless very flat parts of the film are found. The two spectra, however, are good and the interferences satisfactory. The sodium line is sufficiently indicated, though, like the blue image, not quite sharp.

This method of using the unruled edge of the plate of the grating for reflection is, of course, equally applicable and advantageous in the case of the ruled grating. Only the two interfering spectra and no diffused light are present in the field of the telescope, and if sunlight is used the Fraunhofer lines are beautifully sharp.

**62. Equations.**—The equations for $N_e/e$, for normal incidence $I=R=0$, takes its simplest form as

(1) $$N_e/e = \mu - \lambda d\mu/d\lambda = A + 3B/\lambda^2, \text{ nearly}$$

where $N_e$ is the coördinate of the center of a given ellipse on the micrometer $M$, for the thickness of glass grating $e$, index of refraction $\mu$, and color of wavelength $\lambda$.

Hence if two different wave-lengths, $\lambda$ and $\lambda'$, are in question ($\delta$ refers to differences),

(2) $$\delta N_e/e = \delta\mu - \delta\frac{d\mu}{d\log\lambda}$$

$\delta N_e$ being the displacement of the micrometer to pass the center of ellipses from line $\lambda$ to line $\lambda'$.

If $\mu = A + B/\lambda^2$ and $\lambda d\mu/d\lambda = -2B/\lambda^2$, then

(3) $$\delta N_e = 3eB\left(\frac{1}{\lambda^2} - \frac{1}{\lambda'^2}\right)$$

from which $B$ may be obtained without further measurements. If greater approximation is necessary, so that two constants, $B$ and $C$, enter the dispersion equation,

$$(4) \qquad \delta N_e = 3eB\left(\frac{1}{\lambda^2} - \frac{1}{\lambda'^2}\right) + 5eC\left(\frac{1}{\lambda^4} - \frac{1}{\lambda'^4}\right)$$

so that observations at three spectrum lines, $\lambda$, $\lambda'$, $\lambda''$, would be necessary.

The amount of displacement corresponding to the thickness $e$ of glass is, at a given spectrum line $\lambda$,

$$\Delta N_e = e\left(\mu - 1 - \lambda\frac{d\mu}{d\lambda}\right) = e(\mu - 1) + \frac{2Be}{\lambda^2} = e(A - 1) + \frac{3Be}{\lambda^2}$$

where $2B/\lambda^2$ is constant for all values of $e$, or

$$A = \frac{\Delta N_e}{e} - \frac{3B}{\lambda^2} + 1 \qquad\qquad \mu = \frac{\Delta N_e}{e} - \frac{2B}{\lambda^2} + 1$$

It is therefore not possible to obviate the term in $B$, determined as shown, if $\mu$ is to be measured.

If equal distances are cut off at $M$ and $N$, the interference pattern, of course, remains stationary in the spectrum. It is interesting to inquire to what degree this may be guaranteed. Equation (3) is available for the purpose, and, since $\lambda$ and $\lambda'$ are nearly the same, $\lambda' - \lambda = \delta\lambda$ and

$$\delta N_e = 3eB\frac{2d\lambda}{\lambda^3} = \frac{6eB}{\lambda^3}d\lambda$$

Let $\delta\lambda$ be the width of the sodium lines:

$\delta\lambda = 6 \times 10^{-8}$ cm.     $\lambda = 59 \times 10^{-6}$ cm.     $e = 0.68$ cm.     $B = 4.6 \times 10^{-11}$

data for the above grating and sodium light. Hence

$$\delta N_e = \frac{6 \times 0.68 \times 4.6 \times 10^{-11} \times 6 \times 10^{-8}}{(59)^3 \times 10^{-18}} = 5.5 \times 10^{-5} \text{ cm.}$$

i.e., about a half of $10^{-4}$ cm. This would be equivalent to the space on a grating with about 20,000 lines to the centimeter, or 50,000 to the inch. The ellipses can not be set as closely as this, but the order of sensitiveness is within that of a good micrometer.

It is interesting to inquire whether the sensitiveness will change markedly for larger angles of incidence $I$. If $\mu$ is the index of refraction, the largest angle $R$ obtainable at grazing incidence, $I = 90°$, would be $\sin R = 1/\mu$. It may then be shown that

$$\frac{dN_e}{d\lambda} = \frac{2eB}{\lambda^3}\frac{2B/\lambda^2(\mu^2 - 1) + 3\mu}{\sqrt{\mu^2 - 1}}$$

Putting $\mu = 1.5$ and the other data as above, where $d\lambda = 6 \times 10^{-8}$ cm.,

$$dN_e = \frac{1.34 \times 4.6 \times 10^{-11}}{(59)^3 \times 10^{-18}} \frac{9.2 \times 10^{-11}/(59)^2 \times 10^{-12} + 4.5}{1.12} = 7.7 \times 10^{-5} \text{ cm.}$$

The datum is of the same order as above, so that the sensitiveness changes but very little for different angles of incidence. Thus there is no disadvantage in using $I = 0$.

# CHAPTER IX.

## THE USE OF COMPENSATORS, BOUNDED BY CURVED SURFACES, IN DISPLACEMENT INTERFEROMETRY.

**63. Introduction.**—The method of increasing the sensitiveness of the displacement interferometer by increasing the dispersion of the grating readily suggests itself, but unfortunately the interference pattern loses sharpness in the same ratio and ultimately becomes too diffuse for practical purposes. Similar sensitiveness is secured when the air-paths and the glass-paths of the component beams of light are respectively identical, with the same inadequacy in the huge mobile figures, for the purpose of adjustment. In fact, if for simplicity we consider the incidence normal ($I = R = 0$, linear interferometer), the sensitiveness becomes

$$d\theta/dn = \lambda^2/[2eD \cos \theta. \ ((\mu + 2b/\lambda^2) - N))]$$

where $\theta$ is the angle of diffraction for the wave-length $\lambda$, $e$ the thickness of the plate of the grating, $\mu$ its index of refraction, $D$ the grating space, $n$ the order of the fringe, and $b$, $N$, constants. Hence, other things being equal, $d\theta/dn$ increases as $D$ and $e$ grow smaller, where $e = 0$ is obtained by a compensator counteracting the thickness of the plate of the grating.

It occurred to me that the difficulty of diffuse interference patterns might be overcome, in part, by the use of compensators with curved faces, when the case would become similar to the conversion of the usual interference colors of thin plates into Newton's rings. Naturally a cylindric lens with its elements normal to the slit is chiefly in question, though an ordinary lens also presents cases of interest, chiefly because of the easy conversion of elliptic into hyperbolic patterns, and the lens is more easily obtained.

Other methods were tried. For instance, on using a Fresnel biprism with its blunt edge normal to the slit, two sets of interference patterns, one above the other in the spectrum, are obtained. When the blunt edge is parallel to the slit, either side of the prism gives its own interferences, but they can not be made clearly visible at the same time. A doubly reflecting plate or a *thin* sheet of mica covering one half of the beam will produce two intersecting patterns, but these also are of little use for measurement.

**64. Lens systems.**—If but a single compensator is to be used, *i.e.*, compensation in one of the component beams only, the lens in question must be of very small focal power; otherwise the adjustment will be impossible, as the two direct images of the slit will be in very different focal planes. Moreover, the focal power should be variable. All this makes it necessary to use a *doublet*, preferably consisting of lenses of the same focal power, respectively convex and concave. If these lenses are themselves weak, say 1 meter in focal distance, both slit images may easily be seen in the telescope and be

113

sufficiently sharp for adjustment. If the lens first struck by light is convex and the second concave, their focal distances $f_1$ and $f_2$, respectively, and their distances apart $D$, the focal power $1/F$ of the combination used is

(1) $$D/f_1 f_2 = D/f^2$$

since $f_1 = f_2 = f$. The position of the equivalent lens is $d = DF/f_1 = f_2 = f$. $D$, $d$ are both measured from the second or concave lens to the convex lens, and $D$ would always be smaller than $f$. If the lens system is reversed, $F$ remains the same as before for the same $D$, the system being again convex, but $d$ is reversed. The equivalent lens again lies toward the convex side of the system. In other words, the equivalent lens generally lies on the same side of the doublet as the convex lens.

In the actual experiment, however, the rays go through the lens system twice. In this case it is perhaps best to compute the distances directly. Of the two adjustments, the one with the concave lens toward the grating and the convex lens toward the mirror has much the greater range of focus relative to the displacement $D$. Supposing the mirror appreciably in contact with a convex lens, therefore, if $b$ is its principal focal distance measured from the concave lens, $b + D = M$ its principal focal distance from the convex lens or mirror,

(2) $$\frac{1}{b} = \frac{2/f_2 - 1/(f_1+D)}{1 - D(2/f_2 - 1/(f_1+D))} - \frac{1}{f_1}$$

where $f_1$ is the (numerical) focal distance of the concave and $f_2$ that of the convex lens. If we now write

(3) $$b = B(1 - D(2/f_2 - 1/(f_1+D)))$$

equation (2) is easily converted into

(4) $$\frac{1}{2B} = \frac{1}{f_2} - \frac{1}{f_1} + \frac{D}{f_1 f_2}$$

so that the usual value of the principal focal distance has been halved relatively to the new position of the equivalent lens. If, as in the present case, $f_1 = f_2 = f$

$$2B = f^2/D \qquad b = \frac{f}{2D}\frac{f^2 - 2D^2}{f+D} \qquad M = b + D = \frac{f^2 + 2D^2}{2D(f+D)}$$

The following table shows roughly the corresponding values of $D$ and $M$ in centimeters:

| $D$ | $M = C + D$ | $2B$ | $d$ |
|---|---|---|---|
| 2 | 2450 | 2500 | 49 |
| 5 | 950 | 1000 | 47 |
| 10 | 455 | 500 | 45 |
| 15 | 292 | 333 | 41 |
| 20 | 212 | 250 | 38 |
| 25 | 165 | 200 | 35 |

As $b$ is smaller than $B$ by equation (3), the equivalent lens is on the side of the convex lens and at a distance

$$B-M=(f^2-2D^2)/2(f+D)$$

behind the mirror, or

$$B-b=f(f+2D)/2(f+D)$$

behind the concave lens.

If the system is reversed, $f_1$ and $f_2$ are to be replaced by $-f_1$ and $-f_2$, whereas $D$ remains positive. Thus the equations become successively

$$\frac{1}{b}=\frac{1/(f_1-D)-2/f_2}{1-D(1/(f_1-D)-2/f_2)}+\frac{1}{f_1}$$

$$b=B(1-D(1/(f_1-D)-2f_2))$$

$$\frac{1}{B}=-\frac{2}{f_2}+\frac{1}{f_1}+\frac{2D}{f_1f_2}$$

If $f_1=f_2=f$, then

$$B=f^2/2D \qquad b=\frac{f}{2D}\frac{f^2-2D^2}{f-D} \qquad M=b+D=\frac{1}{2}\frac{f^2+2D^2}{D(f+D)}$$

$$B'-b=-\frac{f}{2}\frac{f-2D}{f-D} \qquad B'-M=-\frac{1}{2}\frac{f^2-2D^2}{f-D}$$

Hence the equivalent lens has the same focal distance as before, but it is now placed in front of the system, at a greater distance than it was formerly behind it. Measured from the mirror (mirror distances, $M$) the data (in millimeters) are roughly as follows:

| $D$ | $2B$ | $B-M$ |
|-----|------|-------|
| 2   | 2500 | −51   |
| 5   | 1000 | −52   |
| 10  | 500  | −54   |
| 15  | 333  | −56   |
| 20  | 250  | −57   |
| 25  | 200  | −58   |

The total displacement of the equivalent lens on reversal is about 1 meter, falling off to 96 cm. in the extreme case. The image is larger if the convex lens is nearer the grating and the concave lens nearer the mirror.

**65. Effective thickness of the lenticular compensator.**—The compensator with curved faces may change the interference pattern in two ways; viz, by changing the angle of incidence and refraction of the rays at the grating, and by changing the path-difference of successive rays passing through it. Both conditions are virtually the same, or at least occur simultaneously. If there is but one compensator, as above, the two effects must be small, since the rays reflected from each of the opaque mirrors, $M$ and $N$, of the interferometer, must eventually enter the telescope, to unite in two nearly identical images of the slit. It was rather unexpected to observe that the interferences are still obtained, even when the two slit images are quite appreciably different in size, but they are then confined to a single plane, as will be shown in § 69.

Since the beam of light coming out of the collimator and traversing the grating is a vertical ribbon of light, several centimeters high vertically, but very thin in comparison (a few millimeters) horizontally, it is relative to the vertical plane that the marked effect must be expected. In figure 81, $G$ is the grating, $cc$ the principal plane of the concave, $cv$ that of the convex lens, $M$ the opaque mirror. If the beam consists merely of the axial pencil $c$, the distorting effect due to the introduction of the lens doublet is slight for any value of their distance apart, $D$. The two lenses are practically equivalent to a plate. If a broad beam $dd$ is in question and the rays retrace their path, the same is still true. But if, on changing $D$, the rays do not retrace their path, so that the equivalent lens is convergent or divergent, then the rays after leaving $M$ re-impinge on the grating at different angles than before and the interference pattern is correspondingly changed, principally in its vertical relations.

Thus it is the lens system which changes the obliquity of rays lying in a vertical plane and passing through the grating, to the effect that the axial rays may represent a case of either maximum or minimum path-difference. The latter will be the case when the divergent pencil which usually traverses the grating becomes convergent in consequence of a sufficiently large value of the $D$ of the lens system.
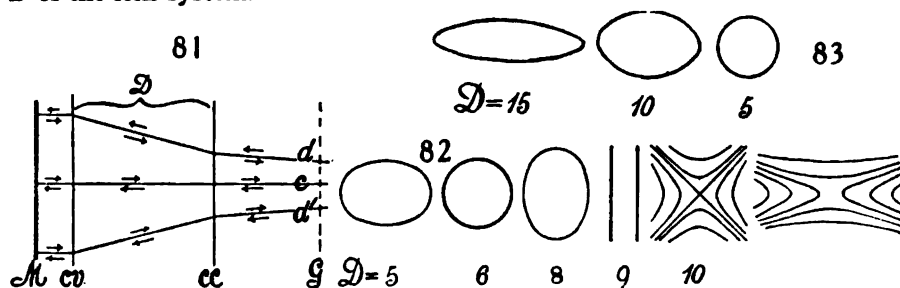


**66. Observations largely with weak lenses and short interferometer.**—The film grating used (Wallace, 14,500 lines to the inch) was cemented with canada balsam to a thick piece of plate glass, so that the total thickness of plate at the grating was 1,734 cm. This introduces a large excess of path in one of the component beams; but it is generally necessary, if the stationary interferences, due to the reflection at the two faces of the plate of the grating, are to be obviated and if the ellipses produced are to be reasonably large for adjustment (cf. § 69). The lens doublet was to be added on the same side as the glass specified, so that the excess of glass thickness on one side was further increased by about 0.19 cm., on the average. Under these circumstances the ellipses were strong, but (in view of the large dispersion) with inconveniently long horizontal axes.

On inserting the doublet (convex and concave lens, each 1 meter in focal distance) with its concave lens at the mirror and gradually increasing the distance $D$ by moving the convex lens toward the grating, a series of forms

was obtained which passed from the initial horizontally long ellipse, through circles, vertically long ellipses, vertical lines, into hyperbolic forms of increasing eccentricity, as recorded in figure 82.

On reversing the system, keeping the convex lens fixed near the mirror and increasing the distance $D$ by moving the other lens toward the grating, the original ellipse usually flattened out further, as shown in figure 83. Moving the lenses sideways parallel to themselves had no definite effect; moving them fore and aft together ($D$ constant) produced results similar to the above. The vertical lines of figure 82 are liable to be sinuous or to resemble the grain of wood around a knot. In case of figure 82, as the equivalent lens lies in front of the mirror, the rays reaching the grating are thus necessarily converging. In figure 83 the equivalent lens lies behind the mirror, so that the rays at the grating are more convergent. Both positions furnish essentially convergent rays.

If corresponding to figure 82, the convex lens is kept fixed near the grating and the concave lens gradually moved up to it, the order of forms is reversed, but not quite completely. They usually terminate in long, vertical ellipses, before reaching which the wood-grained forms are sometimes passed. The same is similarly true for the case of figure 83.

With cylindrical lenses (respectively convex and concave, each 1 meter in focal distance) very little effect was observed when the axes of the cylinders were parallel to the slit. With the axes perpendicular to the slit, the effects of spherical lenses were virtually reproduced, except that the central fields partook of a more rectangular character.

To carry out the purposes of the present paper with strong lenses, respectively convex and concave, the vertical sheet of light from the slit must be diverged into a wedge by the concave lens and then collimated by the convex lens. The mirror, normal to the rays, reflects them, so that they retrace their path and become a sheet of light before the final reflection and diffraction at the grating. The following experiments were made with strong lenses:

At first lenses of double the preceding focal power, $f = \pm 50$ cm., were tried, but with no essential difference in the results. Thereupon strong lenses of focal distances $f_1 = -73$ cm. and $f_2 = 13.1$ cm. were used together, the convex lens being, as usual, near the mirror. For $D = 7.5$ cm., about, these gave fairly clear images of the slit and it was easy to find the ellipses, which were now very eccentric, almost spindle-shaped in form. They could be obtained strong and clear without difficulty, and the nearly horizontal lines filled the whole spectrum. Reversal of lenses practically failed to give results, the rays after reflection being too divergent.

On the large interferometer, where the distances between mirror and grating are nearly 2 meters, adjustment was more difficult and the result (if parallel rays are retained) less satisfactory, because the slit images are not in focus at the same time. This is particularly the case when the convex lens is nearest the mirror and the concave lens toward the grating. Thus when $f = \pm 100$ cm. and $D = 15$ cm., the modified slit image may be twice as large as the other and

the interferences in the principal focal plane of the telescope are only just seen. At $D = 5$ cm., however, the results are acceptable. When the concave lens is nearest to the mirror and the convex lens toward the grating, the modified slit image is smaller than the other. Adjustment is then easier and the usual elliptic and hyperbolic forms may be observed without trouble. In both cases the flickering of the arc lamp used passes the rays through different parts of the lenses relatively to the center, and the adjustment is thus easily destroyed.

If the spectra from $M$ and $N$, however, are observed, not in the principal focal plane but in advance of it (toward the eye), interferences of great interest will be observed, to be discussed in § 69.

**67. Remarks.**—A few explanatory observations may here be inserted. The occurrence of the elliptic or oval and the hyperbolic type of fringes may be most easily exhibited by laying off the order of the fringe in terms of the distance (in arbitrary units) above and below the center of the image of the slit. If we call the latter $y$ and consider the allied colors of thin plates, for instance,

$$n = 2e\mu \cos r / \lambda \text{ or more generally } n = (e\mu/\lambda) f(y, r)$$

(where $e$ is the thickness of the plate, $\mu$ its index of refraction, $\lambda$ the wavelength of light in case of a dark locus of the order $n$) is to be expressed in terms of $y$, which itself determines $e \cos r$, $r$ being the angle of refraction in the plate of the grating. The phenomenon will thus be coarser for red light than for violet light, since $\mu$ decreases when $\lambda$ increases, and any two curves, $r$ and $v$, figure 84, may be assumed as the loci of the equation in question. If, now, horizontal lines be drawn for $n = 1, 2, 3$, etc., they will determine the number of dark bands in the spectrum for any value of $y$.

If the central ray is also a line of symmetry and intersects the grating normally, it must correspond to a maximum or a minimum of $n$. These conditions are shown in the diagram at $M$, where the maximum number of bands occurs, and at $m$, where the reverse is true. The question is thus referred to two sets of loci, $rr'$ and $vv'$, or $r'r''$ and $v'v''$, etc. In the former case $e \cos r$ varies with $y$ in the same sense as $\mu/\lambda$; in the latter in the opposite sense and is preponderating in amount. Both may vary at the same rates in the transitional case, in which, therefore, the two curves $r$ and $v$ are at the same distance apart for all values of $y$.

Suppose, furthermore, that the same phenomenon is exhibited in terms of wave-length $\lambda$, as in the lower part of the diagram, the spectrum being now equally wide for all values of $y$, while at any given $y$ the upper diagram still shows the number of dark points (bands) between $r$ and $v$. If now, we suppose that under any conditions these dark points are grouped symmetrically with reference to any given color (which is probable, for a maximum or a minimum of any value of $y$ will be so for all values), and that the successive dark points have been connected by a curve, the interference pattern will be of the elliptic type in case of $aa'$, $a''a'''$, and of the hyperbolic in the case of $a'a''$.

The other features of the phenomenon are secondary and therefore left out

of the diagram. Thus, for instance, the distance apart of the bands shrinks from red to violet, and the ovals, etc., are only appreciably symmetric, because they occupy so small a part of the spectrum. The horizontal distribution of dark bands around the center is determined by variations $e \cos r$ and is not linear. Whether the long axes of the ellipses are horizontal or vertical depends
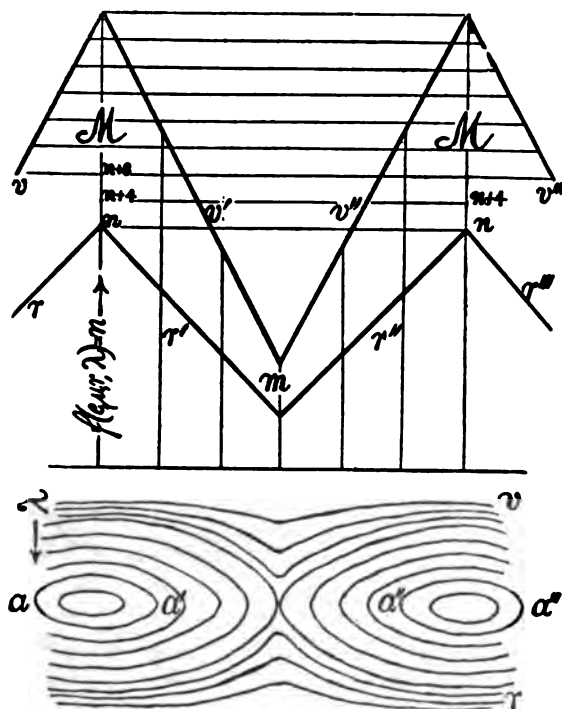


**84**

upon the slope of the lines $r$ and $v$. Maxima and minima will not, as a rule, occur close together, though in certain wood-grain-shaped patterns this seems to be the case.

In conclusion, therefore, the main feature in modifying the type of interference pattern is the varying thickness of the compensator. For oval types the preponderating lens is convex; for the hyperbolic type it is concave. Neither of these lenses is here appreciably affected in modifying the horizontal distribution of path-difference, because the dispersion of the grating requires a horizontally parallel system of rays.

**68. Observation with lens systems on both sides.**—The method shown in plan in figure 85 ($L$ and $L'$ convex lenses, $G$ grating, $M$ and $N$ mirrors, telescope at $T$) was tested. The outcome can not at once be foreseen, since the focal distances for different colors is different and since slight displacements of either lens must greatly modify the interference pattern. The latter, however, as obtained in every case, proved to be exceedingly fine lines, tipping in the

usual way with the motion of the micrometer and indicating a center of ellipses very distant in the field of the spectrum. In other words, the interference pattern is no longer automatically centered and is therefore useless.

A modification of this plan is the method shown in figure 86 (horizontal section), where $B$ is the beam from the collimator, $L$, $L'$,$L''$,$L'''$, four condensing lenses of the same power ($f = 50$ cm.), $G$ the grating, $M$ and $N$ opaque plane mirrors, $T$ the telescope. In all the above cases the horizontal rays from the collimator traverse the grating in parallel and eventually condense to a single point in the field of the telescope. The same is true of all rays having the same angle of altitude. These rays, therefore, act as a whole, since they pass through the plate of the grating at the same angle of incidence. On the other hand,



85



86
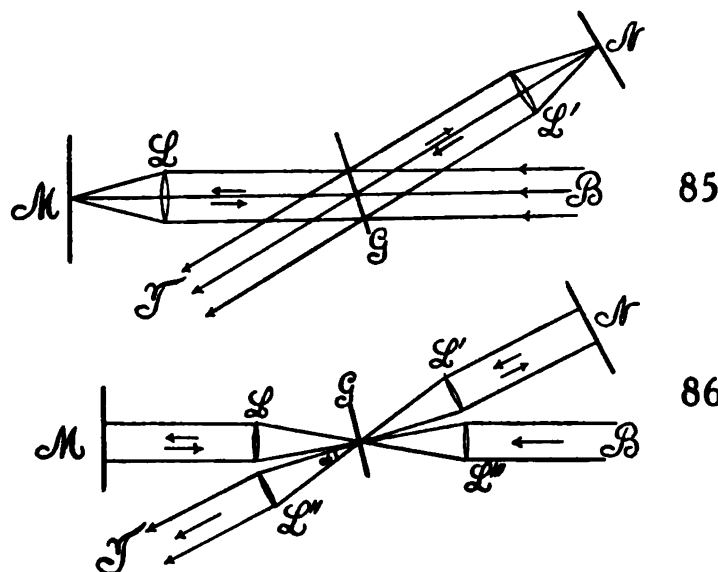
relative to a vertical plane, the rays traverse the grating at different angles, each angle corresponding to a horizontal strip of the spectrum. It is by the easy modification of this obliquity that the curved compensator becomes effective. In figure 86 the rays are also oblique relative to a horizontal plane; but the result, unfortunately, is not available, since each of these oblique rays must have its own complete spectrum. Consequently the diffracted pencil will consist of an infinite number of overlapping spectra, the extreme cases lying within the same angle $\alpha$ shown in the figure. A large telescopic objective would then reunite these spectra into a white image of the slit, while a small objective will show colored slit images, passing from impure red to impure violet. Naturally, the interferences will also overlap, and therefore vanish.

**69. Telescopic interferences.**—If interference patterns of small angular extent are to be obtained, it is essential that the rate at which obliquity increases from ray to ray be made as large as practicable. Probably, therefore,

an opportunity for realizing these conditions will be found within the telescope; *i.e.*, after the rays pass the objective. The endeavor would therefore be directed to bringing two spectra, focussed in two planes, one of which is behind the other and consequently of different sizes, both vertically and horizontally, to eventual interference.

The experiment was made on the long interferometer (fig. 87), the distances between mirror $M$ and grating $G$ and from the latter to the mirror $N$ being nearly 2 meters each. $C$ is the lenticular compensator, consisting of two lenses, respectively concave and convex, each having the same focal distance, $f = \pm 50$ cm. The distances apart, $D$, of the lenses may be varied. The glass plate $C'$, which is revolvable about the vertical, is thick enough to exactly counterbalance, if necessary, the thickness of the glass plate of the grating and of the lens system $C$. A sharp wedge sliding transversely may also be used. It is best to replace $C'$ by two plates of glass, one thick and the other thin, so that the latter may be removed.

The telescope directed along the axis $R$ will therefore, in general, see two white slit images, $A$ and $A'$ (fig.88), not both in focus at once, $A'$ coming from



87

88
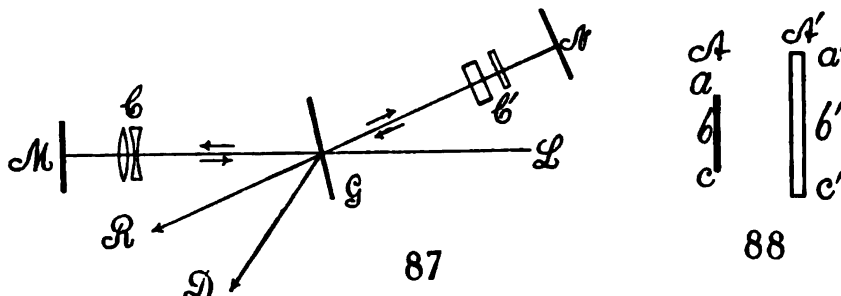
$M$ being larger, $A$ from $N$ (parallel rays) smaller. The focal plane of $A'$ will be towards the grating as compared with $A$, and $A'$ is larger than $A$, in proportion as the distance apart of the lenses $C$ is larger. Similarly, the two spectra are observed along the diffraction axis, $D$, not in focus at once and of different areas.

To obtain the interferences the slit image $A$ must be placed anywhere within $A'$, and they will occur at the top of the spectrum if $a$ and $a'$ are vertically in coincidence; in the middle if $b$ and $b'$ coincide, etc.

The plane of the new interferences is no longer the principal focal plane, containing the Fraunhofer lines, but lies in front of it; *i.e.*, towards the eye of the observer and away from the grating. This distance, measured along $D$ for the given small telescope used, was fully 1 cm. The focal planes of the two spectra are usually not so far apart. $A'$ corresponds to a virtual object behind the observer.

If the vertical plane in which the interferences lie be taken as the image, the object would be situated about 3 meters beyond the objective of the telescope used. This would place it 30 cm. in front of the mirror $M$ or $N$, where there is but a single beam in each case. In fact, the telescope may be brought quite

up to the grating. Hence interference is produced in the telescope itself, where rays are relatively very divergent, a condition which accounts for the smallness of the interference pattern. This understanding of the case is tentatively shown in figure 89, where $O$ is the objective of the telescope, $M$ the larger image from the mirror with the lens compensator, and $N$ the image from the other mirror (parallel rays). If the corresponding rays be drawn through the extremity of $M$ and $N$, their fields of interference, $F$ and $F'$, would begin in the plane $I$ and $I'$. For axial rays it would be at $i$. Thus the locus as a whole would not be a plane, and this seems to be the case. If the telescope moves toward the grating, $II'$ moves toward the right in the figure, as though the virtual object beyond the grating were fixed in position. At all events, the problem is to find the interference diagram of two symmetrical plane parallel spectra, of different areas and placed at definite distances apart.
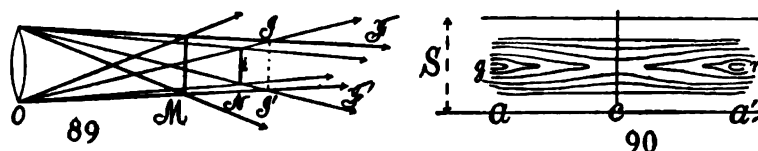


The appearance of the fringes is indicated in figure 90, where $S$ is the height of the spectrum, usually quite out of focus. There are many more lines than could be drawn in the sketch. The ends $a$ and $a'$ seem to surround small ellipses, but these are not quite closed on the outer edge. The center of symmetry is at $C$. The demarcations are stronger and broader vertically if the distance apart of the lenses $C$ (fig. 87) is small; fainter, but nevertheless clear and narrower, if this distance is large. Horizontally the fine lines thread the spectrum. The best results were obtained when the lenses $C$ are less than 1 cm. apart, the middle band being about half as high as the spectrum. Two contiguous lenses gave a design which nearly filled the spectrum vertically.     For practical purposes the lens compensator $C$ is to be attached to the mirror $M$, just in front of and moving with it. It makes little difference here whether the concave lens or the convex lens of the doublet $C$ is foremost.

If the micrometer $M$ is moved, or if the telescope is slid to the right or left, or forward, so as to take in other parts of the spectrum, the nearly closed lines at $a$ and $a'$ become finer and finer crescent-shaped lines, always open outward, till they pass beyond the range of vision. The whole phenomenon remains on the same level of the spectrum. On moving the telescope forward as far as $G$ (fig. 87), the ocular has to be drawn outward (towards the eye) till it is fully 2 cm. beyond the position of the principal focal plane. The whole spectrum is now seen with the interferences from red to violet (no ellipses), but having the same relative position as before. The central horizontal band measures about one-fifth the height of the spectrum, while the fine parallel horizontal lines extend to the upper and lower edges. The
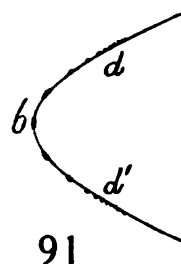
appearance is now curiously like a blunt wedge (fig. 91), with a band at *b* nearest the eye, and the lines *dd* extending quite to the rear. This impression is probably an illusion, due to the shading; the lines grow finer and are more crowded toward the bottom and top of the spectrum. The illusion of a reëntrant wedge is not possible.

To use this interference pattern for measurement, the cross-hair is supposed to pass through the region *c* (fig. 90) symmetrically. Very slight motion of the micrometer mirror *M* then throws *c* either to the right or the left of the cross-hair. In this case the lens doublet, *C*, is attached to the mirror and moves with it, as stated. To obtain the extreme of sensitiveness, the path-difference of *NG* and *GM* must be all but zero; *i.e.*, the grating plate *G* and the lens doublet *C* (fig. 87) must be all but compensated for equal air-distances by the compensator *C'*. In this case of full compensation, the interference pattern, in the absence of a doublet *C*, would be enormous and diffuse, seen preferably in the principal plane of the telescope, but useless for measurement. The introduction of a lenticular compensator, balanced by a compensator in *GN*, transforms the huge pattern into the small interference fringes in question, with the advantage that the high mobility of the coarse design has been retained. In other words, an index suitable for adjustment has been found, compatible with extreme sensitiveness. In fact, it is difficult to place the micrometer mirror *M* so that the region *c* (fig. 90) is exactly bisected. As the plane in which these interferences are seen most distinctly is 1 cm. or more anterior to the principal focal plane, the Fraunhofer lines are unfortunately blurred and a cross-hair is needed as a line of reference.

I may in conclusion refer to a similar series of experiments now in progress, in which the compensators placed in the *M* and *N* pencils (fig. 87, *C, C'*), instead of being of different shapes as above, are plates of different kinds of glass (crown and flint, for instance). Here the successive differences of dispersive power, from wave-length to wave-length, produce effects closely resembling those discussed, with the advantage that difficulties inherent in the curved system are avoided.

# CHAPTER X.

## THE DISPERSION OF AIR.

**70. Introduction.**—In view of the long-armed interferometer available, it seemed interesting to test the refraction of air at different wave-lengths, $\lambda$. An iron tube of inch gas-pipe, 138 cm. long, was therefore placed in one or the other of the component beams. The tube was closed at both ends by glass plates, about one-eighth of an inch thick, kept in place with resinous cement. A lateral tube communicated with an air-pump and drying train, so that the tube could be alternately exhausted and refilled with air. By using sunlight, the different lines of the spectrum were obtained with sufficient clearness, and the method consisted in finding the reading of the micrometer for successive Fraunhofer lines, both for the case of a plenum of air and for a vacuum. If $\Delta N$ is the (monochromatic) displacement of micrometer corresponding to the latter difference of pressure, $\mu$ being the index of refraction of air, $e$ the thickness,

(1)
$$\Delta N_\lambda = e\left(\mu_\lambda - 1 - \lambda\frac{\partial\mu_\lambda}{\partial\lambda}\right)$$

To determine $\mu_\lambda$, we must know $\partial\mu_\lambda/\partial\lambda$. It has been omitted above, because it enters differentially and because of its small value. It appears as a constant decrement of $\Delta N_\lambda$, as $\lambda$ is constant and $\partial\mu_\lambda/\partial\lambda$ is negative. In the present case, where $\mu$ is actually to be measured, $\partial\mu_\lambda/\partial\lambda$ enters directly and is essential; but it follows from any two experiments when $\mu$ is found for different colors.

TABLE 8.—Values of $B$. Inch iron gas-pipe, 138.0 cm. long. $D$ line.

| $t$ Bar | $p$ | $10^3\Delta N$ |
|---|---|---|
| 22.0° 76.20⎫ 20° ⎭ | 75.0 | 38.0 |
| 22.3° 75.83⎫ 20° ⎭ | 74.5 | 37.9 37.7 37.6 37.9 37.7 37.6 37.6 37.7 37.5 37.7 |
| Mean.... | ............ | 37.69 |

**71. Observations with arc lamp.**—In table 8 results are given as obtained with the electric arc, in which the sodium line usually appears with sufficient distinctness in the spectrum to be available as a line of reference for measure-

124

ment. Disregarding earlier results, the following are mean values of the ten independent data for $\Delta N$ (each comprising a reading for vacuum and for plenum):

$$10^6\lambda = 58.9 \text{ cm.} \quad t = 22.3^\circ \quad p = 74.5 \text{ cm.} \quad 10^3\Delta N_D = 37.69 \text{ cm.} \quad l = 138.0 \text{ cm.}$$

Thus

$$(2) \qquad \mu - 1 = \frac{\Delta N}{e} + \frac{\lambda \partial \mu}{\partial \lambda} = (\mu_0 - 1)\frac{p}{76}\frac{273}{\tau}$$

where $\mu_0$ refers to normal pressure and absolute temperature $(\tau)$. If $\mu_0$ is given for the $D$ line, $\partial \mu / \partial \lambda$ is determinable. It will be sufficient for the present purposes to put $\mu_0 = A + B/\lambda^2$, or $\lambda \cdot \partial \mu / \partial \lambda = -2B/\lambda^2$

$$(3) \qquad \frac{\Delta N}{e} - (\mu_0 - 1)\frac{p}{76}\frac{273}{\tau} = \frac{2B}{\lambda^2}$$

$B$ referring to $\tau$ and $p$. Mascart's * value for $\mu_0 - 1$ (agreeing with Fabry's) is $10^{-6} \times 292.7$, whence

$$B = 10^{-14} \times 1.34 \text{ at } \tau \text{ and } p$$

If the value $B$ be computed from Mascart's observations between $C$ and $E$, $D$ and $F$, respectively,

$$B_{CE} = \frac{2.1 \times 10^{-6}}{1.28 \times 10^{-8}} = 1.64 \times 10^{-14} \qquad B_{DF} = \frac{2.3 \times 10^{-6}}{1.39 \times 10^{-8}} = 1.65 \times 10^{-14}$$

so that the mean value $10^{14}B = 1.65$ may be taken. Since the last decimals of $\mu$ are in question, it will not be correct to more than 5 to 10 per cent.

The value found above ($10^{14}B = 1.34$) is therefore somewhat too small. True, since from equation (3)

$$(4) \qquad \frac{\partial B}{\partial(\Delta N)} = 10^{-14} \times 1260$$

an error of $10^{-4}$ cm. in $\Delta N$ is an error of $0.13 \times 10^{-14}$ or 10 per cent in $B$. Very close agreement can not therefore be expected in either result. One is tempted to refer the present low value of $B$ to flexure of the glass end plates of the tube, which, when the tube is exhausted, become slightly saucer-shaped and introduce a sharp concentric wedge of glass into the component beam, whereby the interference pattern is changed, probably in the direction of smaller values, as found. But the direct experiments below do not show this. In any case, the measurement of $B$ lies at the limits of the method. An advantage may possibly be secured by using two identical tubes, one in each component beam, the tubes to be exhausted alternately. The sensitiveness would then be doubled.

**72. Observations with sunlight. Single tube.**—These observations are given in table 9, the exhaustion throughout being 75 cm. and the temperature about 16°. In the first set sunlight was used without a condensing lens; in

---

* See excellent summary in Landolt and Boernstein's Tables, 1905, p. 214.

the second set the sun was focussed with a weak lens (0.5 meter in focus) at the point formerly occupied by the electric arc. The spectrum (particularly in the second case) was brilliant and the lines clear. The focus of sunlight is to be placed just outside the focus of the collimator lens, in order that a nearly linear pencil may be available to penetrate the long refraction tube twice. The distance of the collimator lens to the grating was about 2 meters. The spectrum is then a bright band in the telescope, the width being limited by the height of the ruled part of the grating. The strip of white light on the grating should not be more than a few millimeters wide. It must therefore be narrowed by an opaque screen (wide slit of the given width) in the path of the beam (see fig. 92 below).

TABLE 9.—Dispersion of air. Tube $l = 138.0$ cm. Bar. 77.25 cm. at $19.5°$. $p = 75.0$ cm

| Line. | Temp. | $10^9 \Delta N$ | $10^{+14}B$ |
|---|---|---|---|
| C | 16.0° | 38.5 ⎫ | |
| D | " | 39. ⎬ | 1.5 |
| b | " | 39.4 ⎭ | |
| C | 16.0° | 38.5 ⎫ | |
| D | " | 38.9 ⎬ | 1.4 |
| b | " | 39.3 ⎭ | |
| Improved seeing, weak condensing lens. | | | |
| C | 16.4° | 38.8 ⎫ | 1.51 |
| D | " | 39.2 ⎭ | |
| C | 16.4° | 38.9 ⎫ | |
| D | " | 39.1 ⎬ | 1.65 |
| b | " | ?39.3 ⎪ | 1.4 |
| F | " | 40.1 ⎭ | |
| C | 16.4° | 38.8 ⎫ | 1.61 |
| F | " | 40.1 ⎭ | |

The equation for $B$ in this case, if the symbol $\delta$ refers to differences for two given values of $\lambda$, is

$$3B_0 = \frac{\delta \Delta N / \epsilon}{\delta \frac{1}{\lambda^2}} \frac{76}{p} \frac{\tau}{273}$$

if the value of $B$ is to hold for normal conditions.

The data are shown in table 9, series 1 and 2 being obtained without condensing lens. These are inferior, as regards definition of lines, to the subsequent set, in which condensed sunlight was used. In all cases there is sometimes an irregularity (marked by ? in table 9) in which the observation is obviously discordant, but the reason could not be found. Possibly values of $\tau$ and $p$ taken were not the actual values. The data for $B \times 10^{14}$ given in the table are mean values. Some of these are low. Later values, where the $F$ line is included, come out larger, the range being from 1.3 to 1.8 or 1.5, on the average. It is desirable to use the whole of the available range of the spectrum (sufficiently luminous from $C$ to $F$) to obtain an acceptable value of the coefficient $B$ and additionally to improve the method by using two

identical tubes, alternately exhausted as suggested above. The attempted B measurement is at the limits of the method, as has already been instanced in the discussion of errors in the preceding paragraph, and it is not to be concluded that data which happen to agree with Mascart's result from a correct application of the present method. In fact, there is no reason for excluding the exceptional values, and the present results are to be regarded as preliminary.

**73. Two (differential) refraction tubes.**—In the following experiments two identical iron tubes (138 cm. long, of inch gas-pipe) were installed, one being placed in each of the component beams of light, which subsequently interfered, and the tubes were exhausted alternately. There are apparently three advantages in this arrangement. In the first place, the sensitiveness is doubled; in the second, the flexure of glass plate should be the same at each tube, in each experiment, and thus fail to disturb the interference pattern. Furthermore, by using the tubes in parallel (*i.e.*, exhausting both at the same time), any irregularity of flexure effect, etc., should be determinable, as the air in both tubes will be identically circumstanced. Finally, the air being inclosed in a thick metallic envelope at both beams is not subject to incidental disturbances. An unexpected difficulty, however, was encountered; for there is reflection of direct spectra from the eight glass surfaces, and this must be specially met. The direct spectrum is easily eliminated by inclining the grating until the reflected interference spectra are at a different level; but reflections of this spectrum are not so easily dealt with. Fortunately they are weak. Even so, they are very annoying, as they overlap the interference pattern and dull it. They could be eliminated by attaching the glass plates obliquely to the axis of the pipes, but this remedy was not thought of at the outset.



92
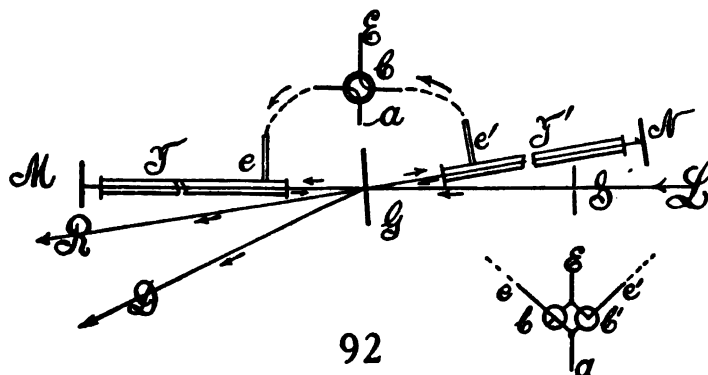
Figure 92 is a diagram of the disposition of the parts of the apparatus. L is the beam of white sunlight from the collimator limited laterally by the wide slit (⅛ inch) S. G is the grating, T and T' the two refraction tubes, M (micrometer) and N the opaque mirrors, R the refracted and D the diffracted (spectrum) beam of light. C is virtually a four-way stopcock (or two 3-way glass stopcocks) leading respectively to the exhaust pump E and dry

air supply $A$, from the tubulures $e$ and $e'$ of both refraction tubes $T$ and $T'$. These are therefore alternately exhausted.

Preliminary results are given in table 10, the arc lamp with its sodium line being used in the absence of sunlight. It will be seen that $\Delta N$, apart from temperature (which is here higher than above), has been doubled. The deflections were symmetrical within $0.15 \times 10^{-3}$ cm.

TABLE 10.—Dispersion of air. Differential tubes, each 138 cm. long. $D$ line in electric arc.
$p = 74$ cm.

| Barometer. | Temp. | $10^3 \Delta N$ | $(\mu_0 - 1) \times 10^6$ | $B_0 \times 10^{14}$ |
|---|---|---|---|---|
| 75.93 cm., 22° | 21.5° | 75.4<br>75.3<br>75.4 | 291.6 | 1.47 |
| 76.02 cm., 19.5° | 18.0° | 76.3<br>76.4<br>76.4 | 291.8 | 1.49 |
| (Single tube) | 23.0° | 37.8 | 293.6 | 1.80 |

The values of $B$ found in the first two series of this table, if the standard value of $\mu_0 - 1 = 0.0002927$ is assumed, is somewhat small, but as near to the true values as may be expected. Again, if $B \times 10^{14} = 1.65$ is assumed, the $\mu_0 - 1$ values given in the table are similarly small, being 0.3 per cent short of standard values. A single-tube experiment made for comparison (series 3), similarly, came out too large in each case. It follows from this that $p$ and $t$ observations are not sufficiently guaranteed. It is hardly probable, however, that with a micrometer reading to $10^{-3}$ cm. and estimated to $10^{-4}$ cm. (vernier) the precision can be much enhanced; for since

$$B_0 = \frac{\lambda^2}{2} \frac{\Delta N}{e} \frac{76}{273} \frac{\tau}{p} - (\mu_0 - 1)$$

$$\frac{\partial B_0}{\partial p} = -\frac{\lambda^2}{2} \frac{\Delta N}{e} \frac{76}{273} \frac{\tau}{p^2} \qquad \frac{\partial B_0}{\partial \tau} = \frac{\lambda^2}{2} \frac{\Delta N}{e} \frac{76}{273} \frac{1}{p}$$

or at the $C$ line and $D$ lines, respectively,

$$\delta p = 1 \text{ cm.} \qquad \delta B = {}_0 \begin{cases} 0.8 \times 10^{-14} \\ 0.7 \times 10^{-14} \end{cases} \qquad \delta \tau = 1° \qquad \delta B_0 = \begin{cases} 0.2 \times 10^{-14} \\ 0.2 \times 10^{-14} \end{cases}$$

Now, unless the measurement can be made in terms of rings, it is difficult to detect a few millimeters of pressure difference by displacement only.

The interesting question now occurs whether the two tubes, if identical for a plenum of air, remain identical (no shift of the interference pattern) throughout all the stages of identical exhaustion. On trial, nothing could be detected, the fringes remaining stationary during the whole period of exhaustion, or during the influx of air following a high vacuum. Hence there is no perceptible difference effect of flexure of the glass ends, and the ultimate question of accuracy depends on the measurement of $\tau$ and $p$. To eliminate the possible effect of flexure, an air column of negligible length, in which the glass effect only is present, will have to be tested; otherwise there is no possibility of separating the air and glass effect.

**74. Differential and single refraction tubes. Sunlight.**—The direct experiments for the coefficient $B$ were now resumed and conducted with sunlight, with the results given in table 11. The first two series were made with the two identical tubes specified, exhausted alternately, one tube containing a plenum of air, while the other was nearly empty in each experiment. The $C$ and $F$ lines alone were used for measurement. In spite of the large displacement ($\Delta N = 0.076$ to $0.078$ cm.), the results were not as satisfactory as was expected, owing to the fact that sharpness of vision is made difficult by the stray reflected spectra to which reference has already been made. But the data for $B$ obtained with one exception (No. 2 in the first series) are consistent and reasonably good. In every other respect the work was satisfactory and could have been improved by using oblique cover-glasses. The values of $B$ obtained are therefore disconcerting.

TABLE 11.—Dispersion of air. First and second series, Differential Tubes, each 138.0 cm. long. $C$ and $F$ lines. Third and fourth series, Single Tube, good adjustment.

| Barom. | $p$ | Line | $10^3\Delta N$ | $10^{14}B$ | Temp. | Barom. | $p$ | Line | $10^3\Delta N$ | $10^{14}B$ | Temp. |
|---|---|---|---|---|---|---|---|---|---|---|---|
| | cm. | | cm. | | °C | | cm. | | cm. | | °C |
| 77.05⎱ 22°⎰ | 74.0 | C | 76.4 | 1.0 | 17.4 | 77.22⎱ 21°⎰ | 74.0 | C | 38.4 | 0.99 | 18.0 |
| | | F | 78.0 | .... | .... | | | F | 39.2 | .... | .... |
| | 74.0 | C | 76.1 | 1.3 | 17.4 | | 74.0 | C | 38.2 | 1.11 | 18.0 |
| | | F | 78.2 | .... | .... | | | F | 39.3 | .... | .... |
| | 74.0 | C | 76.3 | 1.1 | 17.4 | | 74.0 | C | 38.3 | 1.18 | 18.0 |
| | | F | 78.0 | .... | .... | | | F | 39.3 | .... | .... |
| | 74.0 | C | 76.2 | 1.1 | 17.4 | | 74.0 | C | 38.2 | 1.06 | 18.0 |
| | | F | 78.0 | .... | .... | | | F | 39.0 | .... | .... |
| 76.27⎱ 23°⎰ | 74.0 | C | 75.8 | 1.0 | 21.4 | 77.22⎱ 21°⎰ | 76.0 | C | 39.3 | 0.99 | 18.1 |
| | | F | 77.4 | .... | .... | | | F | 40.1 | .... | .... |
| | 74.0 | C | 75.4 | 1.1 | 21.4 | | 76.0 | C | 39.2 | .99 | 18.1 |
| | | F | 77.2 | .... | .... | | | F | 40.0 | .... | .... |
| | 74.0 | C | 75.4 | 1.1 | 21.4 | | 76.0 | C | 39.0 | .99 | 18.2 |
| | | F | 77.1 | .... | .... | | | F | 40.0 | .... | .... |
| | | | | | | | 76.0 | C | 39.2 | .99 | 18.2 |
| | | | | | | | | F | 40.0 | .... | .... |

I then went back to the single-tube experiments (in series 3 and 4), and these are the smoothest results obtained. The $C$ and $F$ lines were used as before. In the last series, for instance, the micrometer reading is the same to $10^{-4}$ cm. throughout. In spite of this satisfactory behavior, the value of $B$ obtained is again of the same low order, all the data, both for double and single tubes, being consistent throughout in this respect. Series 3 and 4 agree, although $p$ is changed from 74 cm. to 76 cm. of mercury.

In table 12 I have summarized the data in comparison with the standard results, computing $\mu_0 - 1$ and $B_0$, for each of the cases, reducing all values to $0°$C. and 76 cm. of mercury. The difference of $\mu_0 - 1$ for the $F$ and $C$ lines, which is $3.2 \times 10^{-6}$ for the standard data, is but $2.3 \times 10^{-6}$ on the average in the present results. Similarly, the mean values of the latter are $10^{-6} \times 4.1$ and $10^{-6} \times 3.2$ larger for the $C$ and $F$ lines, respectively, than the standard results.

These conditions are particularly puzzling, since in §73, with the use of the arc lamp, both results were nearly normal. I therefore endeavored to detect the causes for this difference of behavior.

TABLE 12.—Summary of Table 11. "St." refers to standard data. $A = (\mu_0 - 1)$.

| Line, etc. | $\lambda \times 10^8$ | St. $10^8 A$ | Series. | | | | Ser. (1) to (4) $B_0 \times 10^{14}$ | $(\mu_0 - 1)$ St. | |
|---|---|---|---|---|---|---|---|---|---|
| | | | (1) $10^8 A$ | (2) $10^8 A$ | (3) $10^8 A$ | (4) $10^8 A$ | | $B_0 \times 10^{14}$ C. | $B_0 \times 10^{14}$ F. |
| C.............. | 65.63 | 291.8 | 295.0 | 296.0 | 296.3 | 296.5 | 1.18 | 1.85 | 1.33 |
| $10^8$ Diff. from St. | ..... | ..... | −3.2 | −4.2 | −4.5 | −4.7 | 1.20 | 2.37 | 1.56 |
| F.............. | 48.61 | 295.0 | 297.3 | 298.0 | 298.7 | 298.6 | 1.28 | 2.22 | 1.70 |
| $10^8$ Diff. from St. | ..... | ..... | −2.3 | −3.3 | −3.7 | −3.6 | 1.08 | 2.55 | 1.50 |
| $10^8$ Diff. F and C. | ..... | 3.2 | 2.3 | 2.3 | 2.4 | 2.1 | .... | .... | .... |

The standard of length was first compared with a normal meter, showing that the $1 = 138.0$ cm. for the $M$ tube should be replaced by $137.75$ cm. and for the $N$ tube by $137.59$ cm. As this correction affects all the results, $\mu_0 - 1$ and $B$, in the same ratio, it contributes nothing to modify the discrepancy in question. The correctness of the micrometer screw was assumed, as it was of good manufacture.

The test next was made to see if the lines taken as $C$ and $F$ actually had the accepted wave-lengths. A revolvable arm, with its axis at the grating and 125.5 cm. long, was therefore installed for the direct measurement of the diffraction of the grating. The results obtained for the wave-lengths of the lines taken showed that no mistake had been made in their selection.

To endeavor to obtain further evidence, the values of $B$ were computed for the mean data of table 11, by using the standard values for $\mu_0 - 1$ in case of the $C$ and $F$ lines and the $\Delta N/e$ given by the observations. The results so obtained are given in the last columns of table 12, for each of the four series and the $C$ and $F$ lines at normal temperature and pressure. The mean results are thus—

$B_0 \times 10^{14} = 1.19$ from observations with sunlight directly
between $C$ and $F$ lines.

$B_0 \times 10^{14} = 2.25$ from standard $\mu_0 - 1 = .0002918$ at $C$ line.

$B_0 \times 10^{14} = 1.52$ from standard $\mu_0 - 1 = .0002950$ at $F$ line.

The $B$ values of table 10 show a march to be referred to temperature and pressure. So the present unsatisfactory differences are probably pressure-temperature effects beyond the discrimination of the method.

One reason for this discrepancy which suggests itself is the possible distortion of the glass plates at the end of the exhaust tubes during the exhaustion. There may be a residual temperature effect due to the heating of the air by the beam which passes twice through it, above the indicated temperature of the surrounding tube of iron. But as $\mu_0 - 1$ is already too large compared with standard values, this would make the case worse. Similarly, a larger thermal coefficient than the normal value (1/273) would further increase

the data for $\mu_0 - 1$. For the case of the $F$ lines, the $B$ values found by comparison with the standard $\mu_0 - 1$ (last column of table 12) might be taken as correct within the error of method. Nothing, however, has been found to account for the correspondingly large values of $B_0$ for the $C$ line.

**75. Distortion of glass absent.**—To test the effect of possible distortion of the end plates of the tube, a shallow cell was constructed but 0.8 cm. deep, closed by plates of the same glass. The diameter of the tube was identical with that of the long refracting tubes. Tests made with the electric arc and sodium line gave the mean values

$$\text{Plenum} \ldots \ldots \ldots 10^8 \Delta N = 5.47; \quad 6.6 \text{ cm.}$$
$$\text{Vacuum} \ldots \ldots \ldots \quad\quad 5.25; \quad 6.4 \text{ cm.}$$

Thus the effect of exhaustion is 0.00021 cm. The long tube gave, on the average, 0.039 cm. for 138 cm. of length. Hence the air effect should be

$$0.039 \times 0.8 / 138 = 0.00022$$

which is practically identical with the value found. Hence there is no perceptible distortion referable to the glass plates.

TABLE 13.—Dispersion of air. $D$ and $F$ lines. Single Tube, length 138 cm. Barom., 75.40 at 28°. $p=74$ cm. Temp. 20°. St. refers to standard data. $A=\mu_0-1$.

| Line. | $10^3 \Delta N$ | $10^6 \dfrac{\Delta N_0}{e}$ | $10^{14}B_0$ | Line, etc. | $\lambda \times 10^6$ | St. $10^6 A$ | Mean $10^6 A$ | St. $\mu_0 - 1$ | |
|---|---|---|---|---|---|---|---|---|---|
| | | | | | | | | $10^{14}B_0,F$ | $10^{14}B_0,D$ |
| | *cm.* | | | | *cm.* | | | | |
| $F$ | 39.4 | 312.8 | 2.24 | $F$ | 48.61 | 295.0 | 304.0 | 2.10 | 19.2 |
| $D$ | 38.2 | 303.8 | .... | $10^6$ Diff. from St. | ..... | ..... | −9.0 | .... | ..... |
| $F$ | 39.0 | 310.1 | 1.38 | | | | | | |
| $D$ | 38.3 | 304.6 | .... | $D$ | 58.93 | 292.7 | 299.4 | 1.78 | 2.06 |
| $F$ | 39.0 | 310.5 | 1.49 | $10^6$ Diff. from St. | ..... | ..... | −6.7 | .... | ..... |
| $D$ | 38.3 | 304.6 | .... | $10^6$ Diff. $F$ and $D$ | ..... | 2.3 | 4.6 | 1.83 | 2.06 |

**76. Further observations with sunlight.**—In the absence of other than inferential reasons to account for the difficulties met with, a final series of observations was made between the $D$ and $F$ lines and a single tube, with the results given in table 13. The mean value of $B_0$ found directly, viz, 1.70 $\times 10^{-14}$, would be admissible; but the corresponding values of $\mu_0 - 1$ as compared with the standard values are again too large and worse than above. The same is true of the values of $B_0$ found by comparison of $\Delta N/e$ with the standard values of $\mu_0 - 1$, and their coefficients come out differently for the $C$ and $F$ lines. In fact, the discrepancy of $\mu_0 - 1$ is now about 3 per cent, whereas observations for $\Delta N/e$ should not be in error more than ($2 \times 1/400 =$ 0.0025) 0.5 per cent. There is thus something variable at the limit of application of the present method which has persistently escaped detection. I have thought that a distortion associated with the form of the interference pattern in passing from $C$ to the $F$ line may be in question, as the discrepancy

varies in different, otherwise satisfactory experiments; or the failure to completely exhaust the tube may leave a small error which becomes appreciable in $B$.

**77. Conclusion.**—If allowance is made for the fact that $\Delta N$ at the micrometer is measured for air, at barometric pressure $p'$ and absolute temperature $\tau$, the equation for $\mu_0 - 1$ at normal conditions would be

$$\mu_0 - 1 = \frac{\Delta N}{e}\frac{76}{p}\frac{\tau}{273}\frac{1}{1 - p'\Delta N/ep} - \frac{2B_0}{\lambda^2}$$

where the correction factor $1 - \Delta N p'/pe$ would not appreciably modify the results.

It is difficult to see, therefore, why the promising results of §4, which are quite as near the standard data as the method warrants, did not bear consistent fruit in the sequel. The direct values of $B_0 \times 10^{14}$ are usually too small, sometimes too large, and range from 1 to 2. On the other hand, $\mu_0 - 1$ usually comes out too large, whereas it should be correct to a few tenths percentage. None of the causes examined, temperature, pressure, thermal coefficient, flexure of glass, etc., quite account for such a result. If $B_0 \times 10^{14}$ is computed from standard results for $\mu_0 - 1$ and observed at different spectrum lines, the data are nearly correct for some lines, but too large for other lines, so that a single constant does not reduce the series. It does not seem probable, however, that equation (1) is inadequate; for the results obtained with equal care at different times for the same $\mu_0 - 1$ or $B_0$ are not in accord. The discrepancies, in other words, are not persistent in value and are therefore due to some incidental cause which has not been detected. It has seemed to me that the change in shape of the interference pattern on passing from red to violet, which in case of ordinary glass mirrors is marked, may be responsible for some of the difficulties encountered. This pattern, which for optically flat surfaces would remain elliptical, becomes more and more irregular as the distances, $e$, of the mirror and grating are increased. The distorted image shrinks laterally from red to violet fully one-half, so that it is not certain that the center of figure is actually a fiducial point. The question, however, would have to be tested.

# CHAPTER XI.

## THE CHANGE OF THE REFRACTION OF AIR WITH TEMPERATURE.

**78. Apparatus.**—In the earlier report (Carnegie Inst. Wash. Pub. 149, III, Chap. 15, p. 223) I began some experiments on the change of the refractive index of air with rise of temperature. The question is interesting, inasmuch as the temperature coefficient has not in most investigations been found identical with the coefficient of expansion of air, as Lorentz had obtained it and as would otherwise be anticipated; but a value, over 3 per cent larger, first put forward by Mascart, seems preferable. My earlier work was left unfinished, however, because the design of the apparatus, in which the refraction tube was heated in an independent annular steam-bath, was unsatisfactory. It seemed to be impossible to reach the temperature of the steam in that way, even after half a day's waiting. In the present work, therefore, the apparatus is modified, so that the steam may play directly on the long refraction tube. In this way the temperature difficulty was quite eliminated.
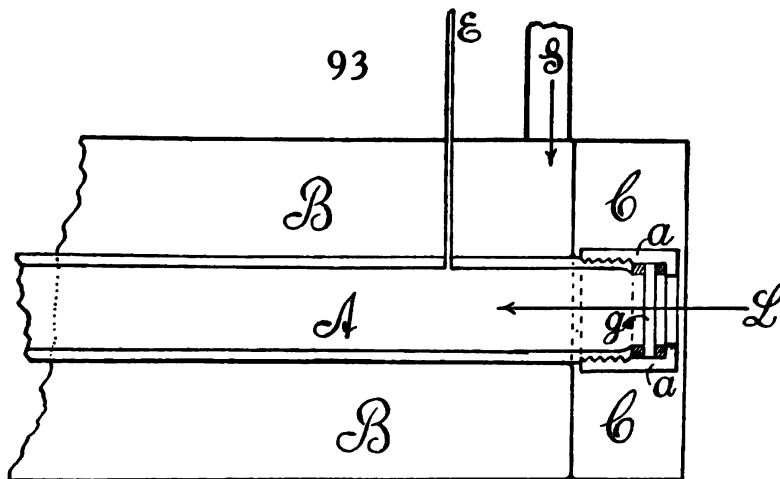


The tube containing the air column was made of inch brass gas-pipe, 71.7 cm. long (between windows) and 2.5 cm. in internal diameter (*A*, fig. 93, which shows one end of the apparatus). The ends were closed with the usual brass caps *a*, in which round windows, about 2 cm. in diameter, had been cut on the lathe. The ends were closed by plates of glass *g*, secured between two jackets of rubber and " vulcanized" fiber. *L* shows the axis of the beam of light.

*BB* is the steam chamber, steam entering at *S* and leaving by a similar tube at the other end of the apparatus. Steam is thus directly in contact with the tube. The projecting end of *A* is inclosed by a recess packed with wadding,

*CC.* As the walls of the brass pipe were thick and the ends relatively short, there seemed to be no objection to this arrangement. Care was taken to conduct the escape steam and hot gases away from the interferometer.

The displacement interferometer was of the linear type described above, the mirrors $M$ and $N$ and the grating $G$ being attached directly to the wall of the pier and without an intervening rail. Unfortunately the pier in a large city is also in incessant vibration, so that the interference patterns quiver. It is this insuperable difficulty which has prevented me from reaching results as accurate as were anticipated. A few of the data, however, will be added as an example of the efficiency of the method.

TABLE 14.—Refraction of air at different temperatures. Tube, 71.7 cm. long, 2.5 cm. in diameter.

| Barometer. | Temp. | $p.$ | $10^5 \times \Delta N$ | Barometer. | Temp. | $p.$ | $10^5 \times \Delta N$ |
|---|---|---|---|---|---|---|---|
| 77.04 cm. 22° I | 19.7° | 75.3 | 19.3 19.4 19.3 | 75.12 cm. 20° VI | 19.9° | 74.3 | 19.3 19.1 19.0 19.2 |
| 76.25 cm. 20° II | 21.7° | 75.5 | 19.1 19.3 19.2 19.4 19.4 19.3 | 76.98 cm. 18.7° VII | 100.4° | 75.5 | 15.0 15.0 15.0 |
| 77.22 cm. 20° IV | 19.1° | 75.7 | 19.8 19.7 19.8 19.7 19.7 | 76.55 cm. 23° III | 100.2° | 75.3 | 15.0 15.0 15.4 |
| 76.25 cm. 20° V | 22.2° | 75.5 | 19.1 19.2 19.4 19.6 19.5 | 75.12 cm. 20° VIII | 99.7° | 74.3 | 15.0 15.0 14.9 15.0 15.1 |

**79. Observations.**—The data are given in table 14, where the temperature and barometric pressure are shown in the first column, the differences in the pressure $p$ between the plenum of air and the exhausted air in the refraction tube in the second column, while the third shows the values of $\Delta N$, the displacement of the micrometer corresponding to $p$, as found in successive independent experiments at the temperature given. For such long distances between grating and mirrors the ellipses are visually distorted, and much depends on finding a satisfactory sharp interference pattern. This was the case, except in series 3 and 5, when for incidental reasons (outside tremors) the patterns were disagreeably flickering. The observations are usually for room air, as the special drying of air in series 3 and 5 made no perceptible difference. At 100° care must be taken to obviate convection currents of air, so far as possible. The endeavor was made to keep $p$ as nearly as possible at the same value, apart from the barometer pressure, which does not enter into the equations. In series 4 the values of $\Delta N$ are relatively large,

but quite consistent with each other. The reason for this could not be made out. But for the inevitable tremors the observations would all have been acceptable.

**80. Computation.**—Since the ends of the air-tube are perpendicular to the beam of light

$$(1) \qquad \Delta N = e\left(\mu - 1 - \lambda\frac{\partial\mu}{\partial\lambda}\right)$$

where $\Delta N$ is the difference of the displacements of the micrometer in the presence and absence of air in the tube, $e$ the effective length of the air column, and $\mu$ the index of refraction of the air for the given wave-length $\lambda$. The equation presupposes a knowledge of the dispersion of air $\partial\mu/\partial\lambda$; but, as this is small, the term may be temporarily omitted. If $\lambda$ is constant, it corresponds to a constant correction of $\Delta N$ throughout the experiments.

Again, if we have an equation of the form of Mascart's, $\mu_n$ referring to o° C. and normal barometer, and $N_0$ to the absence of air in the tube,

$$(2) \qquad \frac{\mu-1}{\mu_n-1} = \frac{p}{76}\frac{1+\beta(p-76)}{1+\alpha t} = \frac{N_p-N_0}{N_n-N_0} = \frac{\Delta N_p}{\Delta N_n}$$

where $\alpha$ and $\beta$ are two constants. If the tube is not quite exhausted ($\delta B$ remaining), the observations for a plenum (barometric pressure, $B$) and exhausted air being made at the same temperature,

$$\frac{\delta B}{B}(1-\beta(B-\delta B)) = \frac{N_{\delta B}-N_0}{N_B-N_0}$$

or nearly

$$\frac{B-\delta B(1-\beta B)}{B} = \frac{N_B-N_{\delta B}}{N_B-N_0} = \frac{\Delta N_{B-\delta B}}{\Delta N_B}$$

Thus if one neglects the small correction $1-\beta B$ of $\delta B$

$$(3) \qquad \Delta N_B = \Delta N_{B-\delta B}\frac{B}{B-\delta B}$$

the micrometer displacement $\Delta N_B$ in case of complete exhaustion at the barometric height, $B$, and the displacement $\Delta N_{B-\delta B}$ corresponding to partial exhaustion $B-\delta B$, are proportional to those pressures. Since $\delta B$ was quite small, this equation was assumed, and $p-\delta B$ is thus nearly the height of the mercury column of the partially exhausted tube. In the table this is briefly called $p$, and differs from the barometric height.

Finally, for two partial pressures $p$ and $p'$ and temperatures $t$ and $t'$ of the air

$$(4) \qquad \frac{p}{p'}\frac{1+\alpha t'}{1+\alpha t}(1+\beta(p-p')) = \frac{\Delta N}{\Delta N'}$$

$\Delta N$ and $\Delta N'$ being the micrometer displacement corresponding to $p$, $t$, and $p'$, $t'$, respectively. Hence if care be taken to make $p=p'$, nearly,

$$\frac{1+\alpha t'}{\Delta N} = \frac{1+\alpha t}{\Delta N'} = \frac{\alpha(t'-t)}{\Delta N-\Delta N'N\delta} = \alpha\delta t$$

if, for brevity, $t'-t=\delta t$ and $\Delta N-\Delta N'=\delta N$; or

(5)
$$\frac{1}{\alpha}=\Delta N\left(\frac{\delta t}{\delta N}-\frac{t'}{\Delta N}\right)$$

If $p$ is not quite equal to $p'$, $\beta(p'-p)$ may still be neglected, but $\Delta N/p$ and $\Delta N'/p'$ must replace $\Delta N$ and $\Delta N'$, or $\Delta N(1-\delta p/p)$ replace $\Delta N$ where $\delta p = p-p'$.

On applying equation (5) to series 1, 2, 3, for which $p$ is nearly constant,

$$\delta t = 79.5° \qquad \delta N = 0.00423 \qquad \alpha = 0.00380$$

applying it to series 4, 5, 7, similarly,

$$\delta t = 79.8° \qquad \delta N = 0.00404 \qquad \alpha = 0.00404$$

The mean value is thus $\alpha = 0.00392$. The reason of this difference is found in series 4, where $\Delta N$ is excessive. In fact, if we compare percentage errors of $\alpha$ and $\delta N$

(6)
$$\frac{d\alpha/\alpha}{d(\delta N)/\delta N}=\alpha\frac{\Delta N}{\delta N}\,\delta t=1.4$$

so that an error of 5 per cent in $\delta N$ would be an error of over 5 per cent in $\alpha$. For the case where the fringes tremble this is inevitable. If the mounting were without tremor, however, $\delta N$ should be guaranteed to $5\times10^{-5}$ cm., corresponding to the evanescence of a single interference ring, so that $\alpha$ should be determinable to 1 per cent, even in case of a tube of the length 71.7 cm. given.

If $\delta t$ is small or $t'$ small, equation (5) becomes, approximately,

$$\frac{\delta N}{\Delta N}=\alpha\delta t \text{ or } \Delta N'=\Delta N(1-\alpha\delta t)$$

This equation may be used to find the successive values of $\Delta N$ in the table, if the second, for instance, is supposed to be correct. It appears that the first and fifth differ about equally ($\doteq0.0001$ cm.) from the second, but the error of the fourth ($-0.00028$) is excessive. Hence if this second datum be taken as the mean of series 1, 2, 5, and combined with the two data for 100°,

$$\Delta N=19.28 \qquad \delta N=0.421 \qquad \delta t=78.6° \qquad t'=100.3° \qquad \alpha=0.00385$$

This is the more probable result of table 14 and would agree with Mascart's value, 0.00382.

Somewhat later, the independent series of observations 6 and 8 were carried out. The interference pattern at 99.7° was exceptionally quiet and clean, but at lower temperatures this was not better than usual. The results are

$$10^3\delta N=4.15 \qquad \delta t=79.8° \qquad \alpha=0.00372$$

somewhat below the preceding value.

**81. Final experiments at 100°.**—Somewhat later, at a time when the laboratory was relatively quiet and after the same effective improvements had been made in the mounting of the interferometer mirrors, the experiments

at 100° were repeated. The optical measurements were satisfactory, or at least just short of the counting of interference rings for measurement. The arc lamp, moreover, which is unsteady, would scarcely suffice for this purpose. The results obtained were as follows (table 15):

TABLE 15.—Refraction of air at different temperatures.

| Bar. | Temp. | $p$ | $10^4 \Delta N$ | Bar. | Temp. | $p$ | $10^4 \Delta N'$ |
|------|-------|-----|-----------------|------|-------|-----|------------------|
| 75.6 cm. | 21.8° | 74.0 | 19.3 | 76.72 cm. | 100.3° | 74.0 | 15.1 |
|  |  |  | 19.2 | 20.5° |  |  | 15.4 |
|  |  |  | 19.3 |  |  |  | 15.0 |
|  |  |  | 19.1 |  |  |  | 15.1 |
| 76.65 cm. | 21.8° | 74.0 | 19.6 |  |  |  | 15.5 |
|  |  |  | 19.4 |  |  |  | 15.0 |
|  |  |  | 19.5 |  |  |  | 15.2 |
|  |  |  | 19.2 |  |  |  | 15.4 |
|  |  |  | 19.3 |  |  |  | 15.2 |
|  |  |  |  |  |  |  | 15.3 |
|  |  |  |  |  |  |  | 15.2 |

If the mean values of $\Delta N$ and $\Delta N'$ be taken and $\alpha$ computed

$$10^4 \Delta N = 19.22 \qquad 10^4 \Delta N' = 15.22 \qquad \delta N = 4.00 \qquad \delta t = 78.5°$$

the result is

$$\alpha = 0.00361$$

As these experiments were the smoothest and were made under the most satisfactory conditions, they are probably the most trustworthy. I have not, therefore, been able to obtain evidence for a value of $\alpha$ (between 0° and 100°) greater than the coefficient of expansion of gases, though it must be confessed that the method in its present surroundings is not sufficiently sensitive to furnish a definite criterion.

Later results at low temperatures (series 3) like the above series 4, table 14, again gave a high result for $\Delta N$, in each case consistently. It is probable that the interference pattern changes between the case of a plenum and of highly exhausted air, owing either to flexure of the glass ends or to some other cause, or possibly depending only on the form of the pattern which happens to appear. In such a case the lines of symmetry for $N$ (plenum) and $N$ (exhaustion) would differ, introducing a systematic error very difficult to obviate. Thus different values of $\Delta N$ often follow a difference of adjustment of the mirror at the micrometer, while all cases for the same adjustment are practically identical.

**82. Experiments at red heat.**—To investigate the feasibility of such experiments, an inch steel tube (bicycle tube), 68 cm. long, with flanges brazed on at the ends, and an exhaustion tube near the middle, was heated in an organic combustion furnace to low red heat. The ends just projected outside the furnace and were closed by plate-glass windows with a jacket of asbestos between (applied wet and dried); or, finally, with a jacket of aluminum cement, clay, plaster, etc. These short but relatively cold ends are, of course,

an objection to the method, but no better device was found. Even so, the windows frequently cracked and had to be replaced. Such an apparatus naturally leaks, particularly at low temperatures, where the viscosity of air is relatively small, so that the experiments as a whole are merely tentative. To maintain the exhaustion as high as 70 cm., it was necessary to keep the air-pump at work. To reduce this annoyance the exhaustions were at first not carried above 60 cm. of mercury. With the interference fringes, however, no serious difficulty was experienced after the tube had taken definite shape. Distortion of fringes was inevitable, but centers of symmetry for measurement were always available.

The first experiments were made without exhaustion, at low and high temperature (low red heat). The difference of displacement $\delta N$ between cold ($25°$) and hot was (for instance) in two different experiments

$$
\begin{array}{llll}
25° & 10^3N \ =35.0 \text{ cm.} & 35.2 \text{ cm.} \\
\text{red hot} & 10^3N' =28.5 & 28.6 \\
\text{or} & 10^3\delta N= \ 6.5 & 6.6
\end{array}
$$

at atmospheric pressure. The $\delta N$ so obtained makes no allowance for the change of refractive index of the hot glass ends, nor for any displacement or rotation or warping of the ends during the course of the experiment, which required a lapse of an hour or two.

In the next experiment, therefore, the method of exhaustion was attempted, the partial vacuum used being about 16.6 cm. when the full barometer read 76.64 cm. Thus $p=60$ cm. An example of the results obtained is given in the following data.

$$
\begin{array}{llll}
& \text{Cold Tube.} \\
\text{Pressure } 76.6 \text{ cm.} & 10^3N \ =34.8 \text{ cm.} & 34.7 \text{ cm.} \\
\text{Pressure } 16.6 & 22.7 & 22.5 \\
p= \ \ \ 60.0 & 10^3\Delta N=12.1 & 12.2
\end{array}
$$

$$
\begin{array}{lllll}
& \text{Red-hot Tube.} \\
\text{Pressure } 76.6 \text{ cm.} & 10^3N \ =24.6 & 24.5 & 26.8 & 26.0 \text{ cm.} \\
\text{Pressure } 16.6 & 20.1 & 19.4 & 20.0 & 20.0 \\
p= \ \ \ 60. & 10^3\Delta N \ \ 4.5 & 5.1 & 6.8 & 6.0
\end{array}
$$

In the two experiments at the end readjustment was necessary, as the red-hot tube warped during the exhaustion. In the last case the glass cracked. The first two data should therefore be taken, so that

$$10^3\Delta N = 12.1 \text{ cm.} \qquad 10^3\Delta N' = 4.8 \text{ cm.} \qquad 10^3\delta N = 7.3 \text{ cm.} \qquad t=25° \ p=60 \text{ cm.}$$

If equation (5) above is solved for $t'$ the result is

(7)
$$t' = \frac{1}{\alpha}\frac{\delta N}{\Delta N'} + \frac{\Delta N}{\Delta N'}t$$

or if $\alpha = 1/273$

$$t' = 478°$$

This result is certainly small, as one would estimate the temperature (red heat) at several hundred degrees higher. Unfortunately the relatively cold

ends of the tube and the leakage at the windows both contribute to a low value of $t'$. But these do not seem to be adequate reasons. It is more probable that the longitudinal radiation of the air on the one hand and the value of $1/\alpha = 273$ assumed (if this is too small) may be the chief causes for the low value of $t'$. It is not, of course, possible to come to any further decision; but the experiments are distinctly unfavorable to the large value of $\alpha$ (small $1/\alpha$) above considered.

The method is not adapted for very high temperatures, since equation (7) may be written

(8)
$$\tau' = \frac{1}{\alpha} + t' = \frac{\Delta N}{\Delta N'}\left(\frac{1}{\alpha} + t\right)$$

and therefore, since $\tau'\Delta N' = \tau\Delta N$,

$$\frac{\partial t'}{\partial(\Delta N')} = -\tau\Delta N/(\Delta N')^2$$

where ($\tau$ referring to absolute temperature) $\Delta N'$ rapidly reaches the limit of accurate measurement.

**83. Further experiments at high temperatures.**—A variety of experiments were now made to obtain a more nearly tight joint at the ends, by using various clays, aluminum, etc., as cements, but without success. Finally, an improvement was obtained by using plaster of paris in the way shown in figure 94. $A$ is the end of the hot tube in the combustion furnace $F$. The flange $f$ is set somewhat back, so that packing of plaster $p$ may secure the window $g$ to the end of the tube. The plaster is put on wet and allowed to dry thoroughly. Lying outside of the furnace, it is never heated to redness. The joint is at



first fairly good, though it gradually deteriorates at high temperatures, and must be replaced. In this way the following results were found:
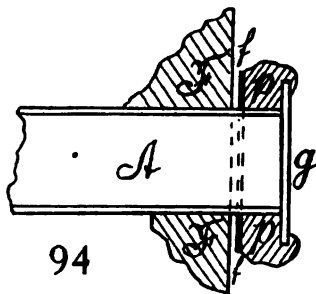
TABLE 16.

| | $p.$ | $10^3\Delta N$ | | $p.$ | $10^3\times\Delta N$ | | $p.$ | $10^3\Delta N$ |
|---|---|---|---|---|---|---|---|---|
| Just below red heat | 74.5 | 12.4 | Cold tube (22°) | 74.0 | 17.6 | Low red heat | 73.5 | 8.9 |
| | | 12.5 | | | 17.7 | | | 8.5 |
| | | 12.0 | | | 17.8 | | | 8.6 |
| | | | | | 18.1 | | | 8.8 |
| | | | | | 17.8 | | | |

Thus, from the first and second series, $t' = 154°$; from the first and third series, $t' = 330°$. As in the first experiments tried, both of these data are much too low. Here they can hardly be referred to the leak, since this was smaller. The ends are exposed not more than 1 or 2 cm. each, or a total length of about 70 cm. of tube.

Some adjustment is needed at the mirrors, to place the slit images in coincidence for the case of an exhaustion, as compared with a plenum of air. This adjustment is slight, but unfortunately its effect on $\Delta N'$ can not be estimated.

Cooling of gas as resulting from longitudinal radiation might be suggested, but, as it was not encountered in the case of the steam tube, it would not seem to be menacing here.

Finally, it will be seen from equation (8) that the effect of a leak is to make $\Delta N'$ too small. It will be larger as the vacuum is more perfect. Hence $t'$ should be too large for this reason. A small $t'$ can not be due to a leak. The exhaustion effect, since the gas expands into a vacuum, can not be serious. None of these incidental difficulties seem adequate to account for the large temperature discrepancies consistently obtained. All things considered, it seems to me most probable that the temperature coefficient, as the gas enters the region of red heat more fully, continually decreases, and that this is the real explanation of the low temperature values obtained.

The apparatus was now taken apart and provided with a fresh jacket. After drying, the cold apparatus again appeared in good condition. The results with the barometer at 75.55 cm. were

| Cold (22°) $p$ | $10^3\Delta N$ | Red hot $p$ | $10^3\Delta N'$ |
|---|---|---|---|
| 73.0 | 17.7 | 73.0 | 8.0 |
| .... | 17.8 | .... | .... |
| .... | 17.8 | .... | .... |

Unfortunately the glass cracked after the first experiment at red heat. The data for $\Delta N$ (cold) agree almost exactly with the preceding results. The high temperature would be $t' = 383°$, again enormously too low. Nevertheless, if the values of $\alpha$ were in question, as the temperature must have been at least 850°, this would come out as low as $\alpha = 0.0015$. The misgivings already enumerated apply here as before. As the experiments are very laborious they were abandoned at this point, for it did not seem that further work would materially enhance the result; nor was it thought necessary to actually measure the high temperatures.

**84. Flames.**—In the earlier report on the refraction of flames an abnormally low result of $\mu$ was obtained for the ignited gases. I have since repeated this work with additional improvements. It appears that it is quite possible to look through the peak of the blue case (symmetrically) without destroying the interference pattern as a whole, though this naturally quivers excessively. The last of the new results showed for the presence ($N'$) and ($N$) of the flame the micrometer readings:

| $N'$, flame | 0.029 | 0.029 | 0.029 | 0.029 | 0.029 |
|---|---|---|---|---|---|
| $N$, air | .0297 | .0295 | .0294 | .0296 | .0296 |

Hence the mean difference is 0.00056 cm., or per centimeter of breadth (2.3 cm.),

$$\delta N = 0.00024 \text{ cm.}$$

If the space occupied by flames were vacuum, the difference would have been 0.000268 per linear centimeter. Thus $\Delta N' = 0.00002$ cm., which lies within the error of observation, but is otherwise quite of the order to be expected for the hot gases in question.

**85. Conclusion.**—Though the experiments made are of a tentative character, the inference seems warranted that, so far as my work goes, the temperature coefficient $\alpha$ of air at low temperature is identical with the coefficient of expansion of gases. At high temperatures the value of $\alpha$ seems to decrease rapidly, in proportion as the gas is more highly ionized at red heat.

It has occurred to me that such ionization might load the gas in relation to the light-wave passing through it, and that the observed excess of index of refraction over the value anticipated at high temperatures might be explained in this way. But air ionized by the X-rays shows no such effect. Neither does the refraction of flames at high temperatures, so far as can be made out, show a large value of the refractive index of the ignited gases.

It is difficult to see how the experiment at red heat can be improved, unless a quartz tube is made for the purpose. But even here the difficulty of obtaining adequately plane parallel ends and a tube of sufficient breadth is formidable. The attempt to grind in reëntrant glass cylinder-like stoppers at the end of the tube was thought of, but did not succeed.

# CHAPTER XII.

## ADIABATIC EXPANSION OBSERVED WITH THE INTERFEROMETER.

**86. Introductory.**—In the preceding report[1] I tested a number of receivers in which air was expanded adiabatically, by passing one of the component beams of the displacement interferometer through the air contained. The vessels then used were not very satisfactory, being, as a rule, not long or capacious enough to insure trustworthy results. Moreover, the interferometer did not at that time admit of the introduction of long or bulky apparatus, whereas in the new form a length of almost 150 cm. is available. The main purpose of the research will thus be to ascertain how long and thin a tube may be made to be serviceable for expansion experiments. Furthermore, it seemed worth while to repeat the work preliminarily with a large, staunch tank since found in the laboratory. This was a heavy cylinder of cast brass, about 27.1 cm. (inside) and closed by plates of heavy glass, each 0.56 cm. thick and 20.3 cm. apart (inside), the whole containing a volume of air of about 11,713 cubic centimeters, to be increased to 12,800 cubic centimeters, because of the efflux pipe. The expansion pipe was 2 inches in diameter and closed by a 2½- inch brass stopcock, with a plug practically floating in oil to prevent the ingress of air from without. The glass plates were secured by iron bolts, a layer of resinous cement (equal parts of beeswax and resin) between glass and the flat end faces of the cylinder being introduced to prevent leakage.

To expand the gas in the receiver, the 2-inch pipe communicated with a tall, galvanized iron boiler used as a vacuum chamber, 29.4 cm. in diameter and 147 cm. high, thus containing a volume of 99,800 cubic centimeters, or 100,200 cubic centimeters with the influx pipe. It was in communication with a large air-pump and provided with a mercury gage for the measurement of the partial vacuum produced by the pump. The air flowing into the air-chamber after exhaustion was dried in the usual way and the influx controlled by a fine screw stopcock. There was a special opening for a thermometer. Vacuum and air-chamber were rigidly connected by a brass union with a rubber washer. There was no appreciable leakage so far as the atmosphere without was concerned. The 2-inch stopcock, however, was not quite tight within, so that air passed very slowly from the air to the vacuum chamber, in proportion as their pressures were different; but as the air-chamber is in service, either at atmospheric pressure (the influx cock being open) or, after exhaustion, at approximately the same pressure as the vacuum chamber, this leakage was of no appreciable consequence. Otherwise the interference pattern would not have been stationary.

While this apparatus was not long enough to fully realize the advantages of the method of displacement interferometry for the purposes in question,

[1] Carnegie Inst. Wash. Pub. 149, Part II, Chapter IX, 1912.

it was useful for testing the ring method in comparison with the former. The equivalent of a vanishing interference ring is here not immediately given in terms of the wave-length of light, since the rings move through the spectrum.

With the exception of a few incidental experiments of my own, optic methods of the present kind have not hitherto been used. They are here particularly applicable, since the number of the rings vanishing in a given region of the spectrum has merely to be counted after the sudden exhaustion and during the period of slow influx of air.

Succeeding parts of the chapter will refer to other available forms of apparatus with similar ends in view, and the additional purpose of ascertaining how long and narrow an apparatus may be shaped, without seriously interfering with the adiabatic measurements; for if the apparatus is increased indefinitely in length and diameter, it is obvious that the suddenness of the exhaustion through any available pipe will be more and more impaired. The same is true if the apparatus, for a given (sufficient) length, is too narrow, though for a different reason.

TABLE 17.—Values of $\gamma$. Bulky air chamber, $V=99,800$ cub. cm., $v=11,620$ cub. cm. $(V+v)/V=1.116$.  $C=952.6$; $1+x=1.0341$; $e=20.3$ cm.

| Series. | $t$ | $p_0$ | $p$ | $10^3\Delta N$ | $\gamma$ | Number of rings. | $\gamma'$ |
|---|---|---|---|---|---|---|---|
| | °C. | cm. | cm. | cm. | | | |
| I | 22.4 | 75.88 | 56.38 | 1.15 | 1.15 | 30 | 1.49 |
| | .... | ..... | 56.88 | .95 | 1.39 | 29 | 1.50 |
| | .... | ..... | ..... | .92 | 1.44 | 29 | 1.50 |
| | .... | ..... | ..... | 1.02 | 1.28 | 29 | 1.50 |
| II | 22.4 | 75.88 | 47.68 | 1.53 | 1.29 | 46 | 1.58 |
| | .... | ..... | ..... | 1.33 | 1.53 | 46 | 1.58 |
| | .... | ..... | ..... | 1.45 | 1.38 | 46 | 1.58 |
| | .... | ..... | ..... | 1.47 | 1.36 | 46 | 1.53 |
| III | 22.8 | 75.70 | 38.50 | 1.95 | 1.38 | [1]61 | 1.54 |
| | 23.2 | ..... | ..... | 2.25 | 1.14 | [1]60 | 1.54 |
| | 23.6 | ..... | ..... | 2.05 | 1.29 | 61 | 1.53 |
| | 24.0 | ..... | ..... | 1.91 | 1.42 | 62 | 1.50 |
| IV | [2]22.5 | 76.75 | 30.35 | 2.65 | 1.28 | 77 | 1.58 |
| | [2]22.5 | ..... | ..... | 2.20 | 1.65 | 76 | 1.59 |
| | 23.6 | ..... | ..... | 2.73 | 1.21 | 78 | 1.54 |
| | 23.6 | ..... | ..... | 2.49 | 1.39 | 78 | 1.54 |

[1] Count broken owing to flicker of arc; obtained from rhythm.   [2] Sunlight.

**87. Experiments with short, bulky air-chambers.**—An example of the data obtained is given in table 17, where the ratio of specific heats, $\gamma$, computed directly both from displacement of ellipses and $\gamma'$ from interference rings, is shown in detail. The original pressure of the air-chamber is that of the barometer, $p_0$. The pressure of the vacuum chamber is given under $p$. The displacement, $\Delta N$, from four independent observations in each case and the number of interference rings vanishing from exhaustion to plenum are the data chiefly of interest. It has not been possible, according to the table, to

* Carnegie Inst. Wash. Pub. 149, Part II, § 83, p.129; § 85, p. 135.   1912.

place the micrometer with an accuracy of more than 0.0002 cm. or 0.0003 cm. in successive cases, $\Delta N$ being the difference of two readings, each uncertain to $10^{-4}$ cm. But the effect of this is to throw out $\gamma$ by about the same number of tenths, so that the roughness of values in the table is inevitable. On the other hand, however, $\gamma$ obtained by displacement is usually too small, whereas the value computed from the evanescence of rings is always much too large. Thus in the first series there should have been an evanescence of 31 rings, in the second of about 50 rings, in the third of 64 rings, in the fourth of 85 rings. The reason for this discrepancy is very hard to determine, but will be considered in the next paragraph. The mean values of $\gamma$ from displacement and from rings are usually more nearly correct than either, as if the errors were equal and opposite in the two cases. The error is, in some way which has not been made out, associated with the placing of the micrometer. Thus, without apparent cause, the micrometer reading with a *plenum* of air may differ by several $10^{-4}$ cm., so that if these discrepancies are in opposite directions the value of $\gamma$ shows such large divergences as in series 4, for instance. In other words, the error appears to be extraneous to the method of experiment.

It has been suggested that the number of vanishing rings observed is approximately about 10 per cent too small throughout, and that the corresponding data for $\gamma$, though excessive, are nevertheless of the same order of value. Experiments were made to determine whether the change of wave-length, $\lambda$, influenced this result. This was done by allowing the center of ellipses in one case to move from the $D$ line towards the red, in the other from the yellow into the $D$ line. The mean wave-length would in the last case be smaller, and one may estimate the former as

$$\lambda = \lambda_D + \frac{\lambda_C - \lambda_D}{2} \frac{\Delta N}{\Delta N_0}.$$

where $\Delta N_0$ is the displacement of mirror which passes the center of ellipses from the $C$ to the $D$ line. This was found to be $10^2 \Delta N_0 = 28.1$ cm. Hence

$$\lambda = \lambda_D + 3.35 \times 10^{-4} \times \frac{\Delta N}{0.0281} = 10^{-6}(58.93 + 119 \Delta N)$$

Even in the final case, therefore, where $10^2 \Delta N = 2.5$, $\lambda_D$ would not be in error by more than 0.5 per cent. Using sunlight and at

$$p_0 = 76.75 \text{ cm.} \qquad p = 48.65 \text{ cm.} \qquad \tau = 294.5° \text{ (abs. temp.)}$$

the number of rings $R$ were counted when the ellipses traveled into the $D$ line and from the $D$ line, respectively, with results of which the following are examples:

From $D$ line, $R = 47$   46   46          Mean $R = 46.3$
Into $D$ line, $R = 45$   47   46.5   46   Mean $R = 46.1$
Indifferent, $R = 46$   46                 Mean $R = 46.0$

These results agree with the second series of table 17, and there is thus no appreciable difference.

One may note that the results for $\gamma$, when rings are counted, are consistently too large, but always of the same order. In fact, if $R$ were increased by the reduction factor $7.76/273p_0$, the values of $\gamma$ would all be nearly correct; but there is no reason for such a correction. Moreover, since the data for $\gamma$ obtained from $\Delta N$ (ellipses brought back to fiducial position) and from $R$ (ellipses displaced) are each separately consistent with each other, the discrepancy can not be due to leakages of air, as these would affect both measurements in the same way. The only source of error which is not common to both (apart from the displacement of ellipses) is the possible distortion of the glass upon exhaustion; for, in case of $\Delta N$, measurement is made at a plenum and at maximum exhaustion only, but at varying pressures for the case of rings. Thus if the rings needed are supposed to increase in the ratio of

$$p_0/p = 1.3 \quad 1.6 \quad 2.0 \quad 2.5$$

roughly, an approximate adjustment of the two sets of observations would also be obtained. Moreover, the effect of flexure would be an increase of the path of the beam in glass and so counteract the negative effect of decreased density.

**88. Effect of strained glass.**—To detect the possible effect of the inward flexure of the two plates of glass, a metallic ring about 25 cm. in internal diameter was provided. To this, two glass plates of about the same thickness (0.8 cm. each) as in the above vessel were cemented free from leakage and kept in place by clamps. The distance apart of the two plates within was but 1.8 cm., so that the micrometer displacement due to exhaustion of air was reduced to a small value. Hence, if the flexure of the glass plates due to exhaustion and the reverse were optically appreciable, it should here be detected.

To compute the residual air effect for the lamella of air, $e = 1.8$ cm. thick, we may write

(1) $$C\vartheta_0 = p/(\mu - 1) = p_0/(\mu_0 - 1)$$

where $C = 952.6$, $\vartheta_0$ is the temperature of the isothermal experiment, $\mu$ and $\mu_0$ the index of refraction of air at the pressures $p$ and $p_0$. Furthermore,

(2) $$\mu - 1 = \mu_0 - 1 - \Delta N/e$$

if $\Delta N$ is the micrometer displacement for the pressure difference $p - p_0$ at $\vartheta_0$.

Finally, if $n$ is the number of rings vanishing or of fringes passing at the sodium line, then

(3) $$\Delta N = n\frac{58.93}{2 \times 10^5}$$

Thus if $p - p_0 = \delta p$, then

$$n = \frac{2 \times 10^5}{58.93} \frac{e}{C\vartheta_0}\delta p = 0.216 \; \delta p$$

so that $n$ and $\delta p$ are proportional quantities. The following results were found:

| | $\delta p$ | No. of rings observed. | No. of rings computed. |
|---|---|---|---|
| Middle of glass plate.. | 30 cm. | 7.2 | 6.5 |
| | 45 | 10.0 | 9.7 |
| | 60 | 13.2 | 13.0 |
| 4 cm. above middle.... | 45 | 9.8 | 9.7 |
| 8 cm. above middle.... | 45 | 10.0 | 9.7 |
| At edge.............. | 45 | 10.5 | 9.7 |

The observed data are the means of 5 or 6 trials. As it is difficult to observe the rings without interruption in an agitated laboratory, there is no doubt that observed and computed values are coincident. The first and last rings are not easily counted, and individual data were found to agree with the computed results perfectly. Finally, if the glass strain were effective (for there is actual flexure), it would be shown in the observations made by passing the beam through different parts of the plate of glass, between the center and the edge. No consistent difference was found.

Hence an appreciable strain effect is also absent, and the reason for the discrepancy in the two sets of values from $\Delta N$ and from $n$, in table 17, remains outstanding.

**89. Equations.**—In the preceding report* the equation for the value of $\gamma$ is deduced as

$$\gamma = \frac{\log p/p_0}{\lg(1 - C\vartheta_0 \Delta N/e(1+x)p_0)}$$

or

$$\Delta N = (1+x)\frac{ep_0}{C\vartheta_0}\left(1 + \left(\frac{p}{p_0}\right)^{1/\gamma}\right)$$

Here $p_0$ and $p$ are the pressures in the air-chamber (barometric) and the vacuum chamber respectively, before exhaustion, $\vartheta_0$ the original temperature of the air, $\Delta N$ the displacement of the micrometer corresponding to the shift of the ellipses on exhaustion. If the air-chamber is quite tight, $\Delta N$ may be taken at any time. $C$ and $1+x$ are the optic constants

$$C = p_0/\vartheta_0(\mu_0 - 1) = 952.6$$

for dry air, being the optic gas constant, if $\mu_0 - 1$ replaces $\rho_0$, the normal density of the gas. To allow for the dispersion of air an empirical equation (convenient in the present calculation),

$$\mu - 1 = B/\lambda^2 = 0.0002101/\lambda^{0.241}$$

was constructed. The deduction assumes that the centers of ellipses are brought back again to the fiducial line $D$, of the spectrum, the micrometer displacement in question being $\Delta N$.

* Carnegie Inst. Wash. Pub. 149, Part II, pp. 166–168.

In the case where rings are counted, however, the center of ellipses leaves the $D$ line by a short distance, less than one-tenth of the interval between the $C$ and $D$ lines. In such a case, if $\mu_a = A_a + b_a/\lambda^2$ for air and $\mu_g = A_g + b_g/\lambda^2$ for glass, the micrometer displacement to bring the ellipses back again from $\lambda'$ to $\lambda$ should be

$$\delta N = 3(e_a b_a + e_g b_g)(1/\lambda^2 - 1/\lambda'^2)$$

$e_a$ and $e_g$ being the lengths of air and glass* in the beam. Here

$$e_a = 20.3 \text{ cm.} \quad b_a = 10^{-14} \times 1.65 \quad e_a b_a = 10^{-14} \times 33.5$$
$$e_g = 2 \text{ cm.} \quad b_g = 10^{-12} \times 48 \quad e_g b_g = 10^{-12} \times 96$$

so that the effect of air, where $b_a$ is variable with pressure, is but 0.3 per cent of the glass effect and may in the first approximation be neglected. The equation may therefore be written:

$$\delta\frac{1}{\lambda^2} = -\frac{2\delta\lambda}{\lambda^3} = \frac{\delta N}{3e_g b_g} \qquad -\frac{\delta\lambda}{\lambda} = \frac{\delta N \times \lambda^2}{6e_g b_g}$$

If the mean data from series I be inserted ($\delta N = 960 \times 10^{-4}$ when $\lambda$ refers to the $D$ line)

$$-\frac{\delta\lambda}{\lambda} = \frac{960 \times 10^{-4} \times 10^{-8} \times 0.3473}{6 \times 96 \times 10^{-12}} = 10^{-2} \times 0.58$$

For the case of the $C$ and $D$ lines $\delta\lambda/\lambda = 3.35/58.9 = 0.057$, roughly, about ten times the preceding distance.

In fact, the observations made for the estimate given in the preceding paragraph (semi-displacement),

$$-\frac{\Delta\lambda}{\lambda}2(\lambda-\lambda_0) = \frac{2 \times 119}{58.9}\Delta N = 4\Delta N$$

compared with the present

$$-\frac{\delta\lambda}{\lambda} = \frac{10^{-8} \times 0.3473 \delta N}{576 \times 10^{-12}} = 6\delta N$$

are quantities of the same order, though one would have expected closer coincidence.

The discrepancy observed between the method of measurement in terms of the displacement ($\Delta N$ to bring the ellipses back to the fiducial position) and the method of counting rings can not, therefore, be explained as the result of a change of wave-length $\lambda$ in the latter case; *i.e.*, the equation

$$\Delta N = (n_0 - n)\lambda/2$$

where $n_0 - n$ is the number of vanishing rings of the mean wave-length $\lambda$, is at fault for some other reason. Curiously enough, the ring method is essentially simple, as it reduces to $\gamma = \dfrac{\log(p/p_0)}{\log(n/n_0)}$, if $n_0$ and $n$ are the number of rings

---

* Thickness of glass plates of air-chamber, 1.3 cm.; of the plate of the grating, 0.7 cm.

vanishing when a plenum of air and the adiabatically exhausted air, respectively, are introduced into one of the beams. Since

$$\mu_0 - 1 = n_0\lambda/2e = p_0/C\vartheta_0$$

this is equivalent to

$$\Delta N = (n_0 - n)\lambda/2$$

**90. Experiments with long tubes. Diameter, one inch.**—The difficulty encountered in the case of the preceding experiments was the small value of the displacement $\Delta N$ obtained. As a consequence, every little incidental disturbance produced a large effect in $\gamma$. It is the purpose of the present experiments to remedy this defect by using long tubes by which $\Delta N$ may be increased over ten times. It was particularly of interest, moreover, to begin with relatively thin tubes, and inch gas-pipe suggested itself for the purpose. The value of $\gamma$ to be expected will necessarily be too small, as the air must undergo reheating before the exhaust cock can be closed. The question, however, is whether consistent values of $\gamma$ will be found, even for these extreme conditions and for large variations of pressure. Obviously the window plates will not produce discrepancies, as has been directly shown in paragraph 88.

The gas-pipe installed was 143.4 cm. long within. To make the junction with the vacuum chamber, a straight pipe of the same diameter and about 75 cm. long was needed between the main pipe and the 2½-inch stopcock. The connecting pipe, together with the tube itself, is probably the chief cause of the resistance to flow and the low value of $\gamma$ found, but it was not possible to shorten it.

The large stopcock inevitably leaked slightly when the pressures were different in the two chambers; but immediately after exhaustion this made no appreciable difference, as the two pressures are then nearly the same. In fact, no rings vanish from the spectrum from this cause. Just before exhaustion, however, after closing the gas-pipe by the fine influx stopcock, appreciable leakage is shown by the spectrum. Hence the exhaustion must be made immediately after the influx cock is closed. Some low results at the outset are referable to this difficulty.

The tube was, as usual, filled with dry air after exhaustion. The results are given in table 18, in the same way as in the preceding case. The experiments themselves were throughout satisfactory, no difficulty being encountered at the interferometer. The work, moreover, is equally trustworthy at low and at high exhaustions, a result which is rather surprising. In the latter case, as the total displacement, $\Delta N$, is over 0.0276 cm., the $\gamma$ contained should be correct within 1 per cent.

Only one attempt was made to find $\Delta N$ by the march of the interference fringes. Fully 276 were observed, and it is here necessary to count the fringes passing the $D$ line, since the ellipses are displaced throughout the greater part of the length of the spectrum; but this introduces no inconvenience whatever. The difficulty is due to the time needed in counting so many evanescences; for during this interval the electric lamp is liable to flicker seriously, or some

commotion will occur in the laboratory or without, tending to make the count uncertain. The rings disappear temporarily during the tremor. In a quiet laboratory, however, and with sunlight replacing the arc light, this would be a method of precision. Thus, for instance, at the highest exhaustions used, over 900 fringes would have to pass the $D$ line, a datum from which $\gamma$ could be accurately obtained.

TABLE 18.—Values of $\gamma$. Iron gas-pipe, 1 inch internal diameter.  $C=952.6$.
$e=143.4$ cm.   $1+x=1.0341$.

| Series. | $t$ | $p_0$ | $p$ | $10^3\Delta N$ | $\gamma$ | No. of rings. | $\gamma'$ |
|---------|-----|-------|-----|----------------|----------|---------------|-----------|
|         | °C. | cm.   | cm. | cm.            |          |               |           |
| I       | 19.2 | 76.84 | 57.84 | 8.75 | 1.18 | 276 | 1.28 |
|         | .... | ..... | ..... | 8.60 | 1.21 | ... | .... |
|         | .... | ..... | ..... | 8.35 | 1.24 | ... | .... |
|         | .... | ..... | ..... | 8.40 | 1.24 | ... | .... |
| II      | 19.1 | 76.28 | 48.08 | 12.95 | 1.20 | | |
|         | .... | ..... | ..... | 13.15 | 1.18 | | |
|         | .... | ..... | ..... | 13.15 | 1.18 | | |
|         | .... | ..... | ..... | 13.25 | 1.17 | | |
|         | .... | ..... | ..... | 13.10 | 1.19 | | |
|         | .... | ..... | ..... | 13.25 | 1.17 | | |
| III     | 19.2 | 76.28 | 38.98 | 18.05 | 1.14 | | |
|         | .... | ..... | ..... | 18.10 | 1.14 | | |
|         | .... | ..... | ..... | 17.95 | 1.15 | | |
|         | .... | ..... | ..... | 17.80 | 1.17 | | |
| IV      | 19.3 | 76.28 | 29.78 | 22.70 | 1.15 | | |
|         | .... | ..... | ..... | 22.80 | 1.14 | | |
|         | .... | ..... | ..... | 22.65 | 1.15 | | |
|         | .... | ..... | ..... | 22.80 | 1.14 | | |
| V       | 19.3 | 76.28 | 20.88 | 27.85 | 1.12 | | |
|         | .... | ..... | ..... | 27.60 | 1.14 | | |
|         | .... | ..... | ..... | 27.60 | 1.14 | | |

If we compare the mean results for $\gamma$ with the exhaustion used (pressure $p$ in the vacuum chamber, full barometric pressure $p_0$ in the air-chamber), the results decrease slightly as the vacuum is higher. Thus

| If   | $p=$      | 58 cm. | 48 cm. | 39 cm. | 30 cm. | 21 cm. |
|------|-----------|--------|--------|--------|--------|--------|
| Then | $\gamma=$ | 1.23   | 1.18   | 1.15   | 1.14   | 1.13   |

which is what might have been expected, except that the rate of decrease is much less than would be surmised. There seems thus to be no objection to the use of high exhaustions, which in turn give a better value of $\gamma$ from the large range of $\Delta N$ obtained.

The low mean value of $\gamma$ obtained has been referred to the resistance of the inch piping to the outflow of air. It is probably not due to the stop-cock, as incidental differences in the speed of opening and closing would otherwise have shown a marked effect. One may conclude that the air in the long inch gas-pipe expands adiabatically with a coefficient $\gamma$ between 1.1 and 1.2, in case of such exhaustions as the above.

**91. The same. Diameter of tube, two inches.**—The experiments were now continued by enlarging the diameter of the tube to 2 inches. Brass gas-pipe, 1.35 cm. long, to be closed with thick glass plates, was at hand. To connect the same with the vacuum chamber, a similar 2-inch pipe, 115 cm. long, as far as the 2½-inch stopcock, was necessary. Moreover, as this was in the way of the light received from the grating, the beam was reflected by an offset consisting of two silver mirrors in parallel. No difficulty was found with this arrangement, and the sodium line was in view to give evidence if any accidental displacement should occur.

Unfortunately, the ellipses obtained were somewhat irregular open forms (*i.e.*, half ellipses), and the endeavor to secure small closed patterns did not succeed. This annoyance depending chiefly on the parts of the mirror and grating used, and on shifting accessories, is not easily controlled. The individual measurements of $\Delta N$ are therefore not as good as those recorded in table 18, where a displacement of $10^{-4}$ cm. was assured. They suffice, however, for the present purposes.

The new data are given in table 19, $t$ being the temperature of both chambers, $p_0$ the initial normal pressure of the air-chamber (2-inch pipe), and $p$ that of the vacuum chamber.

TABLE 19.—Values of $\gamma$. Brass gas-pipe, 2 inches internal diameter.
$C = 952.6$; $1+x = 1.0341$. $e = 135.3$ cm. $(V+v)/v = 1.049$.

| Series. | $t$ | $p_0$ | $p$ | $10^3\Delta N$ | $\gamma$ |
|---------|-----|-------|-----|------------|----------|
|         | °*C.* | *cm.* | *cm.* | *cm.* |        |
| I       | 17.0 | 75.66 | 56.46 | 7.15 | 1.35 |
|         | .... | ..... | ..... | 7.35 | 1.30 |
|         | .... | ..... | ..... | 7.25 | 1.33 |
|         | .... | ..... | ..... | 7.55 | 1.27 |
| II      | 17.0 | 75.66 | 47.36 | 10.85 | 1.33 |
|         | .... | ..... | ..... | 10.95 | 1.31 |
|         | .... | ..... | ..... | 11.10 | 1.29 |
|         | .... | ..... | ..... | 11.05 | 1.30 |
| III     | 16.1 | 75.86 | 38.36 | 14.93 | 1.31 |
|         | .... | ..... | ..... | 15.15 | 1.28 |
|         | .... | ..... | ..... | 15.10 | 1.29 |
|         | .... | ..... | ..... | 15.38 | 1.26 |
| IV      | 16.2 | 75.86 | 29.36 | 19.53 | 1.25 |
|         | .... | ..... | ..... | 19.57 | 1.25 |
|         | .... | ..... | ..... | 19.27 | 1.28 |
|         | .... | ..... | ..... | 19.75 | 1.23 |
| V       | 16.4 | 75.86 | 20.36 | 23.71 | 1.27 |
|         | .... | ..... | ..... | 23.95 | 1.25 |
|         | .... | ..... | ..... | 23.70 | 1.27 |
|         | .... | ..... | ..... | 23.75 | 1.26 |

The effective value of $\gamma$ in these experiments is, for the lower exhaustions, above $\gamma = 1.3$, showing a considerable improvement over the data for the inch tube, which were not much above $\gamma = 1.1$. This was to be inferred, of course; but it was not expected that the increment of $\gamma$ due to increased diameter

would be so rapid. It would seem to be probable, therefore, that if a 4-inch tube were used the conditions for obtaining a trustworthy value of $\gamma$ would be nearly met.

As the exhaustions in a successive series are gradually increased (initial partial vacua from $p = 56.46$ cm. to $p = 20.36$ cm. in the vacuum chamber), the observed values of $\gamma$ gradually but slowly decrease, the mean values being ($p_0 = 75.7$ cm. to 75.9 cm.)

$$p = 56.46 \quad 47.36 \quad 38.36 \quad 29.36 \quad 20.36 \text{ cm.}$$
$$\gamma = 1.32 \quad 1.31 \quad 1.29 \quad 1.25 \quad 1.26$$

where the fourth value is too small, for incidental reasons. This general result is also to be expected; but it is rather remarkable that with such high exhaustions as those finally used the decrease of $\gamma$ is not more marked.

The work, as a whole, progressed smoothly throughout, the only interference with precision being the incidental occurrence of open ellipses. To obtain other patterns would have required longer additional adjustment than the work at the present stage seemed to warrant.

**92. The same. Diameter of tube, four inches.**—The first experiments made with the 4-inch tube are given in table 20. The completed apparatus showed a slight leak, which could not be detected after long searching. The tube was therefore admitted for a tentative series of experiments. The exhaust pipe here, as above, was rigid and straight, but only 2 inches in diameter, with a 2½-inch stopcock. To exhaust the air-chamber, the handle of the cock was suddenly jerked over an angle 180° between the two closed positions. The plug virtually floated in oil, as shown elsewhere.

TABLE 20.—Values of $\gamma$. Brass pipe, 4 inches internal diameter.
$C = 952.6$; $1+x = 1.0341$; $e = 126.9$. $(V+v)/V = 1.119$. Small leak in apparatus.

| Series. | $t$ | $p_0$ | $p$ | $10^3 \Delta N$ | $\gamma$ |
|---------|-----|-------|-----|-----------------|----------|
| I | °C. 19.9 | cm. 76.15 | cm. 57.00 | cm. 5.90 | 1.42 |
|  | .... | ..... | ..... | 6.10 | 1.37 |
|  | .... | ..... | ..... | 6.23 | 1.34 |
|  | .... | ..... | ..... | 6.15 | 1.36 |
| II | 23.0 | 75.79 | 38.39 | 12.40 | 1.36 |
|  | .... | ..... | ..... | 12.73 | 1.32 |
|  | .... | ..... | ..... | 12.60 | 1.30 |
|  | .... | ..... | ..... | 12.75 | 1.31 |
| III | 23.2 | 75.79 | 29.39 | 15.50 | 1.40 |
|  | .... | ..... | ..... | 15.71 | 1.37 |
|  | .... | ..... | ..... | 15.77 | 1.37 |

As a whole, the results are disappointing; and they are irregular, for mean readings could not be made because of the leak. They are, nevertheless, interesting, inasmuch as with some of the above data they point out a special source of discrepancy. It will be seen that the $\gamma$ values tend to decrease in successive measurements, beginning with a high value, which is here nearly

correct. This can not be referred to the temperature of the 4-inch tube, because the initial optic density is necessarily measured. It must therefore be due to the temperature of the vacuum chamber. It follows, therefore, that the time allowed in these experiments, between observations, though sufficient for establishing the initial temperature of the air-chamber, is not sufficient for the much larger vacuum chamber. The two chambers are thus no longer at the same temperature, a condition which the equations implicitly assume.

The apparatus was now taken apart and thoroughly overhauled. After reassembling the parts, the chamber was found free from leakage. As the exhaust pipe was in the way of the beam of light entering the telescope, the offset, consisting of two parallel mirrors firmly adjusted, was used without annoyance, here as above. The work throughout progressed smoothly, though the ellipses were again not as satisfactory in form as would have been desirable.

TABLE 21.—Values of $\gamma$. Data as in Table 11, 4″ brass pipe.

| Series. | $t$ | $p_0$ | $p$ | $10^3 \Delta N$ | $\gamma$ |
|---|---|---|---|---|---|
| I | °C. 16.5 | cm. 75.90 | cm. 56.80 | cm. 6.34 | 1.33 |
|  | .... | ..... | ..... | 6.15 | 1.37 |
|  | .... | ..... | ..... | 6.27 | 1.34 |
|  | .... | ..... | ..... | 6.30 | 1.35 |
| II | 16.6 | 75.90 | 47.60 | 9.25 | 1.38 |
|  | .... | ..... | ..... | 9.40 | 1.36 |
|  | .... | ..... | ..... | 9.30 | 1.34 |
|  | .... | ..... | ..... | 9.20 | 1.39 |
|  | .... | ..... | ..... | 9.55 | 1.33 |
|  | 16.7 | 76.19 | 47.89 | 9.31 | 1.37 |
|  | .... | ..... | ..... | 9.45 | 1.35 |
| III | 16.9 | 76.19 | 38.69 | 12.87 | 1.34 |
|  | .... | ..... | ..... | 12.70 | 1.36 |
|  | .... | ..... | ..... | 12.80 | 1.35 |
|  | .... | ..... | ..... | 12.76 | 1.35 |
| IV | 17.0 | 76.19 | 29.69 | 16.26 | 1.35 |
|  | .... | ..... | ..... | 16.23 | 1.35 |
|  | .... | ..... | ..... | 16.25 | 1.35 |
|  | .... | ..... | ..... | 16.04 | 1.38 |
| V | 17.1 | 76.19 | 20.69 | 20.00 | 1.35 |
|  | .... | ..... | ..... | 19.60 | 1.40 |
|  | .... | ..... | ..... | 19.73 | 1.38 |
|  | .... | ..... | ..... | 19.69 | 1.39 |

Table 21 contains the results. Changes in the values of $\Delta N$ in a given series are most likely referable to the form of the interference pattern, indirectly to the flickering of the electric lamp. There seems to be no evidence to associate them with the manner in which the 2½-inch stopcock is opened and closed. This was merely jerked around 180°, between the two closed positions of the plug, and, so far as can be seen, the rate of motion is adequate. The successive observations show no consistent difference, as was the case

in the preceding table. Hence this discrepancy has been eliminated. What is most interesting is that the 4-inch tube shows no consistent difference in the $\gamma$ values for high or low exhaustion. Thus the mean values under increasing exhaustion, $p$, are

$$p = 56.8 \quad 47.6 \quad 38.7 \quad 29.7 \quad 20.7$$
$$\gamma = 1.35 \quad 1.36 \quad 1.35 \quad 1.36 \quad 1.38$$

Accidentally the highest value of $\gamma$ belongs to the highest exhaustion.

The chief anticipation of the work (*i.e.*, that with a 4-inch tube the true value of $\gamma$ would appear) has not been fulfilled. The value obtained is still much below normal, successive results ranging as follows:

| | | | |
|---|---|---|---|
| Diameter of tube........ | 2.5 | 5.0 | 10.0 cm. |
| Mean $\gamma$............... | 1.17 | 1.29 | 1.36 cm. |
| Diameter of exhaust pipe | 2.5 | 5.0 | 5.0 cm. |

The relatively small increase between the tubes 5 cm. and 10 cm. in diameter is disappointing. At the rate obtained from the first two experiments (see fig. 95) a 3-inch tube should have been nearly sufficient. At the rate established by the last two observations, however, a tube at least 5.5 inches
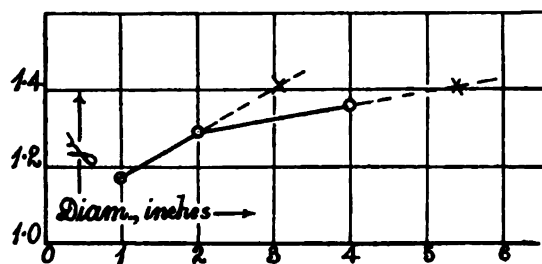


95

in diameter would be needed to obtain trustworthy values of $\gamma$. These differences are possibly due to the exhaust pipe, which in case of the last observation does not increase in size. Hence a 3-inch pipe with a 4-inch stopcock may be estimated as being adequate for $\gamma$ measurement, provided the exhaust pipe is straight and clear throughout.

The observations were broken off at this point, with the object of searching for some means of obtaining a more sensitive and regular interference pattern. If the method is to be ultimately successful, then $10^{-4}$ cm. on the micrometer must be guaranteed. If the ellipses are not quite regular or not closed, this is not the case. A more sensitive method of defining optic density is thus in question.

# CHAPTER XIII.

## MISCELLANEOUS EXPERIMENTS.

**93. Effect of ionization on the refraction of a gas.**—It seemed interesting to test this question carefully, although a negative result was to be expected. Accordingly one component beam was surrounded by a thick iron tube, while the other was allowed to travel freely in air, along a path energized by the X-rays. For this purpose the X-ray bulb was placed near the grating and the radiation directed toward the mirror $N$, the beam $GM$ being inclosed. A thick sheet of lead, 1 foot square, was placed behind the bulb to additionally screen off radiation along $GM$. Under these circumstances the ionization along $GN$ must have been enormous by comparison with $GM$. Quiet ellipses were produced in the interferometer, and the effect of opening the X-ray current and closing it again, alternately, was observed. Not the slightest deformation of the ellipses or any motion of the fringes could be detected. An ionization effect is therefore wholly absent. It might have been supposed, for instance, that the ions present might load the wave of light and produce an appreciable result in the interferometer (cf. fig. 92).

Since a shift of 0.1 of a ring would probably have been detected, $\Delta N =$ 0.000005 cm. would have produced a perceptible effect. Hence, since $\mu - 1$ is, roughly, equal to $\Delta N/s$, the value of the ionization effect could not exceed

$$\frac{5 \times 10^6}{2 \times 138} = 1.8 \times 10^{-8}$$

The ionization effect can not, therefore, exceed 0.01 per cent of $\mu - 1$.

To further test this question, the iron tube, 1 inch in diameter and 138 cm. long, was provided with a fine axial wire about 0.02 cm. in diameter, passing through central holes in the glass plates at the end. The ends of the wire were drawn tight by hard-rubber rods on the outside, so that the tube became a cylindrical condenser. All holes were sealed hermetically with resinous cement. The interference fringes were clearly producible.

The poles of an induction coil were now connected with the inner wire and the tube, respectively, to alternately charge the condenser and discharge it, with the object of strongly ionizing the air within. On partial exhaustion the whole tube became luminous, on account of the discharge, in the usual way.

The best results were obtained with a plenum of air when but two storage cells actuated the coil. Under these circumstances no sparks passed from core to shell of the iron condenser tube, while the air within was intensely ionized by the silent discharge. On closing the current, from 0.5 to 1 per cent of the rings was swept inward at once. On opening it, the rings again emerged. This inward motion, however, was in the same sense as the effect of a decrease of

154

density, such as would result, for instance, from rise of temperature or from partial exhaustion. Hence the effect observed, though very definite, would correspond to a temperature effect due to electrical currents traversing the air. One should expect the effect of ionization, if appreciable, to be the reverse of this. With voltages high enough to produce sparks in the tube, the interference figures naturally show violent agitation or quiver. If the displacement in question is one ring and $\delta$ denotes differences, $\delta(\Delta N) = 30 \times 10^{-4}$ cm.

If only temperature changes, one may write, roughly, $\Delta N . \tau = $ constant, $\tau$ referring to absolute temperature, whence

$$\delta\tau = \tau\delta(\Delta N)/\Delta N = 293\frac{30 \times 10^{-4}}{40 \times 10^{3}}$$

if results found for a similar tube, above, be taken.

Thus $\delta\tau = 2.2 \times 10^{-7}$ degrees centigrade is the average temperature increment, for the whole length of the tube.

When but a single cell was used to energize the coil, no effect could be recognized. In case of two cells, moreover, when the plenum of air was replaced by a partial vacuum of 1 cm. or less, so that an arc was seen, no effect was observable, although the reddish light colored the field of the telescope.

There are two points of view, however, from which the assumption of a temperature effect is not admissible. If the pipe is closed, so that the density of the air contained remains unchanged, there is no difference in the phenomenon. But there should not, for the case of constant density, be any effect, unless the nature of the gas is changed. Again, the effect is instantaneous and not increased on keeping the circuit closed. The simple explanation in terms of temperature made above must therefore be taken with reservation. At all events, the effect of ionization would be small and equivalent to a dilution of the gas of but

$$\frac{1}{273} \times 2.2 \times 10^{-7} \text{ or about } 10^{-9}$$

of its density, when sparks are about to occur.

**94. Mach's interferences.**—It is frequently necessary to use the interferometer in such a way that but one ray passes in a given direction; $i.e.$, the rays are not to retrace their path. Interferometers of this kind are treated above, but Mach's design offers advantages, which will be presently pointed out. As a rule, in using these interferometers, the center of the elliptic interference pattern is remote and the lines are hair-like and found with great difficulty. These annoyances are overcome when the apparatus is put together as follows:

In figure 96, $L$ is the vertical sheet of light from a collimator impinging on the strip of plate glass $gg$, half-silvered on one side, toward or near the ends. The pencil $L$ is thus reflected to the opaque mirror $N$ and transmitted to the opaque mirror $M$ (on a micrometer), and then reflected to the other end $g'$ of the glass strip $gg'$. Thereafter, both the pencils, $Mg'$ and $Ng'$, are available;

but it is generally more convenient to use the former $(Mg')$, reflecting it from the plane opaque mirror $m$ to the telescope at $T$. When $L$ came from sunlight, or from an arc light, etc., the white images of the slit were very bright. After putting them in coincidence, horizontally and vertically, by aid of the three adjustment screws on the mirror $M$, Ives prism-grating $G$ may be placed in front of the objective of the telescope. A very brilliant spectrum thus appears, and the fringes are easily found by moving the micrometer slide which carries $M$ to the proper position. In my apparatus $gg'$ was about 50 cm. long and $gM = gN$ about 2 meters. The telescope is sufficiently near $M$ to manipulate the micrometer, the mirror $m$ being so placed that the beam just misses the strip $gg'$.



96
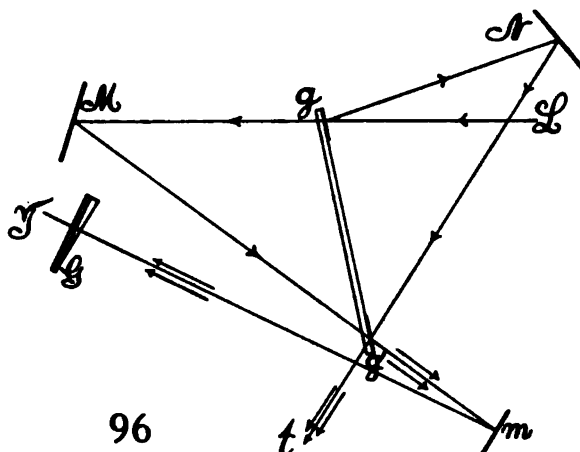
The interference pattern, found at once and satisfactorily centered, consisted of large, broad circles. On moving the micrometer $M$ from evanescence on one side of the center to evanescence on the other, the slide was found to have moved over about 2 mm. With a stronger telescope to magnify the fine, hair-like fringes, this distance would have been larger. It is interesting to compare this datum displacement with the datum found in the case of the phenomenon above, where a range of over 0.5 cm. (double path-difference) was observed. In the present experiment the range is smaller, because the interference pattern falls below the limit of visibility before the possibility of interference is exhausted. $Mg'$ slides along $g'$ when $M$ moves.

**95. A Rowland spectrometer for transmitting and reflecting gratings, plane or concave.**—In the above experiments I had occasion to examine a variety of gratings, and it was therefore desirable to devise a universal instrument by which this could be accomplished without delay. The method chosen is similar to that previously described,* but its details have been greatly simplified, on the one hand, and made more generally applicable, on the other. It seems permissible, therefore, to give a brief description.

---

*Carnegie Inst. Wash. Pub. No. 149, Chapter I, 1911.

In figure 97, $GG'$ and $HH'$ are double slides like the carriage bed of a lathe, each about 1.5 to 2 meters long and 10 cm. wide, rigidly fastened together. They are placed at right angles to each other on a flat table, the vacant distance between $G'$ and $HH'$ being less than a meter. For ordinary purposes they need not be screwed down. $A$, $B$, $D$, $K$, are flat carriages, or tables, provided with screw sockets for supporting the different standards, and capable of sliding to and fro with a minimum of friction. $A$ carries the micrometer slit $S$. $B$ and $C$ are joined by the Rowland rail $R$, whose length is thus equal to the radius of the concave grating to be examined, or nearly so, so that the ends of $R$ are on vertical axes at $b$ and $d$. $B$ also supports the table $C$ (somewhat enlarged in the side elevation, fig. 98), on which the table $t$ of the grating $g$ may be adjusted on its leveling screws. To secure a common axis, $b$, $e$, the rod at $ace$ is twice bent at right angles. Moreover, if $c$ is turned to one side, the supporting rod $e$ may be screwed into the vacant socket $b$ at the end of $R$. For the case of figure 98, the angle of diffraction $\theta$ is varied and $\lambda = D \sin \theta$, where $D$ is the grating space. For the other case ($c$ being turned aside and $C$ screwed into and turning with $b$) the angle of incidence is varied and $\lambda = D \sin i$. This is much simpler in form than the early method used.
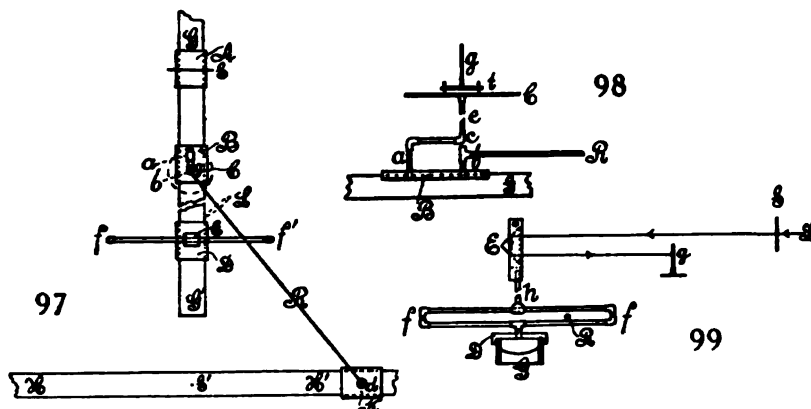


Finally, the table $C$ carries the essentially new addition to the apparatus (shown in front elevation in fig. 99), viz. the long slot $ff$, adapted to support the right-angled reflecting prism $E$ and at the same time to allow free play to the rail $R$ within $ff$. Figure 99 then shows the progress of the rays (turned 90° to the front in a horizontal plane) from the slit or collimator, $S$. They are doubly reflected at $E$, return in a vertical plane and then impinge on the grating at $G$. The rays thereafter pass along the rail $R$ (fig. 97) and are examined by a strong eyepiece at $d$ (not shown), rigidly but adjustably attached to the near end of the rail.

The displacement of $K$ along $HH'$ is accurately measurable on a parallel scale with vernier (not shown). If $x_1$ and $x_2$ are the two symmetrical readings on opposite sides of the virtual slit image at $S$ (fig. 97), and $R$ the radius of the concave grating, and $x = x_2 - x_1$

$$\sin \theta = x/2R, \text{ or } \sin i = x/2R$$

If a plane grating is used, a weak lens $L$ is attached to the rail $R$ and moves with it, so that its focus is in front of the ocular $d$ (with cross-hairs). In this case $S$ is a collimator. If a transmitting grating is examined, the collimator $S$ (fig. 99), etc., are merely to be lowered, and the prism $E$ is superfluous. It need not even be removed. Naturally, it is in the interest of accuracy to have all the standards like $e$ and $h$ as short as possible.

Finally, in the equation $\lambda = \dfrac{Dx}{2R}$, if $D = 10^6 d$, the values $d$ and $R$ are usually of the same order (175 cm.) for gratings with about 15,000 lines to the inch. In this case we may make the rail length $R = d$, whence

$$\lambda = x/2$$

Even in case of the concave grating, when ultimate precision is not aimed at, some variation of the distance $SS' = 2SE$, nearly, is admissible without destroying the definition. The carriage $D$ with the prism $E$ may be moved fore and aft on the slides $GG'$ until the focus at $d$ is sharp. The values of $x$ are usually of the order of 100 to 125 cm., so that an accuracy of Ångström units is easily obtainable without special refinement.

# THE INTERFEROMETRY OF REVERSED AND NON-REVERSED SPECTRA

## PART II

By CARL BARUS

*Hazard Professor of Physics and Dean of the Graduate Department in Brown University*

# THE INTERFEROMETRY OF REVERSED AND NON-REVERSED SPECTRA

## PART II

By CARL BARUS

*Hazard Professor of Physics and Dean of the Graduate Department
in Brown University*

CARNEGIE INSTITUTION OF WASHINGTON

PUBLICATION No. 249, PART II

# CONTENTS.

3

# PREFACE.

In the present volume I have pursued the work on the interferences of reversed and non-reversed spectra, begun in my last report (Carnegie Inst. Wash. Pub. No. 249, 1916), in a variety of promising directions, such as the original investigation suggested. It will be remembered that the reversal (180°) here contemplated takes place on a transverse line of the spectrum (*i.e.*, a line parallel to the Fraunhofer lines), which thereby becomes a line of symmetry for the phenomena. The apparatus has been extensively modified, so as to admit of measurements relating to individual fringes. The object of such quantitative work, however, is to furnish a guide for the development of the experiments and to corroborate equations, not to collate standard data. These could hardly be satisfactorily obtained, moreover, unless the work were done with optical plates and mirrors, whereas the work in this volume and the preceding has been done with ordinary window-plate and usually with film gratings.

A large part of Chapter I is devoted to the treatment of prismatic methods, developed with the additional purpose of securing a greater intensity of light. A very curious intermediate case between the interferences of reversed and non-reversed spectra is the pronounced interference of spectra from the same source, but of different lengths (dispersion) between red and violet. The phenomena of crossed rays find a parallel occurrence in the present paper, in the behavior of duplicated fringes, when similar gratings or prisms disperse and subsequently recombine a beam of white light. A type of fringes is detected which depends merely on the grating space and is independent of wave-length. An interesting question as to the limits of micrometer displacement within which fringes of any kind are discernible (observations which were at first supposed to be due to the degree of uniformity of interfering wave-trains) is eventually shown to be a necessary result of dispersion. Finally, the direct interference of divergent rays obtained from polarizing media is exhibited.

In Chapter II the interferences of inverted spectra, a subject merely touched in the preceding volume, are given greater prominence. In this case one of the two spectra from the same source is inverted (180°) relatively to the other on a longitudinal axis (*i.e.*, an axis normal to the Fraunhofer lines), which thus becomes a line of symmetry. In the development of the subject, spectra half reversed and spectra both reversed and inverted are treated successfully. In the latter case the conditions of interference are fulfilled at but a single point in the whole area of the spectrum field; and yet the phenomenon is pronounced and not very difficult to realize. The limits of micrometer displacement within which interferences may be obtained are again determined. At the end of the chapter it was thought useful to collate available equations in the treatment of phenomena of the present kind.

The third and fourth chapters are incidental applications of the displacement interferometer and contain experiments on the expansion of metal tubes by internal pressure and on a promising method of measuring the refraction of glass, irrespective of form. To carry out the experiments in the last case with requisite rigor, optic plate-glass apparatus would unquestionably be essential. Nevertheless the tentative data obtained are noteworthy.

I have begun in Chapter V the development of displacement interferometry in connection with the older Jamin-Mach interferometer, an instrument which has certain peculiar advantages and is in a measure complementary to the Michelson interferometer. The work was undertaken in connection with the micromeasurement of the difference of heights of communicating columns of liquids, though the latter had to be abandoned in consequence of the excessive tremor in a laboratory surrounded by active city traffic. I shall hope, however, to carry out such work elsewhere.

The chief result of Chapter V is the detection of the achromatic interferences, as I have called them for convenience—interferences which are ultimately colors of thin plates seen at oblique incidence; but with the new interferometer, and obtained with white light, they are peculiarly straight and vivid and resemble a narrow group of sharp Fresnellian fringes with the central member nearly in black and white. They are capable of indefinite magnification and their displacement equivalent is a fraction of a mean wavelength per fringe. Notwithstanding their strength and clearness, they are so mobile in connection with micrometric displacement that in general it would be almost hopeless to attempt to find them but for the fact that they coincide in adjustment with the centered ellipses or hyperbolæ of the spectrum fringes of the displacement interferometer.

The fine white slit-image which is dispersed to produce the latter carries the achromatic fringes when the slit is indefinitely broadened or removed. Once found, moreover, they are not sensitive to small differences of adjustment if a change of focal plane is admissible. The chapter shows a curious method for the measurement of vertical displacements, possibly available for the detection of ether drag, which, though just insufficient in connection with the spectrum fringes, would be promising in connection with the achromatic fringes. Finally, the chapter contains some repetitions of the old experiments of Fizeau on the periodic evanescence of fringes due to the sodium lines. Curiously enough, the achromatic fringes also show periodic recurrence sometimes, which as yet remains unexplained.

The peculiar adaptability of the new interferometer to the measurement of small angles, either in a horizontal or a vertical plane, is developed in the final chapter. The ratio of the angular displacement of fringes to the angle to be measured (i.e., the rotation either of the paired mirrors or of an auxiliary mirror in the apparatus) may be made enormously large, and the paper shows cases in which, with strong luminous fringes, the angle to be measured is magnified 500 times. Moreover, this is by no means a limiting performance. Again, while angles as small as a few tenths of a second or less are measured, angles

as large as several degrees come naturally within the scope of the method. Similar remarks may be made with respect to the ratio of angular displacement and micrometer displacement. Given, therefore, an apparatus which measures very small angles without constraint or forced approximations, the measurement of long distances is the next result in order; for it is merely necessary to place the angle to be measured at the apex of the distance triangle on the length of the ray parallelogram as a base. This may be done in a variety of ways, some of which are shown in the chapter. The sensitiveness may again be made remarkably large.

The fringes here in question are preferably the very luminous achromatic fringes. They have been identified as ultimately colors of thin plates, but they look like Fresnel's fringes. In connection with this work, however, another type of fringes was detected obtainable with a fine slit, white light, and in case of centered spectrum fringes when the ocular of the telescope (or the eye) is out of focus. These are actually Fresnellian interferences, but being made up of broad concentric hyperbolic areas, brilliantly complementary in color, they resemble the lemniscates of biaxial crystals without the shadows.

My thanks are due Miss Lena F. Uhlig, who has assisted me efficiently in the preparation of this volume for the press.

CARL BARUS.

BROWN UNIVERSITY,
  *Providence, Rhode Island, June 1917.*

# CHAPTER I.

## METHODS FOR REVERSED AND NON-REVERSED SPECTRUM INTERFEROMETRY.

**1. Introductory.**—Thus far it has been impossible to use the fringes of reversed spectra individually, because of the tremor of the apparatus. It is therefore desirable to endeavor to obviate this annoyance as far as possible, and the end would appear to be most easily obtainable if the distances corresponding to the same path-difference are made smaller. At the same time the results for small distances will be interesting for this very reason in contrast to the long-distance methods.

Furthermore, the development of different methods, with a consideration of the peculiarities of each, will constitute an essential contribution to the theory of the phenomena; for from this the degree of importance which is to be attached to the original diffraction at the slit of the collimator (*i.e.*, the limiting angle at the slit, within which diffracted rays must lie to be subsequently capable of interference, whether reversed or inverted) will appear in its relations to the total dispersion of the system. The slit, however fine, is still a wave-front of finite breadth.

**2. Apparatus.**—In the first experiment, the device with two identical reflecting gratings, $GG'$, figure 1, was firmly mounted on a massive spectrometer, the four mirrors, $m$, $n$, $M$, $N$, being specially attached. White light received from the collimator $L$ after two dispersions was viewed at the telescope $T$. Both gratings were on a slide $ss$, enlarged in figure 2, set in the direction $LT$ of the previous figure. The carriage $c$, figure 2, was provided with universal joints ($a$ with a vertical axis, $b$ and $e$ with horizontal axes normal to each other), while the swiveling of the grating $G$ was controlled by set-screws at $d$, relative to the axle at $e$.

Unfortunately, the displacement of the mirror $M$, figure 1 (on a micrometer), passes the corresponding pencil across the face of the grating $G'$ and thus virtually includes a fore-and-aft motion of the latter. Thus the fringes pass, with rotation, from very fine, hair-like striations, through a horizontal maximum of coarseness, back to vertical lines again, when homogeneous light and a wide slit are employed. The annoyances due to tremor, however, were not overcome. Moreover, there is difficulty in obtaining Fraunhofer lines normal to the longitudinal axis of the spectrum. This method was therefore abandoned.

The design shown in figure 3, with a transmitting grating at $G$ (grating space $D = 352 \times 10^{-6}$ cm.) and a stronger reflecting grating at $G'$ ($D = 200 \times 10^{-6}$ cm.), was next tested, $M$ being the micrometer mirror. The mean distance of $M$ from $N$ was about 15 cm., from $MN$ to $G'$ about 10 cm. and to $G$ 40 cm.

9

Later these distances were enlarged. First-order spectra were used and the fringes obtained easily and brilliantly, particularly with mercury light, in both green and yellow. They rotated as above, admitted a displacement $M$ of about 1 cm. But they were still too mobile to be used individually.

The same design, figure 3, was now mounted on a round, heavy block of cast iron $B$, 30 cm. in diameter and 4 cm. thick, the distance $G$ to $MN$ being about 20 cm. A number of screw-sockets, $b$, $b$, were drilled into $B$ on the right and left, for mounting subsidiary apparatus. $G'$ as before was on the universal slide (fig. 2), movable in the direction $LT$. The tablets $t$, $t'$, etc., of $G$, $M$, $N$, and $G'$ were mounted tentatively on standards of gas-pipe 1.5 cm. in external diameter and 6 cm. long. Slight pressure by the finger-tips showed a passage of several fringes across the field, but the fringes were stationary in the absence of manual interferences and in spite of all laboratory tremors. A parallel arm of the same pipe was therefore firmly attached to the stem of
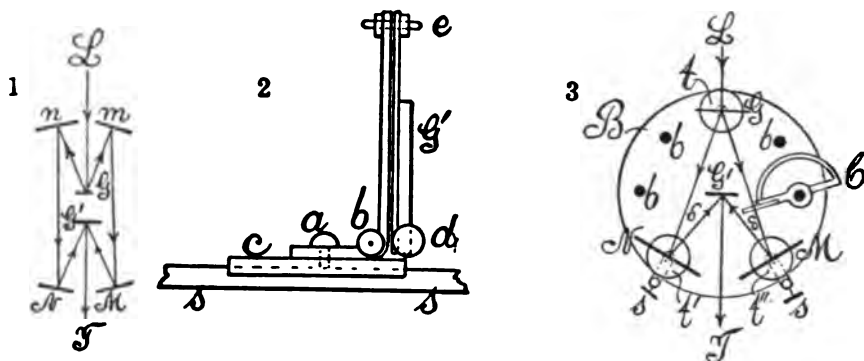


$N$ and $M$, each arm terminating in a fine horizontal set-screw, $s$, $s$, below, adapted to push against the rim of the iron block. In this way adequately stationary conditions and an elastic fine adjustment for superposed longitudinal spectrum axes were both secured with advantage. Similar elastic adjustments have been recently applied. It was now possible to manipulate the micrometer at $M$ by hand; but a glass-plate compensator $C$, rotated by a tangent screw over a graduated arc, was also convenient. Later other types were attached, including an air-compensator, in which path-difference was secured by exhausting the air within a closed pipe provided with glass-plate ends. These contrivances were eventually superfluous, however, as it was found that on reducing the rotation of the micrometer-screw the latter could be used at once.

In case of homogeneous light and a wide slit, fringes were visible in an ordinary telescope for a play of over 2 cm. of the micrometer-screw, passing, however, between extremes of fineness. The slit images are not of equal breadth, if first- and second-order spectra are superposed; but if the longitudinal axes are coincident, any position of the narrow image within the broader produces a wide vertical distribution of fringes, usually more or less horizontal. They are very easily found. The sodium flame is too feeble for use. The mercury

arc is unfortunately too flickering, so that the fringes jump about and are useless for measurement. Excellently sharp quiet fringes are obtained with sunlight (white), in which the cross-hatched interference pattern is nearly linear at the line of symmetry of the reversed spectra. The fringes climb very decisively up and down this line with the motion of the micrometer, reduced as suggested. The electric arc and a Nernst filament are equally available as a source of light. Finally, by suitably rotating the grating $G'$, figure 2, on the axis $e$, by aid of the set of screws $d$, fringes whose distance apart is over one-third of the width of the telescope field may be obtained quite sharply. As this distance represents but $30 \times 10^{-4}$ cm., there is no difficulty of realizing $10^{-4}$ cm. in case of these long fringes.

**3. Measurements. First- and second-order spectra.**—The steadiness of the fringes, even in an agitated location, induced me to make a few measurements for orientation. Accordingly, the Fraunhofer micrometer, reading to $10^{-4}$ cm., was provided at its screw-head with a light wooden wheel $w$, figure 4, about
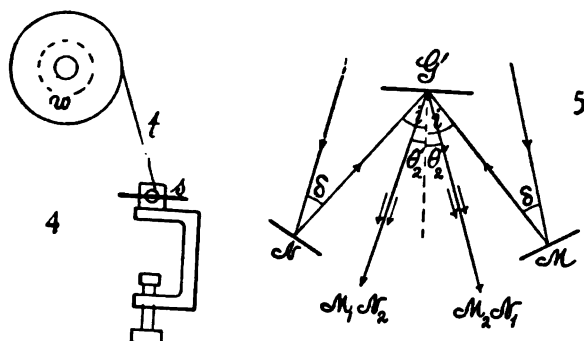


10 cm. in diameter and 3 mm. thick. A groove was cut in the circumference of the wheel, so that a silk thread $t$ could be wrapped around it. The other end of the thread was wound around a brass screw $s$, about 6 mm. in diameter, turning in a nut, preferably of fiber, which was fastened to the edge of the table by a small brass clamp. In this way it was possible to control the motion of individual fringes crossing a fiducial line in the field of the telescope. This simple device worked surprisingly well, a smoothly running micrometer being presupposed. In fact, it was possible to set a fringe to a few millionths of a centimeter. Later the micrometer-head was grooved and a finer turning-screw suitably attached to the base $B$ of the apparatus. (*Cf.* § 70, below.)

The fringes should be widened as far as convenient, by rotating the grating on the axle $e$, figure 2, by aid of the set-screws $d$. In this case they climb up or down the transverse strip as $s$ in figure 4 is slowly rotated. Fringes moving horizontally are not serviceable, because they are too near together. It is not difficult to obtain the single vertical line, black or bright, on suitable rotation about $e$. On either side of this transitional adjustment the fringes move vertically (climb or fall) in opposite directions for the same micrometer

displacement. The arrow-shaped forms are also often satisfactory, and may be obtained by adjusting the two bright patches on the reflecting grating into coincidence, by the eye, in the absence of the telescope. The grating $G'$ is moved fore and aft for this purpose on the slide $s$, figure 2, until the two bright strips become one.

In making the first adjustment, I incidentally combined the first-order spectrum from $N$ with the second-order spectrum from $M$, as shown in figure 5, under the impression that the wider $D$ groups from the latter were due to slight curvatures of mirrors. The fringes were nevertheless easily found and showed no anomalies, except that observation had to be made near $M$ or $N$.

It appears from figure 5 that the equations for this case imply

$$\sin i + \sin \theta''_2 = 2\lambda/D_2$$
$$\sin i - \sin \theta'_2 = \lambda/D_2$$

where the angles $i$ and $\theta$ are equal ($\theta'_2 = \theta''_2$). Thus $\sin i = 3\lambda/2D_2$ and $\sin \theta = \lambda/2D_2$, $D_2$ being the grating constant ($D_2 = 200 \times 10^{-4}$ cm.).
Hence

$$\sin i = 0.4420 \quad \sin \theta_2 = 0.1423$$
$$i = 26°14' \quad \theta_2 = 8°11'$$

while from the first grating, $D_1 = 352 \times 10^{-4}$ cm., $\theta_1 = 9°38'$; whence
$$\sigma = i + \theta_1 = 35°52' \qquad \delta = i - \theta = 16°36'$$

The trial readings given in table 1 of the micrometer for a passage of 20 fringes each were found without special precautions, which is equivalent

TABLE 1.

| Scale parts. | $10^{-4}$ cm. |
|---|---|
| 19.7 | 9.85 |
| 21.0 | 10.5 |
| 22.2 | 11.1 |
| 23.4 | 11.7 |
| 24.6 | 12.3 |
| 25.8 | 12.9 |
| 27.0 | 13.5 |
| 28.2 | 14.1 |

to an average of $10^{-4} \times 30.1$ cm. per fringe. As the line of symmetry lay very near the two $D_1D_2$ doublets, this is obviously an approach to half a wave-length. For accurate work $D_1D_2$ and $D'_1D'_2$ should be superposed, in which case the fringes would lie between and actually correspond to their mean wave-length.

A number of measurements like the above were now made with different types of fringes. The mean values successively taken from 3 or 4 batches of 20 fringes each were

$$10^4\delta e = 29.4, \ 30.0, \ 31.2, \ 30.6, \ 29.7, \ 30.1, \ 30.0, \ 30.0, \ 30.8 \text{ cm.}$$

The results were less decided when long fringes were used. The mean value of the 10 sets is thus $\delta e \times 10^4 = 30.19$ cm. per fringe. Actual or approximate coincidence of the $D$ lines made no appreciable difference.

In the following results the reflection from the mirror $M$, figure 5, was used in the first order and from $N$ in the second order, after leaving $G'$. Observations were made near $N$, figure 5. The displacement corresponding to 80 fringes was successively 0.0024, 0.0024, 0.0024, 0.0024 cm., so that the mean value

$$10^6\delta e = 30.0 \text{ cm.}$$

agrees with the above.

Similar trial observations (combined first order from $N$ and second order from $M$) were made with red light near the $C$ line in series of 6 with a mean value $\delta e \times 10^6 = 34.0$ cm. Again, near the $b$ line (green), giving $\delta e \times 10^6 = 27.2$ and 27.8 cm. per fringe. These should therefore be distributed in terms of wave-length, as in table 2.

TABLE 2.

|   | $10^6\lambda$ | Ratio. | $10^6\delta e$ | Ratio. |
|---|---|---|---|---|
| $C$ | 65.6 cm. | 1.11 | 34.0 cm. | 1.13 |
| $D$ | 58.9 | 1. | 30.2 | 1. |
| $b$ | 51.7 | 0.88 | 27.5 | 0.91 |

and they are as nearly as may be expected in the ratio in question, seeing that the total displacement for 60 fringes does not exceed 0.004 cm. For accurate data it would be necessary to count many hundreds of fringes, and to correct the $\delta e$ values by multiplying by sec $(\theta_2 - \theta_1)/2$. I have not done this, as the red and green fringes are not so distinctly seen as the yellow.

**4. Continued. First-order spectra.**—The apparatus was now readjusted in such a way that first-order spectra were available from both mirrors. This puts the grating $G'$ at a greater distance from the line $M$ and $N$ than before, for the angle $\theta_2$ is smaller. A series of trial results were investigated in the same manner as above, the mean values from 4 successive pairs of 80 fringes each being, in three repetitions,

$$\delta e \times 10^6 = 29.0, 29.4, 29.5 \text{ cm.}$$

and from 5 pairs of 100 fringes each,

$$\delta e \times 10^6 = 29.1 \text{ cm.}$$

This makes an average of

$$\delta e \times 10^6 = 29.25 \text{ cm.}$$

somewhat smaller than half a wave-length of the $D$ light used. Unfortunately, the screw at $s$ (fig. 4) here worked jerkily, to which the low value is probably due.

In this case sin $\theta_1 = \lambda/D_1$, where $D_1 = 352 \times 10^{-6}$ cm. or $\theta'_1 = 9°38'$; sin $\theta'_2 = \lambda/D_2$, where $D_2 = 200 \times 10^{-6}$ cm. or $\theta'_2 = 17°9'$, whence

$$\sigma = 26°47' \text{ and } \delta = 7°31'$$

In a later series of experiments, the play of the screw $s$ was improved, so

that it ran more smoothly. The following values were found in two repetitions, from 4 pairs of 80 fringes each:

$$\delta e \times 10^6 = 30.1, \ 30.0 \text{ cm.}$$

and in 5 pairs of 100 fringes each,

$$\delta e \times 10^6 = 29.5 \text{ cm.}$$

If the mean value of these data is compounded with the above mean, the average is

$$\delta e \times 10^6 = 29.56 \text{ cm.}$$

**5. Continued. Second-order spectra.**—The same phenomenon was not sought in the two second-order spectra from $G'$. Magnificent arrows were obtained, useful throughout about 5 mm. of the micrometer-screw, after which they lost clearness. This limited range could no doubt be immensely increased if optical plate glass were employed in place of the ordinary plate used. The data for pairs of observations, including 60 or 80 fringes, were (5 repetitions) $\delta e \times 10^6 = 30.3, \ 30.5, \ 30.0, \ 30.8, \ 31.1$ cm. per fringe, giving a mean value of $\delta e \times 10^6 = 30.5$ cm. In the last two measurements the sodium doublets coincided.

In this case $\sin \theta''_2 = 2\lambda/D_2$, where $D_2 = 200 \times 10^{-4}$ cm. and $D_1 = 352 \times 10^{-4}$ cm. (first grating). Thus

$$\sigma = 45^\circ 44', \ \delta = 26^\circ 28'$$

If the above mean data are summarized the results appear as follows ($\lambda = 58.93 \times 10^{-6}$ cm.):

G first order, $G'$ first order, mean $\delta e \times 10^6 = 29.56$ cm.
G first order, $G'$ first and second order, mean $\delta e \times 10^6 = 30.2$ cm.
G first order, $G'$ second order, mean $\delta e \times 10^6 = 30.5$ cm.

And if computed as $\delta e = \lambda/2 \cos \delta/2$, these become

TABLE 3.

| $\delta e \times 10^6$ | Diff. |
|---|---|
| 29.53 cm. | +0.03 cm. |
| 29.78 | + .42 |
| 30.27 | + .23 |

The maximum error of $4 \times 10^{-7}$ cm. is equivalent to but a little over 1 per cent of the distance between fringes, and it would be idle to suppose that the apparatus, figure 4, could be set more accurately. In fact, the largest error occurs in the second set, which were first made and in which the play of the apparatus was inadequately smooth.

**6. Theory.**—Hence the theory of the apparatus (fig. 6) may be regarded as justified. Here the rays $Y$ and $Y'$ come from the first grating ($G$ transmitting), and after reflection from the opaque mirrors $M$ and $N$ (the former on a micrometer) impinge on the second reflecting grating $G'$, with a smaller

grating space, and thereafter interfere along the line $T$, entering the telescope. To treat the case the mirrors $M$, etc., may be rotated on the axis $T$ normal to $G'$ in the position $M_1$. $G'_n$ and $G'_m$ show the reflections of $G'$ in the mirrors
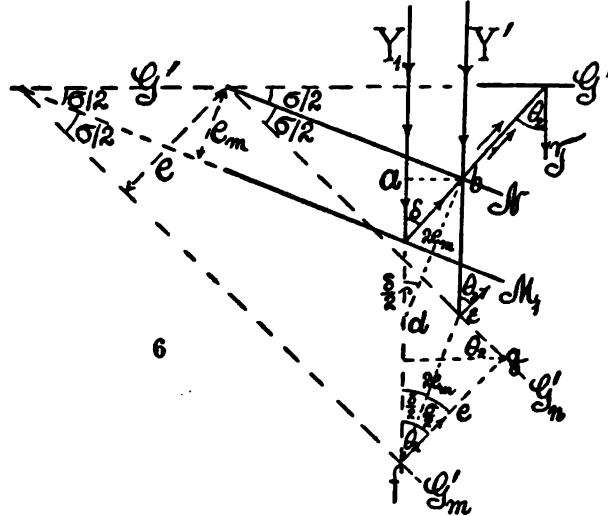


$N$ and $M_1$. We thus have a case resembling the interferences of thin plates, and if $e_m$ is the normal distance apart of the mirrors $M_1$ and $N$, the displacement $\Delta e_m$ per fringe is given by

$$\lambda = 2\Delta e_m \cos \delta/2$$

where $\delta$ is the angle between the rays incident and reflected at the mirrors. This is the equation used above. If the mirrors and the reflections of the gratings $G'$ make angles $\sigma/2$ and $\sigma$ with $G'$, the actual lengths of the rays (prolonged) before meeting to interfere terminate in $e$ and $f$ respectively. Let the image of $G'$ be at a normal distance $e$ apart. Then $e = 2e_m \cos \sigma/2$, for the figure $fdbe$ is a parallelogram. If the distance $eg$ is called $C$ we may also write

$$\lambda = e \cos \theta_2 + C \sin \theta_2$$

since $C = 2e_m \sin \sigma/2$ and the angle of diffraction $\theta_2 = (\sigma + \delta)/2$.

**7. Compensator measurements. Sharp wedge.**—With the object of testing the interferometer under a variety of conditions, measurements were made with a number of different compensators and the experience obtained may be briefly given here. The first of these was a very sharp wedge, such as may be obtained from ordinary plate glass. The piece selected, cut from an old mirror, on being calipered, showed the following dimensions: Length, 5 cm.; thickness at ends, 0.375 and 0.367 cm. Hence the angle of the wedge is $\alpha = 0.0016$ radian, or about 0.1°. No difficulty is experienced from the deviation of the rays for so small an angle, though sometimes the fringes are unequal and the lines presumably curved. This wedge was attached to a Fraunhofer micrometer moving horizontally, and the normality of the rays passing through

the glass was found by rotating it around an axis perpendicular to the rays until the direction of motion of the fringes was reversed. In view of the small angle $\alpha$ and the micrometric displacement, it was easy to count single fringes, or fractions as far as about 1/30 of a fringe, even though the beam traversed the glass twice. In the first experiment the following data of the horizontal displacement, $r$, of the wedge were found for successions of 7 fringes:

|  |  |  |  |
|---|---|---|---|
| 0.2044 cm. | 0.2042 | 0.2043 | 0.2067 |
| 0.2058 cm. | 0.1976 | 0.1946 | 0.18888 |

Mean, 0.2008 cm.    Per fringe, $\delta r = 0.0287$ cm.

The last three results are low, the discrepancies probably resulting from slight wabbling of the micrometer slide. In another series made with care as to the normal adjustment, the horizontal displacement, $r$, of the wedge for successions of 11 parallel fringes was

|  |  |  |  |  |  |
|---|---|---|---|---|---|
| 0.3022 cm. | 0.2997 | 0.2974 | 0.3002 | 0.2991 | 0.3078 |
| 0.3081 cm. | 0.3101 | 0.3170 | 0.3183 | 0.3155 | |

Mean, 0.3014 cm.    Per fringe, $\delta r = 0.0274$ cm.

If $x$ be the distance from apex of the wedge, its thickness is $e = x\alpha$, or per fringe $\delta e = \alpha \delta x$. The index of refraction was found to be $\mu = 1.526$ by total reflection. Thus, without correcting for dispersion,

$$2(\mu - 1)\delta e = \lambda$$

and with the above values

$$\alpha = \frac{10^{-4} \times 5.893}{2 \times 0.526 \times 0.028} = 0.0020 \text{ radian}$$

This is larger than the calipered value because the rays go through the wedge twice obliquely. The reduction, however, would be too complicated here and will be treated later.

The irregularities above are referable to the micrometer, which was not very accurate, and no particular care was taken with details. The method is interesting as allowing of the complete control of a single fringe; i.e., the equivalent of $30 \times 10^{-4}$ cm. As this corresponds to 0.028 cm. on the micrometer, the displacement $\delta x = 0.001$ is equivalent to $10^{-4}$ cm. Furthermore, the method presents an expeditious means of finding $\alpha = \lambda/2(\mu - 1)\delta x$ when $\alpha$ is very small.

**8. Continuation. Revolving plate.**—In the next place, the revolving compensator $C$, figure 3, was employed. This also proved to be an admirable device for controlling the fringes, and it was much more rapid than the preceding. Unfortunately the computation is inconvenient, as the normal position can not be ascertained with sufficient accuracy. To find it, the plate was revolved until the fringes changed their direction of motion. This is an indication of the insertion of the minimum thickness of glass, but is not sharp enough for precision. Hence data in A, table 4, are not coincident, $i$ denoting the angle of incidence. Another somewhat better and thicker plate was now inserted with the results shown in B.

TABLE 4.

| A. Same plate as in the preceding work, $e = 0.370$ cm. | | | | B. Thickness $e = 0.489$ cm. | | | |
|---|---|---|---|---|---|---|---|
| No. of fringes. | $i$ | | $i$ (probable value). | No. of fringes. | $i$ | | $i$ (probable value). |
| 0  | 0° 0° 0° | | 0° | 0  | 0° 0° 0° | | 0° |
| 10 | 4.4 5.8 7.3 | | 5.4 | 10 | 6.0 5.5 4.9 | | 5.2 |
| 20 | 7.4 8.0 9.5 | | 7.8 | 20 | 7.9 7.3 7.0 | | 6.8 |
| 30 | 9.6 9.7 11.1 | | 9.5 | 30 | 9.5 8.9 8.5 | | 8.3 |
| 40 | 11.4   12.6 | | 11.0 | 40 | 10.9 10.3 9.9 | | 9.6 |
| 50 | 13.0   13.8 | | 12.3 | .. | .... .... ... | | .... |

The second series here is practically the mean of the two, though the reason for these large discrepancies is not clear to me, even in consideration of the wedge-shaped plates. The mean of the results may, however, be used for computation.

The path-increment introduced by the glass of thickness $e = 0.489$ cm. and index of refraction $\mu = 1.526$, at an angle of incidence $i$ and refraction $r$ for $n$ fringes, beginning at $i = 0$, may be written (see fig. 7, where $I$ is the incident ray)
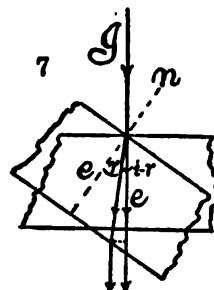


$$n\lambda = e\mu\left(\frac{1}{\cos r} - 1\right) - e\left(\frac{\cos (i - r)}{\cos r} - 1\right)$$

This is a cumbersome equation. If the angles $i$ are small, the cosines may be expanded and then approximately

$$2n\lambda = e\left((\mu - 1)r^2 + (i - r)^2\right)$$

which, since $i = \mu r$ nearly, may be further simplified to

$$n\lambda = e(\mu - 1)i^2 / 2\mu$$

Thus for the second set (mean)

$$r = 3.6° \qquad 4.8° \qquad 5.9° \qquad 6.8°$$
$$10^5\lambda = 6.7 \qquad 6.4 \qquad 6.9 \qquad 6.5 \text{ cm.}$$

The wave-length thus comes out very much too large, but in consideration of the inadequacy of the fiducial position, $i = 0°$, this is not unexpected. Thus the probable values of $i$ in the tables (computed from $\lambda$ correct) agree with the third series. In addition to this the effect of slightly wedge-shaped plates, etc., can not be ignored. For the first set (mean values) the results are similar, being

$$10^5\lambda = 6.8 \qquad 7.0 \qquad 6.9 \qquad 7.0 \qquad 7.0 \text{ cm.}$$

if computed by the approximate equation. This is again too large, but the probable value of $i$ computed from the correct $\lambda$, as before, agrees nearly with the first series of this set.

**9. Continuation. Air column.**—An air compensator was now installed consisting of a tube $\epsilon = 15$ cm. long and about 2 cm. in diameter, closed with glass plates. The fringes were easily found and sharp. Unfortunately the pump was not quite tight, so that, on breaking the count of fringes at low pressures, it was difficult to state when the conditions had become isothermal. Hence the results in table 5 are rough. Temp. 19.7°.

TABLE 5.

| No. of fringes. | Exhausted to ($p$). | $\dfrac{dp}{dn}$ | $\lambda 10^6$ |
|---|---|---|---|
| 0 | 75.1 cm. | .... | .... |
| 30 | 41.8 | 11.1 | 59.7 cm. |
| 67 | 0 | 11.1 | 60.0 |
| 0 | 75.1 | .... | .... |
| 30 | 43.0 | 10.7 | 57.6 |
| 70 | 0 | 10.6 | 57.1 |
| 0 | 75.1 | .... | .... |
| 40 | 32.1 | 10.7 | 57.8 |
| 68 | 0 | 11.2 | 60.0 |

The mean value thus appears as $\lambda = 10^{-5} \times 5.88$ for sodium light. The equations used are

(1)  $\qquad\qquad\qquad n\lambda = \epsilon(\mu - 1)$

where $n$ is the number of fringes counted, $\epsilon$ the tube-length, and $\mu$ the index of refraction of air. Again,

(2)  $\qquad\qquad\qquad p = C(\mu - 1)\vartheta$

where $p$ is the pressure, $\vartheta$ the absolute temperature, and the constant $C$ computed from normal conditions (76 cm. and 0° C.) is (Mascart's values) $C = 952.6$. Hence

(3)  $\qquad\qquad \lambda = \dfrac{\epsilon}{C}\dfrac{p}{n\vartheta} = \dfrac{\epsilon}{C}\dfrac{dp}{d(n\vartheta)} = \dfrac{\epsilon}{C\vartheta}\dfrac{dp}{dn}$

when $\vartheta$ is constant. It is this assumption which is not quite guaranteed above. To obviate this in the following experiments, the total number of fringes were counted (table 6) from exhaustion to plenum. Their number was definite to the fraction of a fringe.

TABLE 6.

| Temp. 19.3° C.; $C = 15$ cm. | | | |
|---|---|---|---|
| No. of fringes. | Exhausted to ($p$). | $\dfrac{dp}{dn}$ | $\lambda 10^6$ |
| 0 | 75.8 cm. | ..... | .... |
| 69.5 | 0 | 1.090 | 58.8 cm. |
| 0 | 75.8 | ..... | .... |
| 69.5 | 0 | 1.090 | 58.8 |
| 0 | 75.8 | ..... | .... |
| 69.5 | 0 | 1.090 | 58.8 |

These results are correct to 0.5 per cent and are as close as the estimation of *p*, *c*, *ϑ*, and fractions of a fringe will warrant. If results of precision were aimed at, a long tube should of course be used. What was particularly marked in these experiments was the motion of fringes in the passage from any approximately adiabatic to isothermal conditions and on approaching a plenum of air.

Since the refraction depends on density, there should not (apparently) be any motion at all; but the thin tube is always more nearly isothermal than the much larger barrel of the air-pump. As a consequence there is residual expansion from the former to the latter.

**10. Continuation. Babinet compensator.**—The behavior of an old Babinet compensator, placed nearly normal to one of the beams, figure 3, was peculiar, though the fringes were clear and easily controlled. The dimensions of the right-handed quartz wedge were roughly calipered and found to be: length, 4.2 cm.; thickness at ends, 1.017 and 0.934 cm. Thus there is a grade of $0.083/4.2 = 0.0193$, or something over $1°$ of arc. A vertical displacement of 2.5 cm. of this wedge was available behind the stationary counteracting left-handed wedge.

The fringes were not uniform and they required an inclination to the vertical of the rulings of the grating $G'$. The fringes were evidently curved lines, intersected by the vertical strip within which they are visible. Consequently they appeared as in figure 8, with linear elements in the middle, shortening into dots at either end of the strip. On motion of the compensator wedge they moved toward or from the center of symmetry, as is also indicated in the figure. Tiled forms were frequent. The most interesting feature, however, was their alternate appearance and evanescence in cycles. While the wedge was moved over 2.5 cm. of its length, 7 of these cycles appeared and vanished, each consisting of about 36 to 40 fringes. The disappearance was not always quite complete, but the fringes could not be restored by any adjustment for coincidence of spectra.

An attempt was made to find the angle of the quartz wedge by the first method. Data, 0.0023, 0.0024, 0.0024 cm., were found for the displacement of the micrometer per fringe. Hence, apart from dispersion,

$$\alpha = \frac{10^{-5} \times 5.893}{2 \times 0.5442 \times 0.0024} = 0.022 \text{ radian}$$

which, as in case of the glass plate, is again slightly above the calipered value.

In another somewhat thinner Babinet compensator the constants were: length, 3.35 cm.; thickness, small end, 0.494 cm., large end, 0.496 cm. The prism angle is $\alpha = 0.062/3.35 = 0.0185$ radian, also about $1°$.

In this case there was no periodic phenomenon, but in its place the degree of longitudinal coincidence of the axes of the two spectra continually changed.

The fringes at once sharpened, however, on readjustment of either mirror, indicating a continuous small change of deviation, due to curvature, probably, in the quartz wedge. In the preceding periodic case, no readjustment of deviation sufficed to restore the fringes. The wedge was now detached and used alone. In spite of the relatively large angle (1°), no difficulty was experienced in adjusting or controlling the fringes; but the face curvature just suggested appeared as before, so that readjustment for varying wedge-angle was required from time to time.

**11. Micrometer displacement of the second grating, G'** (fig. 3).—In the preceding report (Carnegie Inst. Wash. Publication 249, Chapter III, § 28) it was shown that if the angle between the gratings $G$ and $G'$ is $\varphi$ and the angle between the mirrors $M$ and $N$ (which in a symmetrical adjustment would be $180° - (\theta_1 + \theta_2)$, $\theta_1$ and $\theta_2$ being the angles of diffraction at $G$ and $G'$ for normal incidence at $G$) is decreased by $\alpha$, so that the adjustment is non-symmetrical, then the displacement $\delta s$ of the grating $G'$ per fringe will be very nearly

$$\delta s = \frac{\lambda \cos^2 \theta_2}{2(\alpha - \varphi) \sin \theta_2}$$

if $\alpha$ and $\varphi$ are small. Here $\alpha$ is effectively the angle between the mirrors $M$ and $N$, since, if $M$ is rotated 180° on the line of symmetry (normal to the grating $G$), the two mirrors would intersect at an angle $\alpha$. The result of fore-and-aft motion thus depends on the angle $\alpha - \varphi$, and if $\alpha = \varphi$, $\delta s = \infty$ per fringe; i.e., fore-and-aft motion would produce no result. This is necessarily

TABLE 7.

| i = increasing; d = decreasing. | | |
|---|---|---|
| No. of fringes. | Total displacement. | Mean $\delta s$ displacement per fringe. |
| i 3 | 0.0234 cm. | 0.0088 cm. |
| 3 | 267 | ...... |
| 3 | 293 | ...... |
| i 4 | .0302 | .0080 |
| 4 | 317 | ...... |
| 4 | 318 | ...... |
| 4 | 346 | ...... |
| 4 | 330 | ...... |
| d 4 | .0285 | .0073 |
| 4 | 285 | ...... |
| 4 | 287 | ...... |
| 4 | 315 | ...... |
| 4 | 288 | ...... |

the case when but a single grating is used, as in the earlier methods. In the case of two gratings, however, it is not only difficult to make a perfectly symmetrical adjustment of mirrors and grating, but it would not be of any

special advantage. Hence the fore-and-aft displacement $e$ of the grating $G'$ will probably be accompanied by a slow motion of the fringes, from which the angle $\alpha - \varphi$ may be computed.

The experiments recorded in table 7 were made with the grating $G'$ on a micrometer-slide moving normally to the face of the grating. With the mirrors, etc., placed so that optical paths were nearly equal, the adjustment screws on $M$ and $N$ sufficed to bring the fringes strongly into view. Successions of 3 and of 4 fringes were tested, as these required an adequately large displacement of the micrometer, which was moved both forward and backward.

The mean of the three results is $\delta e = 0.008$ cm. per fringe. The data are not smooth, because the micrometer placed between the mirrors $M$ and $N$ is in an inconvenient position for manipulation. The different sets of values, moreover, correspond to different adjustments and therefore to slightly different values of $\alpha - \varphi$. As an order of values only is wanted, it was not considered worth while to remedy the deficiencies.

In accordance with the equation given, if $\delta e = 0.008$ cm., $\lambda = 58.9 \times 10^{-6}$ cm., $\theta_2 = 20°$ be inserted,

$$\alpha - \varphi = \frac{\lambda \cos^2 \theta_2}{2 \delta e \sin \theta_2} = 0.0095 \text{ radian} = 0.54°$$

The adjustment is thus about half a degree out of symmetry, a result which in case of improvised apparatus is inevitable and moreover without significance in the precision of the method.

**12. Prism method. Reflection.**—The grating $G$ was now removed and replaced by a silvered prism, as shown in figure 9 ($P$, prism; $M$, $N$, mirrors; $G$, grating; $T$, telescope). A small prism angle, $\varphi$, is essential ($\varphi = 18°$, about), as a large divergence of rays would not be accommodated on the interferometer, figure 3. The fringes were found without difficulty, in the second order, the arc lamp being used. They are also easily distorted, if the edge of the prism is not parallel to the rulings of the grating. In such a case the symmetrical arrow-shaped forms become one-sided and, as it were, curved or faintly fringed beyond the limits of the strip. To get the best adjustment, the lamp should shed about the same amount of undeviated light from both faces of the prism, on a screen temporarily placed behind it. The illuminated strips on the grating must coincide to the eye while making the fore-and-aft adjustment. Finally, the grating is to be slowly rotated on the axis normal to itself, until fringes of satisfactory shape and size appear. Naturally this is done through the telescope, and a readjustment of the longitudinal axes
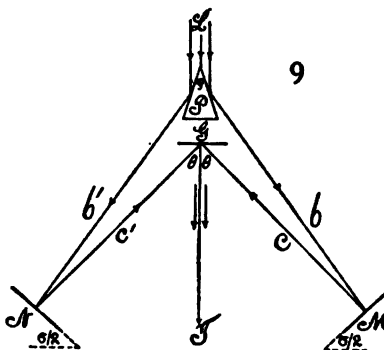
of the spectra is necessary after each step of rotation. Fringes so obtained are as good as those obtained by any other method.

The range within which the fringes are sharp is small, not exceeding 2 mm. of displacement of the micrometer mirror, $M$. A partial reason for this will appear from figure 9 and results from the fact that the illumination on the grating due to $M$ moves laterally across the stationary strip due to $N$. Clearly if the latter were also on a micrometer it might, in turn, be displaced relatively to the direction of $M$ and restore the fringes to full brilliancy. The range in this case may be increased till either illuminated strip gets beyond the edges of the grating. This test will presently be made.

If the prism angle is $\varphi$ and the angle of diffraction for normal incidence is $\theta$, the angle $\delta$, between the incident and reflected ray at $M$, is

$$\delta = \theta - \varphi$$

Thus $e \tan \delta/2$ is the displacement of the strip of light on the mirror $M$, if $e$ is the normal displacement of the latter. Hence the corresponding displacement $x$ on the grating is

$$x = 2e \sin (\delta/2)/\cos \theta$$

If $b$ be the distance from the prism to the light spot reflected on $M$, and $c$ the distance from there to the bright spot on the grating, $\varphi$ may be computed as

$$\sin \varphi = \frac{C \sin \theta}{b} = \frac{2\lambda c}{b}$$

for the spectra are in the second order.

The data are:

$$10^6\lambda = 58.93 \text{ cm.}; \quad b = 38.0 \text{ cm.}; \quad c = 20.4 \text{ cm.}; \quad D = 200 \times 10^{-4} \text{ cm.}$$

Whence

$$\varphi = 18° 12' \qquad \theta = 36° 6' \qquad \delta = 17° 54'; \ \delta/2 = 8° 57'$$

Hence

$$x = \frac{25 \times 0.1556}{0.808} = 0.096 \text{ cm.}$$

if $e = 0.25$ cm., as found. Thus the rays of the same origin, or rays capable of interfering, are found in a vertical strip on the grating, not more than 1 mm. wide. It is interesting to note that the fringes vanish by becoming coarser and wider, corresponding to the narrowing of effective edges in contact.

The attempt to produce these fringes with homogeneous (sodium) light and a wide slit again failed, although much time was spent in the endeavor. Even with a narrow slit and accentuated sodium lines (impregnated arc) the phenomenon may be produced between the doublets, however close together, but it fails to appear with the same adjustment when two corresponding lines coincide. I was only able to produce it in a continuous spectrum, between the two doublets and with a fine slit. It is very important to ascertain the reason.

Both mirrors, $M$ and $N$, were now placed on micrometers moving nearly normal to their faces. Beginning with a coincidence of the illuminated strips on the grating, the $M$ micrometer was moved until the fringes disappeared. The $N$ micrometer was then moved in the same direction, until the reappearing fringes passed through an optimum and finally vanished, in turn. Thereafter the $M$ micrometer was displaced again, always in the given direction, and the same cycle repeated, etc. It was possible to pass through about 8 cycles with each micrometer before the illumination reached the edge of the grating, each cycle corresponding to a displacement of about 2 mm. for a single mirror; but a total displacement of 2.5 cm. was registered, which would obviously have been increased much further if the grating had been wider. The data given in table 8 give a concrete example:

TABLE 8.

| Position of $N$. | Advance of $N$. | Remarks. | Position of $N$. | Advance of $N$. | Remarks. |
|---|---|---|---|---|---|
| 2.42 cm. | .... | Broad arrows | 1.75 cm. | .... | Vertical lines |
| 2.20 | .... | | 1.54 | .... | |
| .... | 0.22 cm. | $M$ advanced | .... | 0.21 cm. | $M$ advanced |
| 2.20 | .... | Narrow arrows | 1.54 | .... | Vertical lines |
| 1.98 | .... | | 1.37 | .... | |
| .... | .24 | $M$ advanced | .... | 1.7 | $M$ advanced |
| 1.98 | .... | Upright lines, inclination changed | | | |
| 1.75 | .... | | | | |
| .... | .23 | $M$ advanced | | | |

As both mirrors move in the same direction, the two illuminated strips on the grating gradually separate until they are quite distinct. Meanwhile the fringes pass with rotation from the original sagittate forms to very fine hair-like striations; whereas the part of the spectrum within which the former occur is less than the distance apart of the sodium lines (doublets), the hair-lines are visible within a strip of spectrum many times as broad as the sodium doublet. Ten such lines may be visible. In good adjustments the sagittate forms are seen to be a nest of very eccentric, identical hyperbolas, as in figure 10, $A$, arranged or strung on the same major axis. The vertices $a$ are therefore thick and pronounced, but taper rapidly down into hair-lines, $b$, $b'$, on both sides. Frequently but half of the coarse vertices, $a$, abundantly fringed on one side, $b$ or $b'$, appear. Nevertheless this does not seem to be an exhaustive description of the phenomena; for it is not uncommon, when partial hyperbolas appear, to find the striations (which are always faint) in the same direction on both sides, as in figure 10, $B$; $i.e.$, the striations are apt to be non-symmetrical on the two sides, as if they constituted a second diffraction phenomenon superimposed on the first phenomenon. Roof-shaped forms (fig. 10, $C$), strongly dotted, are also common, often irregularly awned.

Figure 11 may be consulted to further elucidate the subjects under consideration. $G$ is the grating, $PP'$ the principal plane of the objective of the telescope, $a$ and $b$ are two rays interfering at the focus $f$, and leaving the grating parallel and symmetrically placed to the axial ray $of$. The passage

of the coarse sagittate phenomena into the hair-like striations, as $a$ and $b$ move farther apart, may then be accounted for in accordance with the general theory of diffraction; *i.e.*, if the distance apart of $a$ and $b$ is $d$ and the principal focal distance *of* is $R$,

$$\frac{\lambda}{d} = \frac{s}{R}$$

where $s$ is the distance between the two fringes of wave-length $\lambda$. Hence $s$ will increase as $d$ decreases, agreeing with the effect of fore-and-aft motion, or with the effect of simultaneous, large (2.5 cm.) displacement of both mirrors, neither of which destroys the symmetry of the interfering rays.
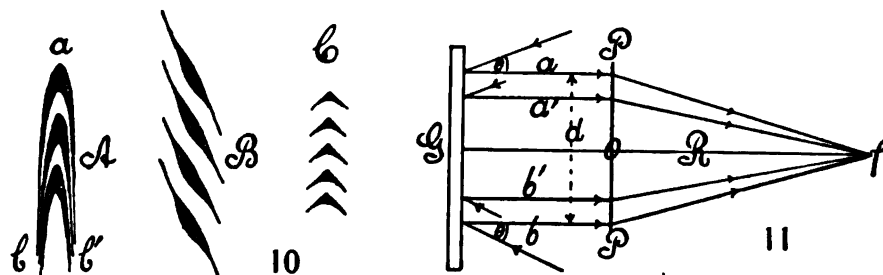


The motion of a single mirror, $M$ or $N$, for instance, does destroy the symmetry, and it was shown in § 12 that the limiting range of displacement of 0.25 cm. moves either $a$ or $b$ 0.096 cm. out of symmetry. The interferences thus vanish without much changing in form or size, and vanish in all focal planes.

The breadth of the blades of light $aa'$ and $bb'$, figure 11, capable of interfering is $x$ on the grating and

$$x \cos \theta = 0.096 \times 0.808 = 0.078 \text{ cm.}$$

normally. Since the rays are parallel after leaving the collimator, this would be about half the breadth of the effective beam on the objective of this appurtenance. Thus $2 \times 0.0776 = 0.155$ cm., increased by the width of the refracting edge of the prism, is the width of the strip of white light which, after separation by the knife-edge of the prism, furnished the two component beams which potentially interfere on recombination. It is reasonable to suppose that the elements of these beams come from a common source and that the width in question is produced by the diffraction of the slit.

This datum is more appropriately reduced to the angle at the slit $\alpha$, within which lie the rays capable of interfering with each other after the interferometer cleavage. As the collimator used was $l = 22$ cm. from slit to lens,

$$\alpha = 2x \cos \theta / l = 0.155/22 = 0.0070$$

Hence the angular width of the wedge of white light, with its apex at the slit of the collimator and containing all the rays which can mutually interfere, is about 0.007 radian, or less than half a degree of arc. One would infer that a long ($l$) collimator (*i.e.*, one with weak objective) is advantageous, as the blade of parallel rays issuing is proportionally wide and the range of displace-

ment at $M$ or $N$ larger. Similarly, divergence subsequently imparted by dispersion (prism, grating), before the rays reach the mirrors, $M$, $N$, should have the same effect. The results obtained for dispersion bear this out, but not those for a long collimator. Moreover, the width of the slit, so long as the Fraunhofer lines do not vanish, is of no consequence. It thus seems tenable (to be carefully investigated below) that the positive effect of dispersion has a deeper significance, bearing directly on the structure of the interfering wave-trains—$i.e.$, the length of the coördinated, uniform wave-train is possibly greater as the dispersion to which the wave-train has been subjected is greater. Two parts of it will therefore fit over a correspondingly longer range of path-difference.

A number of other results point in the same direction. Thus, I may again point to the impossibility of obtaining fringes with homogeneous light and a wide slit, whereas two identical sodium lines ($D_1$ and $D'_1$), superposed, show the interferences strongly. The lines actually become helical in shape and much broader. The range of displacement of $N$ may be decreased from 0.25 cm. to 0.10 cm. by narrowing the beam emerging from the collimator with a slotted screen, while the fringes themselves are coarsened by this process. With the screen removed the fringes are not only sharper and finer, but apparently they may be seen to slowly move laterally across the fiducial sodium lines. This is in accord with the increased range of displacement of the mirror. The observation, however, is complicated by the fact that the sodium doublets are not quite in the same focal plane. The fringes must, in a reduced case, lie midway between them, in the line of symmetry of the spectra.

**13. Prismatic refraction.**—The method indicated in figure 12 ($P$, prism; $M$,$N$, mirrors; $G$, grating; $T$, telescope) was next tested for small distances and the experiments begun in the third order of spectra of the grating $G$. The prism was a small right-angled sample, with faces only about 1 cm. square; but it sufficed very well. Its distance from the grating being about 13 cm. and the illuminated spots on the mirrors 18.8 cm. apart, the mirrors were nearly normal to each other. In fact, as $\theta$ in the third order is about 62° and $i'$ about 28°, $\delta = 34°$ and $\sigma = 90°$. Hence, on displacing the micrometer mirrors $M$ or $N$, the illuminated strips move relatively rapidly across the face of the grating. Nevertheless, the fringes are easily found and controlled. Their range of visibility is larger than in the cases of the preceding paragraph. They remain in view for normal displacement of $M$ of 3 to 4 mm., passing from hair-like striations, through sharp arrows, back to the hair-like forms. The range has thus been increased by the dispersion. The arrows are of the type shown in figure 13, with reëntrant sides and part of the outline accentuated.

In the second order of spectra from $G$, the phenomena were much the same, but far more brilliant. The arrows were now evenly wedge-shaped and very slender. The fringes entered as nearly vertical hair-like striations, and, after

passing the optimum, vanished as inflated arrows. The range of visibility was, as before, about 3.5 mm., so that the change of order has not had any further marked effect, such as might be anticipated. As in the preceding paragraph, if the impinging collimated beam is narrowed, the range of visibility decreases; in fact, the arrows themselves are reduced to slightly oblique lines. Within the limits given the fringes are well adapted for interferometry.

First-order spectra are not available because of the large value of $i'$ in the case of the right-angled prism.

Taking the results of the last two paragraphs together, the increase of the range of displacement is due to the dispersion of the prism. The breadth of the pencil, diffracted at the slit, after leaving the collimator and prism,
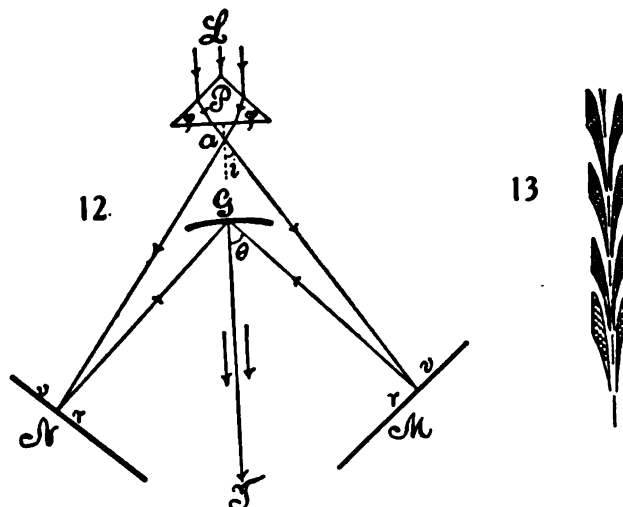


increases. It was shown in the earlier report that inversion of spectra on a longitudinal axis does not preclude the possibility of interference. Taken as a whole, therefore, the present results have a direct bearing on Huyghens's principle.

**14. Prism methods without grating.**—A more interesting method, in some respects, in which the grating is entirely dispensed with, is shown in figure 14. $L$ is the beam of white light from a collimator, $P$ a refracting prism (here with a 60° prism angle), $M$ and $N$ the opaque mirrors, with either or both on a micrometer, $P'$ a silvered reflecting prism (here right-angled). The telescope is at $T$ and should have high magnification. The rays $L$ are refracted into $a\,b\,c$ and $a'\,b'\,c'$ and the two spectra observed by the telescope at $T$. Each of the prisms should be on 3 adjustment screws, as well as the mirrors. $P$ must be revolvable slightly around a vertical axis and capable of fore-and-aft motion. $P'$ is preferably a large prism placed on a tablet. The rays $b$ and $b'$ are made collinear before $P'$ is inserted, and both the rays $c$ and $c'$ must come from near its edge.

The fringes are strong and large and lie within a remarkably wide transverse strip. This may be 10 or 20 times as wide as the $D_1 D_2$ doublets, which, in view of the small dispersion, are hardly separated. For the same reason, moreover, the range of displacement of $M$ within which fringes are visible rarely reaches 0.5 mm. Within this the fringes grow from the fine hair-lines, usually oblique, to their maximum coarseness. Apart from the small range of displacement, these fringes are available for measurement. If both mirrors $M$ and $N$ are on micrometers, they may be brought forward or the reverse, alternately, and the range increased 5 or 10 times.

To change the form of the fringes, the first prism, $P$, may be tilted slightly on an axis parallel to $LT$, figure 14. The fringes then pass through a maximum in the vertical direction (linear phenomenon). Fore-and-aft motion of $P$ rotates the fringes, partially, toward the horizontal; but, as a rule, the com-





ponent beams $b$ and $b'$ pass beyond the edge of $P'$ and the fringes vanish. Just before this (the spectra separating), the strip within which the fringes lie widens enormously. In other words, the breadth of the phenomenon depends on diffraction, not on dispersion, so that even though the prism $P$ scarcely separates the $V$ lines, the striated strip has about the same width as when it is produced by highly resolving gratings.
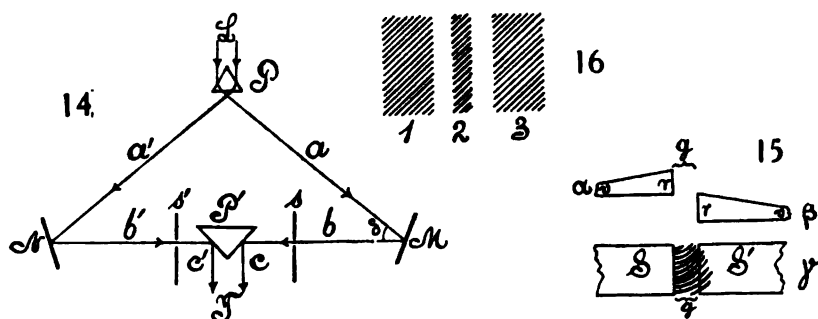
It is preferable to use sunlight directly (without a long-focus condensing lens), as there is a superabundance of light. The best results are attained with a large collimator. A spectacle lens with a focal distance of 1 meter is excellent. The range of displacement of $M$ is not increased, but the spectra and fringes become very sharp. If, with the large collimator, the spectra are just separated in the field of the telescope, by fore-and-aft motion of $P$, a magnificent display appears, resembling a thick, twisted golden cord. With further separation confocal elliptic fringes often cross the gap, as in figure 15. Here $\alpha$ and $\beta$ are graphs suggesting the wave-lengths of the two spectra, $g$ being the gap or deficient overlapping. The appearance in the telescope is shown at $\gamma$, $S$ and $S'$ being the spectra. When the fringes are erect, huge vertical furrows may lie in the gap. When the gap is closed, the linear phenomenon reappears. These enlarged fringes vanish, however, within 0.25 mm. of displacement at $M$. On the other hand, when the spectra are made

to overlap considerably (by fore-and-aft motion of $P$) the fringes become fine and vertical and the parallel blades of light, which interfere at the focus of the telescope, are 0.5 to 1 cm. apart at the objective.

In further experiments, screens $s$, $s'$ (fig. 14) were placed in the paths of the pencils $b\ b'$, so that they were compelled to pass through vertical slits 0.5 mm. wide in the screens. In this way the interfering rays were identified. The first vertical hair-line fringes came from rays about 5 mm. behind the edge of the prism $P'$. Hence the pencils were here about 1.2 cm. apart when they entered the telescope. The largest and last of the fringes came from close to the edge of $P'$. The experiment was varied as follows: Supposing both screens $s$ and $s'$ placed as far to the rear as the visibility of fringes permits; let the former, $s$, be slowly pushed forward. The fringes then contract from the very broad set, figure 16, case 1, to the strong and narrow set 2 (which is a mere line for a full wave-front), and then expand again to case 3. If, now, $s$ is left in place and $s'$ moved forward slowly in the same way, the identical contraction and expansion, cases 1, 2, 3, are reproduced. The screen $s'$ may then be left in place and $s$ in turn slowly moved forward with the same results, etc. (there may be 6 alternations), until finally the effective parts of the pencils $b$ and $b'$ are beyond the edge of the prism $P'$. In case 2 the two slits $s$ and $s'$ are obviously symmetrical to the interfering rays, whereas in cases 1 and 3 the diagonally opposite edges of the slits $s$ and $s'$ limit the efficient pencils to a sheet. If the edge of the prism were truly a knife-edge, the last fringes would be very large, since the distance $cc'$, figure 14, would vanish. If the fringes are vertical (obtained by tilting $P$ around an axis parallel to $LT$), the case 2 is given by 2 or 3 strong vertical lines, whereas 1 and 3 consist of 10 or 20 lines, all of about the same width and distance apart. If the slits $s$, $s'$ are finer (1 mm.), the fringes are throughout sharper. A single displacement, 1, 2, 3, corresponds to about 2 mm. When the edge of $P'$ is approached the case 2 often shows vertical strands of fringes, a strong central strand, and two or three fainter ones either side of it. The cases 1 and 3 are not stranded.

A similar result (passage of case 2 into 3, fig. 16) may be produced by moving $P$ forward, the case 3 appearing just before the pencils $b\ b'$ leave the edge of $P'$. Again, when $M$ is moved rearward, when both $b$ and $b'$ are near the edge of $P'$, the cases 2 and 3 are obtained. In general, the width of the diffraction pattern increases without changing the size of fringes, as the width of the available wave-front decreases. A similar result will be described in connection with figure 48, Chapter II. Naturally, if the displacement is considerable, it is accompanied by some rotation of fringes.

**15. Displacement parallel to rays.**—It now becomes of importance to test the range of displacement as modified by the angle of reflection, increasing from $\delta = 0$. It is therefore desirable to make a few direct measurements. The angle $\theta$ at $P$, figure 14, was found to be about $49° 45'$, so that the total angle at $M$ is $\delta = 40° 15'$. $M$ and $N$ are both on micrometers, with the screws normal

to their faces. $P'$ is on a micrometer with its screw parallel to $bb'$, so that this prism is shifted right and left. The range of displacement was found at

$M$, about 0.04 cm.; $x = 2 \times 0.04 \times 0.939 = 0.076$ cm.

$P'$, about $y = 0.07$ cm.; $2y = 0.140$ cm.

where $x = 2e \cos (90-\theta)/2$ and $2y$ are the corresponding path-differences between the inception and evanescence of fringes. With a very fine slit, $2y$ was possibly smaller (see fig. 17).

The question at issue is thus, in the first place, how the value of $2y$ compares with $x$; for in the former case the angle $\delta$ is effectively zero. In other words, when $M$ is displaced from $M$ to $M'$, over a distance $e$, the pencil $b$, figure 17, changes to $b_1$, and is soon lost at the edge of $P'$, whereas, when $P$ is displaced in the direction $bb'$, over a distance $y$, the rays $b$ and $b'$ do not change their point of impact at the prismatic mirror $P'$. If $PP$ represents the principal plane of the objective of the telescope and $F$ its principal focus, there should be no accessory effect for the case $y$ as compared with the case $x$.

Results bearing on this subject are given in table 9, in which the displacement $e$, observed at $M$ and at $N$, as well as the displacement $y$ at $P'$, are recorded when a plate of glass of thickness $E$ is inserted normally to the rays $b$, $b'$. The corresponding air-path difference computed from $E$, $\mu$, $B$, and $\lambda$ should be $s$, nearly. This is about the value $(2y)$ observed, remembering that to set the micrometer, fringes of a particular pattern must be selected. The rotation of fringes being but 90° or less, there are no fiducial horizontal lines.

TABLE 9.—Reversed spectra. Refracting prism. $\theta = 49° 45$. $B = 4.6 \times 10^{-11}$ (assumed). $x = 2e \cos (90° - \theta)/2$; $s = E (\mu - 1 + 2B/\lambda^2)$.

| Detail. | E | μ | s | e | x | 2y |
|---|---|---|---|---|---|---|
| | cm. | cm. | cm. | cm. | cm. | cm. |
| Mirror right, plate right... | 0.736 | 1.526 | { 0.3901<br>{ +.0195 | 0.204<br>{ .199<br>{ .206 | 0.381<br>.....<br>..... | 0.400<br>.410 |
| Mirror left, plate left...... | .736 | 1.526 | = .4096 | .208 | .391 | { .410<br>{ .406 |
| Mirror right, plate right... | .736 | 1.526 | = .4096 | { .201<br>{ .205<br>{ .202 | } .381 | { .406<br>{ .402 |
| Mirror left, plate left...... | .736 | 1.526 | = .4096 | .207<br>{ .207<br>{ .208 | .389<br>} ..... | .402<br>.400 |
| Mirror right, plate right... | .736 | 1.526 | = .4096 | { .205<br>{ .207 | } .387 | .406 |
| Mirror left, plate left...... | .736 | 1.526 | = .4096 | { .206<br>{ .208 | } .389 | .406 |
| Mirror right, plate right... | .434 | 1.533 | { .2313<br>{ +.0115 | { .125<br>{ .124<br>..... | } .234<br>..... | { .248<br>{ .250<br>.248 |
| Mirror left, plate left...... | .434 | 1.533 | =.2428 | { .126<br>{ .125 | } .236 | { .255<br>{ .248<br>{ .246 |
| Mirror left, plate right.... | .434 | 1.533 | =.2428 | { .127<br>{ .126 | } .237 | ..... |

Furthermore, though $\mu$ was determined by the total reflectometer for each of the two plates used, $B$, the Cauchy dispersion coefficient, had to be assumed from similar results in my earlier work. Finally, the first plate ($E=0.736$ cm.) was slightly wedge-shaped and some adjustment for coincidence of spectra was needed. The second plate ($E=0.434$ cm.) was optically nearly plane parallel. One may therefore conclude from these details that $2y=s$ as nearly as could be expected.

The values of $x$, computed from $\theta$ and $\epsilon$, however, certainly fall below $s$, being about 6 per cent and 3 per cent short of it in the two cases, respectively; or, again, $x$ is 0.019 cm. and 0.014 (about 5 per cent) smaller than the mean values observed for $2y$. This extra 5 per cent of path-difference can not be an error of observation or of adjustment, but must be interpreted as the path-difference added when the pencil shifts towards the edge of the prism ($x$) instead of being stationary as in $y$. In case of inverted spectra, moreover (next chapter), $x$ is usually in excess of $s$, and the shift is the other way. The deficiency in $x$, though not equally marked, is present in observations both on the right and left sides of the prism $P'$.

**16. Breadth of efficient wave-fronts. Apparent uniformity of wave-trains. Rotation of fringes.**—It follows from figure 17 that if $M$ is displaced to $M'$, over a distance $\epsilon$, the pencil $b$ is displaced parallel to itself over

$$s = 2\epsilon \sin \delta/2$$

where $\delta = 90° - \theta$. The pencil $c$ is then displaced parallel to itself over a distance

$$t = s \tan \varphi'/2 = s$$

since $\theta = 49° \ 45'$, $\delta/2 = 20° \ 7'$, and therefore $s = 2\epsilon \times 0.344 = 0.7\epsilon$, nearly. If the rotation of fringes is but 90°, either $s$ (or $s/2$) is also the breadth of the strips, or patches of like origin, which, when sliding over each other more
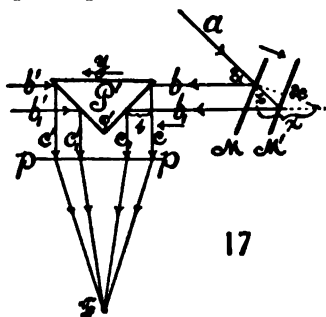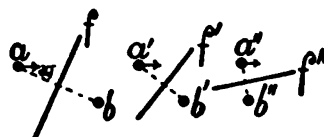


17                                        18

or less, produce the fringes. This may be treated from a graphic point of view as follows, a theory not being aimed at:

In figure 18, let $a$ and $b$ be two patches of light of like color and origin at the objective $pp$, figure 17, producing interferences at the focus $F$. Hence the fringes will be arranged in the direction $f$, figure 18, at right angles to the

line joining $a$ and $b$. Since $a$ and $b$ here correspond to $c$ and $c'$ in figure 17, let $a$ be continually displaced to the right, as indicated by the arrows, figure 18. In proportion as the positions $ab$, $a'b'$, $a''b''$, are taken, the fringes must pass by rotation from $f$, into $f'$, into $f''$, etc.—*i.e.*, over about 90°. In the present experiment, $c$, figure 17, can never pass across $c'$, for they are essentially separated by the edge of the right-angled prism $P'$. Hence the rotation can not exceed 90°, for the vertical through $a$ can not cross the vertical through $b$. This is not the case when a grating replaces $P'$, as in figure 12; nor is it the case when, as in Chapter II, inverted spectra are treated, and the patches $a$ and $b$ slide *along* the edge of the prism. In such cases figure 18 may be continued symmetrically toward the right (mirror images), and the limit of rotation is therefore 180°. All these suggestions are borne out by experiment.

Moreover, if the first prism $P$, figure 14, is tilted slightly on an axis parallel to $LT$, $a$ (fig. 18) will be lowered and $b$ raised. If $a$ and $b$ are on the same level, the fringes are always vertical and pass through a *vertical* maximum, when $ab$ is a minimum. On the other hand, if $a$ and $b$ are not in the same level, as in the figure, fore-and-aft motion brings the rays $c$ and $c'$ (fig. 17) to or from the edge of the prism $P'$. Hence the case $ab$ passes into $a''b''$, or the reverse; in other words, the fringes pass through a *horizontal* maximum when $ab$ is a minimum, etc. This is also shown by experiment.

Moreover, if $\alpha$, figure 18, is the angle (in the observer's vertical plane) of $ab$ to the horizontal, the horizontal distance between $c$ and $c'$ will be $ab \cos \alpha$, which is zero when $\alpha = 90°$, and both $c$ and $c'$ are at the edge. Suppose the full breadth of the strips are at the edge, so that the fringes present the strongest, coarsest, but narrowest field of case 2, figure 16. Then if either $c$ or $c'$ retreats until the fringes vanish, the width of the appreciably efficient strip $cc'$ will be $ab \cos \alpha = t = s = 0.7e$, nearly. This is probably the best method of estimating the width in question. Usually, however, away from the edge, the succession 1, 2, 3, figure 16, is obtained. In such a case the breadth of efficient strip is $t/2 = 0.35e$.

The experiment made by moving screens with slits, forward or rearward, successively, by which the appearance and evanescence of fringes may be repeated through several cycles, is next to be explained. Here it is merely necessary to remember that the spectra $c$ and $c'$ are reversed, or that the colors of like origin and wave-length are successively farther apart. When the screens are alternately moved, therefore, the same phenomenon is in turn produced in slightly different colors. But as $ab$ continually increases, whereas the efficient breadth of the strips does not, the fringes soon pass beyond appreciable smallness.

When, as in the earlier methods, but a single grating is used with two successive diffractions through it, the patches $a$ and $b$ are obviously in the same level when the longitudinal axes of spectra coincide. Hence the fringes are essentially vertical.

In the experiment with screens, $s$, $s'$, figure 14, it is obvious that path-difference remains constant. The distance from the same wave-front in the

pencils $b$ and $b'$, figure 17, to the principal plane $pp$, is always the same; but pencils different in lateral position are successively selected. On the other hand, when the prism $P'$ is moved in the direction $y$, parallel to $bb'$, path-difference only is introduced, while the pencils selected remain the same. Supposing the ordinary conditions of visibility (magnification, etc.) to remain unaltered throughout, the wave-fronts are, as it were, explored in depth as to their uniformity—*i.e.*, the distance is apparently recorded throughout which a wave-train consists of identical wave-elements. Effectively, however, the rapidity with which fringes decrease in size beyond visibility is directly in question. Finally, when the opaque mirror $M$ (or $N$) is moved from $M$ to $M'$, both effects occur together. Path-difference $x = 2e \cos \delta/2$ is introduced and the pencil is displaced from $b$ to $b'$.

The $x$-effect is thus probably the same as if $P'$ were displaced to the left and $s$ were brought forward. Hence it is of great interest to determine the extent in which the values of $y$ and $x$ are different. It appears as if the distance within which the wave-trains are uniform is definitely limited and that it increases with the breadth of effective wave-front just instanced, while both increase with the amount of dispersion to which the incident white pencil has been subjected. Diffraction at the slit of the collimator may be regarded as the first dispersion. This seems to me to be a very important observation, and a systematic investigation of the lengths of uniform wave-trains, so understood, in their dependence on dispersion, is desirable, even if the geometry of the system should prove to be adequate to explain the phenomena.

**17. Film grating.**—The method of two gratings was now again resorted to, except that the first at $G$, figure 3, was a film grating. This attempt failed in my earlier work, when but a single film grating was used for the two diffractions, because of insufficient light.* In the present case, where two gratings ($G'$ being reflecting) are employed, the method succeeded at once. The first grating constant was $D = 10^{-6} \times 167$ cm.; observations were therefore necessarily made in the second order of $G'$, so that the spectra are not as intense as with prisms. But the fringes are perfect and may be made as large as desirable—with but two in the breadth of the spectrum, for instance. They come in and go out of range with inflation of form, and they are free from the awns seen in the preceding paragraph (with prism), probably because the light is less intense.

The phenomena in general are the same in character; but the range of displacement of either mirror is enhanced, conformably with the increased dispersion at $G$. This range was found to be about 6 mm. under the best conditions (arrows). If both $M$ and $N$ are successively displaced in the same direction, the total displacement available between the hair-like fringes at the extremes is about 1.5 cm. for each mirror.

---

* I have since obtained the fringes with a single film grating.

At these extremes the two patches of light on the grating $G'$ may have been separated by several millimeters. The nature of the transformation from arrows to the oblique striations would be well reproduced if equidistant vertical wedges were moved from right to left, or the reverse, behind a vertical slit.

The distance between $G$ and $G'$ was about 10.2 cm., and between the spots of light on mirror $M$ and gratings $G$ and $G'$, respectively, 22.2 and 12.6 cm. This corresponds to $\theta_1 = 20.5°$ and $\theta_2 = 36.2°$, so that $\delta = 15.7°$ and $\sigma = 56.7°$.

It is obvious that if the slit of the collimator is displaced right or left, the range of displacement, within which the interferences lie, will have different positions on the micrometer, because the path-differences are changed. A flickering arc may also introduce annoyances.

The present method has an advantage for ordinary practical purposes, as it does not require a ruled-glass grating at $G$.
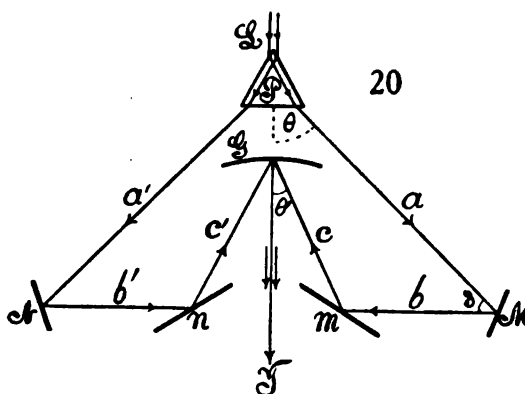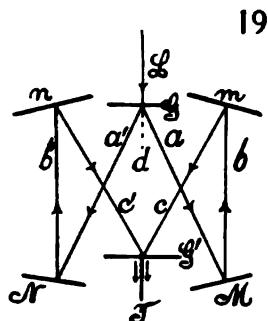


The surprising success obtained with the film grating at short distances induced me to test similar methods at long distances. Figure 19 is an apparatus of this kind, in which $L$ is the white beam incident from a collimator, $G$ and $G'$ are the transmitting gratings, $M$, $N$, $m$, $n$, pairs of opaque mirrors, $T$ the telescope. The undeviated ray, $d$, is screened off. The component paths $a+b+c$, $a'+b'+c'$ were each about 4 meters long. The method of adjustment again consisted in bringing the shadow of the thin wire across the slit into the same position of the spectra seen in the telescope when the spectra coincide. For this purpose the adjustment screws for horizontal and vertical axes on $M$, $N$, $m$, $n$ must be actuated together. To facilitate this tiresome work, with the observer at $T$, long levers brought from $m$ and $n$, with their ends near his hands, as well as a lever from $G'$ (fore-and-aft motion), were very useful. Since the adjustment screws at $M$ and $N$ are already within reach, it is thus easy to bring any Fraunhofer line to the middle of the field and to make these fields overlap, with the guide-wire central in both.

The attempt made with sunlight, to find the fringes when both $G$ and $G'$ are film gratings ($D = 167 \times 10^{-6}$ cm.), did not succeed. The light, moreover,

is not as bright as desirable, owing to the strong dispersion. When the grating $G'$ was replaced by a ruled-glass grating ($D = 352 \times 10^{-6}$ cm.), the dispersion was not much reduced, but the light was better. The fringes were now found after some searching and seemed to be of $D_1D_2$ breadth, a strip of oblique lines of the usual character. But they were not brilliant and were hard to recover when lost. The Fraunhofer lines were still disagreeably blurred.

On exchanging the gratings (ruled-glass grating at $G$ and film at $G'$), though the dispersion was smaller, the brilliancy of spectra was greatly improved. The fringes came out fairly sharp. However, on cutting down the incident beam at the collimator and near $G$ to a breadth of not more than 0.5 cm., the fringes were acceptable and capable of high magnification. They remained visible for a displacement of 5 mm. at the micrometer at $M$. With fore-and-aft motion of $G'$, the fringes rotated as usual from fine vertical hair-lines, through the horizontal (probably arrow-shaped forms of maximum size), back again to hair-lines. Here the excursion of $G'$ was about 1.5 cm. On tilting the grating $G'$ in its own plane and readjusting $M$, the rotation is through the vertical maximum (the linear phenomenon). With a slotted screen (0.5 cm.) at the collimator, the slit may be widened until the Fraunhofer lines just vanish. If the slit is but 0.2 cm., the fringes become bulky and the play at $M$ is but 2 mm.

The film grating may be used by reflection, on adapting the apparatus in figure 12 for this purpose, by supplying a ruled grating or prism at $P$ and the film grating (with its ruled side toward $P$) at $G$. If a ruled grating is put at $P$, the spectra and fringes are good; but naturally there is deficient illumination. Nevertheless a strong telescope may be used and a range of displacement of 4 mm. at $M$ is available. This may be increased indefinitely by using a micrometer at $M$ and $N$ alternately. The chief difficulty was the (incidentally) unequal brightness of spectra.

Again, the method of figure 14, apart from the drawbacks to which that method is incident, succeeds almost perfectly, both in the first- and second-order spectra. The fringes are strong and clear. An Ives grating of high dispersion ($D = 167 \times 10^{-6}$ cm.) was tested.

The method of figure 20, with auxiliary mirrors $m$ and $n$ to accommodate the dispersion of $G$, was also successfully tried. Here $G$ was originally a concave *reflecting* grating. It was replaced by a film grating used as a reflecting grating, with entire success. The ruled side of the film should be free (without cover-glass), but the reversed side cemented on plate-glass as usual and the latter placed towards the telescope at $T$. The prism $P$, in other words, admits an abundance of light, so that even the loss in reflection from the film is not serious. Sunlight should be used without a condensing lens; or, if the latter is added, the light leaving the telescope is to be narrowed laterally.

**18. Non-reversed spectra.**—The prismatic method of cleaving the incident beam of white light is available for the superposition of non-reversed spectra,

under conditions where the paths of the component rays may have any length whatever. It is thus an essential extension to the method (fig. 21) given in the preceding report ($PP'$, prisms; $M$, $N$, mirrors; $Gp$, Ives prism grating; $T$, telescope), where the path-differences were essentially small and the spectra reversed.

In figure 22, $P$ is the first prism cleaving the white beam $L$, diffracted by the slit of the collimator. $M$ and $N$ are the opaque mirrors, the former on a micrometer. For greater ease in adjustment, the second prism $P'$ is here right-angled, though this is otherwise inconvenient, since the angle $\delta = 90° - \varphi$ is too large. The rays reflected from $P'$ impinge normally on the reflecting grating $G$ ($D = 200 \times 10^{-6}$) and are observed by a telescope at $T$. $P$, $P'$, $M$, and $N$ are all provided with the usual three adjustment screws. $P'$ must be capable of being raised and lowered and moved fore and aft. The field is
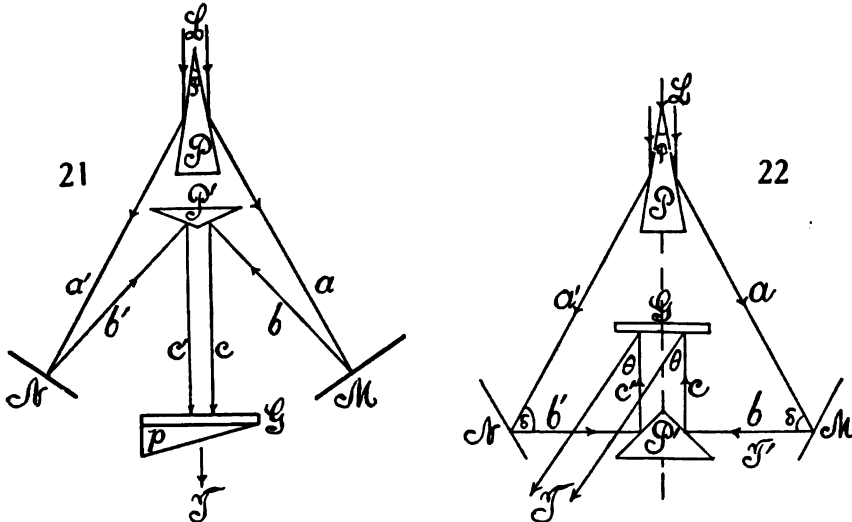


brilliantly illuminated. When the path-difference is sufficiently small, the fringes appear and cover the whole length of superposed spectra strongly. They are displaced with rotation if $M$ is moved normally to itself.

As first obtained, the fringes were too closely packed for accurate measurement. But the following example of the displacement $e$ of the mirror $M$, for successions of 40 fringes replacing each other at the sodium lines, shows the order of value of results: $10^3 e = 1.55$, $1.40$, $1.60$, $1.55$ cm., so that per fringe

$$\delta e = 39 \times 10^{-6} \text{ cm.}$$

The computed value would be ($\varphi$, the prism angle)

$$\delta e = \frac{\lambda}{2 \cos \delta/2} = \frac{58.93}{2 \times .81} 10^{-6} = 36.4 \times 10^{-6} \text{ cm.}$$

assuming $\delta = 90° - \varphi$. The difference is due both to the small fringes, which are difficult to count, and to the rough value of $\delta$. The range of measurement is small (if $M$ only moves), not exceeding 1.6 mm. for a moderately strong

telescope. But one-half of this displacement is available, as the fringes increase in size (usually with rotation) from fine vertical hair-lines to a nearly horizontal maximum, and then abruptly vanish. This is one-half of the complete cycle.

If we regard the component beams, $a\,b\,c$ and $a'b'c'$, as being of the width of the pencil diffracted by the slit of the collimator, it is clear that the maximum size of fringes will occur when $c$ and $c'$ are as near together as possible; furthermore, that as $M$ moves toward $P'$, $c$ continually approaches $c'$, until $b$ drops off (as it were) from the right-angled edge of the prism $P'$. To get the best conditions—*i.e.*, the largest fringes—$c$ must therefore also be moved up to the edge of $P$ and very sharp-angled prisms be used at both $P$ and $P'$. The largest fringes (lines about 10 times the $D_1D_2$ distance) obtained with the right-angled prism were often not very strong, though otherwise satisfactory. Much of the light of both spectra does not therefore interfere, being different in origin.

Results very similar to the present were described long ago* and found with two identical half-gratings, coplanar and parallel as to rulings, etc., when one grating was displaced normally to its plane relative to the other. The edges of the two gratings must be close together, but even then the fringes remain small and the available paths also. Strong, large fringes, but with small paths, were obtained by the later method† of two identical transmitting gratings, superposed.

If the prism $P'$ is right-angled (a special case of fig. 21), it may be rotated as in figure 23, so that the rays $c$ and $c'$ pass off towards the observer. They are then regarded through a prism-grating $G$ and a telescope at $T$. This method admits of much easier adjustment. With the component beams $a\,b$, $a'b'$, coplanar, horizontal, and of about equal length in the absence of the prism $P'$, the latter is now inserted with its edge vertical (rotation) and the white slit images in $T$ (without $G$) superposed, horizontally and vertically. $G$ is then added and the micrometer at $M$ or $N$ manipulated till the fringes appear. As above, they are largest when $c$ and $c'$ are as nearly as possible coincident and vanish as horizontal fringes at the maximum; for the effective parts of $c$ and $c'$ are component halves of the same diffracted beam from the slit. It is interesting to observe, seeing that interference also occurs when one of the superposed spectra is inverted on a line parallel to its length, that such diffraction is demonstrable in case of homogeneous light, even when a slit is absent. Both beams must be nearly at the edge of $P'$ in order that strong, large fringes may be seen.

The case of figure 22 was subsequently again tried on the large interferometer, the distance $P$ to $M-N$ being about 2 meters. $G$, in these experiments, was a concave grating and $T$ a strong lens near the principal focus of $G$. The adjustment for long distances is not easy. The equilateral triangle of rays, $a$, $a'$, $b'$, $b$, should be first carefully leveled, the edges of $P$ and $P'$ being on

---

* Phil. Mag., XXII, pp. 118–129, 1911; Carnegie Inst. Wash. Pub. 149, chap. VI.
† Physical Review, VII, p. 587, 1916; Science, XLII, p. 841, 1915.

the median line. With $G$ placed at the proper distance, the two spectra seen at $T$ will usually be quite distinct in the field. They should show the shadow of the black line across the slit, at the same level in the spectra. The longitudinal axis of the spectra may then be made collinear by slightly tilting the edge of $P'$ to the vertical, on a horizontal axis, with the adjusting screws. $M$ and $N$ are then rotated on a vertical axis till the $D$ lines coincide. Small changes may be completed at $M$ and $N$. The fringes when found are usually strong, but very fine, less than the $D_1D_2$ distance in width. I have been able to increase them to a width of $2D_1D_2$, but they are then faint. The two illuminated strips on the grating may even be an inch apart, but the fringes are as usual large when this distance is the smallest attainable (virtual
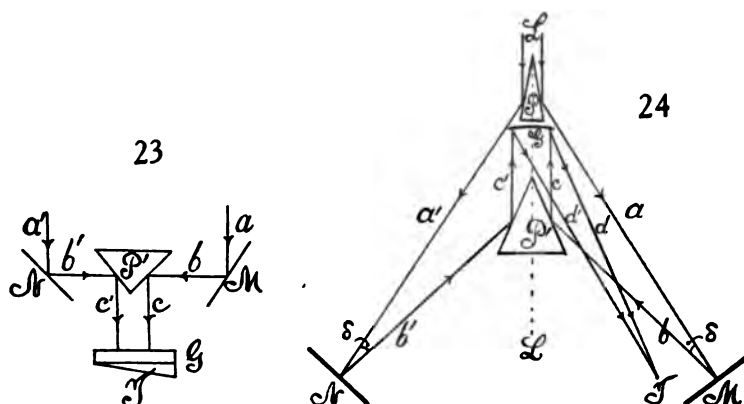


coincidence). The grating may be moved fore and aft without effect. As $N$ is moved on its micrometer, the interferences are first seen as vertical hair-like striations, which gradually enlarge, rotate, and vanish just before reaching the horizontal and at maximum size. The range of displacement did not exceed 0.15 cm. for this rotation of 90°, so that the total displacement for 180° of rotation would be about 3 mm. Since $N$ and $T$ are close together, the manipulation is convenient here, but with another lens at $T'$ the phenomenon could be traced further on the $M$ side.

To secure a smaller angle of incidence and reflection, $\delta/2$, at $M$, figure 24, the combination of a silvered 20° prism $P$ and a 30° prism $P'$ was tested. $M$ and $N$ are the opaque mirrors, $G$ the concave grating with its focus at $T$ for inspection by a strong lens. $L$ is the incident beam of white sunlight from the collimator, which is split into the component pencils $abcd$ and $a'b'c'd'$ and interfere at $T$. The results, however, were about the same as above, the range of displacement at $M$ for 90° of rotation of fringes being about 0.15 cm. As $a$ and $b$ make angles $\varphi$ and $\varphi'$ with the line of symmetry $LL'$,

$$\delta = \varphi' - \varphi$$

was about 10°.

At a subsequent opportunity I made further trials with the paired prisms of 20° and 30°, but failed to increase the fringes above about $D_1D_2/2$ width.

Two micrometers, one at $M$ and the other at $N$, were installed, and moved forward in alternate steps, within a range of over 2 cm., naturally without modifying the fringes. These are now observed on both sides ($N$ and $M$), each with the micrometer which is manipulated. One may note in passing that the two screws are being incidentally compared. To set the 30° prism properly it would have to be provided with a fine fore-and-aft, right-and-left slide adjustment, in order that its edge may be set sharply in the line where the two component rays intersect. An attempt was made to increase the dispersion by allowing a spectrum to fall on the first prism (20°), but without success.

It is noteworthy that the 30° prism at $P'$ is no marked improvement as to range of displacement over the 90° prism at $P'$, previously used. In other words, the effect of decreasing the angle of reflection $\delta$ at $M$ is, unexpectedly, of small importance, in relation to the range of displacement at $M$. This result already treated in §16 will be accentuated in other ways below (Chapter II).

**19. Non-reversed spectra. Restricted coincidence.**—In figure 25, the white ray $L$ from the collimator is diffracted by the grating $G$ and the two spectra $a$ and $a'$, thereafter reflected by the parallel opaque mirrors $M$ and $N$, to be again diffracted by the grating $G'$. The rays are observed by a telescope at $T$. If the gratings $G$, $G'$ have the same constant, it is obvious that the field of the telescope will show a sharp white image of the slit, for each mirror. If $M N G G'$ are adjusted for symmetry by aid of the adjustment screws on each and the rulings are parallel, the two white slit images will coincide horizontally and vertically. If now a direct-vision spectroscopic prism or a direct-vision prism-grating $G''$ is placed in front of the telescope, the superposed white slit images will be drawn out into overlapping non-reversed spectra, which will usually show a broad strip of interference fringes.

In my first experiments, $G$ and $G'$ were film gratings of high dispersion ($D = 167 \times 10^{-6}$). The field was therefore too dark and the fringes were obtained with difficulty because of the cumulative distortion of images from the gratings. When found, the fringes were very fine parallel lines, filling an irregular strip in the orange-yellow region, and it was already obvious that an enormous play of the micrometer-screw at $M$ would be permissible.

A number of film gratings were now tested and the best samples selected ($D = 175 \times 10^{-6}$), although the dispersion was still too large and the $D$ lines not clear. To secure more light, a beam of sunlight 15 cm. in diameter was condensed to a focus on the slit by a large lens of about 2 meters in focal distance. The illumination was now adequate and the fringes were found at once, as they should be; for they are always present, though not in the same colored region. These fringes, found with more accurate adjustment, were also larger than before.

Figure 25 shows, if $ab$, $a'b'$ and $cd$, $c'd'$ are pairs of corresponding rays of the same order but different wave-lengths, $\lambda$ and $\lambda'$ respectively; that for the given position of $G$ and $G'$ only the rays $a$ $a'$ issue coincidently at $T$. The rays $cd$, $c'd'$ issue at $e_1$, $e'_1$, and, though brought to the identical focus

by the telescope, the distance $e_1e'_1$ may be too large to admit of appreciable interference. Hence the colored strip within which interferences occur will comprise those wave-lengths which lie very near $\lambda$, whereas the colors lying near $\lambda'$, etc., will be free from interference.

If, however, the mirror $M$ is displaced parallel to itself to $M'$ by the microm-eter-screw, the rays $c''d''$ and $c'd'$ will now coincide at $e'_1$, whereas the rays from $ab$ and $a'b'$ will no longer issue coincidently and may not interfere. Thus the interferences are transferred as a group from rays lying near $\lambda$ to rays lying near $\lambda'$. It is obvious, therefore, that with the displacement of $M$ the strip carrying interferences will shift through the spectrum and that an enormous play of the micrometer-slide at $M$ will be available without the loss
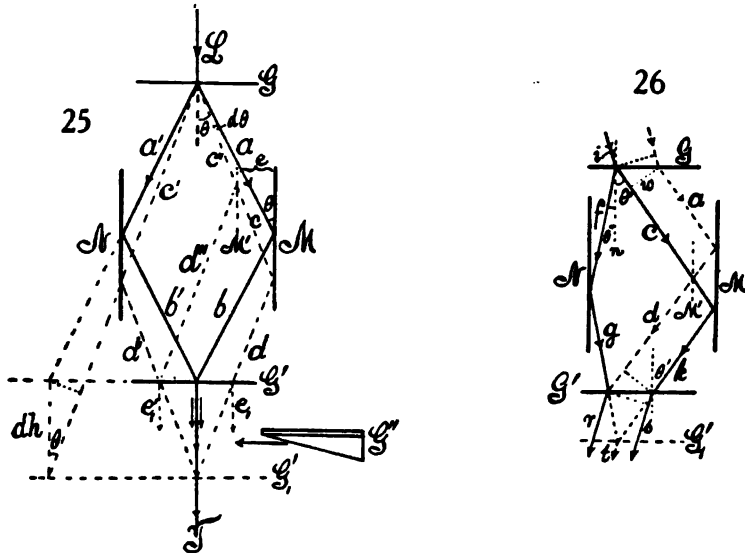


of interferences. In fact, a displacement $e$ of over 3 cm. of $M$ normal to itself produced no appreciable change in the size or form of fringes, but they passed from the green region into the red. In consequence of the film gratings used, the strip in question was naturally sinuous and somewhat irregular, but the fringes themselves in the clear parts were straight, parallel, strong lines. They did not thin out to hair-lines at their ends, nor show curvature, as one would be inclined to anticipate. On the contrary, they terminated rather abruptly at the edges of a strip occupying about one-fourth of the visible length of the spectrum.

It follows, therefore, from figure 25, that the displacement of $M$ does not change path-length or path-difference, for the rays are inclosed between parallel planes, as it were. Since the double angle of reflection is $\delta = 180° - 2\theta$, where $\theta$ is the angle of diffraction of $G$ and $G'$, the displacements of $M$ over a normal distance $e$ will shorten the path of $M$ in accordance with the equation

(1) $$n\lambda = 2e \cos \delta/2 = 2e \sin \theta$$

where $n$ is the number of fringes passing at wave-length $\lambda$. This equation is not obvious, since for constant $\lambda$, the distance between $G$ and $G'$, measured along a given ray (prolonged) for any position of $M$ or $N$, is also constant. The equation may be corroborated by drawing the diffracted wave-front, which cuts off a length $2e \sin \theta$ from $d''$.

Since $\sin \theta = \lambda/D$ if $D$ is the grating space, the last equation becomes

$$n = 2e/D$$

or per fringe

$$\delta e = D/2$$

a remarkable result, showing that the displacement of the mirror $M$ per fringe is independent of wave-length and equal to half the grating space. An interferometer independent of $\lambda$ and available throughout relatively enormous ranges of displacement is thus at hand. It will presently appear that it is also independent of the angle of incidence at $G$.

In case of the given grating and sodium light, $\theta = 19° 37'$. Hence if $\delta e$ is the displacement per fringe,

$$e = \lambda/2 \sin \theta = 10^{-4} \times 88 \text{ cm.}$$

Actuating the micrometer at $M$ directly by hand (this to my surprise was quite possible without disturbing the fringes, except for the flexure of supports), the following rough data were successively obtained from displacements corresponding to 10 fringes:

$$10^6 \times \delta e = 65 \quad 95 \quad 90 \quad 80 \quad 60 \text{ cm.}$$

Without special precaution the fine fringes can not be counted closer than this, so that the data are corroborative.

If the incidence is at an angle $i$, as in figure 26, the rays entering at $G$ obviously leave at the same angle $i$ (symmetrically) at $G'$. In other words, rays enter and leave in pencils of parallel rays. The optic path of the component $N$ ray, $f+g$, is

$$h/\cos \theta''$$

where $h$ is the normal distance between $G$ and $G'$ and $\theta''$ the angle of diffraction on the left. Similarly the optic path of the $M'$ rays $c+d$ which meet $f+g$ in $r$ is

$$h/\cos \theta'$$

where $\theta'$ is the angle of diffraction on the right. If now $M'$ is displaced to $M$, $c+d$ is changed to $a+d$ of the same length; but if the wave-front $w$ is drawn, it appears that the optic path of the $M$ ray has been shortened to $2e \sin \theta'$, where $e$ is the normal displacement of $M'$ to $M$. Hence the path-difference is now

$$h/\cos \theta' - 2e \sin \theta' - h/\cos \theta'' = n\lambda$$

$n$ being the ordinal number of fringes of wave-length $\lambda$. Furthermore, since $h$, $i$, $\theta'$, and $\theta''$ do not change, the displacement per fringe is as above

$$\delta e = \lambda/2 \sin \theta'$$

For the angles in question the usual equations are given:

$$\sin \theta' - \sin i = \lambda/D \qquad \sin \theta'' + \sin i = \lambda/D$$

so that

$$\delta e = \lambda/2(\lambda/D + \sin i)$$

which is thus not quite independent of $\lambda$ unless $i$ is very small. It is obvious that the optic paths of $a+d$ and $c+k$ are identical. Hence the path-differences of the rays $r$, $s$ are the same. If now the grating $G'$ is shifted to $G'_1$, over the distance $e'$, the same path-length is cut off from both $r$ and $s$, and hence the fringes do not move. The locus or strip of fringes, however, is displaced in wave-length, bodily, as shown in figure 25.

The equation in $n\lambda$, which may be written ($\delta$, a differential symbol)

$$n\lambda = h\delta(1/\cos \theta) - 2e \ (\lambda/D + \sin i)$$

suggests the phenomena to be expected both when $\lambda$ is constant and $i$ varies and when $i$ is constant and $\lambda$ varies. The former require a wide, the latter a narrow slit.

Some time after, with an improved micrometer, not directly manipulated by hand, I obtained the following data from a succession of 50 small fringes (arc lamp):

$$e \times 10^3 = \quad 3.7 \quad 3.9 \quad 4.0 \quad 4.1 \quad 4.2 \text{ cm}$$
$$\delta e \times 10^6 = 74 \quad 78 \quad 80 \quad 81 \quad 84 \text{ cm.}$$

Again, from successions of 30 large fringes:

$$e \times 10^{-3} = \quad 2.6 \quad 2.6 \quad 2.4 \text{ cm.}$$
$$\delta e \times 10^{-6} = 87 \quad 87 \quad 79 \text{ cm.}$$

All of these are below the value computed for sodium light, from imperfect adjustment. The march of values in the first series is probably incidental, for I was not able to eliminate the effects of flexure in my improvised apparatus. Again, the precise symmetry of the apparatus is not guaranteed.

Simple as the method appears in figure 25, it is in practice quite difficult to control. Fringes may be lost and thereafter hard to find again, and this in spite of the large range of displacement. The cause was eventually located in the circumstances under which the incident pencil $L$ strikes the grating $G$. If $L$ shifts to right or to left the symmetrical rhombus of figure 25 will be converted into a non-symmetric rectangle or into a figure as in figure 26. If $G$ and $G'$, $M$ and $N$ were rigorously parallel this should not produce any effect; but as they are not and as the surfaces are not optically flat (film gratings) the effect is very marked and probably of the same nature as a rotation of $G'$ on an axis normal to its face. It requires but slight displacement of $L$ to right or left to make fringes in the yellow change to hair-lines in the green or the red; or they may even be lost altogether. These fine fringes may sometimes be enlarged, at other times made smaller, by adding or thickening (rotation) the compensator. Naturally in all these cases the overlapping spectra are perfect. The only method of finding the fringes

after the parts are symmetrically placed relatively to the light is to move $L$ successively and gradually toward one side or the other and to test each case with compensators 1 to 2 mm. thick, placed in the $b$ or $b'$ pencils. It would be advisable to place the slit on a right-and-left micrometer. When found, however, the fringes, if reasonably treated, are very persistent, strong, and easily enlarged.

Finally, the fore-and-aft motion of $G'$ must produce a bodily shift of fringes, while the strip as a whole is displaced in mean wave-length; for figure 25 shows at once that if $G'$ were displaced to $G'_1$, the $\lambda$ rays $bb'$ would lose their coincidence in $T$, while that property would now be possessed by the $\lambda'$ rays, $dd'$. If $G'$ is on a fore-and-aft micrometer, therefore, one might suppose a second method of interferometry to be available in which symmetry is retained throughout and (since the angle at which the rays $bb'$ meet is $\delta = 2\theta$) subject to the equation

$$n\lambda = 2\epsilon' \cos \delta/2 = 2\epsilon' \cos \theta$$

where $\epsilon'$ is the displacement corresponding to $n$ fringes passing in wavelength $\lambda$.

This equation, however, is inapplicable, as already explained, because the pencils $bb'$ are not reflected, but diffracted into $T$. In the symmetrical apparatus, therefore, no perceptible motion of fringes is produced by the fore-and-aft motion of $G'$, because in all cases the rays $bb'$ meet the grating with a constant phase-difference. If the phases are identical they remain so while $G'$ is displaced. The strip of fringes as a whole, however, is slowly though imperceptibly displaced through the spectrum, without accentuated motion of the fringes within the strip. This inference was tested by placing $G'$ on a fore-and-aft micrometer. Large displacements of the screw (fractions of a centimeter) shifted the strip from color to color as specified. A micrometric displacement of $G'$, however, was unaccompanied by any appreciable displacement of fringes. On the other hand, any flexure of the supports of $G'$ at once produced a marked displacement of fringes, while from mere micrometer displacement no measurement could be obtained.

Equation (1) is of interest in interferometry, in view of the very long ranges of displacement available. For such purposes gratings of lower dispersion (preferably ruled gratings or else prisms) should be used, to obtain greater luminous intensity in the spectrum. Of course, the gratings $G$ and $G'$ may have different constants, but in such a case $GNG'M$ will no longer be a rhombus. Since for constant $\lambda$ the ray-lengths in figure 25 are constant for all positions of $G$ parallel to $G'$, $M$ parallel to $N$, large path-difference may conveniently be introduced by compensators. If a thin sheet of mica is moved in either the $b$ or $b'$ pencils, there is a lively skirmish of fringes, but they do not change size appreciably. A glass plate 5 mm. or more thick placed in *both* rays $b$ and $b'$ and rotated produces the same results, but the fringes move more slowly. A plate 2.8 mm. thick, with strong fringes horizontal in the yellow, if placed in the $b'$ pencil produces hair-lines inclined toward the left in the red; if placed in the $b$ pencil, hair-lines inclined to the left in the green,

etc. In contrast with this, the shift from red to green, if produced without compensator by the displacement of $M$, shows scarcely any change of fringes, either as to size or inclination.

To change the size of fringes it is necessary to rotate the grating $G'$ (relatively to $G$) on a horizontal axis normal to itself. They then both rotate and grow larger, attaining the maximum of size when the fringes are vertical. Fringes quite large and black, which are naturally much more sensitive to compensators, may be obtained in this way; but the fringes are still easily controlled by hand. Limitations of the incident light in breadth, or simultaneous rotation of $M$ and $N$, produced no marked effects.

Fringes may also be enlarged on moving the collimator with slit micrometrically right or left, as already stated, though this must be done with caution, as the effects are often surprisingly abrupt; for when the system is not quite symmetric displacements on $G$ will be equivalent to accentuated displacement on $G'$, owing to the reflections. The reflected rays soon cease to intersect and the displacement on $M$ and $N$ is invariably large. Furthermore, by the insertion of compensators (glass plates 1 to 2 mm. thick) in the $b$ or $b'$ pencils, either directly or differentially, larger or smaller fringes may be obtained.

It is now of interest to return to the equation referring to the displacement of $G'$, normal to itself, and to consider the resolving power of the system; for the latter bears a close analogy to the experiments made in a preceding paper (Carnegie Inst. Wash. Pub. 249, Chap. V, 1916) on the remarkable behavior of crossed rays. If $G'$ is displaced to $G'_1$ over a distance $e'=dh$ (see fig. 25, where $h$ is the distance apart of $G$ and $G'$), the rays $\lambda'$ meeting in $T$ will now be in the same condition as were originally the rays $\lambda$. In other words, $e_1$ and $e'_1$ have become coincident at $G'$. If we assume that the same type of fringe results in these cases, and if $\lambda'-\lambda=d\lambda$, $\theta-\theta'=d\theta$ (for the passage of $bb'$ into $dd'$ is in the direction from red to violet),

(2)                    $d\theta=dh \sin\theta \cos\theta/h$, nearly

Since $\lambda=D\sin\theta$ and $d\lambda=-D\cos\theta\, d\theta$, this may be changed to

(3)                    $d\lambda/\lambda=dh(1-\lambda^2/D^2)/h$

when $D$ is the grating constant. This is the expression used heretofore.

In general it is to be noted that the present method, apart from any practical outcome, is of great interest as to the data it will furnish of the width of the strip of spectrum carrying interference fringes under any given conditions. For here the spectra are not reversed or inverted and the latitude of interference of diffraction throughout $\lambda$ is much broader than in case of reversed spectra. But for this purpose films will not suffice and rigid refracting systems must be devised.

**20. The same, continued. Homogeneous light. Dissimilar gratings.**—To show the close relation of the present experiments with one reflection to the

earlier work with crossed rays and two reflections (*l.c.*), experiments may be made with homogeneous light. Accordingly, the sodium arc with a wide slit was installed and the fringes found without difficulty. Strands of fringes with nodules were obtained as before. These rotated in marked degree (180°) from vertical hair-lines, through coarse vertical strands with horizontal nodules, back to vertical hair-lines again, as either $M$ or $G'$ was suitably displaced normally to its plane. To shift the fringes of any form into the middle of the wide-slit image, a glass compensator in either $b$ or $b'$ may be resorted to, or both $M$ and $G'$ may be displaced together. Again, whereas the micrometric displacement of $M$ produces a marked displacement of fringes within the strip in accordance with equation (1), the micrometric displacement of $G'$ leaves the fringes stationary within the strip. While the strands and nodules were strong, the reticulation of fringes could not be clearly made out, in view of the use of film gratings in place of the ruled gratings used in the earlier report.

In equation (4), $D = 169 \times 10^{-6}$ cm., if $d\lambda/\lambda = 6 \times 10^{-8}/6 \times 10^{-5} = 10^{-3}$, $h = 60$ cm., $D = 169 \times 10^{-6}$ cm.; whence $dh = 10^{-3} \times 60/(1 - (60/169)^2) = 0.07$ cm., nearly. Thus, if with ruled gratings the fringes due to the $D_1$ and $D_2$ lines could be separately recognized, it should be possible to distinguish between them here also, as the same phases require a differential displacement of $G'$ of nearly a millimeter. The same result would be recognized at $M$ by a displacement of $dh \tan \theta$, where $\theta = 21°$ nearly, being the mean angle of diffraction. The $M$ displacement is thus $0.07 \times 0.36 = 0.025$ cm.

In case of homogeneous light the prism grating $G''$ is not needed and much more light is available if the telescope is used directly. The strands of interferences, being on a yellow ground, are not very strong. Nevertheless a few measurements of ranges of displacement were made by moving both $M$ (displacement $e$) and $G'$ (displacement $h$), alternately. The following values of $e$, $h$, and $h \tan \theta'$ were found, the film gratings having nearly the same constants:

$e = 0.5$ cm.   $h = 1.30$ cm.   $h \tan \theta' = 0.49$ cm.   $\theta = 19° 37'$   $\theta' = 20° 40'$

$e$ and $h \tan \theta'$ coincide as closely as may be expected, seeing that the fringes in neither case can be quite brought to vanish.

Experiments were next made with a grating of less dispersive power ($D = 352 \times 10^{-6}$ cm.), ruled on glass and a stretched film grating of the same strength. It was found, however, that the long rhombus $GMG'N$ was very difficult to control, owing to the reflection at almost grazing incidence. The spectra also were not quite clear. The method was therefore eventually abandoned, as no fringes could be found.

The trial was then made with a weak grating at $G$ ($D = 352 \times 10^{-6}$ cm.) and a strong grating at $G'$ ($D = 167 \times 10^{-6}$ cm.). In adjustment the latter naturally overpowers the former and two reversed spectra are seen in the telescope (without prism grating) immediately behind $G'$. Both spectra were quite strong and sharp. With white light no fringes could be found even after long trial and a variety of adjustments.

The sodium arc was now used with a very wide slit and the fringes were found without difficulty. They consisted as usual of vertical hair-lines rotating through a usually horizontal maximum back to vertical hair-lines again, as either $M$, $N$, $G'$ were displaced normal to their faces on their respective micrometers. These fringes are simply due to either one or the other sodium line separately and therefore seen on a yellow ground free from interference. Even after this, with the apparatus in adjustment for homogeneous light, white light was tried again in alternation, but no fringes appeared.

With sodium light a few measurements of the ranges of displacement were made. If $\theta$ and $\theta'$ are the angles of diffraction, $\delta = 180° - (\theta + \theta')$ and $x = 2e$ cos $\delta/2$, when $x$ is the path-difference cut off at one end by the displacement $e$ of the mirror $M$. The displacement of $G'$ being $y$, it appears that, apart from sliding, $e$ and $y$ tan $\theta'$ should be nearly equal. The results were

| | | | | |
|---|---|---|---|---|
| $e = 0.42$ | 0.42 | 0.45 cm. | $\theta =$ | $9° 39'$ |
| $x = 0.81$ | 0.81 | 0.87 cm. | $\theta' =$ | $20° 40'$ |
| $y = 1.74$ | | 1.80 cm. | | |
| $y$ tan $\theta = 0.66$ | 0.68 cm. | | $\delta =$ | $149° 41'$ |

It was not practicable to make the hair-lines quite disappear without a large excess of displacement in both cases. Even so the difference of $e$ and $y$ tan $\theta'$ is too large to be explained by such an error. But the work with the present apparatus (screws not long enough) is not sufficiently accurate to make further discussion fruitful. The error will probably be associated with the oblique incidence of rays in case of a wide slit.

Very remarkable results were finally obtained with compensators of glass plate. Placed in one or both beams and rotated around a vertical axis, they rotate the fringes. This would be referable to the sliding of the ends of the two pencils on the grating $G'$. If, however, they are placed nearly normally in one beam, they produce no effect either of rotation or on the size of the fringes; but the pattern is displaced bodily across the wide yellow slit image. Glass plates 0.2 and 0.5 cm. were used. It is not until the thickness of plate reaches 2 cm. that appreciable thinning of the interference fringes occurs when the plate is placed in one beam. With optic plate this would be an excellent method for testing the lengths of uniform wave-trains. Finally, with a fine slit and coincident sodium lines, the fringes could be seen in the presence of a continuous spectrum as marked dots on the enhanced sodium lines. But nothing could be detected with non-coincident lines.*

**21. The same, continued. Duplicate fringes.**—The occurrence of strands and apparently duplicated fringes has already been suggested in the preceding paragraph. In further experiments definite results were eventually obtained *with sunlight*. These occur in very great variety, but two typical phases may be accentuated, given in figure 27. In the case *a* the two sets are more

---

* Such fringes were since found, incidentally, in the white flash of a sodium arc. They were very clear, but could not be controlled.

nearly parallel, but one is always very large in comparison with the other. In case *b* the difference in size is even more marked and the fringes are nearly orthogonal. In intermediate cases fine large strands occur. These pass into each other continuously; the manner does not admit of description. They are seen best in the principal focal plane and both sets are about equally strong.

To obtain these fringes the adjustment was first carefully made with the sodium arc. Thereupon the arc was replaced by concentrated sunlight and fine fringes were recognized in the superposed spectra (longitudinal and transverse axes coinciding). These fine fringes were then enlarged both by rotating the grating *G'* (fig. 25) on its normal axis and readjusting *M* in each case, and by adding trial compensators in the *M* or *N* pencils. A glass plate 3 mm. thick gave the best results and they were very striking. The following are the chief characteristics:

When the mirror *M* is slowly rotated on a horizontal axis, moving one spectrum vertically, slightly over the other, the fringes pass through all their phases.

When *M* is slowly rotated on a vertical axis, which slides one spectrum horizontally over the other, the fringes are displaced, more or less, bodily in the spectrum. Thus in the case *b*, figure 27, the *D* doublets are many
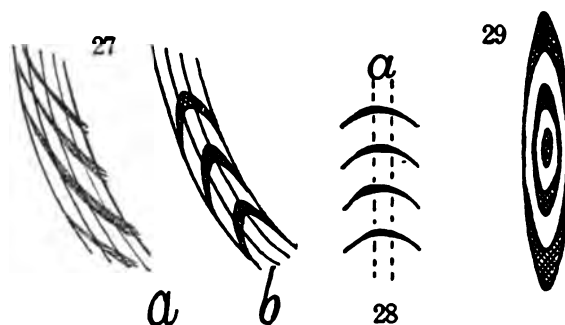


times their own spacing ($D_1D_2$) apart. If the two *D* doublets approach each other, the fringes approach the *D* line from larger wave-lengths and *vice versa*. The fringes were lost when the doublets crossed over each other.

Rotation of the compensator in the first place moves the fringes as in interferometry, as does also the normal micrometric displacement of *M*. If this motion requires readjustment of *M*, the range of displacement is curtailed and the corresponding change of phase appears. In the second place, the compensator, on rotation, traces the contours of the curves by successively accentuating the vaguer parts, as will presently be explained.

The fore-and-aft motion of *G'* also moves the fringes bodily through the spectrum without marked change of phase. All fringes, whether produced with or without compensators, are ultimately curved lines.

The most remarkable results occurred on widening the slit. Supposing that large strands were visible in case of the fine slit, and that this was gradually widened until the slit width was 0.5 mm. or more, the strands were found

to have coalesced in a way which defies description. In their place appeared a wide strip of equidistant parallel crescents, as shown in figure 28. The Fraunhofer lines had long vanished and the appearance of the spectrum was whitish and intense. The fringes in question are thus in a measure achromatic. The strips appear quite regular through the breadth of the spectrum and its width may be one-third of the length of the spectrum. The fringes move with the normal displacement of $M$ (interferometry) and the range is large (0.5 cm. without adjustment), provided $M$ does not require readjustment by rotation. Simultaneously the strip is displaced longitudinally in the spectrum in the usual way.

On closing the slit the ellipses break up into sharp strands again without offering a systematic clue as to the manner in which this is done. The strands usually trend more or less vertically with two sharp, strong groups, flanked by one or more weak groups on each side.

On removing the condenser these crescents became more slender but much sharper, so that in spite of the diminished light they could be well seen. They were then found to be like the approximately confocal ellipses of displacement interferometry, though not subject to the same laws. They embraced over one-third of the visible overlapping (green-yellow through red) spectra, terminating in very fine hair-lines on one side but coarse lines on the other. On opening the slit to about 0.1 mm. the evolution was curious. With a very fine slit a relatively narrow strip of strong slanting lines was seen in the yellow. As the slit widened these developed curvature, adding the more slender complements of the ellipses on the red side, until this part of the spectrum was filled with confocal half-ellipses having a transverse major axis. ˉ The range of displacement of $M$ is practically indefinite, depending simply on the degree to which the spectra overlap; 3 to 4 cm. were tried. A horizontally wide mirror at $M$ is needed; for the ellipses travel through the spectrum and the pencil along the mirror, from end to end. Both sides of the ellipses may be traversed by rotating the plate compensator, which successively accentuates (in a transverse strip) a definite part of their contours. In this way the thick apices or either of the hair-like lateral ends may be clearly brought out. Thus the two lines $a$, in figure 28, limit the strong part of the ellipses. When $a$ moves to right or left, the hair-lines appear more and more strongly until they terminate, showing that the inclusive strip is also limited.

To further study this result, the grating* $G'$ was successively rotated in small amounts on a normal axis with adjustment at $M$. It was thus possible to find both the ends of the ellipses, as well as the central parts. As a result the form figure 29 was definitely brought out. The confocal ellipses are extremely eccentric, with very turgid apices, so that the central part, if in the spectrum, consists of transverse straight lines. Motion of $M$ shifts the fringes to and from the center where they originate or evanesce.

---

* When nearly centered, rotation of $M$ about a horizontal axis is also sufficient to complete the centering of the ellipses.

The ellipses move as a whole with $M$, without changing form appreciably, throughout the spectrum; but they move *very slowly*, quite differently in this respect from the round ellipses in displacement interferometry, which are extremely sensitive to displacement of $M$. In the present work it may take 5 or 10 cm. at $M$ to pass the ellipses quite through the spectrum. They are strong and fine in spite of the film gratings used.

In the endeavor to explain these phenomena one may notice that the main features have already been accounted for. As to details, since the gratings are films which may act from both sides, explanations are hazardous. I do not believe, however, that the films (cemented with balsam on glass plate) had any other discrepant effect here than to make straight lines sinuous. The character of the phenomena, as a whole, is trustworthy.

In the case of the duplicated fringes (fig. 27, *a*, *b*, and the strands) seen with a fine slit, the danger is perhaps greatest. But it appears to me that the coarse lines in figure 27 are vestiges of the ellipses of figure 29, due to a wide slit. These are superimposed on special fringes resulting from the diffraction of the narrow slit. It is difficult to conjecture any other cause of duplication.

The shift of ellipses through the spectrum follows as before from figure 25. Their occurrence in case of a wide slit might be associated with the equation

$$ne = D/2$$

or with their independence of wave-length. They would therefore result merely from the obliquity introduced by dispersion. But the presence of the glass-plate compensator militates against this. In the peculiar behavior of the compensators when added or rotated around a vertical axis, the dispersion of the glass itself comes prominently into play, for the effect of introducing a corresponding air-path is negligible in its effect on form. Thus the removal of a 3 mm. compensating plate may leave the fringes almost too small to be seen, whereas the displacement of $M$ over 3 cm. produces but little change of form.

Finally, the ellipses are developed in arc or contour from left to right, for instance, when the slit is widened; and they vanish from right to left as the slit is more and more nearly closed. The last lines for a closing slit make a narrow grid of fringes quite straight and strong.

**22. The same. Prismatic adjustment.**—The 60° prism has certain advantages in experiments like the present, particularly when non-reversed spectra are to be obtained. Figure 30 is a device of this kind, in which $P$ is the separating prism and $P'$ the collecting prism, the beam of white light $L$ from a collimator entering the flat face normally on the front side and issuing normally on the rear side at $c$ and $c'$. $M$ and $N$ are opaque mirrors parallel to each other, $G$ a direct-vision prism-grating. The telescope is at $T$. The reflection may be either internal, as in the strong lines of figure 30, or it may be external on silvered faces of the prisms $p$ and $p'$, the appurtenances being shown in dotted lines. In this case the separated rays $a$, $a'$, $b$, $b'$ are collected

at $c''$, $c'''$, to be joined in the telescope at $T$. The internal reflection being total, with the rays entering and leaving at right angles to the faces and requiring no silvering of the latter, I made use of it for the following experiments: $M$ and $N$ are on micrometers with the screw in the direction normal to their faces. $P$, $M$, $N$, $P'$ must all be adjustable. After preliminary measurement for equal distances, the fringes were found without trouble. They were strong but fine, beginning with vertical hair-lines and gradually rotating as they grew coarser, till they rather abruptly vanished. The displacement of the $M$ mirror did not exceed 0.6 mm., nor the rotation 30°. The spectra being non-reversed, the fringes covered the whole field. Nevertheless these lines must probably be regarded as arcs of circles or ellipses with enormously distant centers. In fact, the appearance of the whole of the elliptic symmetry, in the preceding experiments (§ 21) with gratings, is also to be associated with a slight difference of length of two overlapping spectra. This is necessarily the case, since the two gratings $G$ and $G'$, figure 25, have never quite the same constant. The third grating must therefore produce two spectra, the one slightly incremented and the other decremented in length, respectively, as compared with the case for white light.
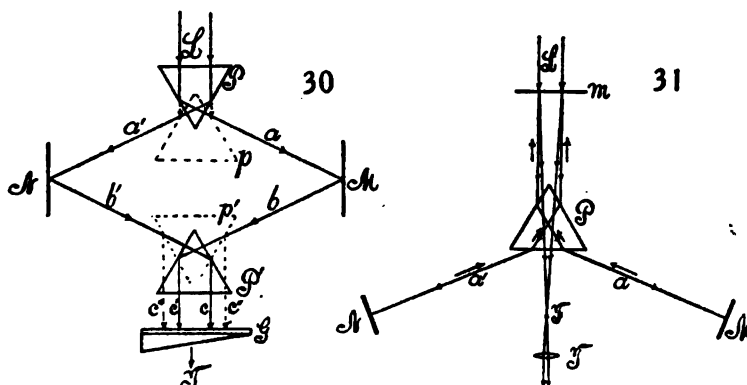


One would naturally suppose that the abrupt evanescence of fringes was due to the escape of the $b$ beam at the edge of the prism $P'$; but this is not possible, as the mirror $M$ was traveling toward the rear. Furthermore, the fore-and-aft motion of the prism $P'$ over several millimeters had scarcely any effect on the fringes. This is unexpected; for the rays, $c$, $c'$, are compelled to approach or recede from each other by this motion. Finally, the sodium doublets may be moved at some distance (many times their breadth) apart without destroying the fringes. They are often most distinct when the $D$ lines are not superposed. The same is also true for the longitudinal axes, though to a less degree.

These features are therefore peculiar. The rays $c$ $c'$ were about 5 mm. apart. Unfortunately the faces of the prisms were optically inadequate, so that the sodium lines were not sharp. For this reason no results were obtained with homogeneous light and a wide slit.

To enlarge the fringes, the prism $P'$ may be rotated around a horizontal axis parallel to $LT$. The fringes then also rotate, but the increase of size so obtained is usually not striking. Moreover, no observable effect, either on the size of fringes or on the range of displacement, is produced by inserting compensators in one beam or both. If $M$ and $N$ are moved together toward the right or left, the result is not appreciable. A great variety of different adjustments showed a range of displacement, at $M$, about the same (0.06 cm.), whether the patch of light on the prism was wide or narrow. The range of fore-and-aft motion of $P'$ within which fringes are visible was 0.52 cm. They vanish quite abruptly when the light is near the edge of the prism, although *both spectra* are still strongly visible. When the light is nearer the base of the prism they vanish more gradually. Definite strips of white light on both sides of the prism, therefore, coöperate to produce the fringes. The remainder of the illumination is ineffective. The distance apart of $c$ and $c'$, as modified by fore-and-aft motion, curiously enough, is here without marked influence. It is true, however, that the largest fringes were obtained when the two pencils of light from $M$ and $N$ coincided at the objective of the telescope, although the $D$ lines were in this case far apart. The attempt to find a systematic method for enlarging the fringes failed, possibly because the prism angles were not quite identical. The striking contrast in the results obtained here in comparison with those of the preceding paragraph, although both methods are essentially the same, is noteworthy.

It is for this reason that I thought it desirable to test the method in figure 31, which accomplishes with a prism what was done in my original experiments with reversed spectra, by the aid of a grating. In the figure the incident beam of white light $L$ from a collimator strikes the 60° prism at its edge, and is then refracted into the paired pencils $a$, $a'$. These are reflected normally by the opaque mirrors $M$ and $N$, again refracted by $P$ as each pencil nearly retraces its path. The return beams, however, are given a slightly upward trend, so as to impinge on the opaque mirror $m$ (curved or plane). The rays reflected from $m$, in such a way as to avoid the prism $P$, may be reunited in the focus $F$ observed by the lens $T$, or (if parallel) collected by a telescope at $T$. In view of the prism, the spectra are small and reversed, but may be brought to overlap at the red ends, which are towards each other.

The small dispersion makes it necessary to use a strong telescope if the Fraunhofer lines are to be visible and the $D$ lines separated. Usually the two doublets will be at a small angle to each other, but this does not mar the interferences. When the adjustment has been made symmetrically, a strong linear phenomenon may be found not differing in appearance from the results obtained when a grating was used at $P$, figure 31. When the mirror $M$ is displaced, however, the fringes appear in the form of multiple vertical hair-lines, which grow coarser until but a single dark line flanked by a bright line is visible. With further displacement the phenomenon again vanishes in passing through multiple hair-lines. This appearance of hair-lines is one distinguishing feature; but a much more important result is the small range

of displacement.  It was found to be, between appearance and evanescence of fringes,

$$\delta e = 0.112 \quad 0.119, \quad \text{etc., cm.}$$

thus scarcely larger than a millimeter, whereas in the case where a grating $(D = 352 \times 10^{-4}$ cm.) was used in place of $P$ the range of displacement was of the order of 5 mm.

If the spectra be regarded with a prism grating, they become relatively long and short, respectively; but the phenomenon is none the less strong, although it is apt to lie outside of the two sodium doublets and not midway between them, as with the telescope.  It seeks out the line of coincident wave-lengths.  Now, inasmuch as the refraction from $M$ is normal and the rays virtually retrace their paths both in the case of the prism and the grating (in the original adjustment), it seems at first difficult to avoid the conclusion that wave-trains are more uniform in proportion as they have been more highly dispersed.  The only misgiving would be the fact that the phenomenon with prism appears and vanishes in hair-lines, whereas with gratings it goes out rather abruptly.  Otherwise one would regard white light as consisting of irregular pulses incapable of prolonged interference, whereas the dispersed wave consists of wave-trains in each color, which throughout a considerable number of wave-lengths are plane polarized.  True, if there is sliding, the sections of the two light-pencils, the points of which are capable of interfering in pairs, increase in area proportionately to the dispersion.

Suppose that for low dispersion the fringes may be regarded as extremely eccentric, virtually linear ellipses, the lateral distance between which very rapidly diminishes, so that, since $\delta e = 0.12$, but

$$\frac{1}{2} \frac{0.12}{3 \times 10^{-4}} = 2000$$

can be seen by the given telescope.  These lines would move behind the strip carrying interference fringes as $M$ is displaced.  If now the dispersion were much increased, say from $\dfrac{d\theta}{d\lambda} = 2 \times 760$ for the prism to $2 \times 2880$ for the grating, the ellipses would be much less eccentric as a whole and their lines would have grown coarser, so that many more would be visible by the given optical system.  As the dispersion is increased $2880/760 = 3.8$ times, the range of displacement should increase similarly to $0.12 \times 3.8 = 4.6$ cm.  The plane ruled grating $(D = 352 \times 10^{-4}$ cm.) in question was now again mounted in place of $P$ and under good illumination the range $0.48$ cm. was found experimentally.  This agrees very well with the estimated value.  Moreover, on close inspection it is discernible that the linear phenomenon really consists of extremely eccentric ellipses, which in case of the best adjustments manifest the very sharp arrow-like forms.  It also enters and vanishes in multilinear form, though the lines are not hair-lines.  Thus the assertion that increased uniformity of wave-train accounts for the long range of displacement and

visibility in case of the grating is not warranted. In the second order of the ruled grating or with a grating of higher dispersion ($D = 175 \times 10^{-4}$ cm.) the field was too dark for experiments of this kind. In this work, however, I obtained the linear phenomenon for the first time, from the double diffraction of a film grating.

In conclusion, it is interesting to refer to a relation of the reversed and the inverted spectra and their interferences. If in case of reversed spectra one of the superposed pair is rotated 180° in its own plane, around an axis normal to that plane and through the line of symmetry, the new pair of superposed spectra is an inverted system. At the same time the interferences which are ellipses in both experiments probably rotate their major axes 90°. In the case of reversed spectra this major axis is transverse, coinciding with the line of symmetry in a given wave-length, and the ellipses are *extremely* eccentric, whereas in the case of inverted spectra the major axis is probably longitudinal. It is not unusual to obtain a single line running all the way from red to violet; but arrow-shaped forms never occur, so that the ellipses are rounded forms and belong to distant centers. An adequate reason for the highly eccentric, closely packed elliptic fringes of reversed spectra on their evolution from the round ellipses of inverted spectra by rotation is yet to be given.

**23. Apparent lengths of uniform wave-trains.**—In § 16 certain results were given which made it seem plausible that the path-differences within which interferences are producible (*i.e.*, the apparent lengths of uniform wave-trains) increase, as the dispersion to which the incident collimated white light is subjected is made continually greater. Work with this quest in view is reported in table 10, the plan being to produce the interferences by one and the same method, but with a successive variation of the dispersion of spectra. The method, figure 14, was first selected for this purpose, inasmuch as the use of prisms and gratings of different dispersive power at $P$ meets the requirements, while spectra of the first and second order are equally available.

It is obvious that in work of this kind the spectra must be bright, otherwise the fine lines will escape detection. Deficient values will thus be attained if the spectra are too dark. Moreover, the results can not furnish data of precision, since the exact instant at which fringes, continually decreasing in size, have actually vanished, can not be fixed; and it is the fine fringes which furnish a considerable amount of the displacement. The differences, however, are so large that not only orders of values are clearly apparent, but the ranges more than sufficiently so to substantiate the argument.

It is possible that the method, figure 14, gives the half-ranges only, since the efficient patches of light, figure 8, can not cross each other. The methods applied will nevertheless be trustworthy, since they are identical, the same telescope and other appurtenances being used throughout. Later the grating method (fig. 3), suitably modified, will be used. Path-lengths of a meter or more were usually admissible.

In table 10 the first series of measurements is obtained with a 60° prism,

the dispersive power $d\theta/d\lambda$ being computed (approximately) from Cauchy's equation, so that

$$\mu = A + B/\lambda^2 = \sin(\varphi+\delta)/2/\sin\varphi/2$$

nearly, and therefore

$$d\delta/d\lambda = 4B\sin\varphi/2/\lambda^3\cos(\varphi+\delta)/2$$

$\varphi$ being the prism angle (60°) and $\delta$ the angle of minimum deviation. The constant $B$ was put $4.6 \times 10^{-11}$.

TABLE 10.—Ranges of displacement, $e$, $y$, for different dispersions. Method of figure 14. $B = 4.6 \times 10^{-11}$.   $\mu = 1.6$.

| Disposition. | $e_M \times 10^3$ | $e_N \times 10^3$ | $y \times 10^3$ at $P$ | $d\theta/d\lambda$ | $\theta$ | Remarks. |
|---|---|---|---|---|---|---|
| | *cm.* | *cm.* | *cm.* | | | |
| 60° prism $P$, 90° prism $P'$ | 26 | 19 | 16 | 760 | 49° 45′ | |
| | 25 | 18 | 17 | ...... | ...... | |
| | 24 | 17 | 19 | ...... | ...... | |
| Mean.............. | 25 | 18 | 17 | ...... | ...... | |
| Same. $P'$ brought forward | 28 | 29 | 27 | 760 | 49° 45′ | |
| | 32 | 30 | 23 | ...... | ...... | |
| | ... | ... | 26 | ...... | ...... | |
| Mean.............. | 30 | 30 | 25 | ...... | ...... | |
| Ruled grating $P$, 90° prism $P'$ | 100 | 81 | 65 | 2,880 | 9° 39′ | |
| | 100 | 89 | 76 | ...... | ...... | |
| | 117 | ... | 56 | ...... | ...... | |
| Mean.............. | 106 | 85 | 66 | ...... | ...... | Too dark. |
| Same, mean............. | 161 | 136 | 108 | ...... | ...... | Very bright. |
| Same, second order from $P$ | 250 | 229 | 155 | 6,030 | 19° 34′ | |
| Same, second order near edge................... | 227 | ... | 150 | ...... | ...... | Bright spectra. |
| Film grating $P$, 90° prism $P'$ | 173 | 184 | 155 | 6,400 | 20° 40′ | Too dark. |
| Same................... | 301 | 247 | 183 | ...... | ...... | |
| | 303 | 226 | 200 | ...... | ...... | Very bright. |
| Mean.............. | 302 | 236 | 191 | ...... | ...... | |
| Same, vertical fringes..... | 325 | ... | 234 | 6,400 | 20° 40′ | Very bright. |
| Same, second order from $P$ | 482 | 422 | 450 | 16,910 | 44° 56′ | |
| | 461 | ... | 427 | ...... | ...... | |
| Mean.............. | 472 | 422 | 438 | ...... | ...... | Bright. |
| Same, second order, vertical fringes............ | 500 | ... | ... | ...... | ...... | Strong fringes. |

In the remaining series $d\theta/d\lambda = 1/D\cos\theta$, the usual expression for the grating, $\theta$ being the angle of diffraction and $D$ the grating space. The dispersive power thus increases from about 800 to 17,000, over 20 times. Throughout this whole enormous range good fringes were obtained.

The values $e$ show the displacement of the opaque mirror $M$ during the

presence of fringes, and of the opaque mirror $N$ as specified. Of these, $e_M$ is systematically larger than $e_N$ for reasons which do not appear. The screws were of American and foreign make, but they could not be so different. It is due very probably to residual curvature in the mirrors and surfaces, whereby fringes on the left ($N$) vanish sooner than those on the right ($M$). The datum $y$ is the displacement of the right-angled reflecting prism $P'$, parallel to the component rays $bb'$. This value is smaller than $e$ for reasons already discussed in § 16. All measurements were frequently repeated and the means finally taken for comparison with $d\theta/d\lambda$.

In the third series (ruled grating and concave grating) with specially brilliant spectra, the phenomenon of figure 32 was observed. A wide field of faint fringes was visible, enormously accentuated and clear in the narrow strip of the linear phenomenon. As the micrometer mirror at $M$ moves forward, these faint fringes shift bodily across the stationary bright linear strip, beginning therefore with the pattern $a$ and ending with $b$. The faint fringes follow the rules of displacement interferometry.
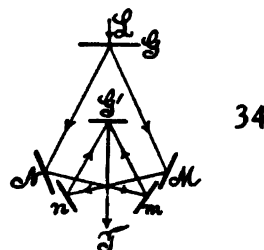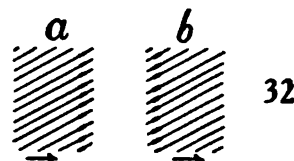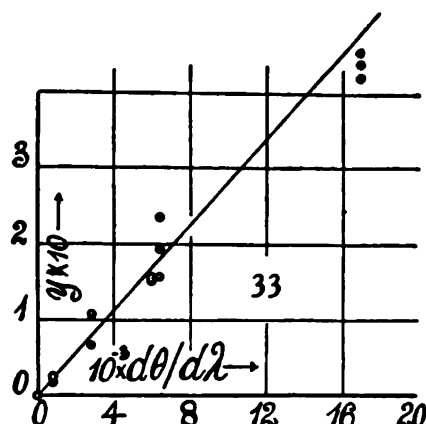


In addition to the data of the table, a large number of miscellaneous tests were made with the reflecting prism in different positions. Unless brought too far to the rear, when the beams are lost at the edge and $e$ too small, the results for fine and coarser fringes were of the same order.

The values of $y$ have been graphically given in figure 33; those for $e$ are not sufficiently regular in the dispersive powers above 1,000 for this treament. It is probable, for instance, that at 16,900 the sliding along the prism surface is interfered with. All the data, in consideration of their limitations, bear out the inference that the range of displacement within which fringes are seen increases in marked degree with the dispersion. The average initial ratio $2\lambda/(d\theta/d\lambda)$ is about $60 \times 10^{-6}$ cm.

A very surprising result in these experiments is the efficiency of the film grating in series IV and V, not only in the first but in the second order of spectra.

After these experiments an attempt was made to obtain similar results with the more comprehensive method of two gratings (transmitting $G$ and reflecting $G'$) of figure 3, above. But here the choice of gratings with appropriate constants was limited and with high double dispersion the fields were apt to be too dark. Good results were obtained with the 60° prism and concave grating and with the ruled grating together with the latter. In the method of figure 3, the second angle of diffraction is necessarily greater than the first, $\theta' > \theta$. To obviate this difficulty the method was modified for prisms as in figure 20, where $G$ is the concave grating, $T$ a strong lens near its focus, and $m$ and $n$ auxiliary mirrors. If this method is used for highly dispersive gratings ($G$ replacing $P$), the rays must be crossed as shown in figure 34. The fringes were found in this case when $G$ was a film grating, but the work had to be abandoned, as the spectra were dull.

The data given in table 11 again show marked increase of displacement with the dispersion $d\theta/d\lambda$, though it is not proportional here. The method with two gratings lacks the brilliancy of the prism method.

TABLE 11.—Range of displacement for different dispersive powers. Method of figure 20, full displacement.

| Details. | $e_M$ | $e_N$ | $\dfrac{d\theta}{d\lambda}$ | $\theta$ | Remarks. |
|---|---|---|---|---|---|
| | *cm.* | *cm.* | | | |
| 60° prism and concave grating..... | 0.357 | 0.315 | 760 | 49° 45′ | Bright. |
| | .300 | .282 | 760 | 49  45 | Too dark. |
| Ruled and concave grating........ | .514 | .520 | 2,880 | 9  39 | Bright arrows. |
| | .509 | ..... | 2,880 | 9  39 | Dark. |
| Film and concave grating......... | ..... | ..... | 6,400 | 20  40 | Too dark. |

**24. Normal displacement of mirrors ($\delta = 0$).**—This desideratum was secured in the original methods, in which a single grating was used for both diffractions. Rays in such a case have to cross the grating somewhat obliquely to the horizontal. The method, furthermore, is restricted to the linear vertical fringes, which are not useful if practical measurement is aimed at.

In the methods with a right-angled reflecting prism (fig. 14), this result is easily secured by displacing the prism. In all other methods ($\delta > 0$), the displacement of mirror is accompanied by sliding of the pencil along it. The effect, as has been shown, is not negligible. It therefore seemed desirable to devise other methods in which $\delta = 0$, and figure 35 is a device of this kind.

Here $G$ and $G'$ are two identical gratings, the first, $G$, receiving the light $L$ from a collimator. The component pencils $a$, $a'$ pass through the half-silvered plate $H$, and thence ($b$, $b'$) to the opaque mirrors $M$ and $N$, one or both on a micrometer. The pencils $b$ and $b'$, impinging normally, retrace their paths and are thereafter reflected at the plate $H$ into $c$ and $c'$. These strike the second grating $G'$ at the proper angle of diffraction and thereafter enter the telescope $T$ together. The path of rays is symmetrical throughout. White light is screened off at $d$. Reversed spectra are seen at $T$. Unfortunately the only identical gratings at my disposal were film gratings of high dispersion

($D = 162 \times 10^{-6}$). As a result of the two diffractions and the half-silver reflection, the spectra were too dull to make it worth while to look for fringes, at length. None was discernible after some searching, to my regret, for the method itself has many points of interest and with gratings of low dispersion it succeeds.

Later I stripped a celluloid film from the ruled grating ($D = 352 \times 10^{-6}$) and mounted it by simple stretching. Using the original grating at $G$ and the film at $G'$, the fringes were found with some patience. The spectra were fairly bright (arc lamp) and the fringes reasonably strong; but they admitted of a displacement of only 1.8 mm., in spite of the vanishing angle $\delta = 0$. Possibly this small displacement is due to the imperfect film grating.

In further experiments I half-silvered plates of glass to different density. In this work I obtained adequately bright spectra and practically perfect fringes, but the range of displacement ($\delta = 0$) could not be increased above 1.8 mm. Within this interval the fringes seem to change form but little, thinning only being evident. Then they become dull and vanish.

The method was temporarily modified, as shown in figure 36, where $G$ is a ruled grating ($D = 352 \times 10^{-6}$ cm.), $G'$ a film grating ($D = 176 \times 10^{-6}$ cm.), and $m$ an opaque mirror. This naturally introduces an angle $\delta = \theta' - \theta$, which is negative when $\theta' > \theta$, or the grating $G$ shows greater dispersion. The mirror is limited in breadth, so that the rays $a$, $a'$ have free access to $M$ and $N$. The fringes were found after some trouble, for the transmitting grating $G'$ also acts as a reflecting grating if the rays $b$, $b'$ fall upon it, and it is not always easy to separate these two cases, each of which will give fringes on proper adjustment. The spectra are very bright and the range was about 2 mm.

The same method was now carried out with prisms, as shown in figure 37, where $L$ is the incident pencil from a collimator, $P$ and $P'$ right-angled prisms, $l$ the half-silvered plate, $N$ and $M$ opaque mirrors on micrometers, $T$ the telescope. The spectra seen at $T$ have each been four times refracted and twice reflected, at $M$ and $H$. They are very bright, so that a very fine slit (here specially desirable) is available. The sodium lines are not separated. On bringing the spectra to overlap at their corresponding edges, the fringes were found. They are peculiar, inasmuch as they show the phenomenon of figure 32, but with the faint fringes curved and more prominent than heretofore. In other words, the faint phenomenon shifts across the field from side to side, but is enormously accentuated at the transverse strip of the linear phenomenon. Narrowing the incident pencil broadens and blackens the fringes. They may be obtained in the gap between two spectra just separated. The range of displacement within which fringes are seen was, however, very small, not exceeding 0.2 mm. This is a characteristic of these fringes and in keeping with the low dispersion.

It is interesting to note that the systems figures 35, 36, 37 constitute an element of a direct-vision spectroscope. It has been shown that it can be made quite powerful.

The same method, figure 37, was now used with two 60° prisms of highly

refracting glass. In contrast with the ease in which the adjustments were made with the symmetrical 45° prisms, the corresponding work with 60° prisms proved to be exceedingly difficult. True, the prisms were large, including long glass-paths. The sodium lines, now clearly separated, were markedly curved, so that on placing them near together they either assumed an O-shape or an X-shape. But the spectra were brilliant and nothing appeared to militate against a successful result. But it was not until after days of searching that the fringes were found, and then only with two prisms of different, highly refracting glass. They were not quite uniform, but it seemed impossible to improve them. The ranges of displacement were found to be 0.088 to 0.093 cm. with the electric arc, 0.103 cm. with (condensed) sunlight. This is again in accord with the large increase of dispersion, the range of displacement being about five times greater than was the case with 45° prism of less refracting glass.
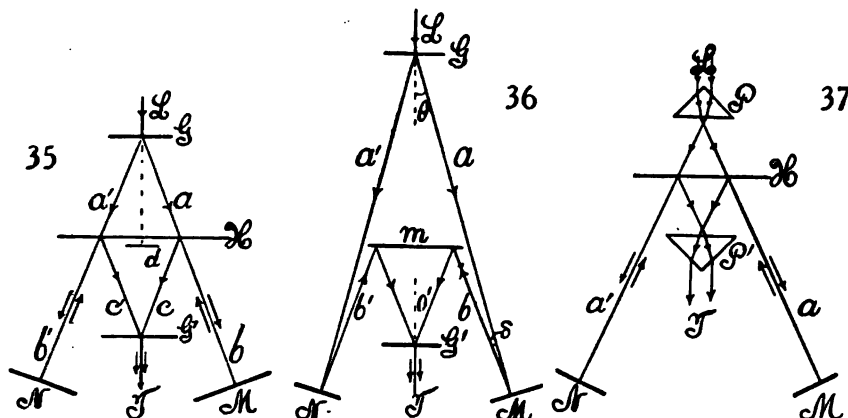


**25. Diffraction at M, N, replacing reflection.**—The present method of observing interferences in the zero, first, second, third, and even fourth order, successively, without essential change of the parts of the apparatus, is noteworthy. I happened to possess a plane reflecting grating $(D \times 10^{-6} = 200)$, cut into two equal parts by a section parallel to the rulings, and it was therefore easy to devise the method. In figure 38, the incident light $L$ from the collimator is separated into two component beams $a$ and $a'$ by the 60° prism $P$. This is essential here, as an abundance of light is needed (sunlight should be focused by a large lens of long focus (5 feet) on the slit). The rays $a$, $a'$ are then either reflected or diffracted in any order by the plane reflecting gratings $G$, $G'$ into the collinear rays $b$, $b'$. They are then reflected by the silvered right-angled prism $P'$ and observed in a telescope at $T$. $G$ and $G'$ and if possible also $P'$ should be on micrometers, so that
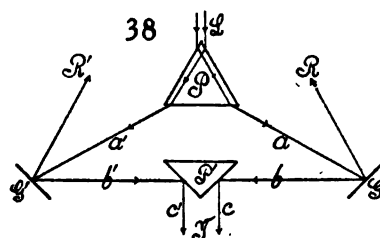
corresponding displacements $\epsilon$, $\epsilon'$, normal to $G$ and $G'$ and $y$ in the direction $bb'$, may be registered.

The adjustments, if symmetry were demanded, would be cumbersome; for, in addition to precise modification of the position and orientation of the prisms $P$, $P'$, the grating requires fine adjustment and a means of securing parallelism of the rulings. But an approximate adjustment does very well and no pains were taken in the first experiments to secure symmetry. The spectra were intensely brilliant in the low-order work; but even in the fourth order the light was adequate. One may note that here the gratings do not reverse the dispersion of the prism $P$, though this is relatively small. Table 12 is an example of results:

TABLE 12.—Ranges of displacement varying with dispersion. Paired gratings and 60° prism. $\theta=46°$. $\delta=44°$. $x=2\epsilon \cos \delta/2$.

| Order | Observed $\epsilon \times 10^3$ | $x \times 10^3$ | $\frac{i}{\theta}$ | $d\theta/d\lambda$ | Remarks. |
|---|---|---|---|---|---|
|   | cm. | cm. |   |   |   |
| 0 | 38 | 70 | 22° | 760 |   |
| 1 | 180 |   |   |   |   |
|   | 200 | 351 | 12.8° | } 3,490 |   |
|   | 180 |   | 31.2° |   |   |
|   | 200 | 351 |   |   |   |
| 2 | 420 |   |   |   |   |
|   | 420 | 777 |   |   |   |
|   | 400 |   | 3.5° | } 6,440 |   |
|   | 380 | 721 | 40.5° |   |   |
| 3 | 320 |   |   |   |   |
|   | 300 | 573 | −6.4° | } 9,930 | { Fringes lost at |
|   | 520 |   | 50.4° |   | edge? |
|   | 520 | 962 |   |   |   |
| 4 | 580 |   |   |   | { Fringes faint. |
|   | 580 | 1070 | −17.6° | } 14,800 |   |
|   | 520 |   | 61.6° |   | Fringes faint. |
|   | 450 | 910 |   |   |   |

The fringes in the zero order were good and strong, not inferior to any of the others, but unfortunately too short-lived. In the fourth order the fringes are weak (although the enormous sodium doublets stand out clearly), doubt-less from excess of extraneous light. Here also it is difficult to prevent the beam from vanishing at the edge of the prism $P'$. Hence the anomalously small displacement, a discrepancy which is already quite manifest in the third order.

The present experiments furnish a striking example of the uniform breadth of the strip of spectrum carrying the fringes, quite apart from the dispersion of the spectra. In the prism spectrum, where the sodium doublets are indicated by a hair-line just visible, to the fourth-order spectra, where they stand apart like ropes, the linear phenomenon has the same width.

The computation of the dispersive power in these cases is peculiar. It will be seen from figure 38 that the angle $\delta = 44°$ between the incident ray $a$ and

the diffracted ray $b$ is constant and is $\delta = \theta + i$ in the first and second and $\delta = \theta - i$ in the third and fourth orders. Hence in succession

$$\sin(\delta - i) - \sin i = \lambda/D \qquad \sin(\delta - i) - \sin i = 2\lambda/D$$
$$\sin(\delta + i) + \sin i = 3\lambda/D \qquad \sin(\delta + i) + \sin i = 4\lambda/D$$

from which equations the angle $i$ may be computed. I did this with sufficient accuracy graphically, and the values of $i$ and $\theta$ so found are given in table 12.

Since $d\theta = di$, apart from sign, it follows that the dispersing power is

$$-d\theta/d\lambda = n/D \left(\cos i + \cos(\delta - i)\right)$$

where $n$ is the order of the spectrum and $i$ changes sign in the third and fourth orders. With the values of $i$ given, the data for $d\theta/d\lambda$ in the table were finally computed. The dispersive power of the prism was computed as above and is to be added to all the succeeding dispersive powers. Figure 39 shows the relation between the dispersive powers and the path-difference $x = 2e$ $\cos \delta/2$ computed from the observed range of displacement $e$ of the grating $G$. The largest values of $x$ are taken, as they are the most probable. The effect of dispersion here breaks down in the third and fourth orders, as already stated, probably from incidental causes. For the spectra themselves were still adequately bright, but the fringes were



faint for some reason and I failed to make them stronger. The rate $x/(d\theta/d\lambda)$ is here about $120 \times 10^{-6}$ initially. This is larger than above, owing to the differences of apparatus used, etc.
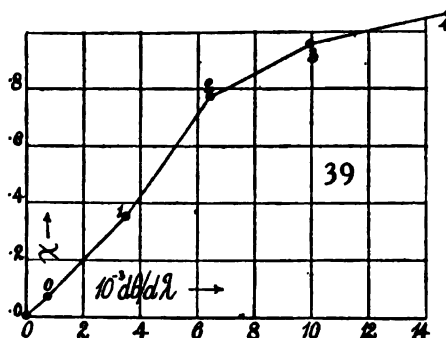
**26. Experiments with the concave grating.**—As there was an excellent Rowland grating in the laboratory with a 6-foot radius and a grating space $D = 177 \times 10^{-6}$ cm., it seemed worth while to obtain the interferences with it. I had hoped to doubly diffract the rays at the same grating, but there is not light enough to make this method fruitful. Accordingly the device, figure 40, promised the best results, where $L$ is a convergent pencil of sunlight, $S$ the slit. The pencil $L$ is carried above the grating $G$ to the opaque mirror $m$, whence it is reflected to the grating and diffracted into the component beams $a$ and $a'$. These are in turn reflected by the opaque mirrors $M$ and $N$ (on micrometers) into the pencils $b$ and $b'$, nearly collinear. The latter are then reflected by the silvered right-angled prism $P$ to the common focus $F$, to be observed with the lens $T$. The spectra are very bright and highly dispersed and are easily made to overlap on their contiguous edges (parallel to a Fraunhofer line $D$, for instance) sufficiently to show the linear phenomenon of reversed spectra.

The fringes are easily found and splendid, though they are not superior in this respect to the fringes obtained by other methods. $P$ is also on a micrometer with the screw in the mean direction $b\,b'$. The range of displacement of $P$ was about $y = 0.55$ cm., so that the available path-difference is considerably above a centimeter. Within this the fringes pass from fine hair-lines through a maximum and back again, apparently without rotation. To enlarge the fringes the grating $G$ may be tilted in its own plane or a similar adjustment made at $P$.

The longitudinal axes of the spectra (wire across the slit) are not in focus with the $D$ line; but though hazy they suffice for adjustment. Naturally the distance $FbaG$ is the radius of the grating $R$ (6 feet) and the distance $Sm + mG$ is $R \cos \theta$. The distances are approximately laid off and the observer at $T$ may then push the mirror $M$ fore and aft by the aid of a lever till the Fraunhofer lines are sharp.

Unfortunately the spectra as a whole are shifted by the micrometers, together when $P$ moves and separately when $M$ or $N$ moves.

**27. Polarization.**—The two rays obtained from calc spar, if corrected for polarization, should be available for interferences of the present kind. Naturally an achromatized calc-spar prism ($C$, fig. 41) is most convenient for the
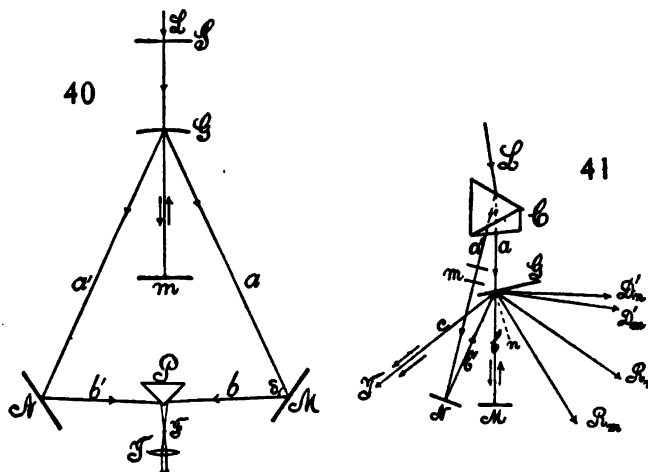


purpose. White light from a collimator, $L$, is doubly refracted by this prism $C$, and the extraordinary ray $a$, just missing the grating $G$ (above or on the sides), impinges on the opaque mirror $M$ and is thence reflected to the grating $G$. The ordinary ray $a'$ is reflected from the opaque mirror $N$ and thence also reaches the grating. These two pencils, $b$, $b'$, are directly reflected by the grating ($D \times 10^6 = 200$ cm.) into $R_m$ and $R_n$ and diffracted into $D'_m$ and $D'_n$. By suitably adjusting the grating between $C$ and $M$ and inclining it as shown, two coincident spectra may be made to pass along the common direction $c$ to the telescope at $T$. These spectra are quite intense. One is somewhat

more dispersed than the other, owing to the difference of angles of incidence $i$, $i'$ and to the residual or differential dispersion at the calc-spar prism, for only the $a$ pencil has been adequately achromatized. In my apparatus the distances $CM$ and $GM$ were about 130 and 100 cm. and the distance $NM$ roughly 30 cm. $N$ is on a micrometer, as it is nearer to the observer at $T$, though it would be preferable to put $M$ on a micrometer.

To obtain interferences of the present kind, the plane of polarization of either $a$ or $a'$ must be rotated 90°. This may be done by two quarter-wavelength micas $M$, in $a'$, the first of which (set at 45° as usual) produces circularly polarized light and the second then erects the vibration into parallelism with the vibration of the pencil $a$. Other methods will presently be resorted to.

With this adjustment fringes were found at $T$ after some searching. They were large, but occurred in a transverse strip of spectrum about $D_1 D_2/2$ in width. True, the spectra are without reversion; but, as stated before, one was about one-fifth longer than the other. This is probably the reason for the narrowness of the strip, for the fringes should otherwise fill the spectrum.

The fringes as first found admitted a displacement of $N$ of about 0.3 cm. only. They were hard to control, needed sharp longitudinal adjustment, and when lost were difficult to find again. They rotate from and to vertical hairlines, through a horizontal maximum. They are always found in the line of symmetry, which for unequal spectra moves more rapidly than the Fraunhofer lines if they are separated. The nearer quarter-undulation plate at $W$ may be considerably rotated without quite destroying the fringes.

If the double quarter-wave-length plate is suitably put in the $a$ beam, results of the same kind are naturally obtained. If a single quarter-wave-length plate is placed in each beam, at 45°, both will be circularly polarized, the position of the micrometer being intermediate. I tested this case at some length, but found no interferences, as was to be expected. Circularly polarized rays of the same sense do not interfere.

In place of the achromatized calc-spar prism, a double-image Wollaston prism or a double-image Fresnel prism (rotary polarization) could be used. Unfortunately I had neither of these, but the latter in connection with an analyzing nicol would have been worth testing.

# CHAPTER II.

**28. Introductory.**—If two identical spectra are superposed in such a way that one is rotated 180°, on a transverse axis (parallel to the Fraunhofer lines), with respect to the other, it will be convenient to refer to the phenomena resulting and described in Chapter I as the interferences of reversed spectra. On the other hand, if one of the superposed spectra has been rotated 180° with respect to the other on a longitudinal axis (parallel to the length of the spectrum), we may refer to the interferences as those of inverted spectra. The absence of either of these adjustments would then be accentuated as non-reversed or non-inverted.

In the case of inverted spectra, therefore, we are dealing with phenomena of virtually homogeneous light, exhibited throughout the length of the spectrum. Such experiments were made cursorily in my first paper on the subject,* but the phenomenon is very peculiar, apparently anomalous, and further treatment is therefore desirable.

**29. Apparatus. Non-inverted spectra.**—The apparatus formerly used for long optical paths is difficult to manipulate. It has therefore been simplified in the present method and used for short distances, so as to be wholly in the observer's control. The parts of the apparatus are conveniently assembled as in a preceding experiment, except that the slit which furnishes the collimated light $L$, figure 42, is now horizontal—*i.e.*, at right angles to the edge of the sharp prism $P$ (about 20° at apex). The rays $a$ and $a'$ (horizontal blades), after leaving the opaque mirrors $M$ and $N$, are then reflected from the sides of the right-angled prism $P'$ into $c$ and $c'$. Thus far the light is white; but $c$ and $c'$ are now diffracted by the grating $G$ with its rulings horizontal (parallel to slit) and with the interposition of an auxiliary prism $p$ (edge horizontal), the two spectra due to $c$ and $c'$ are observed by a telescope at $T$.

The experiment succeeds best with sunlight. The triangle of rays, $a, a'$, $b', b$, is first made isosceles and horizontal by adjusting $P, P'$, being set midway and symmetrically between $M$ and $N$. The two spectra in the telescope (vertical ribands) are now made to overlap at their inner edges and the two sodium doublets placed accurately in contact, by aid of the adjustment screws on the mirrors $M$ and $N$. The latter are then to be moved micrometrically (Fraunhofer slide) until the fringes appear. The experiment is not an easy one.

It is obvious from figure 42 that the two superimposed spectra are non-

---

inverted or direct. Hence with a wide slit, or insufficiently homogeneous light in the direction of a given Fraunhofer line, no fringes will appear. Such fringes as may in any case be found will not, therefore, much outlast the Fraunhofer lines, so far as width of slit is concerned. Furthermore, even if the slit is narrow and the spectra coördinated, there will be no fringes obtainable if the superimposed solar spectra are quite unbroken—*i.e.*, without incidental furrows in the direction of their length (normal to the Fraunhofer lines). For it is to be noticed that the slit is horizontal, and therefore there is no observable diffraction—*i.e.*, virtually no slit in the horizontal direction.

If, however, the spectrum field is interrupted longitudinally by a thin (0.1 mm.) wire drawn across the slit (or, much better, by very fine specks of dust lying incidentally within the slit), then these fine opaque objects will effectively replace the slit, or act analogously to a slit in the horizontal direction. Hence fringes will appear when the path-difference is sufficiently small, associated with the geometric shadow of the opaque objects, throughout the length of the spectrum.
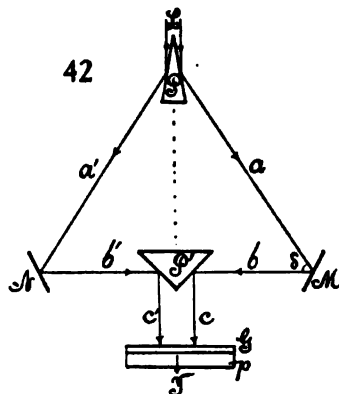


We have here, therefore, a peculiar case of the diffraction of a rod, from two separately controlled half-wave-fronts. The fringes at one extreme of adjustment of mirror $M$ begin with fine horizontal lines, which on moving $M$ incline and enlarge until they gain the maximum of size in the vertical direction. After this, on further motion of $M$ in the same direction, they incline further, diminish in size, and finally become horizontal and hair-like again. They move along the horizontal axis with $M$, subject to the equation

$$\frac{de}{dn} = \frac{\lambda}{2\cos \delta/2}$$

where $\delta/2$ is the angle of incidence at $M$, $\lambda$ the wave-length, and $de/dn$ the normal displacement of $M$ per fringe.

Within the region of overlapping spectra each longitudinal black line is covered from end to end with fringes, the strip being about of $D_1D_2$ width or more if the line is thinner. A broad black line (thicker wire across slit)

shows the fringes at its edges only. While the spectrum may thus be covered with independent strands of fringes, they all move or change phase together. The range of displacement of the micrometer-screw is about 2 mm. When the spectra are about to separate—*i.e.*, when overlapping ceases—the fringes are apt to be particularly wide, say even $4D_1D_2$, and they may be seen in the gap between spectra. In general, the degree of coarseness of fringes depends on the adjustment for parallelism of spectra.

### 30. Apparatus and results for inverted spectra.

—The preceding apparatus may be modified as shown in figure 43. Here $L$ is a collimated beam of white sunlight from the vertical slit, $G$ a transmitting grating. The component pencils $a$ and $a'$ of spectrum light impinge on the opaque mirrors $M$ and $N$, and are then reflected in $b$ and $b'$ to reach the silvered sides of the right-angled prism $P'$. This is now placed with its sides at 45° to the horizontal and its edge in the direction of the incident beam $L$ prolonged. Hence the two pencils $b$ and $b'$ are reflected vertically upward (fig. 44) and appear as two identical and parallel spectra in the field of a telescope, vertically above $P'$. Observation is conveniently made downward to obviate additional reflection. If the triangle $a$, $a'$, $b'$, $b$ is horizontal and isosceles there is no difficulty. On slightly moving the adjustment screen on $M$, $N$, $P'$ (which must be revolvable on a vertical axis, and $P'$, or the beam $L$, movable up or down), to bring the two spectra into coincidence along a given longitudinal axis, and a transverse axis like the $D$ lines, the two spectra are symmetrical—*i.e.*, mirror images one of another with respect to the longitudinal axis. If, now, the mirror $M$ is moved on a micrometer, the fringes of inverted spectra appear when the path-differences are nearly the same.
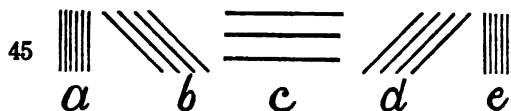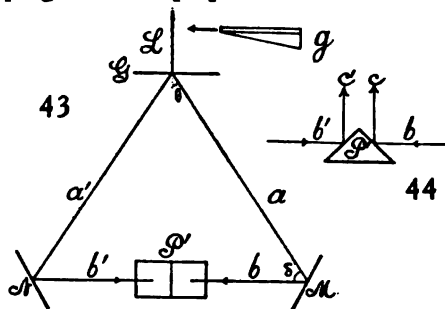
Obtained at short distances (of the order of a foot) on the cast-iron block (Chap. I, fig. 3), these fringes are quiet and better circumstanced for observation; but their characteristics are the same as found for them before (Chap. I, § 4, Carnegie Inst. Wash. Pub. 249). They lie within a narrow strip at the line of symmetry of the two superposed spectra, running from end to end and in breadth about three times the distance apart of the sodium lines ($3D_1D_2$). When the mirror $M$ is moved micrometrically in one direction, the fringes begin to appear as fine hair-lines ($a$, fig. 45) parallel to the $D$ lines. These fine fringes gradually coarsen and rotate until they reach their max-

imum size $c$, when they are perpendicular to the $D$ lines. A single black or bright line may here extend from end to end of the spectrum. Thereafter they grow finer (rotating again) in the same way until they vanish, $e$, as they began. The total angle of rotation is thus 180°.

If the two beams $b$ and $b'$, figure 43, are moved nearer the edge of the prism, the fringes become larger, but usually not much. At least I did not, at first, succeed in separating the fringes much beyond the $D_1D_2$ distance. The width of the longitudinal interference strip remains unchanged. If the light is removed at the line of symmetry (wire across slit), the fringes are sharply outlined across the black line. Being so small, they are naturally always sharp and vivid. The range of displacement of $M$ within which fringes are visible was about 0.2 cm. for the given grating ($D = 352 \times 10^{-6}$), corresponding to the complete rotation 180°, instanced above. If the slit is widened, the fringes slightly outlast the Fraunhofer lines. They also lie in the principal focal plane.

The remarkable feature of these fringes is the definite breadth of strip, from red to violet, within which they lie. With full wave-fronts the striations look as though they were cut between two parallel lines, $3D_1D_2$ apart, In some adjustments, however, suggestions of concealed fringes, very faint prolongations of the strongly marked striations, are unmistakable.

**31. Wave-fronts narrowed.**—The longitudinal strip within which the interferences lie is very sharply limited in breadth, as has been stated. It may, however, be broadened by screening off the white beam, as it leaves the collimator, *from below*. When the whole length of slit is utilized, the strip may not be more than $D_1D_2$ in width. As the vertical blade or beam of white light is cut off, more and more from below, the strip increases to a width of $4D_1D_2$, and when the two inverted spectra in the field of the telescope begin to separate at the line of symmetry, the strip may be over $10D_1D_2$ in width. It is obvious that in such a case the light comes from near the horizontal top edge of the prism. The wave-fronts are slit-like. The field within which diffraction is perceptible in the telescope increases in breadth as the colored wave-front, incident at the objective of the telescope and parallel to the spectrum, decreases in breadth in the same direction. In figure 46, $a$ and $b$ are the two component beams from the two faces of the prism, respectively. The focus is at $f$. The arrows show the effect of narrowing. The oblique rays (omitted) are similarly affected and in step with the axial rays shown. But the fringes are not changed in size. They may, however, be definitely changed in inclination. Size results from the anterior relations of the spectra (distance between paired pencils), and not from the width of wave-front.

These inverted fringes admit of much magnification. With a strong telescope (magnification about 15) they are quite sharp only in a part of the magnified spectrum and grow vague beyond, showing that the component spectra are not quite identical after the two reflections. When not quite in adjustment, the strip is liable to exhibit separate oblique strands, lying within

the same strip or region (fig. 47). They may become sharp by changing the focal plane of the eye-piece. When parallel to the length of the spectrum and seen in a strong telescope, about 7 lines alternately black and white may be counted. The whole lie within a strip of not much above $D_1 D_2$ width. The range of displacement of $M$ for a rotation of 180° of fringes is about 0.25 cm. Change of size of fringes from red to violet is hardly appreciable.
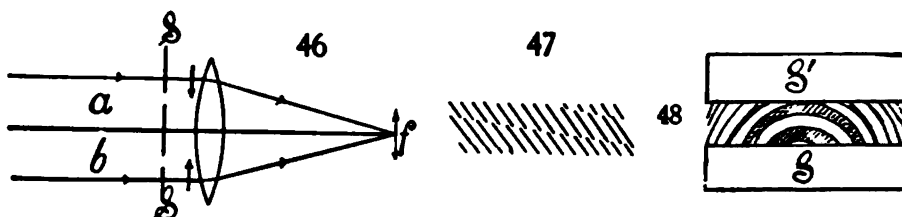


The same results may be obtained by placing a screen $SS$, figure 46, with two parallel slits, under the vertical telescope, to admit and limit the two rays $c$ and $c'$ in figure 44. It was found that slits 3 or even 6 mm. apart may still show fringes, though they are obviously smaller as the distance apart is greater. The most interesting results were obtained by bringing the rays a little beyond the edge of the prism, so that the spectra in the telescope $SS'$, figure 48, are separated at some distance. A long collimator (1 meter) is advantageous. In this way the character of these fringes was definitely established. They are of the elliptic type, as suggested in the figure, characteristic of the displacement interferometer, and the cases, figure 45, $a$, $b$, $c$, $d$, $e$, are thus merely the intercepts of ellipses with the distant centers, between parallels. Very coarse central fringes were obtained in the dark gap, and the displacement at mirror $M$, between the extreme hair-line types, was now only about 0.08 cm., all fringes filing by the coincident $D$ lines while the micrometer shifted.

Hence this method is available for displacement interferometry, the horizontal type $c$, figure 45, normal to the $D$ lines, being used for setting the micrometer at $M$. If a plate of glass of thickness $E$ and index of refraction $\mu$ is inserted normally into one beam, the corresponding air-path is

$$s = E\left(\mu - 1 - \lambda \frac{d\mu}{d\lambda}\right) = E\left(\mu - 1 + \frac{2B}{\lambda^2}\right)$$

when $B$ is Cauchy's constant and the wave-length $\lambda$. I assumed $B = 4.6 \times 10^{-11}$ and $B/\lambda^2 = 0.0265$. On the other hand, the same air-path for a normal displacement, $e$, of the mirror as given by the micrometer-screw is

$$X = 2e \cos (90° - \theta)/2 = 2e \cos \delta/2$$

where $\theta$ is the angle of diffraction of the grating $G$, figure 43, and $b\,b'$ is normal to the direction of incident light. Hence

$$E(\mu - 1 + 2B/\lambda^2) = 2e \cos (90° - \theta)/2$$

A rough experiment was made with a plate $E = 2.2$ cm. thick, $\mu = 1.53$.

The corresponding displacement found was $e=0.92$ cm. The computed displacement should be $e=0.80$ cm. The low value was supposed to be due to the need of readjustment (wedge-shape) and insufficient normality of plate. Further data (table 13) were therefore investigated for thinner plates, but they do not clear away the difficulties.

TABLE 13.—Inverted spectra.   $\theta=9°\ 39'$.   $x=2e\cos(90°-\theta)/2$.
$\mu=1.526$; $B=4.6\times10^{-11}$; $2B/\lambda^2=0.0265$; $s=E(\mu-1)+2EB/\lambda^2$.

| $E$ Observed. | $e$ Observed. | $x$ | $e$ Computed from $x=s$ | $s$ | $E$ Computed from $e$ (observed) and $x=s$ |
|---|---|---|---|---|---|
| 0.736 | 0.298 | 0.455 | 0.268 | 0.3901 +0.0195 | 0.817 |
|  | 0.282 | 0.431 | 0.268 | =0.4096 | 0.774 |
|  | 0.295 | 0.451 | 0.268 | ....... | 0.809 |
|  | 0.314 | 0.480 | 0.268 | ....... | 0.861 |
|  | 0.311 | 0.475 | 0.268 | ....... | 0.853 |

In table 13, $e$ is the observed normal displacement of the mirror $M$, $x$ the corresponding computed path-difference, $s$ the path-difference computed for the glass of thickness $E$ and the index of refraction $\mu$. From $s$ the displacement $e$ or from $x$ the glass thickness $E$ may be computed. These are given in the table. In the second and third parts of the table, the edge of the prism $P'$ was inclined at an angle to the line of symmetry, in opposite directions. The effect of this is manifest, but it does not explain the very large values of $x$ for the symmetrical adjustment (rays from grating to mirror making an isosceles triangle) of the next observations. These were made with care. $P'$, figure 43, lay at the middle of the base of the isosceles triangle of rays from $G$. The long collimator was used, giving two splendid spectra, and rays were raised until magnificent large, cord-like fringes appeared. The longitudinal fringe, a single line normal to the sodium lines extending throughout the spectrum, made it possible to set the micrometer to about 0.0003 cm., or 5 wave-lengths. The motion of fringes with the rotation of plate being very striking, the plate was placed in the normal position to the rays by noting the retrogression of fringes at this point. The total range of displacement between extreme hair-like striations was 0.25 to 0.30 cm. One circumstance was noticed for the first time—that on limiting the blade-like beam from below (as above described) the fringes not only enlarge, but rotate—*i.e.*, path-difference is modified.

It is thus difficult to ascertain the discrepancies in $x$ in table 13, as these values should be nearly 0.41 cm. throughout, or in $e$, which should be about 0.27 cm. when the prism is symmetrically placed.

**32. Inverted spectra.  Further measurements.**—The curious results shown in table 13 induced me to endeavor to detect the nature of the discrepancy by displacing the prism in the direction of the beams incident upon it.  To

do this effectively it was necessary to do the work at long distances (meters), in order that adequate space might be available between opaque mirrors and prism. Accordingly $M$, $N$, $P'$, figure 43, were all placed on micrometers, with the screws normal to the faces of the mirrors and the right edge of the prism, respectively. The fringes were found without difficulty and they were large and perfect near the edge of contact of the spectra. Though the sunlight was waning, a few measurements of ranges of displacement were made. They were on the average ($e$ at $M$ and $N$, $y$ at $P$):

$$e_M = 0.095 \text{ cm.} \qquad e_N = 0.097 \text{ cm.} \qquad y = 0.062 \text{ cm.}$$

and since $x = 2e \cos \delta/2$ should correspond to $2y$,

$$x_M = 0.145 \text{ cm.} \qquad x_N = 0.148 \text{ cm.} \qquad 2y = 0.124 \text{ cm.}$$

Here, as above, $x > 2y$, or the sliding along the edge of $P$ which accompanies $e$ is distinctly effective, being nearly 16 per cent of $2y$.

Next day, with a bright sun, so that much finer fringes could still be detected, the range could be increased to $e_M = 0.2$ cm. or $x_M = 0.3$ cm. when the spectra were all but separated on their near edges and fringes very large. For the case of much overlapping of spectra, $e_M = 0.15$ cm., $x_M = 0.22$ cm., were obtained. Finally, when the spectra were all but separated on the far edges (implying reflection at some distance from the edge of the prism $P$), the fringes were glittering, but too small to be distinctly seen.

TABLE 14.—Inverted spectra. Long distances. Plate. $E = 0.434$ cm.; $\mu = 1.533$; $B = 4.6 \times 10^{-11}$; $z = 0.2313 + .0115 = 0.2428$.

| Series, etc. | Observed $e$ | Observed $e$ | Observed $2y$ | $x$ | $x$ |
|---|---|---|---|---|---|
| | cm. | cm. | cm. | cm. | cm. |
| I. Ruled grating. $10^6 D = 352$ | 0.184 | 0.186 | 0.253 | ..... | ..... |
| | 0.184 | 0.185 | 0.253 | ..... | ..... |
| Mean................ | 0.184 | 0.185 | 0.253 | 0.281 | 0.283 |
| II. Do., another adjustment.. | 0.185 | 0.184 | 0.246 | ..... | ..... |
| | 0.185 | 0.184 | 0.246 | ..... | ..... |
| | 0.186 | ..... | 0.248 | ..... | .. |
| | 0.186 | ..... | 0.248 | ..... | ..... |
| Mean................ | 0.185 | 0.184 | 0.247 | 0.283 | 0.281 |
| III. Do., another adjustment.. | ..... | ..... | 0.244 | ..... | ..... |
| | ..... | ..... | 0.244 | ..... | ..... |
| IV. Film grating. $10^6 D = 167$. | ..... | ..... | 0.234 | ..... | ..... |
| | ..... | ..... | 0.240 | ..... | ..... |
| V. Prism 60°.............. | ..... | ..... | 0.244 | ..... | ..... |

In table 14 the results for $e_M$, $e_N$, and $y$ are given, when these displacements are produced by a glass plate $E = 0.434$ cm. thick. If the coefficient of dispersion $B$ is assumed, the displacement computed from $\lambda$, $\mu$, $E$ would be $z = 0.243$ cm. Although the values of $2y$ are larger than this, the difference

must be ascribed to the assumed value of $B$ and to the difficulty of placing the plate normal to the rays. The method of reversion of fringes, used elsewhere, is not sufficiently sensitive here. The data for $x$ are again in excess of $y$ by about 13 per cent.

Finally, a series of consecutive measurements were made of the ranges of displacement, $2y$, for different dispersive powers at $G$, figure 43, all under (otherwise) like circumstances. The mean results were for

| | | |
|---|---|---|
| 60° prism............$d\theta/d\lambda =$ 760. | $2y = 0.060$ cm. |
| Ruled grating........ 2,880. | .117 |
| Film grating......... 6,400. | .208 |

Three or more measurements, completed in each case, were in good agreement. The attempt was also made to use a 45° prism here, but the spectra were too small and the fringes could not be found. In each of these cases the value of $2y$ for the plate $E = 0.434$ cm., as shown in table 14, series III, IV, V, are virtually the same. The rapid increase of range of displacement with the dispersion of the system is thus again encountered.

**33. Rotation of fringes.**—A word must now be given relative to the rotation of fringes, which is here throughout 180°, whereas in the similar case above (Chapter I, §§ 25, 26) the rotation was but 90°. It will be seen on consulting figure 43 that if $M$ moves micrometrically, normal to itself, the pencil $b$ will slide fore and aft, along the edge of the reflecting prism $P'$. Thus $b$ may be either in front of or behind $b'$ or coplanar with it in a vertical plane. It will not generally be collinear. This is an essential part of the explanation.
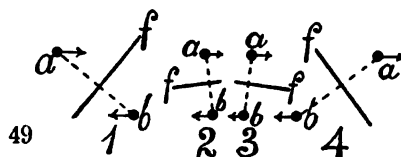


In figure 49, let $a$ and $b$ be the two patches of light of like color and origin, which produce interferences. The fringes will therefore be arranged in the direction $f$, normal to the line $ab$. Now suppose $a$ is moved toward the right or $b$ toward the left, or both, parallel to the edge of the prism, as the arrows in the figure suggest. Then the fringes will successively take the trends of which cases 1, 2, 3, 4 are typical examples. In other words, they will be markedly accelerated and retarded in passing through the cases 2 and 3 respectively. This is precisely what takes place and suggests why the case between 2 and 3 may be used as a fiducial mark in interferometry. If $a$ and $b$ also move vertically, in figure 49 there will be no essential difference, unless the latter motion is large. In such a case the rotation may become 1, 2, 2, 1.

The displacement of $b$ parallel to itself, for a normal displacement $e$ of the mirror $M$, will be, as above, figure 17, if $\delta = \theta' - \theta = 90° - \theta$

$$s = 2e \sin \delta/2$$

and the corresponding displacement of $c$ parallel to itself, since $\varphi' = 90°$, $t = s \tan \varphi'/2 = s = 2e \sin \delta/2$.

If $\theta = 9°39'$, $t = s = 2e \times 0.81 = 1.62e$. Thus if $e = 0.25$ cm., $t = 0.4$ cm., and since $t$ is twice the width of the patches or strips sliding over each other, the width of this strip would be 0.2 cm.

It is the sliding of the pencil $b$ along the edge of $P'$ which introduces additional path-differences whenever $P'$ is not symmetrical and its edge not parallel to the plane $a\,a'$. It is probable also that the same restrictions as to the breadth and depth of efficient wave-fronts will apply here as before; but this should be specially investigated. The nearly circular outline of the locus of fringes, when spectra are both reversed and inverted in § 36, even though homogeneous light is in question in the last case, clearly points in this direction.

**34. Range of displacement varying with orientation of reflector P'.**—The displacement $e$ of the mirrors $M$ and $N$ slides the corresponding pencil $b$ or $b'$, figure 43, along the edge of the reflecting prism $P'$, and a reason for the rotation of fringes is thus easily at hand. It does not at once appear why the right or the left displacement ($y$) of $P'$ should also produce a rotation of fringes; for here the pencils $b$ and $b'$ remain collinear and there is no sliding. It must thus be remembered, however, that the fringes are ultimately elliptic; for the axis parallel to the Fraunhofer lines is conditioned by the obliquity of rays in this plane only, whereas the axis in the direction of the length of spectrum depends on dispersion. The motion $y$ of $P'$ displaces these ellipses bodily through the spectrum. Hence the fringes first appear at any given Fraunhofer line in the form of hair-like striations parallel to it. These enlarge and rotate to a maximum normal to the Fraunhofer line. In fact, a single interference line may now run from end to end of the spectrum. Thereafter the fringes vanish in symmetrically the same manner and are last seen as fine striations parallel to the Fraunhofer line. It is possible, therefore, that the sliding of pencils which accompanies the $e$ displacement accounts for the difference of values of $x = 2e \cos \delta/2$ and $2y$.

Before discussing this question further it seemed necessary to study the effect of different orientations of $P'$ relative to the $b\,b'$ rays. One may note, preliminarily, that a rotation of $M$ and $N$ on a horizontal axis parallel to their faces, or of $P'$ on a horizontal axis parallel to its edge, also rotates the fringes; but it seems probable that these motions are virtually equivalent to a displacement, $y$, of the edge of the prism.

The fringes may be seen in all focal planes, at least the long line parallel to the length of spectrum. The others may often be restored by rotating the grating. The marked occurrence of fringes in the narrow longitudinal gap between two spectra (overlapping just removed by the rotation of $M$ and $N$ on a horizontal axis) can possibly be explained in this way. These fringes in the dark space are very sharp and luminous and seen in the principal focal plane with the Fraunhofer lines. But it will usually be found that on drawing the ocular out the separated spectra will overlap at their edges again,

whereas on pushing the ocular in from the principal position the separation is increased. Hence, to account for the disturbance in the ether gap, as it were, it seems most reasonable to assume that the rays cross and interference occurs after the rays have passed the principal focal plane (*i.e.*, nearer the eye of the observer), and that the interferences occurring here are projected into the principal focal plane. Nevertheless, the fringes are so strong and sharp that the two clearly focused spectra seem to react on each other across the gap at their edges. I have pointed out similar phenomena in the preceding report (Carnegie Inst. Wash. Pub. 249). The case is just as if a telescope or lens focused on a single or a Young's double slit (with the images sharply delineated) should show fringes.

In adjusting the interferometer, figure 43, for these experiments, the following systematic plan was pursued. By a rough adjustment with sunlight and measurement, all parts of the apparatus are first placed symmetrically to each other (as in figure). The direct beam should just graze the edge of the prism $P'$ and the naked eye, viewing the edge from above, should see the two bright rays of the same color (reflected from $M$ and $N$) contiguously near the edge. In the spectra of the same length on the two sides of the prism $P'$, the same colors are opposite each other. On looking down on the edge of the prism with a telescope (fine slit), two sharp and clear spectra should be seen, which can be made to overlap at their edges in any amount by rotating $M$ and $N$ on a horizontal axis. Finally, the $D$ lines are brought into coincidence by rotating the grating $G$ on a vertical axis. The largest fringes are obtained by slightly raising and lowering the incident beam $L$ to the grazing position in question. By displacing $P$ on the micrometer, right and left, the fringes are soon found.

The first experiments were made with the object of testing the effect of a slant, to the right or left, of the edge of the prism on the range of displacement $y$. With a 60° prism at $P$, the search was found to be too difficult and therefore soon was given up. The few data obtained were: Edge of $P'$ symmetrical—range, $y = 0.061$, $0.050$, $0.062$ cm.; edge of $P'$ toward left—range, $y = 0.63$ cm.; showing no certain difference.

$P$ was therefore replaced by a ruled grating ($D = 352 \times 10^{-6}$ cm.) to obtain greater dispersion. The ranges of displacement, $y$, now found were: edge of $P'$ to left, $y = 0.120$, $0.130$ cm.; edge of $P'$ symmetrical, $y = 0.128$, $0.127$ cm.; edge of $P'$ to right—$y = 0.110$, $0.113$ cm.; readjusted, $0.130$, $0.132$ cm. These differences are apparently incidental, as much depends on the light. In a darker field fringes vanish sooner. One may assume that slight inclinations of the edge of the reflecting prism $P'$ are without consequence.

The next experiment was to determine the effect of a lack of collinearity of the rays $b\,b'$. This shows itself to the naked eye looking down upon the edge of the prism from above, since by rotating $M$ and $N$ in contrary directions around a vertical axis the bright spots of light move along the edge of the prism from front to rear, or the reverse. If regarded by a telescope, the axis of the instrument will be correspondingly inclined toward the front

or to the rear. The data obtained for the range of displacement were now: Images and telescope toward rear, $y=0.124$, $0.140$ cm.; $y=0.150$, $0.142$ cm.; images and telescope toward front, $y=0.146$ cm., $y=0.154$ cm.

These differences are again incidental. The following data were subsequently found: Telescope inclined rearward, $y=0.100$, $0.110$ cm.; $0.143$, $0.140$ cm.; telescope vertical, $y=0.150$, $0.150$ cm.; $0.162$, $0.151$ cm.; telescope inclined forward, $y=0.150$, $0.133$ cm.; $0.145$, $0.162$ cm.

In the first experiment the illumination was insufficient, so that the finer fringes escaped detection. Hence, it is here also probable that slight departure from collinearity in the rays $b\ b'$, normal to the edge of the prism $P'$, is without consequence. Discrepancies are introduced by changes in the intensity of light—conditions which are often hard to control.

As the range of displacement is not a quantity which can be accurately ascertained, the effect of the insertion of a glass-plate compensator, $0.434$ cm. thick, was determined, with a similar end in view, for different angles of the rays $b\ b'$ (nearly normal) to the edge of the prism $P'$. The results were: Telescope inclined toward front, $y=0.122$, $0.123$ cm.; telescope vertical, $y=0.122$, $0.122$, $0.122$ cm.; telescope inclined toward the rear, $y=0.120$, $0.121$ cm. These are the differences of the displacement corresponding to the linear central fringes normal to the sodium lines, obtained in the presence and absence of the plate. The path-difference computed above was $s=0.2428$ cm. This is as near $2y$ as the observations warrant.

It follows, therefore, even if the observations are in their nature not very precise, that if the rays $b$ and $b'$ meet at such small angles as any reasonable adjustment may introduce, the effect may be disregarded. Furthermore, that the difference between $x=2s\cos\delta/2$ (where $s$ is obtained by moving the mirrors $M$ and $N$ parallel to themselves) and $2y$ (obtained by moving $P'$ at right angles to its edge) is to be ascribed to the sliding along or across the edge. The rotation of fringes which necessarily occurs in displacement interferometry by the shifting of the ellipses is augmented or decreased in the former case ($x$) by the equivalent of the sliding in question. The reason for this has clearly been suggested in connection with figure 18, Chapter I, and figure 49, Chapter II.

**35. Range of displacement varying with dispersion.**—The interesting method in Chapter I, § 25, where the opaque mirrors are replaced by two identical gratings (halves of the same grating) with the object of obtaining successive orders of dispersion, may be used in connection with figure 43 of the present chapter. It is therefore the object to find the range of displacement $y$ of the prism $P'$ when the fringes pass from the initial transverse hair-lines to the final transverse hair-lines (fig. 45), through the longitudinal maximum of size. The same difficulty inheres in this method as in the above, viz, it is not possible to state precisely when the hair-lines have vanished; but the successive orders of range of displacement are so different that interpretable results are obtained. The experiments in the large interferometer

proved very trying, however, because the ruled faces of the available gratings at $M$ and $N$ were but 0.5 inch square. There is thus, without refined and special instrumental equipment, considerable difficulty in adjusting the rays to this small surface. This was particularly true in the higher orders of spectra.

To obtain sufficient light the resolving grating $G$ was replaced by a 60° prism. The dispersive powers are thus the same as in § 25, Chapter I. The work proceeded smoothly in the orders of 0 (reflection from grating face) and 1. In the third, the fringes were hard to find and hard to retain, for reasons which I do not understand. There was abundance of light, except in the fourth order, which was abandoned for that reason. The best results were:

| Order 0, $y = 0.066$ cm. | $d\theta/d\lambda =$ 760 |
|---|---|
| 1, | .230 | 3,500 |
| 2, | .450 | 6,400 |
| 3, | .650 | 9,900 |

Though much time was spent on this work, the results (excepting the first) are doubtless still too low. Since the path-difference $2y$ corresponds to $x = 2e \cos \delta/2$, *cæteris paribus*, and since the data in $x$, table 12, are essentially half the total range (rotation but 90°, while it is 180° here), $y$ corresponds to $x$. Thus the results in table 12 are larger throughout, but the present data make a smoother series even through the third order.

**36. Spectra both reversed and inverted.**—This is an interesting combination of the two methods of investigation and not very difficult to produce. Retaining the adjustment for inverted spectra as in § 30, figure 43, the light impinging on the grating $G$ is dispersed, preferably by a direct-vision grating (with auxiliary prism). The rulings of both gratings (the prism grating $g$ inserted as shown being between the collimator at some distance and the grating of the interferometer $G$, figure 43) must be parallel. If the grating constants are different ($D = 167 \times 10^{-6}$ cm. film and $D = 352 \times 10^{-6}$ ruled grating were employed), the spectra in the telescope are naturally of different lengths; for the dispersion of the prism grating $g$ is increased on one side and decreased on the other side by the second grating $G$. Moreover, this decrease from the larger dispersion of the first grating $g$ is beyond zero (achromatism) into negative values. Hence, the corresponding duplicate spectrum in the telescope is a small and a large spectrum reversed, while the inversion remains intact. In the experiment made, the larger $D'_1 D'_2$ distance was somewhat more than twice the smaller $D_1 D_2$.

It is now merely necessary to place any longitudinal axis (line of symmetry) of the spectra in contact, or it is but necessary that the spectra are longitudinally parallel and overlap. The phenomenon $a$, figure 50, then appears at the intersection of the lines of longitudinal and of transverse symmetry. It is thus proportionately nearer the smaller $D_1 D_2$ and farther from the larger $D'_1 D'_2$ doublets, but always between them. If the $D_1 D_2$ lie within the $D'_1 D'_2$ lines, the fringes lie within the $D_1 D_2$ pair.

The phenomenon, which should be observed with a powerful telescope, usually consists of three small elongated dots, lying within an elliptic locus, the locus usually having a transverse axis (parallel to the Fraunhofer lines) about two or three times as long as the longitudinal axis (parallel to lengths of spectra). As a rule, the width was $D_1D_2$ and the length larger than $D'_1D'_2$, but this ratio may be changed, as above, by screening off the wave-front. The fringes are not more than one-half of $D_1D_2$ apart and are frequently horizontal (longitudinal), however the micrometer at $M$ is shifted.

The interesting result is here again met, incidentally, that spectra, though of different lengths, are nevertheless quite capable of producing strong interferences.
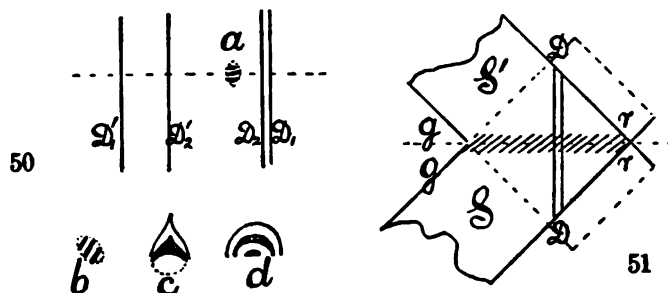
In further experiments with the long collimator and very bright spectra, a variety of other forms were obtained, shown at $b, c, d$, figure 50. In the patterns $a$ and $b$, the elliptic outline, sometimes circular, is always evident from the enhanced brightness of the bright fringes of the spot. The arrow-shaped form, $c$, inclosed a bright egg, whereas $d$ was usually sharply semicircular. As any adjustment of overlapping spectra suffices, the $D$ lines may be quite out of the field, or the spectra may be slightly separated with the interference spot in the gap.

The experiment was also made of crossing the spectra at some other angle than 0° or 180°. To do this the rulings of the prism grating were placed at right angles to those of the interferometer grating, as in Newton's method of crossed prisms. Seen in the telescope (adjusted for inverted spectra, as above, § 30) the two spectra now made an elbow with each other, figure 51, while the $D_1D_2$ lines are still parallel and can be put in coincidence. At first no interferences could be detected in any adjustment. Later, however, on using the large collimator, strong interferences were obtained in the line of symmetry of the elbow and normal to the $D$ lines, as shown. They have the same characteristics as the preceding and persist during a displacement of $M$ of about 0.3 cm.

**37. Experiments with the concave grating.**—If in the device figure 40, Chapter I, the prism $P$ is rotated 90° on an axis parallel to $b\,b'$, so that the rays move upward, the phenomenon of inverted spectra may be realized. The fringes are observed with a lens from above or reflected forward. They

were found without much difficulty and showed a range of displacement ($y$) of the prism $P$, right or left, in various adjustments, of at least $y = 0.71, 0.61, 0.67$ cm. larger, therefore, than with the forward prism, as was inferred. Of course, much depends upon how far the extremely fine fringes at the beginning and end are pursued.

This method is not very convenient for the present purposes. In the first place, the distance $GMPF$ is given, an unnecessary restriction on the adjustment, unless the lens $T$ is replaced by a short-distance telescope, which has other disadvantages. In the second place, the mirrors $M$ and $N$ can not be used for displacement, as they move the Fraunhofer lines of the corresponding spectrum. In fact, $M$ or $N$ affords a method for the adjustment of these lines to coincidence. Finally, the amount of overlapping which is usually secured is always very partial, and if the edge of the prism $P$ is not quite sharp and well silvered, the edges are ragged. Even in the right-and-left displacement ($y$) of $P$, the spectra are carried bodily with it in front of $T$. Although this is no serious objection, it is an unnecessary complication. In spite of the brilliant spectra and large ranges, I did not spend much time in developing the method.

**38. Conclusion. General methods.**—The origin of the phenomenon of reversed spectra seems to be the slit of the collimator, the diffraction of which furnishes a patch of light, effectively 1 or 2 mm. in breadth, out of which the component rays are to be separated. Spectroscopically the slit furnishes the degree of homogeneous light within which the phenomenon may be developed.

In the case of inverted spectra, the slit is not primarily necessary, for here the interferences occur in the direction of (or the fringes lie normally to) the Fraunhofer lines and therefore virtually in homogeneous light. The fringes are due to the continuous changes of the obliquity of rays in each separate color and thus belong to the phenomenon of a wide slit with homogeneous light. The fringes of reversed spectra owe their occurrence to the continuous change of the obliquity of rays produced by dispersion and require a spectroscopic slit. In the case of combined inversion and reversion, the locus of fringes is not far from circular, though the major axis of the ellipse corresponds to the inversion. Obliquity and dispersion are thus about equally effective.

The patch of light rays of identical origin may now be separated into two component rays by a variety of methods. The white pencil may simply be cleaved by the edge of a sharp silvered prism, or the pencil may be refracted into two beams at a blunt-edged prism, or the separation may be produced by the diffraction of a grating, by polarization, etc.

Two entirely distinct pencils are thus obtained, subject to independent control, by which the phenomenon of diffraction may be generalized. In other words, in the classical experiments in diffraction, the diffracting system is rigid. Take, for instance, the following experiment, which has a close bearing on the phenomenon of this paper. In figure 52, $L$ is a distant slit or a fine Nernst filament, $P$ the principal plane of the objective of a telescope

with the principal focus at $F$, to be observed with the eye-piece. The screen $s\,s'$ with a double slit parallel to the linear source $L$ is placed in front of the objective. Brilliant interferences are then seen at $F$, which are coarser as the distance $e$ between the slits $s\,s'$ is smaller, and if the distance $PF$ is $r$ and the distance between fringes is $x$, the usual equation

$$\lambda/e = x/r$$

is applicable. Owing to the direct application of this experiment to the above investigations, its very fundamental importance in the theory of resolution of optical instruments, etc., it seemed worth while to give it experimental treatment here. The screen $s\,s'$ is conveniently made by cutting parallel lines with a sharp triangular cutting stylus and a steel T-square, on a blackened gelatine dry plate. A number of such doublets 0.05 to 0.5 cm. apart may be ruled at a distance of about 0.5 inch apart. When the parts are assembled, the fringes may be seen in all focal planes $F$, and the fringes are in fact much more brilliant with the ocular out of focus. The enormously large diffraction of each single slit is simultaneously visible, and if two doublets are close enough together, their systems may be seen superposed. If $c$ is small (less than 0.1 cm.) the fringes are in fact visible to the naked eye without a telescope. With two identical doublets close together, the fringes may be seen to be alternately in step and out, as the ocular of the telescope moves outward, until finally the diffractions of the "rod" between the doublets is strikingly manifest. This has also been generalized in the present work.
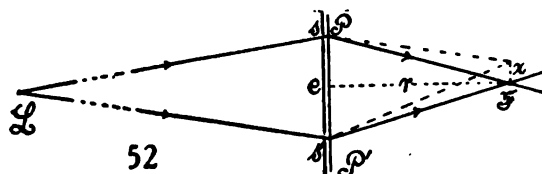


In all these classical cases there is a continuous succession of pairs of corresponding points (one of the pair in each slit of the doublet) between which interferences occur. The line of any two such points is rigidly normal to the direction of the slits. In the above experiments with spectra, however, the two points may not only have any relation to each other, but either point may be moved at pleasure. This gives rise to the bewildering variety of beautiful phenomena, some of them useful, which I have tried to describe in the present and preceding reports.

With the beams of like origin separated, it is next necessary to bring them together again. This requires at least one independently controllable reflection for each beam. In the interesting group of phenomena obtained with crossed rays, two reflections may be desirable, though with a change of apparatus a single reflection here also suffices. Thereafter the beams may be compounded in a manner inverse to the one by which they were produced, for instance, by the reflection of a silvered obtuse prism, by refraction toward the edge of a prism, by a grating, by polarization, etc. To observe the recom-

bined ray, the telescope is always the more convenient instrument, since its use is not restricted to definite distances from the system.

It has been shown that as a whole the above phenomena correspond very closely to the behavior of the ellipses encountered in displacement interferometry. Thus the cases of non-reversed spectra, of inverted spectra, etc., if we disregard certain exceptional accompaniments for the moment, can be at once so classified. The shift of ellipses behind a narrow slit in an opaque screen and observed in front of it, for instance, would exhibit all the rotational occurrences.

**39. Displacement interferometry. Equations.**—It is thus desirable to adduce the equations of displacement interferometry in a somewhat different way, but in the main as taken from my earlier reports. In figure 53, *G* is a thick plate of glass on which the blade-shaped pencil of white light *L* from a collimator impinges at an angle *i*. *M* and *N* are the opaque mirrors of a Michelson device. *G'* is a plate grating by which the white beam *R* (feeble spectrum) is resolved, *P* the principal plane of the objective of the telescope, *rv* the image seen through the ocular. The plate disperses the white light *L* into the spectrum *rv*, as shown in the figure. The direct reflection at *R'* is not used. For convenience in discussion the mirror *N* and its component ray may be rotated 180° around the trace of the grating *G* as an axis, into the position *N'*, where *IN* becomes $x +$



$x'+p+x''$, intercepted between normals. If perpendiculars be let fall from *I* to *N* or *N'* and *I'* to *M*, their difference of length is

(1) $$N = x + x'' = e \cos i + x''$$

*N* is an important coördinate used throughout, below, since it is independent of color ($\lambda$ and $\mu$). In (1) *i* is the angle of incidence, *R* of refraction of the plate of thickness *e* and index of refraction $\mu$.

If we draw the wave-front *w*, the path-length of the red ray through glass to *M*, for instance, is $e\mu/\cos R + p$. The path of the ray through air (only) to mirror *M* is

$$x + x' + p + x'' = e \cos i + e \sin i \tan R + p + x''$$

If $\sin i = \mu \sin R$ be introduced, the path-difference thus becomes, after reduction,

(2) $$n\lambda = 2N - 2e\mu \cos R$$

or

(3) $$n\lambda = 2e \left( \mu - \cos(i-R) \right) / \cos R$$
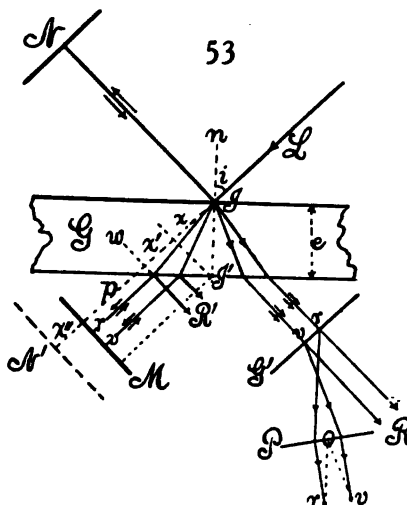
the first equation being more practical. $N$, therefore, is the differences in distances of the extremities $I$, $I'$ of the normal $n$ at the point of impact $I$ from the mirrors $N$ and $M$ respectively; $x''$ is the air-distance apart of the two mirrors (after rotation).

To find the change of wave-length per fringe, $d\lambda/dn$ may be deduced.

(4)  $$2\frac{d\lambda}{dn} = \frac{\lambda^2}{N-\epsilon(\mu\cos R+\lambda(d\mu/d\lambda)/\cos R)}$$

This equation has a maximum when

(5)  $$N=N_\epsilon=\epsilon\left(\mu\cos R + \frac{\lambda}{\cos R}\frac{d\mu}{d\lambda}\right)$$

and this is the coördinate $N_\epsilon$ for centers of ellipses on any given spectrum line $\lambda$. $N=N_\epsilon$ in equation (2) gives

(6)  $$n_\epsilon = \frac{2\epsilon}{\cos R}\frac{d\mu}{d\lambda}$$

In general $\mu=A+B/\lambda^2$; $\dfrac{d\mu}{d\lambda}=\dfrac{-2B}{\lambda^3}$ is adequate for experimental work. Thus

if $B=4.6\times10^{-11}$, $\epsilon=1$ cm., $R=0$, then $n_\epsilon=880$, or 880 sodium wave-lengths are expended in the path-difference at the elliptic center.

If $n'$ fringes pass at a given color $\lambda$ for a displacement $\Delta N$ of the mirror $M$

(7)                    $$\lambda=2\Delta N/n'$$

If $n'$ fringes lie between two given colors $\lambda$ and $\lambda'$ for the same position $N$ of the micrometer mirror $M$

(8)  $$n'=2\epsilon\left(\frac{\mu'\cos R'}{\lambda'}-\frac{\mu\cos R}{\lambda}\right)-2N\left(\frac{1}{\lambda'}-\frac{1}{\lambda}\right)$$

or if $\delta$ is the differential symbol

$$n'=2\epsilon\delta\frac{\mu\cos R}{\lambda}-2N\delta\frac{1}{\lambda}$$

The question next of interest is the change of the angle of altitude of the ray per fringes transversely to the spectrum. Light is homogeneous, $N$ therefore constant. Let $\alpha$ be the angle of altitude of an oblique ray in the horizontal plane $L$, figure 53, impinging at $I$. If $i'$ and $R'$ are the corresponding angles of incidence and refraction, then $i''$, $i$, $\alpha$ make up the sides of a spherical triangle, right-angled at the angle opposite $i'$. Hence

(9)     $\cos i'=\cos i\cos\alpha$, and $\mu\cos R'=\sqrt{\mu^2-1+\cos^2 i\cos^2 a}$

With this introduction of $R'$ for $R$, equation (2) is again applicable, since nothing has been changed in $N$, $\epsilon$, $\mu$, $\lambda$, or $i$. Hence

(10)                $n\lambda=2N-2\epsilon\sqrt{\mu^2-1+\cos^2 i\cos^2 a}$

To determine the change of altitude per fringe,

(11)
$$\frac{d\alpha}{dn} = \frac{\lambda\sqrt{\mu^2 - 1 + \cos^2 i \cos^2 \alpha}}{e \cos^2 i \sin 2\alpha}$$

and this is a maximum when $\alpha = 0$; i.e., in the plane of figure 53. In this case equation (2) is reproduced from (10), so that a double maximum occurs for $\alpha = 0$ and

$$N_e = 2e \left( \mu \cos R + \frac{\lambda}{\cos R} \frac{d\mu}{d\lambda} \right)$$

The other practical datum is the shift of a given fringe per centimeter of displacement of the mirrors. Here $n$ and $e$ are constant while $N$, $\lambda$, $\mu$, $R$ vary, so that

(12)
$$\frac{d\lambda}{dN} = \frac{2}{n + \dfrac{2e}{\cos R}\dfrac{d\mu}{d\lambda}}$$

This is a maximum when $n = n_e = -\dfrac{2e}{\cos R}\dfrac{d\mu}{d\lambda} = 4eB/\lambda^3$, or when $N = N_e$. In other words, there is a minimum displacement relative to wave-length shift of fringe at the centers of ellipses.

Equation (10) is thus inclusive. If $i = 0$, which is nearly the case, experimentally, in my work and no restriction on the apparatus, and since $\alpha$ is always very small, equations (10), (11), (12), etc., may be simplified. Hence approximately ($i = 0$)

(13)
$$n\lambda = 2N - 2e\sqrt{\mu^2 - \alpha^2}$$

(14)
$$\frac{d\alpha}{dn} = \frac{\lambda}{2e\alpha}\sqrt{\mu^2 - \alpha^2}$$

(15)
$$2\frac{d\lambda}{dn} = \frac{\lambda^2}{N - e(\mu + \lambda.d\mu/d\lambda)}$$

(16)
$$\frac{d\lambda}{dN} = \frac{2}{n + 2e.d\mu/d\lambda}$$

where $n$ is the order of the fringe at $\lambda$ for $N$, $e$, $\mu$, $\alpha$. Again, $n_e = -2e.d\mu/d\lambda$.

Equation (13) admits of an interpretation in terms of the approximately elliptic locus found for constant $n$. The equation may be written, if $\mu$ is treated as a mean constant,

$$\frac{e^2(\alpha/\mu)^2}{e^2} + \frac{(\lambda - 2N/n)^2}{(2e\mu/n)^2} = 1$$

Here $e$ $(\alpha/\mu)$ and $\lambda$ may be regarded as the coördinates of a curve described on the face of the plate of glass toward the observer, so that the equation is an ellipse referred to an eccentric axis of ordinates. The axes of this ellipse are $2e\mu/n$ horizontally and $e$ vertically. Of course, the telescope converges all this to a

single white image of the slit; but the grating $G$ reproduces the spectrum and enlarges it, in which case, however, not absolute position but the direction of rays is the determining factor.

**40. Continued. Reversed spectra, etc.**—The equation underlying the greater number of experiments in the work with reversed spectra is of the form

(17) $$n\lambda = 2e \cos \delta/2$$

where $\delta$ is the double angle of incidence at either opaque mirror and $e$ is the effective distance apart of the two mirrors—$i.e.$, the distance between the faces when one is rotated $180°$ about the axis of symmetry into parallelism with the other. In the present case, therefore, $e$ corresponds to $N$ in § 39. The angle $\delta = \theta_2 - \theta_1$, where $\theta_2$ and $\theta_1$ are the angles of refraction of the collecting and the dispersing grating, respectively, so that $\sin \theta = \lambda/D$ if $D$ is the grating space. If the silvered right-angled reflecting prism is used for alining the separated pencils, $\delta = 90° - \theta_1$.

From the above equation the change of $\lambda$ per fringe is

(18) $$\frac{d\lambda}{dn} = -\frac{\lambda^2}{e\left(2 \cos \delta/2 + \lambda(d\delta/d\lambda) \sin \delta/2\right)}$$

Since $\lambda d\delta/d\lambda = \lambda/D \cos \theta = \tan \theta$

(19) $$\frac{d\lambda}{dn} = -\frac{\lambda^2}{e\left(2 \cos \delta/2 + \sin \delta/2(\tan \theta_2 - \tan \theta_1)\right)}$$

This is a maximum if $e = 0$, as the quantity in the parenthesis can not vanish for very acute angles, such as $\theta$ and $\delta$ must be.

If $\delta = 0$, or $D_1 = D_2$, $d\lambda/dn = -\lambda^2/2e$.

Similarly, since $e$ is now the micrometer variable or coördinate, and $n$ constant,

(20) $$\frac{d\lambda}{de} = \frac{2\lambda}{e\left(2 + \tan \delta/2(\tan \theta_2 - \tan \theta_1)\right)}$$

from which the similar conclusions may be drawn with regard to the motion of a given fringe. There is a maximum for $e = 0$. The equation, it will be seen, is quite cumbersome, so that further treatment is inexpedient. Nevertheless equation (20), if $\theta$ and $\delta$ are expressed in terms of $\lambda$, should admit of integration, at least approximately.

The equation $n\lambda = 2e \cos (90° - \theta)/2$ for reflecting prisms needs special treatment, since $90°$ is not derived from $\theta$. The coefficients after reduction become

(21) $$\frac{d\lambda}{dn} = \frac{-\lambda^2 \sqrt{2D(D+\lambda)}}{e(2D+)\lambda}$$

and

(22) $$\frac{d\lambda}{de} = \frac{2\lambda(D+\lambda)}{e(2D+\lambda)} = \frac{2}{C}\frac{(D+\lambda)^{3/2}}{2D+\lambda} \text{ with the aid of (23).}$$

In both cases there is a maximum for $e = 0$.

Equation (22) may be integrated, and if $C$ is an experimental constant,

$$(23) \qquad e^2 = C^2 \frac{\lambda^2}{D+\lambda} = e_0^2 \frac{\lambda}{D+\lambda} \text{ if } e = e_0 \text{ for } D = 0$$

There remains the equation for crossed rays or achromatic conditions,

$$n\lambda = 2e \cos \frac{180^\circ - 2\theta}{2} = 2e\lambda/D$$

or

$$(24) \qquad\qquad\qquad e = nD/2$$

in which there should be no motion of fringes throughout the spectrum, but for secondary reasons.

It is now possible to consider the above results on the increase of the range of displacement within which interferences are visible, with the dispersion of the grating. In this case the equations in $d\lambda/de$, viz., Nos. 20, 22, as well as 23 and 24, may be consulted. Since $\sin \theta = \lambda/D$, all of them involve the dispersion $1/D$, where $D$ is the grating space. In the case of No. 24 the range of displacement should be indefinite, since the locus of fringes is stationary in the spectrum. It is found to be exceptionally large, but limited by special diffraction. Equation (20) is cumbersome, but otherwise similar to equation (22), which may be treated first. The displacement of any given fringe in wave-length increases with $f = 1/D$, the number of lines per centimeter. If a fringe travels between any two wave-lengths $\lambda$ and $\lambda'$ and if $D$ is large relative to $\lambda$, equation (23) shows that approximately

$$\Delta e = e - e' = C\sqrt{f} \left( \sqrt{\lambda} - \sqrt{\lambda'} \right)$$

The range of displacement should therefore be roughly proportional to the square root of the dispersion, and one is not at once at liberty to conclude that the uniformity of wave-trains is enhanced by dispersion.

In fact, if $D$ is not large compared with $\lambda$, as in the higher orders of dispersion, the full equation must be taken. Unfortunately the data of Chapter I, § 25, table 12, which are the most complete, do not easily admit of computation in full. I have compared them both with $e = e_0\sqrt{\lambda/(D+\lambda)}$, in which the ratios of $e$ observed and computed run up with $D$, regularly, from 1 to 7; and with $2de/d\lambda = C(2D+\lambda)/(D+\lambda)^{3/2}$, in which the regular change of ratios for the same $D$ (as $D$ decreases) is again from 1 to 7. In other words, the observed values of $e$ varying with $D$ decrease enormously faster than coefficients of this type, as they should. In view of the equation

$$e = e_0\sqrt{\lambda/(D+\lambda)}$$

it follows that

$$\frac{de}{dD} = \frac{-e_0}{2} \sqrt{\frac{\lambda}{(D+\lambda)^3}}$$

and the comparison of the $e$ observed in table 12 with this coefficient is therefore crucial.

To determine $D$ from table 12 we have $D=D'/n=1/(\cos \theta_n \cdot d\theta_n/d\lambda)$, where $n$ is the order of the spectrum and $d\theta_n/d\lambda$ its dispersive power, like $\theta_n$ is given in the table. In this way the data of table 15 were obtained.

TABLE 15.—Ratio of the range of displacement $e$ observed in table 13 and $de/dD$, computed.

| Order. | $D \times 10^4$ | $10^4 e$ observed. | $\sqrt{\lambda/(D+\lambda)^3}$ | Ratio $e_{obs}/\sqrt{\lambda/(D+\lambda)^3}$ |
|---|---|---|---|---|
| 0 | 1,320 | 38 | 151 | 2.5 |
| 1 | 335 | 200 | 980 | 2.1 |
| 2 | 204 | 420 | 1,800 | 2.3 |
| 3 | 158 | 520 | 2,400 | 2.2 |
| 4 | 142 | 580 | 2,690 | 2.2 |

In view of the *character* of the results for $e$, the ratio $e/\sqrt{\lambda/(D+\lambda)^3}$, where $e$ is the observed range of displacement, may be considered constant. The enormous variation of the range $e$ with the dispersive power, as observed, must therefore be regarded as in keeping with the theory of the phenomenon, although the computation is not direct. The latter would require an integration of equation (22) which may be written

$$e = \frac{e_0}{2} \int_0^\infty \frac{2D+\lambda}{\sqrt{\lambda(D+\lambda)^3}} d\lambda$$

but the simpler comparison given was regarded adequate.

Data bearing on equation (20) are given in table 11 and may after reduction be written as in table 16 ($\theta_2 = 19° 30'$, $D^2 = 177 \times 10^{-6}$).

TABLE 16.

| Range $e$ observed. | $\theta_1$ | $D \times 10^4$ | $\delta$ | $\tan \delta/2 \times (\tan \theta_2 - \tan \theta_1)$ |
|---|---|---|---|---|
| 0.33 | 2° 36' | 1,320 | 16° 54' | 0.0459 |
| .52 | 9° 39' | 352 | 9° 51' | .0156 |

The value of the term in the last column is thus small in comparison with 2 and may be neglected, as a first approximation. Hence roughly

$$e = C\lambda = n\lambda/2$$

and the range of displacement should be nearly independent of the dispersion. As it is not, some corresponding principle must here be active, and this has already been found in the shift of one illuminated strip on the collecting grating relative to the other, when either of the opaque mirrors is displaced.

For the same reason the effect produced by making $\delta = 0$, as in §24, is not marked, so far as equation (20) is concerned. If $\delta = 0$ rigorously, the original experiment with but a single grating did in fact show large ranges of displacement, in view of the absence of sliding.

We thus return to the special diffraction already mentioned in §38. When two spectra from the same source coincide, horizontally and vertically, throughout their extent, they will interfere at every point. The interference

will be visible within a certain range of path-difference. If one spectrum shrinks longitudinally on the other, the strip carrying fringes rapidly diminishes in breadth; but interference is still marked near the transverse line of coincident wave-lengths. If one spectrum is reversed with reference to the other on a transverse axis, the interferences are reduced to a single nearly linear strip coincident with the line of symmetry. The width of this strip is independent of the dispersion of the system. It depends on the breadth of colored region which contributes rays to the strip in question. Hence, if, beginning with both ends of the spectrum, rays are cut off except those very near the line of symmetry, the linear phenomenon rapidly increases in size until all light is extinguished. This is what one would expect from the theory of the diffraction of wave-fronts broad or slender, with the generalization as to the rotation of fringes to which I have already referred.

The association of the two diffractions is well illustrated by the experiments with inverted spectra. Here the edge of the reflecting prism is horizontal and normal to the interfering beams. When this edge is moved normal to itself, path-difference only is introduced. To compensate a plate 0.434 cm. thick the motion should be about 0.243 cm. The displacement found was $2y = 0.247$ cm., the difference being referable to insufficiently accurate dispersive constants. When either of the opaque mirrors moves, the corresponding beam slides along the edge of the prism and the displacement $2e = 0.370$ cm. of mirror was found, corresponding to the path-difference $x = 2e \cos \delta/2 = 0.282$ cm. About 14 per cent *more* path-difference is thus needed with sliding $(x)$ than without $(2y)$.

If now the reflecting prism is turned $90°$, so that the edge is vertical, the corresponding beams slide normally to or from the edge of the prism when the opaque mirrors are moved. The corresponding data were then found to be $2y = 0.250$ cm., $x = 0.235$ cm. Here about 6 per cent *less* path-difference is needed with sliding $(x)$ than without $(2y)$. The smaller effect in the latter case is to be expected, since the two corresponding rays slide toward each other in the same plane and can not pass through each other. In the former case they pass in marked degree across or through each other and must therefore essentially contribute to the rotation of fringes. But the sign of the effect is precisely the opposite to what one would expect. Investigations such as these and the corresponding question of the width of strip carrying interference fringes in case of crossed rays call for apparatus with better optical plate, or for more rigorous instrumental adjustment than I have been able to utilize in the present papers. It is best, therefore, to waive them for the present, however interesting the theoretical results with which they are associated.*

* I have since treated the outstanding difficulties of the text rigorously and the results will be given in a future report.

# CHAPTER III.

## ELONGATION OF METALLIC TUBES BY PRESSURE AND THE MEASUREMENT OF THE BULK MODULUS BY DISPLACEMENT INTERFEROMETRY.

**41. General method and apparatus.**—About 25 years ago[*] I obtained satisfactory results in the measurement of pressures of the order of 1,000 atmospheres by the expansion of steel tubes of suitable thickness. The tube in this case was inclosed in a snugly fitting glass tube filled with water and the volume expansion measured by an attached capillary tube, the system being submerged in water to obviate thermal discrepancies. The whole subject has since been transformed by the famous experiments of Prof. P. W. Bridgman, and I merely touch it here with the purpose of testing the optic apparatus involved and with a view to the experiment explained in the final paragraph of this paper. In the present experiments I shall attempt to measure the increase of length of a steel tube due to internal pressure, by the displacement interferometer. The experiments will lead to an independent method for the measurement of the bulk modulus (Tait) and to a procedure for studying the thermodynamics of the adiabatic expansion of liquids.



54
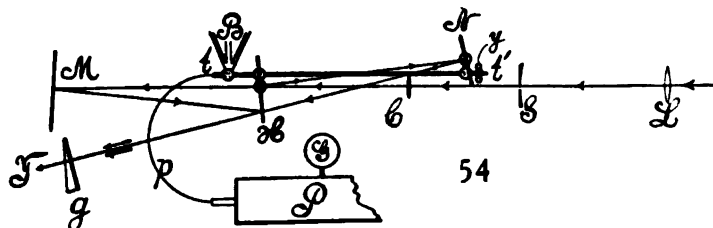
The interferometer used was of the linear type (fig. 54). Here $L$ is a weak lens, about 2 meters in focal distance and 12 cm. in diameter, concentrating a beam of sunlight on the slit $s$. $c$ is the objective of the collimator, being a spectacle lens of about 1 meter focal distance. It is particularly advantageous to have rays of slight obliquity here if a brilliant and wide spectrum is to be seen in the telescope at $T$. $H$ is the half-silvered plate of the interferometer, $N$ and $M$ (on a micrometer) are the opaque mirrors, each about 2 meters from $H$. The rays reaching the telescope $T$ would therefore show two white slit images from $N$ and from $M$, which are to be placed in coincidence both horizontally and vertically by the adjustment-screws on $M$ and

* Phil. Mag. (5), xxx, p. 338, 1890; Bull. U. S. Geol. Sur., No. 96, 1892; cf. Am. Acad. Arts and Sciences, xxv, p. 93, 1890; for effect of pressure on electrical conductivity of liquids, see Am. Journal, xl, p. 219, 1890, and on the mercury pressure-gage, Am. Journal, p. 96, xlv, 1893.

*N.* To bring out the interferences, a direct-vision prism grating *g* is placed in front of the objective of *T*, whereupon, when the path-difference *HM*, *HN* is annulled, magnificent ellipses may be seen in the bright spectrum in the field of the telescope.

The steel or other tube whose elongation under pressure is to be measured is shown diagrammatically at *t t'*. The end *t'*, moreover, is closed by a tinned-steel plug-screw, while *t* communicates, by aid of a thick-walled ½-inch tube *p* of small bore, with the screw-compressor *P* described in my earlier papers (*l. c.*). It is here that the thick hydrocarbon oil is forced into the tube *t t'* and the pressure measured by a Bourdon pressure-gage *G*, reading in steps of 10 atmospheres to 1,000 atmospheres.

The parts of the interferometer are attached directly or indirectly to a brick pier in the laboratory. *M* is separately so attached; so is also the end *t* of the steel tube by the bracket at *B*, this being fixed rigidly. The other end, *t'*, which must be free to expand, is to be supported on knife-edges or rollers of a vertical pendulum hanger *y*, the supports of which are in turn rigidly fixed to the pier. This will presently be further described. It was found that long vertical wires, supporting intermediate parts of the tube, were desirable and quite as good as more complicated arrangements.

With the tube *t t'* thus fixed except as to linear expansion toward the right, the mirror *N* is clamped by a horizontal lateral arm at the end *t'*, and the half-silvered plate *H* by a similar arm on the other side, at the end *t*. Thus the length *HN* varies with the pressure and the increment is compensated at *M* by bringing the center of ellipses back to the *D* lines in the field of the telescope. Accessories like water-jackets, etc., are left out of the figure for clearness and will not be used in these experiments.

To obviate friction, the end *t'* of the tube *t t'* was suspended from a rectangular yoke or pendulum consisting of two vertical rods *y* and *y'*, figure 55, and horizontal smooth round brass cross-rods *r* and *r'*. The latter roll on the round horizontal rods *a* and *b* suitably anchored at the same level in the pier. The rod *r'* supported the free end *t'* of the pressure tube.

To counteract vibrations the rod *y* carries a bell-shaped damper, *d*, below, submerged in oil in the cup *c*. The middle of the tube *t'* is similarly damped at its center by a bell-shaped damper in oil (not shown), against lateral and vertical vibrations.

**42. Remarks on the displacement interferometer.**—As a rule the ellipses are not seen at their best in the principal focus. The ocular must be drawn out somewhat to focus them sharply; but usually the sodium lines are still visible for guidance. No doubt this is due to the fact that ordinary glass plate was employed at *M*, *N*, and *H*, figure 54, or that *H* was not optically plane parallel. Moreover, as *M* is displaced, the focus of fringes changes; but as the centers of ellipses are used in measurement this is no particular disadvantage.

A few trials were made with lens compensators, but the available combinations reduced the ellipses to horizontal sharp spindles or lines, without

The pitch washer was therefore removed and replaced by one of *tallow* slightly hardened with a little resin or wax, the two being melted together. This functioned perfectly within 1,000 atmospheres and was easily inserted in parts which could then be molded into a disk within the stuffing-box on forcing the gland into it.

The measurements given in table 17 were made in steps of 100 atmospheres. $\Delta L$ denotes the elongation per atmosphere.

TABLE 17.

| Series. | Pressure range. | $10^6 \Delta L$ (pressure increasing). | $10^6 \Delta L$ (pressure decreasing). |
|---|---|---|---|
| 7 | 100 to 500 atm. | 8.3 cm. | 6.5 cm. |
| 8 | 100    600 | 9.2 | 6.1 |
| 9 | 100    700 | 7.9 | 6.2 |
| 10 | 100    800 | 7.9 | 7.1 |

An example of the individual results may be given in case of series 9:

Pressure ......... 100 200 300 400 500 600 700 700 600 500 400 300 200 100 atm.
Micrometer reading 1.01 9.4 8.6 7.9 7.0 6.2 5.5 5.4 6.3 7.0 7.7 8.5 9.1 9.8 cm./10³

The elongation here is always greater when pressures increase, although time is allowed for dissipation of temperature, than when they decrease. Four reasons may be assigned for this result: (1) the temperature increase on increasing pressure and *vice versa;* (2) permanent set imparted to the tube; (3) elastic warping of the tube owing to the end-thrust of internal pressures and consequent disadjustment of the interferometer; (4) viscosity of steel. Probably all of these discrepancies are present. That there was set I infer from the gradual displacement of the reading of the interferometer for 100 atmospheres at the beginning and end of a series, though this may be due to new adjustments. The incidental displacements are particularly shown in the values of $\Delta L$ when pressure increases and are specially marked in series 7 and 8. They are also apparent in the change of form of the ellipses. As sunlight was used in the above work the annoyances of a flickering arc do not occur. The ellipses were not centered.

To obtain some notion of the relation of these discrepancies we may proceed as follows: The difference between the elongation per atmosphere during the phases of increasing and decreasing pressures in the four series given is, respectively, 1.8, 3.1, 1.7, 0.8 cm./10⁶, or $1.8 \times 10^{-6}$ cm. per atmosphere of compression. For a tube-length of 160.8 cm. and a coefficient of expansion $12 \times 10^{-6}$ this is equivalent to a rise of temperature $9.3 \times 10^{-4}$, or, roughly, $10^{-3}$°C. per atmosphere of compression.

Supposing the compressibility of the oil to be $dv = 100 \times 10^{-6}$ per atmosphere per cubic centimeter and the mean pressure $p = 500$ atmospheres, the work done is $pdv$ or

$$500 \times 10^6 \times 100 \times 10^{-6} = 5 \times 10^4 \text{ ergs per atmosphere per cubic centimeter at}$$
500 atmospheres

Since the preceding datum corresponds to both increasing and decreasing pressures, the work done must be reckoned per 2 atmospheres or it will be $10^5$ ergs. Taking the specific heat of oil as 0.5 and the mechanical equivalent as $42 \times 10^6$, the rise of temperature of the oil should be

$$\frac{10^5}{0.5 \times 42 \times 10^6} = 5 \times 10^{-3} \,^\circ C., \text{ nearly}$$

Hence the residual temperature discrepancy found, 0.001 C., would be but one-fifth of the full temperature discrepancy to be anticipated—*i.e.*, four-fifths of the heat would have dissipated by conduction, etc., during the waiting between successive compressions.

The residual temperature is thus adequate to account for the full discrepancy, and if a tube of this kind is to be used as a pressure-gage, the tube should be made of "invar" or other metal without thermal expansion. True, a water-jacket surrounding the tube would improve the apparatus, but the thermal increments in question are so small that the device would not be trustworthy. If, however, a temperature discrepancy is shown by the optic gage it should also be shown by the more sensitive Bourdon gage, which is not the case. Thus a residual effect of temperature is improbable. The optical difficulties are slight and could be overcome by suspending the yoke, which in figure 55 rolls loosely on the cylinder *a, b, t'*, from steel pivots bearing on jeweled cups. Elastic and particularly slow viscous yieldings to persistent pressure are thus the probable reason for the errors. This also accounts for the displacement of the fiducial reading.

Two further experiments were now made in which the ellipses were *centered* before each observation (table 18). In the second set (series 12) the tube was attached to the yoke and the latter to the hangers by soft adhesive wax, applied in the molten state. This proved quite adequate.

TABLE 18.

| Series. | Range. | $10^6 \Delta L$ (pressure increasing). | $10^6 \Delta L$ (pressure decreasing). |
|---|---|---|---|
| 11 | 100 to 600 atm. | 7.2 | 7.2 |
| 12 | 100    600 | 7.7 | 7.7 |

The zeros were regained and the results were marked improvement on the preceding series. The same mean elongation is found for increasing and decreasing pressure; but the values are not identical in the two series. The following data give the details of series 11:

Pressure.......... 100  200  300  400  500  600  500  400  300  200  100 atm.
Micrometer reading  50   43   34   28   20   15   21   28   36   43   50 cm./$10^4$

A few units in the cm./$10^4$ place are thus uncertain. The graph is shown in figure 58.

**45. Brass tube.**—A somewhat thinner seamless tube of soft brass was next tested within 600 atmospheres. The dimensions were: length, 161 cm.; diameter within, 0.485 cm.; diameter outside, 0.960 cm. Hence

$$k = \frac{161 \times 0.235}{(0.9216 - 0.2352)3 \Delta L} = \frac{18.36}{\Delta L}$$

The ellipses were centered throughout and the yoke was given additional stability by soft adhesive wax, as above. The tube showed extraordinary variability, but during the trials under increasing and decreasing pressure and in the lapse of time the viscous changes somewhat subsided, as will be seen from table 19.

TABLE 19.

| Series. | Range of pressures. | $10^6 \Delta L$ (pressure increasing). | $10^6 \Delta L$ (pressure decreasing). |
|---------|---------------------|-------------------------|-------------------------|
| 1 | 100 to 500 atm. | .... | 15.6 cm. |
| 2 | 100    500 | 13.6 cm. | 16.5 |
| 3 | 100    500 | 13.5 | 17.0 |
| 4 | 100    600 | 13.7 | 16.7 |
| Mean.. | ............. | 13.6 | 16.7 |

Disregarding the first series, which was preliminary, the remaining data are consistent. Hence $k$ from the mean $10^6 \Delta L = 15.2$ is relative to atmospheres

$$k = 10^6 \frac{18.36}{15.2} = 1.21 \times 10^6$$

Voigt's value for brass is but $0.61 \times 10^6$, i.e., but half this. Throughout these experiments the reading for 100 atmospheres wandered continually, creeping over $7 \times 10^{-3}$ cm. during the time interval of the experiments. The following individual data show this for the fourth series:

Pressure.......... 100  200  300  400  500  600  600  500  400  300  200  100 atm.
Micrometer reading 320  301  290  274  263  250  252  270  290  305  321  336 cm./$10^4$

One would naturally refer this to the viscosity of the brass tube, but, curiously enough, the march is a contraction. Apparently the tube continually contracts in the lapse of time under internal pressure. The contraction occurs, however, for the case of a tube which was not rigorously straight.

Optically, apart from the tremor of the laboratory, one would have no fault to find with the measurements, allowing a micrometer accuracy of a few $10^{-4}$ cm. Interference rings could easily have been utilized, but this would have required two observers.

Two more series of experiments were made with the brass tube (table 20), in one (5) of which it was supported only at the ends with its original curva-

ture convex upward; in the sixth series the tube was additionally supported in the middle on a large pendulum-like wire or hanger.

TABLE 20.

| Series. | Range of pressure. | $10^6 \Delta L$ (pressure increasing). | $10^6 \Delta L$ (pressure decreasing). |
|---|---|---|---|
| 5 (free)........ | 100 to 600 atm. | 12.3 cm. | 15.2 cm. |
| 6 (supported)... | 100    500 | 13.6 | 15.2 |

The individual results are shown in figures 59 and 60. .It will be noticed that an error was introduced when pressures passed from the increasing to the decreasing phase at the highest pressure, and this was particularly the case when a slight leak developed. If the highest pressure is omitted, $10^6 \Delta L$ = 14.7, both for increasing and decreasing pressures in the case of the suspended tube. Hence $k = 1.250 \times 10^6$, not differing essentially from the above. The unsupported tube is highly subject to viscosity.
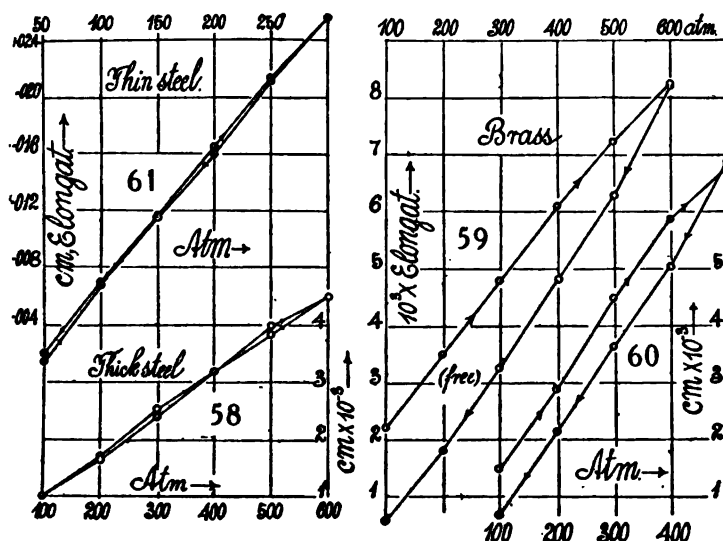


The large effect resulting from viscosity is also shown in the initial and final readings (100 atmospheres) in figures 59 and 60. It is in both cases again an apparent contraction and is present even in the supported tube. The viscous effect in the lapse of time is directly given in the following independent measurements of apparent contraction. The tube was kept charged with an internal pressure of 100 atmospheres.

Time............$9^h 30^m$        $10^h 5^m$        $12^h 12^m$
Length, $L$........0.0173        0.0183        0.0206 cm.

It is difficult to understand, however, how anything of the nature of viscous longitudinal contraction can occur under internal pressure. One might

suppose that the cylindrical tube as a whole is gradually progressing toward an ultimate spherical form, but this seems far-fetched. It is more reasonable to suppose that the viscosity is simply flexural. The tube is curved slightly convex upward and therefore the end mirrors $N$ and $H$, figure 54, rotate continually towards each other on a horizontal axis, under the end-thrusts of the internal pressure. The component beams and $HNH$ and $HMH$ are thereby each modified in length. Though it is difficult to specify why the former should be shortened relative to the latter, such a result is easily conceived.

**46. Thin steel tube.**—The steel tube in §§43 and 44 was adapted for high pressures only, showing but 0.2 interference ring per atmosphere. In contrast with this a thin steel tube was now inserted, adapted for lower pressures. This was more sensitive than the Bourdon gage, the other tube being on the whole less so. The dimensions were: length, $L = 161$ cm.; diameter inside, $a_0 = 0.799$ cm.; diameter outside, $a_1 = 0.951$ cm. The outside diameter was calipered. A short length was then cut off and slit open and the wall thickness similarly found (0.076 cm.). The tube was not quite straight. Snugly fitting brass plugs were carefully soldered into the ends, and these were then tapped to receive the tubes conveying pressure.

The observations shown in table 21 were recorded, the steps of pressure being 50 atmospheres in the first two and 100 atmospheres in the last two series.

TABLE 21.

| Series. | Pressure range. | $10^4 \Delta L$ (pressure increasing). | $10^4 \Delta L$ (pressure decreasing). |
|---|---|---|---|
| 1 | 50 to 200 atm. | 89 cm. | 100.1 cm. |
| 2 | 50    300 | 95.3 | 95.5 |
| 3 | 100    400 | 97.3 | 100.0 |
| 4 | 100    400 | 95.2 | 100.7 |

At 400 atmospheres the tube developed a slight leak at the ends. At 750 atmospheres one of the soldered end-plugs was blown out. It is remarkable that the plugs held so well.

An example of the individual data may be given for the second series. In figure 61 these data are shown, positively.

Pressure............ 50  100  150  200  250  300  300  250  200  150  100   50 atm.
Micrometer reading 260  210  164  115   67   23   24   67  120  163  212  266 cm./$10^4$

Very little viscosity is, therefore, in evidence, but there is some displacement or irregularity, probably in the reading of the Bourdon gage.

Pressure increments and decrements slightly rotated the mirrors in opposite directions around both a vertical and a horizontal axis. These were compensated by adjustment at the mirror $M$ before each reading. As the mirrors inclined towards each other for pressure increments the tube must have been slightly convex upward, and therefore successively straightened as pressures

increased. The mean elongation per atmosphere is $10^6 \Delta L = 97$ cm. and the bulk modulus may be computed as

$$k = \frac{a_0^2}{a_1^2 - a_0^2}\frac{L}{3\Delta L} = \frac{0.6384 \times 161}{(0.9044 - 0.6384) \times 3 \times 97 \times 10^{-6}} = 10^6 \times 1.33$$

In spite of the large difference of dimensions, this datum is of the same order of value as the above ($k = 1.39 \times 10^6$) for the thick tube, particularly as the present $\Delta L$, from the occurrence of flexure, is probably slightly large.

A tube of this kind with well-sealed ends (brazed probably), quite straight, and supported at different points of its length by wire pendula, should make a good pressure-gage within at least 1,000 atmospheres. An individual reading about $10^{-4}$ cm. per atmosphere or over 3 interference rings would be uniformly available throughout.

**47. Conclusion. Thermodynamic application.**—The data given show that an independent method of measuring the bulk modulus of metals is quite within the province of the displacement interferometer. The annoyances encountered, resulting from the viscosity of the metal or from warping, may be considered eliminated in the mean of the pressure-increasing and pressure-decreasing phase of the experiment. The tubes should be supported at various points along their length. Even the temperature discrepancy, if sufficient time is allowed between the successive steps of pressure, seems not to be of serious effect on the mean data.

For the measurement of pressure, however, the device is promising. In such a case the tube section should be chosen to correspond with the pressures to be measured. Within 1,000 atmospheres a steel tube about 1 cm. in diameter, with walls about 0.75 mm. thick, gave fair results, showing the evanescence of about 3 interference rings per atmosphere. Such a tube must be rigorously straight, well supported, and if possible of non-expanding (temperature) steel.



It is interesting to consider the case of the adiabatic expansion of liquids in relation to such a gage. The available thermodynamic equation is

$$\Delta\theta = \frac{\alpha\theta}{J\rho C_p}\Delta p$$

where $\Delta\theta$ is the temperature increment corresponding to the adiabatic compression $\Delta p$ at the temperature $\theta$, in case of a liquid whose coefficient of expansion is $\alpha$, density $\rho$, and specific heat $C_p$, $J$ is the mechanical equivalent of heat. In an apparatus like figure 62, in which $P$ is the screw compressor (with tinned or waxed screw $S$) filled with the liquid in question, $G$ the Bourdon gage, pressures may be suddenly applied without leakage by turning the
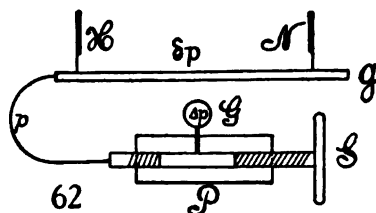
screw $S$. These are also measurable at the interferometer gage $g$, $H$ being the half-silvered and $N$ an opaque mirror, as in figure 54. The subsidence of pressure due to cooling adiabatic compression is, however, also measurable at $g$ in terms of the delaying pressure. For we should have ($v$ denoting volume, $k$ the bulk modulus)

$$\frac{\Delta v}{v} = a\Delta\theta; \quad -\frac{\Delta v}{v} = \frac{\delta p}{k}$$

or, apart from signs, $\Delta\theta = \frac{\delta p}{ka}$, where $\delta p$ is the subsidence of pressure due to the cooling $\Delta\theta$, after adiabatic compression. Hence the original equation takes the form

$$C_p = \frac{ka^2\theta}{J\rho} \frac{\Delta p}{\delta p}$$

an equation for measuring the specific heat of constant pressure of the liquid at temperature $\theta$ and pressure $\frac{2p+\Delta p}{2}$. The observations thus consist in measuring $\Delta p$ (in displacement) and $\delta p$ in interference rings, both at the gage $g$.

One may estimate the value of $\delta p$ per atmosphere of $\Delta p$, for alcohol, by way of illustration. Here in c.g.s. units,

$$k = 1.21 \times 10^{10}; \quad a = 1.1 \times 10^{-3}; \quad \theta = 20°; \quad \rho = 0.79; \quad C_p = 0.58$$

Hence

$$\delta p = \frac{1.21 \times 10^{10} \times (1.1 \times 10^{-3})^2 \times 20 \times 10^6}{42 \times 10^6 \times 0.79 \times 0.58} = 1.52 \times 10^4 \frac{\text{dynes}}{\text{cm.}^2}$$

or

$$\delta p = 0.015 \text{ atm. per atm. of } \Delta p$$

Hence, if $\delta p = 200$ atmospheres, the above gage would show about 10 rings for $\delta p$. Similarly a pressure dropping adiabatically from 1,000 atmospheres would show about 50 rings, residually, after closing.

The present research was planned to be pursued at much greater length; but owing to the annoyances of a quivering pier, which are particularly marked during the term weeks, and to the injury of the screw before the tallow washer was inserted, it was thought wise to discontinue it at present. If the micrometer is to be set to $10^{-4}$ cm., the ellipses must be reasonably quiet, and in case of long-distance interferometry such a condition can be realized only during the summer months.

# CHAPTER IV.

## REFRACTIVITY DETERMINED IRRESPECTIVE OF FORM BY DISPLACEMENT INTERFEROMETRY.

**48. Introductory.**—Some time ago* I made a number of experiments on the use of curvilinear compensators in connection with the displacement interferometer. It is obvious that the curvature in such a case must be very small, so that single lenses for the purpose are not easily obtained. The use of a doublet of two lenses of the same glass, but respectively convex and concave, meets the case fairly well, the necessary refracting power being received by spacing the doublet. Lenses of about 1 diopter each gave the best results, bringing out fringes of quasi-elliptic and hyperbolic symmetry in great variety.

Later it appeared as if plates of different varieties of glass, as for instance crown and flint, if placed in the two component beams $MH$, $NH$, figure 54, would produce the same phenomena. The flint plate used, however, proved to be inadequately plane, so that the result is in doubt.

More recently I have endeavored to secure similar results by submerging the lens (convex or concave) in a liquid of about the same index of refraction. This method would seem to be interesting in other respects, for it is probable that the index of the solid may be determined in this way irrespective of form.† If, for instance, the liquid and the solid have the same index, one would be tempted to infer that the latter may be removed or inserted without displacing the center of ellipses at the particular wave-length under consideration. The index of the liquid in place is then determinable by the interferometer to a few units in the fourth place.

If experiments of the present kind are to be accurate, it is obvious that the walls and cavity of the trough in which the lenses are to be submerged must be *optically* plane parallel; otherwise some compensating adjustment must be made at the opaque mirrors of the interferometer, and for this no adequate allowance is at hand. It did not, however, seem worth while to provide expensive apparatus before the method had been worked out in detail. Accordingly the present experiments were conducted with troughs of ordinary plate-glass put together by myself, and little attention will be given to absolute values of index of refraction, as such.

**49. Preliminary experiments.**—The first experiments were made on a large linear interferometer (see fig. 54) with distances of nearly 2 meters between

---

* Carnegie Inst. Wash. Pub. No. 249, 1916, chapter IX; cf. Amer. Journ. Science, XL, pp. 299-308, 1915.
† Mr. R. W. Cheshire (Phil. Mag., XXXII, 1916, pp. 409-420) has recently used Töpler's method for the same purpose with marked success.

the mirrors. The rays in such a case are all very nearly parallel. Sunlight, arc light, and the Nernst filament were each available for illumination. If the latter is used, the adjustment must be made by aid of the two white slit images, which are to coincide horizontally and vertically. Otherwise the sodium lines are available. With a very long collimator (2 meters) and a wide single-lens objective (10 cm. or more), the Nernst filament may be used directly in place of the slit. If the beam passing the objective is not wider than 1 cm. (opaque slotted screen), very perfect ellipses may be obtained.

On inserting the trough with a thickness of 1.3 cm. of $CS_2$ solution normally into the $MH$ beam, the original very large ellipses were reduced in size and rounded as usual to smaller circles. Submerging a convex lens (1 diopter) into the liquid until the beam passed symmetrically through it changed these circles to very long horizontal spindles. A concave lens similarly produced horizontally very eccentric hyperbolæ. With water in the trough, only the convex lens showed observable fringes, these being very long, practically linear horizontal spindles. All these fringes lie considerably in front of the principal focal plane of the telescope (fig. 54, $T$), and the abnormal forms are necessarily relatively faint. They change in shape and intensity with the focal plane observed.
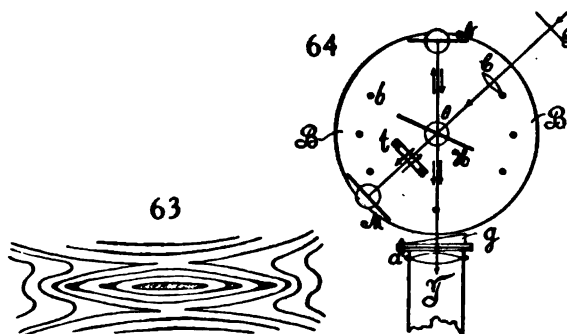


On mixing $CS_2$ with kerosene (about equal parts), types of fringes shown in figure 63, but with many more lines, were obtained. This is a combination of both spindles and hyperbolæ. Probably three layers of liquid are chiefly in question, viz, kerosene, kerosene + $CS_2$, $CS_2$, and the three stages of form and the sinuous lines correspond to them. Fringes were sharp only if viewed in front of the principal focal plane of the telescope. By submerging convex or concave lenses, the hyperbolic parts or the spindles of the fringes could often be removed. Similar results were obtained with mixture of $CS_2$ and sweet oil, though this solution is more homogeneous.

**50. Apparatus.**—To obviate the tremor of apparatus which is inevitable in the case of the long-distance interferometer, the parts were now screwed down at short distances in the cast-iron block $B$, figure 64. Here the ranges $MH, HN$ of half-silvered plate $H$, and opaque mirrors $M, N$, did not exceed

14 cm., but this gives ample room for the manipulation of the trough $t$ placed normally in the beam $MH$. White light enters by way of the collimator $SC$ at any convenient angle $\theta$ (as this does not enter into the equations), and $\theta = 60°$ was used. The opaque mirrors $M$ (and preferably also $N$) are on micrometers with screws normal to their faces, and each must be provided with adjusting-screws relatively to horizontal and vertical axes. An elastic fine adjustment is desirable. The block contains a number of screw-sockets, $b$, for attaching subsidiary apparatus. The trough $t$ should preferably be attached to an independent supporting arm, not connected with $B$, and be revolvable about two axes normal to each other. In such a case the position *normal* to the beam of light may be found from the reverse of motion of the interference rings, while the trough is slowly rotated in a given sense.

The telescope $T$ (relatively much enlarged in the diagram) is not attached to the block. It is to be used both as a simple telescope for the adjustment of the white slit images to horizontal and vertical coincidence, and as a direct-vision spectroscope. The most convenient attachment for this purpose is the direct-vision prism grating $G$ (film grating) just in front of the objective of $T$. Two perforated thin disks of brass are useful for this purpose, one disk being firmly attached (like the cap) to the objective, the other to the flat face of the grating with the prism outward. A swivel bolt $a$, between the disks, thus allows the observer to throw out the grating and use the telescope. A stop arrests the motion of the grating when it is rotated about $a$, back again, for viewing the spectrum. This plan worked very well, and the ellipses obtained were magnificent. It was almost possible to control the micrometer $M$ manually, and all hurtful quiver is absent. The fiducial line to which centers of ellipses, etc., are to be returned is always the sodium doublet present in sunlight and the arc and artificially supplied by an interposed burner in case of the Nernst lamp. The telescopic lens need not be more than 2 cm. wide, and cross-hairs are not needed. For measuring dispersion the Fraunhofer lines $B, C, D, E, b, F$ were used.

**51. Equations.**—The useful equations for present purposes are given in a preceding report,[*] and the following cases only need be repeated here. If $\epsilon$ is the thickness of glass plate of index of refraction $\mu$ for the wave-length $\lambda$, and if the equation $\mu = A + B/\lambda^2$, where $A$ and $B$ are constants, be taken as sufficient,

(1) $$\mu - 1 = \Delta N/\epsilon - 2B/\lambda^3$$

where $\Delta N$ is the displacement of the micrometer at the opaque mirror $M$ or $N$ due to the insertion of the plate normally to the component beam in question. To determine $\mu$, $B$ must be known at least approximately. It may be measured in the same adjustment, however, if two Fraunhofer lines are used fiducially. Let $\delta N$ be the displacement of micrometer to pass the center of

---

* Carnegie Inst. Wash. Pub. No. 229, 1915, §§ 40, 41, 42.

ellipses from wave-lengths $\lambda$ to $\lambda'$. Then if $e'$ is the thickness of the half-silvered plate $H$, and $R$ the angle of refraction within it,

(2)
$$\delta N = B\left(e + e'\cos R + 2\left(e + \frac{e'}{\cos R}\right)\right)\left(\frac{1}{\lambda^2} - \frac{1}{\lambda'^2}\right)$$

If $e = 0$,

(3)
$$\delta N_a = B\left(e'\cos R + \frac{2e'}{\cos R}\right)\left(\frac{1}{\lambda^2} - \frac{1}{\lambda'^2}\right)$$

which may be called the corresponding air displacement. Hence

(4)
$$B = \frac{\delta N - \delta N_a}{3e\left(\frac{1}{\lambda^2} - \frac{1}{\lambda'^2}\right)}$$

Here     $\delta N - \delta N_a = N - N' - (N_a - N'_a) = N - N_a - (N' - N'_a)$

so that the difference of the corresponding positions of micrometer for a given Fraunhofer line, with and without the plate, are to be found.    The method is quite accurate, as will be seen below.    More than two constants $A$ and $B$ may be taken, if desirable.

To return to equation (1), remembering that $2B/\lambda^2$ is small, it is seen that the percentage accuracy of $\mu - 1$ and $\Delta N$ are about equal.    Now $\Delta N$, for a plate 5 to 6 mm. thick and ordinary glass, is about 0.3 cm.    This may be measured within $10^{-4}$ cm. or 3 parts in $10^4$ of $\Delta N$ or one or two units in the fourth place of $\mu$, the index of refraction of the glass.    A much more serious consideration is the consistent measurement of the thickness of plate $e$, which must be given to $10^{-4}$ cm. if the same accuracy is wanted.    Naturally this presupposes optic plate.    Hence the data below will be inaccurate as to absolute values from this cause.    The plates used frequently showed increases of thickness of several $10^{-3}$ cm. within a decimeter of length.    Absolute values are, however, without interest in this paper.

To show that less than $10^{-4}$ cm. is guaranteed on the micrometer in the placing of elliptic centers at the sodium line, the pairs of results given in table 22, made at different times and with entirely independent adjustments, may be cited.    The screw-pitch was 0.025 cm. and the drum divided into 50 parts with a vernier to 0.1 part.

TABLE 22.

| Fraunhofer line. | Pitch, drum. | | Pitch, drum. | | Difference. |
|---|---|---|---|---|---|
| B | x 85 | 17.1 | 74 | 33.2 | 0.25000+0.01695 cm. |
| C | 85 | 23.3 | 74 | 39.3 | + .01700 |
| D | 85 | 41.0 | 75 | 7.0 | + .01700 |
| E | xx 86 | 14.9 | 75 | 30.9 | + .01700 |
| b | 86 | 19.2 | 75 | 35.2 | + .01703 |
| F | f 86 | 36.6 | 76 | 2.6 | + .01703 |

x Ellipses long horizontally.   xx Circles.   f Ellipses long vertically.

The total difference is less than $10^{-4}$ cm. and probably due to the width of the Fraunhofer lines with deficiency of light at the ends of the spectrum.

Apart from measurement of the thickness $e$, therefore, the method is guaranteed for fourth-place work.

' **52. Observations.**—At short distances the ellipses are always rounder and present in all focal planes of the telescope. Doublet lens compensators of relatively large focal power are available. Using the CS₂-sweet oil solution, the submergence of convex and concave lenses in it made but very little difference in the position and definition of the ellipses. There must, therefore, have been approximate equality of the conditions of refraction. With glass in water this was naturally not the case.

A number of experiments were made with the well-known mercury-potassic iodide solution as obtained from Eimer & Amend. The index of refraction in the concentrated state (floating glass) exceeds 1.7. The slight straw-color is no disadvantage.

A plane-parallel trough of ordinary plate-glass, 0.293 cm. internal width, was now constructed, only just large enough to receive a glass plate or a convex lens. With the plate or lens submerged centrally, therefore, the excess of path-difference over the empty trough would be nearly constant. The liquid was then gradually diluted until the excess of path-difference of the liquid over the glass content passed through zero into a deficiency. Considerable stirring was needed to insure homogeneity on each dilution. The results are given in table 23 for the plate and in table 24 for the lens. So long as the diluted solution was effectively more refracting than the glass, the ellipses were nearly circular and very clear both for the submerged plate and lens, as well as for the liquid, but when the solution began to effectively refract less than the glass, the ellipses were washed and could not be obtained strongly. On submerging the lens in these cases it was necessary to so adjust its position horizontally and vertically that the white images (obviously in different focal planes) coincide as nearly as possible. This insures a symmetric position for the lens, after which the spectrum is to be examined and the ellipses placed by moving the micrometer. Unfortunately, as neither the trough nor the plate was optically plane parallel, some readjustment for this was necessary at each observation, an operation which introduces the error in the results shown in tables 23 and 24, so far as absolute values are concerned, which has been alluded to above.

TABLE 23.—Submergence of plate-glass (thickness 0.284 cm.) in mercury-potassic iodide solution. Thickness inside of trough, 0.293 cm. Sodium line. $2B/\lambda^2 = K$. Glass, $B = 4.5 \times 10^{-11}$; $2B/\lambda^2 = 0.0262$.

| Solution. | Liquid $\triangle N$ | Glass in $\triangle N$ | Liquid $\mu - 1 + K$ | Glass in $\mu - 1 + K$ |
|---|---|---|---|---|
| | *cm.* | *cm.* | | |
| 6 | 0.1640 | 0.1468 | 0.6064 | 0.5476 |
| 7 | .1570 | .1466 | .5824 | .5469 |
| 8 | .1494 | .1466 | .5564 | .5469 |
| 9 | .1478 | .1468 | .5505 | .5475 |
| 10 | .1430 | .1466 | .5345 | .5470 |
| 11 | .1426 | .1466 | .5333 | .5468 |

TABLE 24.—Submergence of glass convex lenses in mer-
cury-potassic iodide solutions. Thickness of the trough
inside, 0.293 cm. Focal power, 1 diopter. Sodium line.
$K = 2B/\lambda^3$. Glass, $B = 4.5 \times 10^{-11}$; $2B/\lambda^3 = 0.0262$.

| Solution. | Liquid $\Delta N$ | Glass in $\Delta N$ | Liquid $\mu - 1 + K$ | Glass in $\mu - 1 + K$ |
|---|---|---|---|---|
| | *cm.* | *cm.* | | |
| 1 | 0.2069 | ....... | 0.7525 | ...... |
| 2 | .1841 | x 0.1722 | .6746 | 0.6340 |
| | ..... | .1742 | ...... | .6410 |
| 3 | .1692 | .1638 | .6239 | .6055 |
| 4 | .1599 | .1565 | .5921 | .5805 |
| 5 | .1412 | xx .1432 | .5283 | .5352 |
| | .1411 | f .1445 | .5280 | .5396 |

x Focal power 2 diopter.    xx Washed ellipses.    f Concave lens.

In both these series the trough was not fixed with adequate rigidity, so
that errors crept in from this source. Nevertheless, if the data are con-





structed graphically ($\mu - 1 + K$ for solution as abscissa and for submerged
glass as ordinate), the results (figs. 65 and 66) show a very definite trend
and show also that slight interpolation would be possible. It would be
hasty, however, to infer that the intersection at $a$ of the graph for submerged
glass with the line at 45° through the origin is the index of refraction of the
glass, in so far as the data for the liquid are trustworthy. The method
seems to be deserving of notice; but before discussing the matter further
it will be necessary to determine the dispersion involved in $B$.
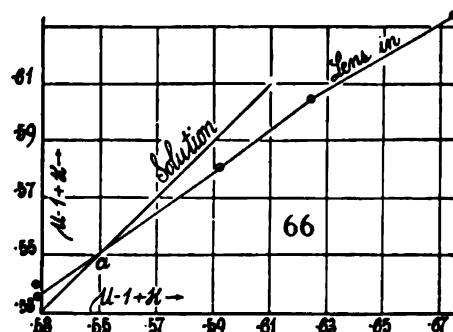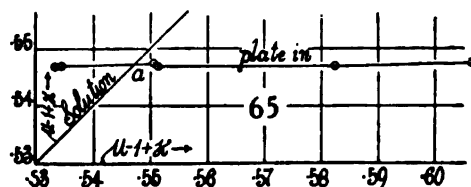
53. Dispersion constants.—As shown in §51, the constant $B$ is found by
passing the center of ellipses between Fraunhofer lines, both in the presence
and absence of the plate to be tested. In the case of liquids the empty and

the filled trough are similarly compared. Data of this kind for a dilute solution of mercury-potassic iodide and two kinds of glass are given in table 25. $N_a$ is the micrometer reading at $M$ for the half-silvered plate alone. In case of the solution, it is to include the glass plate of the trough. $N-N_a=\Delta N$.

TABLE 25.—Dispersion constants.

| Fraunhofer line. | $\lambda \times 10^6$ | $N_a$ | (1) Solution. $e=0.293$ cm. $N-N_a$ | (2) Trough glass. $e=0.562$ cm. $N-N_a$ | (3) Glass plate. $e=0.434$ cm. $N-N_a$ |
|---|---|---|---|---|---|
| | cm. | | | | |
| B | 68.7 | 0.0152 | 0.1530 | 0.3008 | 0.2390 |
| C | 65.63 | .0173 | .1554 | .3023 | .2403 |
| D | 58.93 | .0220 | .1622 | .3065 | .2436 |
| E | 52.70 | .0284 | .1731 | .3121 | .2481 |
| b | 51.77 | .0296 | .1753 | .3130 | .2488 |
| F | 48.61 | .0342 | .1851 | .3171 | .2520 |

The computed values $\mu - 1 + K = (N - N_a)/e = \Delta N/e$ are given in the graph figure 67 (series numbered), from which the characteristic difference in the dispersion of the solution and of the glass is apparent.
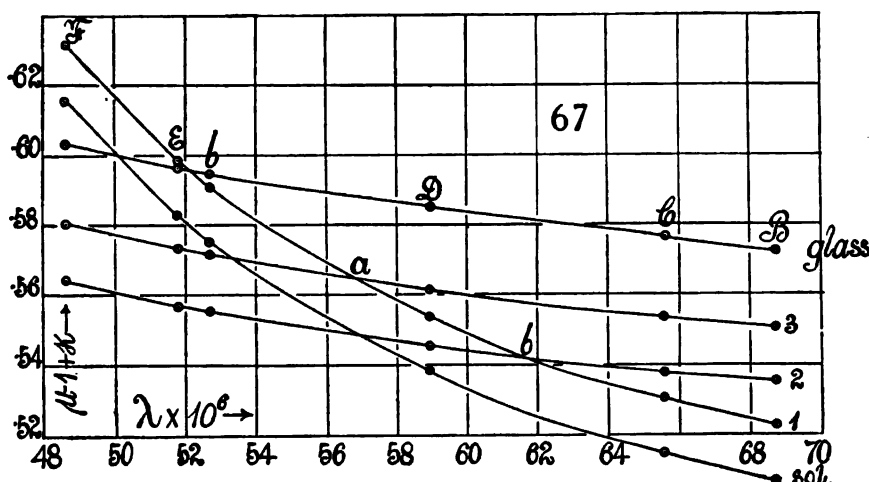


If, now, the value of $B$ is computed by equation (4), between successive Fraunhofer lines $B-E$, $C-b$, $D-F$, the results come out as in table 26 and the coefficient $B$ should be correct to about 1 per cent. For instance, in the case of the solution $(N-N_a)\lambda - (N-N_a)\lambda' = \delta N = 0.0201$, 0.0200, 0.0229, respectively.

TABLE 26.

| Fraunhofer lines. | (1) Solution. $B \times 10^{11}$ | (2) Trough glass. $B \times 10^{11}$ | (3) Glass. $B \times 10^{11}$ |
|---|---|---|---|
| B-E | 15.38 | 4.50 | 4.71 |
| C-b | 16.02 | 4.49 | 4.65 |
| D-F | 19.22 | 4.62 | 4.76 |

It thus appears that in case of the solution the equation $\mu = A + B/\lambda_2$ is far from sufficient up to the Fraunhofer $F$ line. Nevertheless even here the mean of the first two results may be regarded as holding in the region of the $D$ line. The large value of $B$ as compared with the glasses is particularly noteworthy, and from this a reason for the poor ellipses obtained with dilute solutions is suggested. If for two media the $\Delta N/e$ are identical, as at $a$ and $b$ in figure 67, this implies merely that

$$\mu + 2B/\lambda^3 = \mu' + 2B'/\lambda^3$$

Hence, when the coefficients $B$ differ as largely as is the case for the solution and the glass, the indices $\mu$ are far from equal. In the above case, if $\mu - \mu' = 0.071$, the solution should show no displacement at the $D$ line when the glass is submerged. But this difference in the indices of refraction of the glass and the solution is enormous, and if the submerged body is a lens, the corresponding images in the telescope will be thrown quite out of focus. Thus the ellipses are necessarily washed. Conversely, when the indices of lens and solution are nearly equal at the sodium line, the displacement is $2(eB - eB')/\lambda^3$, and therefore considerable (0.035 cm. above, in the example taken); but the ellipses are now sharp and strong. Unfortunately, therefore, displacement is no criterion for equality of $\mu$, and mere dependence on the sharpness of fringes is insufficiently accurate. The only resource left is to compute $B$ and $B'$ for two spectrum lines and adjust the solution for this displacement. Again, this is not convenient, particularly when but a single spectrum line is at hand.

**54. Further observations.**—A somewhat wider trough was now constructed of the same plate-glass as above. The following dimensions were found by calipering: Glass wall plates, top 0.290 cm., bottom 0.283 cm.; internal thickness (liquid plate), top 0.564 cm., bottom 0.563 cm. As the light passed through near the bottom of the trough, the second data are to be taken in each case. The observations were made with sunlight and at each of the Fraunhofer lines B, C, D, E, b, F. In case of a hazy sun the lines B and F were often less strong than desirable; but in other respects the work throughout progressed smoothly, showing magnificent ellipses beginning at the B line with the horizontal axis longer and ending at the F line with the vertical axis longer. Circles occur earlier as the refraction is greater. $N - N_e$ in table 27 is the coördinate referring to the difference of micrometer reading for the presence and absence of the plate under observation. If the glass walls of the trough alone are to be taken, the $N_e$ refers to the half-silver plate alone. If the solution is in question, $N_e$ refers to the half-silver and the trough walls taken conjointly and in place. The trough is, of course, not to be moved; but some adjustment is needed when the liquid is introduced, which mars the absolute result. In series 5 a glass plate $e = 0.293$ cm. thick was submerged in the solution without readjustment. Hence of the resulting refraction $293/563 = 0.5024$ belongs to the glass and $270/563 = 0.4796$ to the solution surrounding it. Table 16 contains ten series of results with the

Table 27.—Refraction of glass and of mercury-potassic iodide solutions. New trough. Glass walls, $e = 0.283$ cm. thick, each; solution, $E = 0.563$ cm. thick; $K = 2B/\lambda^2$. Figure 68 is an exhibit of the more important of these results.

| Series. | Fraunhofer line. | $\lambda \times 10^5$ | $N_d \times 10^3$ | $\Delta N$ | $\mu - 1 + K$ | $\delta N \times 10^4$ | $B \times 10^{11}$ |
|---|---|---|---|---|---|---|---|
| | | cm. | cm. | cm. | | cm. | |
| (1) Glass plate. $e = 0.566$...... | B | 68.7 | 8.1 | 0.3247 | 0.5737 | BE, 117 | 4.65 |
| | C | 65.63 | 9.7 | .3263 | .5766 | Cb, 111 | 4.65 |
| | D | 58.93 | 14.4 | .3306 | .5841 | DF, 110 | 4.78 |
| | E | 52.70 | * 20.8 | .3364 | .5943 | ........ | ..... |
| | b | 51.77 | 22.0 | .3375 | .5963 | ........ | ..... |
| | F | 48.61 | 26.6 | .3416 | .6035 | ........ | ..... |
| (2) Dilute solution.......... | B | Same as above | .... | 0.2855 | 0.5071 | BE, 382 | 15.26 |
| | C | | .... | .2899 | .5149 | Cb, 382 | 16.01 |
| | D | | .... | .3031 | .5384 | DF, 435 | 19.00 |
| | E | | .... | .3237 | .5750 | ........ | ..... |
| | b | | .... | .3281 | .5828 | ........ | ..... |
| | F | | .... | .3466 | .6156 | ........ | ..... |
| (3) Glass plate. $e = 0.566$ cm... | B | Same as above | .... | 0.3178 | 0.5616 | BE, 116 | 4.63 |
| | C | | .... | .3194 | .5643 | Cb, 111 | 4.63 |
| | D | | .... | .3237 | .5719 | DF, 109 | 4.74 |
| | E | | .... | .3295 | .5822 | ........ | ..... |
| | b | | .... | .3305 | .5839 | ........ | ..... |
| | F | | .... | .3346 | .5912 | ........ | ..... |
| (4) Stronger solution...... | B | Same as above | .... | 0.3098 | 0.5503 | BE, 450 | 17.99 |
| | C | | .... | .3151 | .5597 | Cb, 446 | 18.75 |
| | D | | .... | .3304 | .5869 | DF, 524 | 22.89 |
| | E | | .... | .3548 | .6303 | ........ | ..... |
| | b | | .... | .3598 | .6391 | ........ | ..... |
| | F | | .... | .3828 | .6800 | ........ | ..... |
| (5) Glass plate in solution 4. $e = 0.293$ cm... | B | Same as above | .... | 0.3077 | .05465 | BE, 279 | 11.16 |
| | C | | .... | .3110 | .5525 | Cb, 276 | 11.59 |
| | D | | .... | .3207 | .5697 | DF, 309 | 13.52 |
| | E | | .... | .3356 | .5962 | ........ | ..... |
| | b | | .... | .3387 | .6016 | ........ | ..... |
| | F | | .... | .3517 | .6247 | ........ | ..... |
| (6, 7) Glass plate. $e = 0.566$ cm... | B | Same as above | 8.0 | .03193 | 0.5641 | BE, 114 | 4.53 |
| | C | | 9.7 | .3207 | .5666 | Cb, 107 | 4.48 |
| | D | | 14.5 | .3249 | .5740 | DF, 108 | 4.69 |
| | E | | 21.0 | .3307 | .5843 | ........ | ..... |
| | b | | 22.2 | .3315 | .5858 | ........ | ..... |
| | F | | 26.8 | .3357 | .5931 | ........ | ..... |
| (8) Strong solution.......... | B | Same as above | .... | 0.4474 | 0.7947 | BE, 1000 | 39.94 |
| | C | | .... | .4582 | .8139 | Cb, 1003 | 42.03 |
| | D | | .... | .4916 | .8732 | DF, 1224 | 53.47 |
| | E | | .... | .5474 | .9723 | ........ | ..... |
| | b | | .... | .5585 | .9920 | ........ | ..... |
| | F | | .... | .6140 | 1.0906 | ........ | ..... |
| (9) Strong solution.......... | B | Same as above | .... | 0.4474 | 0.7953 | BE, 999 | 39.90 |
| | C | | .... | .4584 | .8143 | Cb, 1004 | 42.06 |
| | D | | .... | .4918 | .8736 | DF, 1216 | 53.14 |
| | E | | .... | .5476 | .9727 | ........ | ..... |
| | b | | .... | .5589 | .9927 | ........ | ..... |
| | F | | .... | .6135 | 1.0897 | ........ | ..... |
| (10) Dilute solution........... | B | Same as above | .... | 0.3255 | 0.5782 | BE, 509 | 20.32 |
| | C | | .... | .3309 | .5879 | Cb, 514 | 21.56 |
| | D | | .... | .3487 | .6194 | DF, 601 | 26.25 |
| | E | | .... | .3764 | .6687 | ........ | ..... |
| | b | | .... | .3824 | .6792 | ........ | ..... |
| | F | | .... | .4088 | .7261 | ........ | ..... |

* Circles.

same trough but with different solutions, dilute and nearly concentrated.
To place the trough normal to the beam, the reflection of the latter from
the face of the trough was made to coincide with the spot on the half-silver.
This is inadequate for fine work, but the interferometer method of retro-
gressing fringes is not applicable unless the trough is separately mounted.

From the data obtained the constant $B$ was computed from pairs of Fraun-
hofer lines, B and E, C and b, D and F. Apart from the effect of the thick-
ness $e$, it should be correct in case of the solutions to about a few tenths per
cent. In case of the concentrated solutions, however, the ellipses already
begin to move sluggishly and are much smaller.
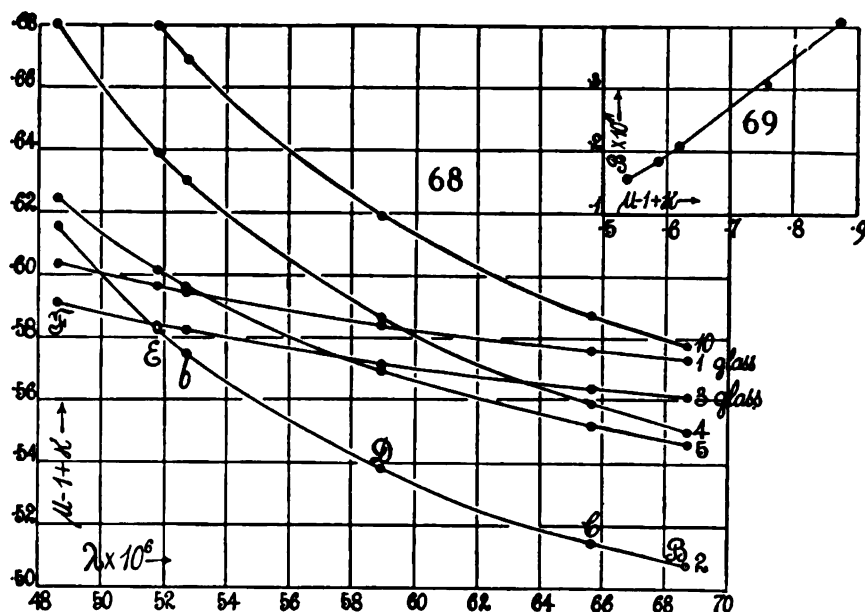


From $\mu - 1 + 2B/\lambda^2$ and $B$, the corresponding indices of refraction in table 27
are easily computed; but these data are of little value here, because the thick-
ness $e$ of the ordinary plate-glass used is not constant to the degree necessary.
It is, however, worth while to exhibit the $B$ for the different mercury-iodide solu-
tions in terms of either $\mu$ or, what is equally serviceable and more convenient,
in terms of $\mu - 1 + K$; for this quantity is directly given by the displacement
measurement $\Delta N/e$. If we regard the mean $B$ for the B to E lines, and C to
b lines as applying to the D line, the coördinated values are:

|  | (2) | (4) | (8) | (9) | (10) |
|---|---|---|---|---|---|
| $\mu - 1 + K$ | 0.5384 | 0.5869 | 0.8732 | 0.8736 | 0.6194 |
| $B \times 10^{11}$ | 15.63 | 18.37 | 40.99 | 40.98 | 20.94 |

For solutions of small concentration the ratio of $B$ and $\mu - 1 + K$ changes
but slowly (29 to 34) as shown in figure 69, so that $B$ may be predicted from
the latter, always remembering that our equation with two constants ($\mu = A$
$+ B/\lambda^2$) is inadequate at the outset.

To take the case of the submerged glass-plate series 5, if $e'$ be the thickness of plate and $e''$ of solution, so that $e'+e''=e$, the thickness of trough,

$$\frac{e'}{e}(\mu'-1+K')+\frac{e''}{e}(\mu'-1+K'')=\frac{\Delta N}{e}$$

Thus, 0.5204 of the data of series (3) added to 0.4796 of the data of series (4) should reproduce series (5). The results are given in table 28.

<div align="center">TABLE 28.</div>

| | B | C | D | E | b | F |
|---|---|---|---|---|---|---|
| 3⎫ 4⎬Computed.... 5⎭ | 0.5561 | 0.5621 | 0.5791 | 0.6052 | 0.6104 | 0.6338 |
| Found........ | .5465 | .5525 | .5697 | .5962 | .6016 | .6247 |
| Difference.... | .0096 | .0096 | .0094 | .0090 | .0088 | .0091 |

These differences are nearly constant and due to the orientation of the glass plate with which its effective thickness (assumed 0.293 cm.) will vary.

**55. Conclusion.**—It appears, therefore, that the expectation of recognizing the equality of refraction of a submerged solid and a solution, at any given wave-length, from the fixity of the fringes in the presence and absence of the solid has not been fulfilled, at least for the mercury-potassic iodide solution. The reason is found in the enormous difference of the dispersions of the solution and ordinary glass. When the ellipses are not displaced, $\mu-\mu'=2(B'-B)/\lambda^2$, and this difference may even approach a unit in the first decimal of $\mu$. The troughs in which such experiments are to be made must be *optically* plane parallel, as otherwise an inadmissible error due to thickness of plates is introduced. With such a trough, however, the ease and accuracy with which the dispersion constants may be found, at least for the solution, are noteworthy.

When the solution is more refracting than the glass, it is curious that the ellipses are not seriously distorted or vague, even when the symmetrically submerged solid is lenticular. Hence the equation just stated is available for a wide variation of form. Furthermore, if $\Delta N$ is the displacement at the micrometer corresponding to the presence and absence of glass of the thickness $e$,

$$\mu-\mu'+\frac{2}{\lambda^2}(B-B')=\frac{\Delta N}{e}$$

But as $\mu'$, $B'$ for the solution are known, $\mu$ and $B$ for the glass may both be computed from observation at a number of wave-lengths, $\lambda$, provided $\mu=A+B/\lambda^2$ for glass, which is sufficiently nearly so to the fourth place of decimals. Hence if $\Delta N/e+\mu'+2B'/\lambda^2=x$ is known,

$$B=\frac{x-x'}{3(1/\lambda^2-1/\lambda'^2)}$$

114



From $\mu - 1 +$
are easily comp
ness $e$ of the o
It is, however,
tions in terms
in terms of $\mu-$
measurement
b lines as app

# CHAPTER V.

n.—A variety of constants in physics may be found from
hts of two communicating columns of liquid. This is, for
e in the classical experiment of Dulong and Petit on the
n of liquids. Again, if one of the tubes is subject to a special
he direction of its axis, this force in its bearing on the liquid
ted from the resulting difference of heads of the columns.
may be surrounded by a magnetizing helix and the effect of
tic field on the liquid in question (i.e., the susceptibility)
displacement of its surface by the presence and absence of
It seemed to me worth while, therefore, to test whether it
ble to measure small displacements of this kind by passing the
t beams of a displacement interferometer axially *through* the
espectively, and to measure the differential effects in question
he resulting displacements of fringes.
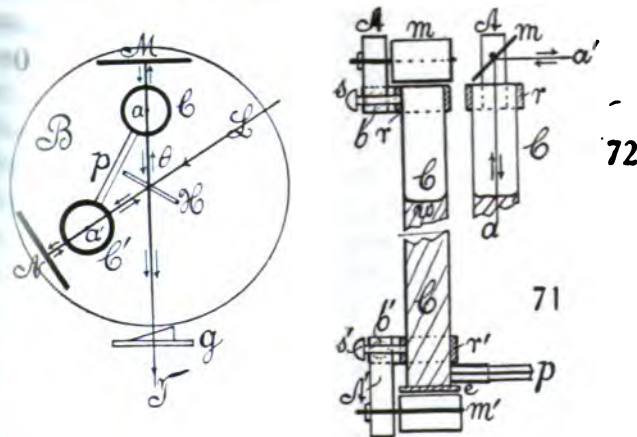


paratus. Michelson interferometer.—The interferometer first used
he same form as that described above (§ 2, fig. 3), B, figure 70, being
iron block, 1 foot in diameter and 1.5 inches thick, on which the
M, N (the latter and preferably both on micrometers) are securely
ed with the usual direct rough and elastic fine adjustment for hori-
and vertical axes. A beam of parallel white rays L arrives from a
ator (not shown) and impinges on the half-silver plate H, to be reflected
nsmitted at a convenient angle θ (about 60°), thus furnishing the two
ent beams which are to traverse the limbs of the U-tube.

The vertical columns of this tube are shown at $C$ and $C'$ (with accessory mirrors removed), and they are joined to the capillary tube $p$ near the bottom of $C$ and $C'$. Details will be given in connection with figures 71 and 72.

The ray $HM$ strikes a mirror symmetrically at 45° to the vertical below $C$, is thence reflected upward along the axis $a$, striking another mirror above, also symmetrically at 45° and parallel to the former, whence it is reflected to the opaque mirror $M$. The latter reflects the ray normally back, so that it retraces its path as far as $H$, by which plate it is now transmitted to be observed by the telescope at $T$. Similarly the transmitted component ray $HN$ is guided by suitable reflectors at 45°, so as to take the path $Ha'Na'HT$, thus passing axially ($a'$) through the tube $C'$.

It is necessary that the U-tube $CpC'$ be mounted independently of the block $B$ on suitable bracket or arm attached to the pier. Otherwise any manipulation at $N$ will disturb the surfaces of water in $C$ and $C'$. Ordinary clamps admit of raising or lowering or rotating $CC'$ satisfactorily, always providing that it shall not touch $B$. The telescope at $T$ is also mounted apart from $B$ on the table below. The direct-vision prism grating $g$ is placed immediately in front of the objective and swiveled as described in figure 64, Chapter IV, so that either the white slit images or their spectra may be seen in the field of view, according as $g$ is rotated aside or is in place.

In figure 71 a front sectional elevation of one of the shanks of the U-tube is given with all appurtenances, and a similar sectional elevation at right angles to the former is added in figure 72 for the top of the tube. In figure 71 the mirrors $m'$ and $m$ are on horizontal axes and the component ray coming from behind the diagram strikes $m'$ below, is reflected axially upward through $CC$, impinging on the mirror $m$ (also on a horizontal axis), whence it is reflected horizontally toward the front of the diagram. The ray $a$ and mirror $m$ are given more clearly in figure 72. The lateral capillary tube appears at $p$ and the tube $C$ is closed below with a plate of glass $e$, cemented in place.

To mount the mirrors $m$, $m'$, snugly fitting rings $r$ and $r'$ encircle the tube $C$ near its top and bottom and can be fixed by the set-screws $s$ and $s'$. In virtue of these rings, the mirrors $m$, $m'$ may be rotated at pleasure around the vertical axis $a$ of $CC$. The horizontal axis of the mirrors $m$, $m'$ rotates at pleasure in the vertical arms $A$, $A'$ of square brass tube. $A$, $A'$ in turn may be slightly swiveled about the horizontal axis $b$, $b'$, in a rigid lateral projection of the rings $r$, $r'$. Thus $m$, $m'$ are capable of rotation around three axes normal to each other and adequately clamped in any position.

The component ray $HN$ may be adjusted to the center of the lower mirror $m'$ by placing the collimator $L$ and then guided axially by $m'$, $m$, $N$ as described, each being adjustable. The component ray $HM$ may be similarly adjusted to the center of the lower mirror $m'$ (at 45°) by slightly rotating the half-silver plate $H$ (on horizontal and vertical axes) and then guided axially by $m'$, $m$, $M$. As a whole the adjustment is difficult, though it need not be much refined. Clear white slit images in the telescope $T$ are an adequate criterion.

In the absence of a liquid in $CC$, figure 71, the fringes are easily found after

careful preliminary measurement, and they are strong and satisfactory. When this adjustment is given, the presence of liquid in $CC$, if the two columns are of nearly equal length, does not much modify the adjustment. In fact, the fringes were found much more easily than I anticipated, and in quiet surroundings they are strong and fine. It is necessary, however, that the tube $CC$ should be of sufficient width to avoid all curvature due to capillarity, at least in the axis. Tubes 2 cm. in diameter and 10 cm. long of thin brass were first tried, but proved to be too narrow. No sharp slit images could be obtained with reasonable care as to setting the mirrors. Thereafter tubes 4 cm. in diameter were used, but even these are somewhat too narrow. Slit images, however, were sharp and parallel and could be easily brought to coincide.

With the wide tubes, however, the mobility of the liquid in $CC$ increases enormously, so that only under exceptionally quiet conditions could the fringes be seen, and never quite without quiver. The wind beating on the house, for instance, threw them nearly out of view, so that only a suggestion of their presence remained. In spite of the very promising beginnings, therefore, it became a serious question whether, with the apparatus as here devised, the purposes of the research could be reached in this laboratory.

Finally, the flickering of the arc lamp may be a grave inconvenience; for if the columns $C$, $C'$ as usual are virtually prisms, the coincidence of spectra will for this and other reasons be destroyed by the displacement of the arc.

**58. Equations.**—Some estimate of the increments to be anticipated may be given here, and expressed in terms of the Dulong-Petit experiment. If $\alpha$ is the mean coefficient of expansion of water at the temperature in question and $\Delta H$ the increment of the head $H$ corresponding to the temperature difference $\Delta t$ between the columns,

$$(1) \qquad\qquad \Delta H = \alpha H \Delta t$$

Again, if $\Delta N$ corresponding to $\Delta H$ is the displacement of centers of ellipses at the wave-length $\lambda$, and $\mu$ the index of refraction of water, so that $\mu = A + B/\lambda^2$, nearly,

$$(2) \qquad\qquad \Delta H = \frac{\Delta N}{\mu - 1 + 2B/\lambda^2}$$

Hence $\Delta t$ may be computed as

$$(3) \qquad\qquad \Delta t = \frac{\Delta N}{(\mu - 1 + 2B/\lambda^2)\alpha H}$$

Since the value of $\Delta N$ is within $10^{-4}$ cm. and $H = 10$ cm. in the above apparatus, we may further write at mean temperatures $(25°)$

$$\alpha = 2.5 \times 10^{-4} \qquad \mu = 1.333 \qquad B = 10^{-11} \times 3.1 \qquad 2B/\lambda^2 = 0.018 \text{ at the } D \text{ line.}$$

Thus $\mu - 1 + 2B/\lambda^2 = 0.351$ and $\Delta t = 10^{-4}/0.351 \times 2.5 \times 10^{-4} \times 10 = 0.114°$. In other words, in case of tubes 10 cm. long, the effect of a difference of tempera-

ture of about 0.1 degree between the tubes should be easily observable by mere displacement, whereas a difference of less than 0.03 would be equivalent to the passage of one interference ring.

Again, from equation (2), if $\Delta N = 10^{-4}$ cm., then $\Delta H = 10^{-4}/0.351 = 10^{-4} \times 2.8$ cm., or about $9 \times 10^{-4}$ cm. per vanishing interference ring are the displacements to be anticipated. These are equivalent to pressures of about 0.3 and 0.1 dyne per square centimeter.

**59. Observations.**—A large number of observations were made with the apparatus described, but as under present surroundings the fringes always quivered violently, no quantitative results of value were obtained. Naturally such experiments imperatively demand a laboratory remote from traffic, since the undulation of mobile liquid surfaces is introduced in addition to the tremors of solid appurtenances.

An attempt was made to register the pressure near an electrically charged point, but no results could be obtained. Again, though the attraction of an electrically charged surface for the free surface of water in either tube was recognized, on using adequately high potentials to measure the forces the surface became troubled and the fringes vanished. In this case, if $p$ is the pressure, $V$ the difference of potential in volts, and $d$ the distance apart of surfaces in centimeters, $f = 4.4 \times 10^{-7} \times (V/d)^2$ dynes/cm.$^2$ if $f = 0.3$ can just be determined by the displacement method, and if $V = 80$ volts (roughly) is the smallest potential difference discernible for quiet fringes. Finally, Dulong and Petit's experiment gave very definite results even for small ranges of temperature, subject to the conditions stated.

By surrounding the top of the tube $C$, figure 71, with a close-fitting helix, the upper face of which reached just below $r$, while the surface of liquid within, $w$, lay at its center, an attempt was made to detect the susceptibility $k$ of water, etc. If the field of the coil be written roughly $H = 0.4\pi i n/l$, where $i$ is the current in ampères, $n$ the number of turns, and $l$ the length of the helix, we may write

$$\rho g.\Delta h = H.kH = kH^2$$

Since $\rho = 1$, the increment of head, $h$, becomes

$$\Delta h = kH^2/g = (0.4 n\pi/l)^2 i^2 k/g$$

Hence if roughly $k = 10^{-6}$, $g = 10^3$, $i = 1$ am., $n/l = 35$ as in the helix used,

$$\Delta h = 44^2 \times 10^{-9} = 1.9 \times 10^{-6} \text{ cm.}$$

Thus if $i = 10$ ampères, $\Delta h = 2 \times 10^{-4}$ cm., nearly, and easily determinable by the displacement of ellipses, or from interference rings. The experiment was tried, but the quiver of rings was such as to admit of no decision. In case of the magnetic solutions, $k$ is of course much larger; but under the circumstances it did not seem worth while to attempt further work. This will be done with other apparatus in the course of this paper.

**60. Jamin's interferometer.**—The ease with which the Michelson inter-
ferometer may be adjusted and its remarkable adaptability have led to its
general preference over the older form of Jamin. Nevertheless, the latter
furnishes two parallel rays which for such purposes as the present are desir-
able. Hence if the four faces of the interferometer be separated in the manner
suggested by Mach (shown in fig. 73), a very available form of interferom-



eter is obtained. Here $M$ and $N$ are half-silvered plates, $M'$ and $N'$ the
opaque mirrors. The white light $L$ impinging from a collimator thus fur-
nishes the two component beams $ac$ and $bd$, which are observed with the tele-
scope at $T$, after passing the direct-vision prism grating $g$. If either mirror
$M'$ or $N'$ is displaced a distance $e$, moving parallel to itself, the path-differ-
ence $2e \cos \theta$ is introduced with the corresponding shift of ellipses. The
U-tubes $C, C'$, with their helices $H; H'$, and connecting pipe $p$ are now con-
veniently installed as shown. But the trouble with the arrangement is the
difficulty of adjusting the *four* surfaces. Not only are the centers of ellipses
liable to be remote from the center of the field, but it is often hard, without
special equipment, to even find the fringes.
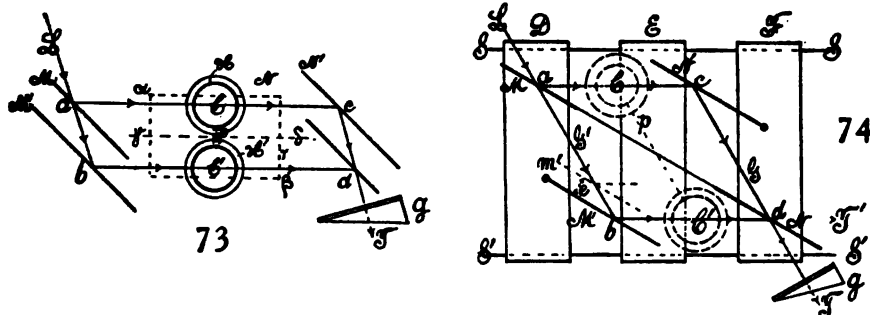
If, however, the device which I suggested in the preceding report is adopted—
*i.e.*, if (fig. 74) the half-silvered plates $M, N$ are at the ends of a single
strip of plate-glass, so that rays terminating in $M, M'\ N\ N'$ after adjust-
ment necessarily make a rhombus-like figure symmetrical to $MN$—the fringes
are found at once; for they appear when the white slit images in $T$ coincide
horizontally and vertically and the rays $bd$ and $cd$ intersect in the common
point $d$. Hence the mirrors $M', N'$ should be on carriages $D, F$, adapted to
move on parallel slides $S, S'$. $M, N$ may also be put on a carriage $E$, though
this is not necessary. $S, S'$ need not be parallel to $ac$ or $bd$. If the mirrors
$M'$ and $N'$ are wide, considerable latitude of adjustment is thus obtained.

If $MN$ is half-silvered on the same side (*i.e.*, toward $N'$) a compensator is
needed in $ac$ or $cd$ if path-difference is to be annulled (symmetry). If, how-
ever, $M$ is half-silvered on the $N'$ side and $N$ on the $M'$ side, no compensator
is required. In the latter case, however, if ordinary plate-glass is taken, $M$
and $N$ are not quite parallel and the ellipses will be eccentric. This, however,
is not necessarily a disadvantage, unless the strip $MN$ is excessively wedge-
shaped.

The ellipses obtained are usually long vertically—*i.e.*, quite eccentric— so that the fringes soon become straight and the rotation is extremely rapid whenever the center of ellipses is out of the field. It is therefore possible to adjust relative to horizontal fringes (parallel to the shadow of wire across slit), as these incline very obviously for a displacement of less than $10^{-4}$ cm. and rapidly become vertical. For this reason it makes little difference in practice whether the half-silvers are on the same or on opposite sides, or whether observation be made at $T$ ($cd$ prolonged) or at $T'$ ($bd$ prolonged). Moreover, the plate $MN$ may be conveniently constructed, as in figure 75, of two mirrors $m$, $n$, attached to the clear strip of plate-glass $g$ by aid of strong steel clips at $c, c'$. With the half-silvers $s, s'$, on the same side, the wedge-angle of the glass is excluded. For shorter diagonals, the plan of figure 76, with the silver surfaces $s, s'$ held together by clips at $c$, is preferable.
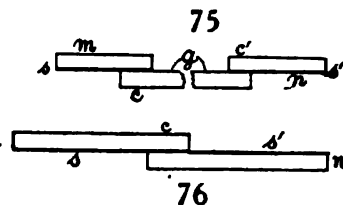
If the mirror $M'$, figure 74, is displaced a distance $e$, where a glass-plate compensator of thickness $E$ and refraction constants $\mu$ and $B$ is introduced normally either into $ab$ or $bd$, the equation is easily seen to be, at wavelength $\lambda$,

$$E(\mu-1)+2B/\lambda^2=2e\cos\theta$$

where $\theta$ is the angle of reflection at $M$. Using the plate $E=0.434$ cm. treated above, the first member is 0.2428 cm. Values of $e$ of 0.2420, 0.2409, 0.2427 were roughly obtained. Hence the mean value of $\theta$ should be about 60°, as it actually was.

The occurrence of this angle and the shift of the beam $bd$ along the mirrors $M'$ and $N$ are the main objections to the method of figure 74, for the rhombus is not necessarily perfect. If the ends of the plate $MN$ are silvered on the same side, the compensator must have double the plate-thickness to annul path-difference. Finally, the half-silvering does not, for large $\theta$, sufficiently exclude the reflection of $bd$ from the naked face of the plate, so that the fringes are never quite black. These difficulties may be met by making $MN$, figure 74, the *short* diagonal of the rhombus and using the strip, figure 76. In such a case $\theta$ at $M'$ is small, and in view of the nearly normal reflection at $M$ and $N$ relatively little reflection comes from naked glass, sliding is largely avoided, and no compensator is necessary. In this case the fringes for no path-difference are actually strong black horizontal lines on a colored ground and far enough apart that 0.1 fringe could easily be estimated. A test experiment with the above plate showed $e=0.1244$ cm., corresponding to the small angle $\theta$, a little over 12°.

When the U-tube $CC'$, figures 71 and 74, is introduced, the strip $MN$ will have to be at a considerable angle (about 45°) to the horizontal, so as to raise the $N$ end about 15 cm. above the $M$ end, corresponding to the height of $m$ above $m'$ in figure 71. The new condition, however, in no way changes

the general procedure. In case of figure 74, the mirror $N'$ must be high and $M'$ low. This is usually less convenient than the case when both mirrors are high ($C$ placed at $G$) or where both mirrors are low ($C'$ placed at $G'$). In the former case, again, the rays have considerably diverged in a vertical plane and the fringes are less marked. If $C'$ is at $G'$ the whole of each component beam may be caught and passed through the respective shanks of the U-tube. The fringes are strong, easily found, and large, so that the center of ellipses is not far outside of the field of the telescope. It is obvious that to facilitate adjustment the mirrors $m$ and $m'$, figure 71, must be nearly parallel. They are made so by the aid of a broad beam of sunlight and then clamped firmly in position at about $45°$ to the respective axis of the U-tube.

Finally, if the connecting-tube $p$ is nearly horizontal when in place, the fringes are usually found at about the same position of the micrometer (at $M'$) after the liquid is introduced into the U-tube. Here it is advantageous and usually permissible to make a part of the connection $p$ of flexible rubber tubing. But unless the free surface $w$, figure 71, is very nearly parallel to the plate $e$, the center of ellipses is liable to be far outside of the field of the telescope and the fringes correspondingly small. The difficulty of adjustment for large fringes is now considerable, because of the two mobile liquid surfaces in the U-tubes. For this reason I did not attempt to make measurements, although the fringes themselves were surprisingly steady and strong and would have been quite available, apart from laboratory tremors. Slight changes in density, due to solution or temperature changes in one shank of the U-tube, were well recorded, after stirring, with curious effects of surface-tension and viscosity.

The fringes being very clear, a number of other promiscuous experiments were tried. Thus, a tube with plate-glass ends and filled with water was made the core of a powerful magnetic helix. The tube, 26 cm. long, was placed in one of the component beams and compensated by a column of glass in the other. Good fringes were easily found; but not the slightest displacement could be detected by alternations of presence and absence of the magnetic field. The water was now replaced by a solution of nickel sulphate. Fringes were again easily found and strong in the green, but the effect of the magnetic field was quite as inappreciable as before. Magnetic fields were thus totally ineffective.

In a set of experiments of a different kind the attempt was made to observe the gradual deposition of silver on plate-glass. Böttger's solutions were poured into a plane-parallel clean glass trough normal to one of the component beams ($cd$, fig. 74) and compensated by a plate of glass in the other ($bd$). Large fringes were produced by setting the micrometer and observed during the formation of the two silver films on the opposite faces of the trough, until they became quite opaque. It was astonishing to find that fringes were still faintly visible long after a highly reflecting mirror had been deposited. But no displacement larger than a fraction of a fringe could be detected, showing the extraordinary thinness of the silver film even when practically opaque.

Similarly, the silver deposit on plate-glass was removed in parallel strips, so that the film had the appearance of a grid. The results when this plate was placed normally in one of the component beams were the same.

**61. Vertical displacement of ellipses.**—If the fringes are too small when horizontally centered by the micrometer, the center of ellipses may be brought into the middle of the field of the telescope by sliding one component beam vertically over the other without appreciably changing the direction of the rays. In other words, one illuminated spot at $d$, figure 74, is to move vertically relative to the other by a small amount. This may be done by placing a thick plate-glass compensator, such as is shown in figure 77, in each of the component beams $abd$ and $acd$ and suitably rotating one plate relative to the other, each on a *horizontal* axis. Very little rotation is required. In the same way elliptical fringes may be changed to nearly linear horizontal fringes when desirable. If the fringes are to be sharp the slit must be very fine. When sunlight is used with a slit not too fine, each of the coincident sodium lines ($D_1D_2$) frequently shows a sharply defined helical or rope-like structure, the dark parts in step with the fringes of the spectrum. It looks like an optical illusion of slanting lines or a shadow interference of two grids (fringes and sodium lines respectively); but later experiments showed it to be an independent phenomenon. (*Cf.* § 63 *et seq.*, 68, 70.)
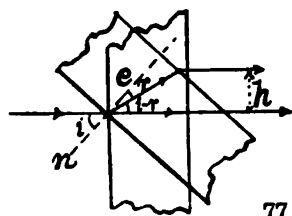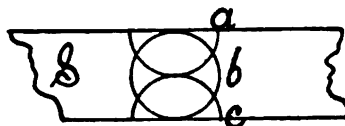


The first result is particularly interesting, inasmuch as it is thus possible to displace the centers of ellipses not only horizontally as usual relative to the fixed sodium lines in the spectrum, but also *vertically* relatively to the fixed horizontal shadow in the spectrum due to the fine wire across the slit. The following experiment was made to coördinate the vertical displacement of the component rays and centers of elliptic fringes: A glass plate $d=0.705$ cm. thick was placed nearly normally in the beam $ac$, figure 74, and provided with a horizontal axis and graduated arc. The amount ($i$) of rotation of the plate, corresponding to the vertical displacement of one central fringe in the telescope (*i.e.*, passage of fringe $a$ into $b$, into $c$, in the duplicate spectrum $S$, fig. 78), was then found to be, if $i$ is the angle of incidence,

|              | $i$    | $h$         |
|--------------|--------|-------------|
| No fringes...... | 3.5°   | 0.0149 cm.  |
| One fringe...... | 5.0°   | .0214       |
| Two fringes..... | 6.5°   | .0281       |

where $h$ is the corresponding vertical displacement of the rays $ac$, figure 74, and computed from ($\mu$ index, $r$ angle of refraction)

$$h = d(\sin i - \cos i \tan r)$$

Thus the vertical displacement of rays corresponding to the vertical semi-axes of the central ellipse or one fringe is between 0.0065 and 0.0067 cm.— *i.e.*, on the average below $7 \times 10^{-3}$ cm. Hence $h = N \times 0.007$ for $N$ such central fringes. It was difficult to get a closer result, owing to quiver.

The interesting question is now suggested, in how far such an arrangement would fall short of being able to exhibit the drag of the ether in a rapidly rotating body, should such drag occur. In figure 73, let $\alpha\beta$ be a cylinder of glass with plane-parallel ends, capable of rotating on the axle $\gamma\delta$. If $l$ is the length of the cylinder, $\mu$ its index of refraction, and $r$ the distance of either component ray $(ac, bd)$ from the axis $\gamma\delta$, $n$ the number of turns per second, and $V$ the velocity of light, we may write, using the above excessive estimate, $N$ being the number of fringes displaced,

$$h = \tfrac{1}{2}N \times 0.007 = 2\pi nrl\mu/V$$

since $ac$ rises while $bd$ falls. If

$$n = 200, \qquad r = 10 \text{ cm.}, \qquad l = 100 \text{ cm.}, \qquad V = 3 \times 10^{10}, \qquad \mu = 1.5,$$

$$N = \frac{6.3 \times 2 \times 10^2 \times 10 \times 10^2 \times 1.5}{3.5 \times 10^{-3} \times 3 \times 10^{10}} = 0.18, \text{ nearly}$$

It would thus be necessary to estimate about one-sixtieth of a fringe, which is just beyond the limit of certainty, even if $nr$ can be increased and $l$ multiplied by reflection. The device suggested is nevertheless of interest and deserves further consideration. It will appear much more promising in connection with the achromatic fringes described below.

### 62. Displacement interferometer. Jamin type.

—These considerations induced me to devote further study to the Jamin type of interferometer (fig. 73). The mirrors $M$, $N'$ were put on one pair of long slides (1.5 meters long) parallel to $ac$ and the mirrors $M'$, $N$ on similar slides parallel to the former. In this way any distance $ac$ or $bd$ was available. The beams were about 16 cm. apart, corresponding to a normal distance between the end mirrors ($NN'$, $MM'$) of about 12 cm. But these distances could also be increased from nearly zero ($M$ and $M'$ nearly contiguous) to about 20 cm. in view of the width of mirrors used. The angles at $a$, $b$, $c$, $d$ were each about 45°, so that a rectangle of rays is in question. (See figure 88 or 93 below.)

The adjustment proved eventually to be greatly facilitated by using a horizontal beam of sunlight with *weak* condenser-lens and collimator. A thin wire is to be drawn across the slit. $M$ and $M'$ are first set for parallelism in the absence of $N$ and $N'$, by adjusting the images of the slit at the same level (horizontal) on a distant wall. The images or shadows of the wire specified on the wall are to be equally far apart, with the beams $ac$ and $bd$ at the mirror. The mirrors $N$ and $N'$ are next put in place with the distances $acd$ and $abd$ about equal. The two images seen in the telescope at $T$ ($g$ removed) are then made to coincide both horizontally and vertically by adjusting $N$ and $N'$,

and these are then slid by a small amount on their slides (direction *ac*) until the rays are coincident at *d* to the eye (light strips on the mirror coincide).

If, now, the grating *g* is inserted, very fine oblique fringes will usually be seen. These may be enlarged to a maximum by moving the micrometer controlling the displacement $M'$ normal to itself. Somewhat coarser *horizontal* lines are thus obtained.

Finally, the distant centers of the ellipses are brought into the center of the telescope by aid of the thick glass compensator, like figure 77 (the equivalent air-path of the other ray being correspondingly lengthened) by rotating the glass plate on a horizontal axis.* It is desirable to have an excess of glass-path in one beam, as otherwise the ellipses are so large as to be unwieldy.

The ellipses so obtained with common plate-glass and a film grating at *g* were magnificent. A rough test of the displacement interferometer was made by using the above plate-glass of thickness $E = 0.434$ cm., where $s = E(\mu - 1) + 2B/\lambda^2 = 0.2428$ cm. In two experiments agreeing to within $10^{-4}$ cm., $2e = 0.3448$ cm. were the displacements obtained. Assuming that $\theta = 45°$, $2e \cos \theta = 0.2438$ cm. This agrees with *s* as nearly as may be expected, unless $\theta$ is specifically measured.

Experiments were now made (as above) with thick plate-glass compensators inserted in one component ray (*bd*) only, to determine the rotation of compensator ($i°$) necessary to raise the center of ellipses in steps of half the diameter of the first ring (see *a, b, c*, fig. 78). The initial angle *i* is already large and shows the rotation of compensator from the vertical needed to bring the ellipses into the field. Two sets of experiments were made with plates respectively $d = 0.965$ cm. and $d = 0.705$ cm. in thickness, with the results given in table 30.

TABLE 30.

| Experiment I. | | | |
|---|---|---|---|
| *d* | *i* | *h* | $\triangle h$ |
| 0.965 cm. | 9.0° | 0.0529 cm. | ........ |
|  | 10.1 | .0596 | 0.0067 cm. |
|  | 11.4 | .0676 | .0080 |
| Experiment II. | | | |
| *d* | *i* | *h* | $\triangle h$ |
| 0.705 cm. | 2.6° | 0.0100 cm. | ......... |
|  | 3.3 | .0139 | 0.0039 |
|  | 3.9 | .0165 | .0026 |

The equation of the preceding section is used for *h*. The first case shows about the same order of sensitiveness ($\triangle h$ per half-ring). In the second case, for the thinner plate, the sensitiveness has been more than doubled. This

---

* The same result may be obtained in the absence of the compensator by rotating $N$ and $N'$ on a horizontal axis, successively by small amounts, into parallelism with $M$ and $M'$.

is in a measure not unexpected, because the amount of displacement, *cast. par.* (*i.e.*, the mobility and size of ellipses), increases in marked degree as the plate compensator is thinner. But apart from this $\Delta h$ is in some way, yet to be stated, associated with the obliquity of rays in a vertical plane.

In case of the rotating compensator, vertical and lateral displacement of centers of ellipses go together. It is therefore next in order to determine the ratio of vertical and lateral displacement.

The equation deduced in § 8, which follows easily from figure 77, may be put in the form (for a single passage of light through the plate)

$$n\lambda = 2e(\sin^2 i/2 - \mu \sin^2 r/2)$$

or into the approximate form for small angles

$$n\lambda = e(\mu - 1)i^2/2\mu$$

From the former equation

$$\frac{di}{dn} = \frac{\lambda}{e(\sin i - \cos i \tan r)}$$

or approximately, again,

$$\frac{di}{dn} = \frac{\lambda\mu}{e(\mu - 1)i}$$

Hence, if $\Delta i$ corresponds to $x$ fringes,

$$\Delta i = x\frac{di}{dn} = x\frac{\lambda\mu}{ei(\mu - 1)} \text{ roughly}$$

Again, for the corresponding normal displacement $\Delta N$ of the micrometer at the opaque mirror,

$$x\lambda = 2\Delta N \cos \theta$$

Hence

$$x = \frac{ei(\mu - 1)\Delta i}{\lambda\mu} = \frac{2\Delta N \cos \theta}{\lambda}$$

The data given in table 31 were found from successive positions of the plate $e = 0.705$ cm., while the center of ellipses moved as in figure 78, at the $D$ line.

TABLE 31.

| | Center at | | | $10^4 N$ | $10^4 \Delta N$ | $x$ | |
|---|---|---|---|---|---|---|---|
| | $i$ | $\Delta i$ | $x$ | | | | |
| Bottom..... | 13.6° | ... | .. | 19 cm. | ... | ... | $\theta = 45°$ |
| Middle..... | 12.5 | 1.1 | 18 | 28 | 9 | 22 | $x = 1.27 i\Delta i$ |
| Top........ | 11.5 | 1.0 | 15 | 35 | 7 | 17 | $x = 24,000\Delta N$ |
| Bottom..... | 7.5 | ... | .. | 111 | ... | ... | $10^6\lambda = 59; \mu = 1.53$ |
| Middle..... | 6.7 | 0.8 | 7 | 115 | 4 | 10 | |
| Top........ | 5.9 | 0.8 | 6 | 119 | 3 | 8 | |

In view of the small values of $\Delta N$ and $\Delta i$ and the estimated $\mu$ and $\theta$, the two sets of values of $x$ are no more divergent than would be expected. The

values of $i$ are very different in different adjustments, because the ellipses may also be raised and lowered by rotating one of the opaque mirrors, as $M$, around a horizontal axis, though in this case with rapid loss of sharpness. Here the rotation of both mirrors of a pair, $M'$ and $M$ for instance, by the same amount, is required as an equivalent to the rotation of the compensator, as has been stated. The aim is to render both parallel pairs themselves parallel.

If $x\lambda$ is eliminated from the two equations on the preceding page,

$$\mu = \frac{1}{1 - 2\Delta N \cos \theta / eiΔi}$$

The above data are inadequate for evaluating $\mu$, but they nevertheless indicate a value entirely too low. It seems, therefore, as if some essential term has been left out of sight. This is also to be inferred from the values of $x$, which differ systematically on the two sides of the table 31.

TABLE 32.—Refraction of a glass plate. $e = 0.434$ cm. $\mu = 1.53$. Rotation around vertical axis. Jamin type displacement interferometer. $\theta = 45°$.

| $i$ | $\Delta N \times 10^3$ | $\mu$ | $i$ | $\Delta N \times 10^3$ | $\mu$ |
|---|---|---|---|---|---|
| | cm. | | | cm. | |
| +12.5° | 2.60 | 1.56 | − 6.5° | .60 | .... |
| 10.5 | 1.65 | 1.47 | − 8.5 | 1.20 | 1.56 |
| 8.5 | 1.25 | 1.51 | −10.5 | 1.75 | 1.52 |
| 6.5 | .70 | .... | −12.5 | 2.60 | 1.56 |
| 4.5 | .45 | .... | −14.5 | 3.35 | 1.51 |
| 2.5 | .05 | .... | −16.5 | 4.60 | 1.57 |
| ± 0.0 | .00 | .... | −18.5 | 5.60 | 1.55 |
| − 4.5 | .30 | .... | | | |
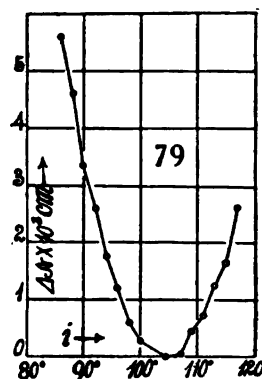


In view of the discordant results obtained here and elsewhere with this type of rotating compensator, the provisional parts of the apparatus were improved by mounting a more accurate graduated circle with vertical axis and tangent screw. A good plane-parallel plate of thickness $e = 0.434$ cm. and refractive index $\mu = 1.53$ was then adjusted normal to the ray passing through it, by noting the position of reversal of motion of the ellipses both when the plate was rotated around a vertical and around a horizontal axis. The data of table 32 and figure 79 were found while the plate was rotated on its vertical axis both in a clockwise and counter-clockwise direction from the normal position. In the former case (left side of curve) the normal position showed the same constants before and after. In the latter this was not quite the case, the micrometer being not sufficiently refined for such purposes.

The results for $\mu$ were computed from the full equation

$$\Delta N \cos \theta = e \sin^2 \frac{i}{2} \cdot \left(1 - \frac{1}{\mu}\right)$$

They are as good as the small values of $\Delta N$ and the impossibility of obtaining the zero of $i$ with sufficient sharpness admit, and they show that the latter cause adequately explains all the irregularities encountered.

The equations are liable to be cumbersome in the cases of greatest interest. I therefore proceeded experimentally to obtain a limit of $\Delta h$ or $\Delta x$ per fringe, using thinner glass compensators. The results are given in table 33. The ellipses were now so large and distorted that it was difficult to define the center of irregular rings. The transverse displacement is therefore largely referred to the top, middle and bottom of the spectrum band, which took up about one-third of the height or diameter of the field of the telescope. The angular width of the latter being about $3°$, the corresponding angular height of the spectrum is thus about $1.0°$. In view of the large rings, moreover, the displacement $\Delta N$ at the micrometer of the mirror $M'$ is difficult to obtain and the data given are estimates. Experiments like the present must be made with optic plate-glass, so that sharp rings nearly circular may be obtained, if the data are to be quite satisfactory. In table 33, $\Delta h$ thus corresponds to a transverse displacement of one component ray parallel to itself, equivalent to a displacement of the centers of ellipses of about $0.5°$ at the sodium line.

TABLE 33.—Vertical (transverse) displacement of ellipses. Glass-plate compensators $\mu = 1.53$. Horizontal axis. Angle of telescopic field $3°$; angular height of spectrum about $1.0°$ or $0.175$ radian. Vertical diameter of first fringe in excess of height of spectrum.

| Fringe centers at | $e$ | $i$ | $h$ | $\Delta h \times 10^4$ | $\Delta N \times 10^4$ |
|---|---|---|---|---|---|
| | *cm.* | | *cm.* | *cm.* | *cm.* |
| Top of spectrum..... | 0.300 | 0.4° | 0.0007 | −26 | ... |
| Middle of spectrum.. | ..... | 1.9 | 34 | 0 | ... |
| Bottom of spectrum.. | ..... | 2.6 | 47 | +13 | ... |
| Bottom of spectrum.. | .300 | 2.3 | .0042 | +22 | ... |
| Middle of spectrum.. | ..... | 1.1 | 20 | 00 | ... |
| Top of spectrum..... | ..... | 0.0 | 00 | 20 | ... |
| B................. | 0.434 | 40.8° | 0.1274 | +15 | 0 |
| M................. | ..... | 40.2 | .1259 | 00 | 7 |
| T................. | ..... | 39.2 | .1217 | −42 | 22 |
| B................. | .434 | 8.1 | .0213 | +12 | 0 |
| M................. | ..... | 7.6 | .0200 | 00 | 0 |
| T................. | ..... | f 7.1 | .0187 | −13 | 2 |
| B................. | .434 | 6.5° | .0170 | +29 | 0 |
| M................. | ..... | 5.4 | .0141 | 00 | 2 |
| T................. | ..... | 4.3 | .0112 | −29 | 7 |
| B................. | .434 | f 3.3 | .0087 | +19 | 0 |
| M................. | ..... | 2.6 | .0068 | 00 | 4 |
| T................. | ..... | 1.5 | .0039 | −29 | 4 |
| B................. | .020 | 20.0 | .00253 | +14 | ... |
| M................. | ..... | 9.4 | .00115 | 00 | ... |
| T................. | ..... | −3.6 | −.00044 | −16 | ... |

The mean result of all data is here about $\Delta h = 0.002$ cm., and this is not influenced in a discernible way, either by the thickness of plate $e$ or by the rotation angle of the compensator $i$. The smallest value $\Delta h = 0.0012$ cm. appears incidentally and not when the system of four mirrors is most nearly in parallel adjustment. The transverse displacement of ellipses changes sign with the sign of the rotation of $i$ in all cases and is independent of the normal position. The longitudinal displacement reverses at the normal position.

**63. Broad slit interferences. Achromatic fringes.**—Some allusion has been made above to a type of interferences totally different in size from the regular fringes and seen in the broadened slit. These were finally isolated and show exceedingly interesting properties. They appear to best advantage, in the absence of the spectroscope, in the broad white field of a very wide slit. The latter may be removed. They have the appearance when vertical of regular Young or Fresnellian fringes, very sharp and fine, achromatically black and white at the middle of the grid, colored and fainter outward. They are vertical when the enormously larger spectrum fringes discussed above are centered. Like these, they partake of displacement here through the broad white slit image, and this displacement is extremely sensitive in relation to the displacement of the opaque mirror $M'$ (fig. 73) to which it is due. Thus a displacement of $\Delta N = 10^{-4}$ cm. of the latter corresponds to a march of fringes through about 0.017 of the telescopic field of $3°$; *i.e.*, to $0.05°$. This comprises two fringes or $\Delta N = 5 \times 10^{-5}$ cm. per fringe. Now, these fringes are so sharp and luminous that it should be possible on proper magnification to measure a few hundredths of this with an ocular micrometer. It is from this point of view that I regard the new fringes important. They supply the fine fiducial mark in displacement interferometry for which I have long been seeking. They appear in a white field, thus requiring no spectrum resolution nor monochromatic light. Moreover, the source of light need not be intense.

To have a distinctive name for these fringes which will be much used in the work following, I shall refer to them under the term "achromatic fringes." If not too large, the central fringes are straight and almost quite black and white.

The displacement of fringes with $\Delta N$ at the mirror (when $n\lambda = 2\Delta N \cos \theta$) is so rapid that if they are lost it is difficult to find them, unless the centered large spectrum fringes in the spectroscope are first reëstablished. The latter are easily found. A removal of the prism grating $g$, figure 73, and a widening of the slit show the achromatic fringes. The datum for sensitiveness may be found directly as follows: The displacement at the mirrors corresponds to about two residual fringes. Thus a single fringe (distance apart of the intensely black lines at the center which can be distinguished and used as fiducial lines for this very reason) corresponds to a displacement of mirror of $\Delta N = 50 \times 10^{-5}$, as above. The white pattern, as a rule, appears but once and is not usually present rhythmically, as is the phenomenon in the next section for homogeneous light.

As a clue to the nature of the residual fringes, one may note in the first place that they may be recovered in the principal focal plane, if the two white slit images which may have separated be put in coincidence. Without such coincidence they are seen sharply in other focal planes.

Later, on more careful adjustment as to parallelism by the auxiliary normal method described below, periodic reappearance of the achromatic fringes was in fact obtained. The central set was exceedingly strong and sharp as usual. To the right and left of it similar patterns or groups rapidly decreasing in strength were discovered. Not more than two patterns on each side of the

central set could be seen. The white field between the patterns was several times the width of the fringed field. Each group as a whole resembles the fringes of the biprism, as usual, and they differ appreciably only in intensity and in their focal planes. It is difficult to account for this periodic reappearance; but it must be due to reflections at the half-silver surfaces. The reflections from the uncovered surfaces are indeed just visible, and naturally, since they are duplicates, they also carry the fringes. But they are easily differentiated by the relative faintness of field and have nothing to do with the recurrences in question.

Ordinary daylight is quite adequate to show the residual fringes in the complete absence of the collimator. They are superimposed on the field of view (landscape, etc.) and hence will subserve other purposes than are here given. When the adjustment for parallelism is not sharp, the fringes may often be found strong in continuously varying focal planes.

**64. Wide slit. Homogeneous light. Sodium flame.**—A further clue to the nature of the residual fringes will be obtained when white light is replaced by homogeneous light. A strong, large sodium flame near the mirror $M$, figure 73, suffices. The fringes now appear of the same size in yellow light, naturally spread over a much larger area of field. But on moving the mirror $M'$ ($\Delta N$ increasing continually) forward very gradually, the homogeneous fringes alternately vanish and reappear, each time, however, enlarged in size (nearly doubled but still straight) until at an intermediate position of symmetry enormous round ovals cover the yellow field. The fringes then diminish symmetrically in the same way. The following data for the micrometer position corresponding to the clearest demarcations of fringes are illustrative. At least six periods ($n$) are easily detected on each side of the ovals ($n = 0$). Thus (originally small fringes, vertical, increasing in size to huge ovals)
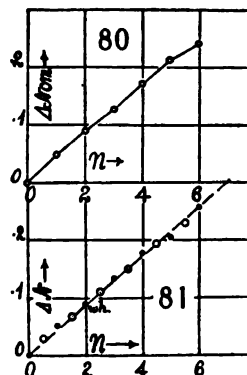
| $n =$6 | 5 | 4 | 3 | 2 | 1 | 0, etc. |
|---|---|---|---|---|---|---|
| $\Delta N \times 10^3 =$0 | 49 | 90 | 127 | 171 | 214 | 243 cm., etc. |

These intervals, since it is impossible to establish the maximum states of presence or absence of fringes quite sharply, are practically equidistant, as figure 80 indicates. Thus the mean period of reappearance is $\Delta N = 0.042$ cm.; or a path-difference of $2\Delta N \cos \theta = 0.059$ cm.; or a shift of ray parallel to itself ($2\Delta N \sin \theta = 0.059$ cm.) of the same amount.

The reason for this rhythm can only be the two wave-lengths of the $D_1$ and $D_2$ lines of the sodium flame, originally detected in the colors of thin plates by Fizeau. Hence a relatively enormous shift of micrometer of nearly 0.5 mm. is equivalent to the wave-length interval $\Delta \lambda = 6 \times 10^{-6}$ cm., or $\Delta \lambda / \Delta N = 6 \times$

$10^{-6}/42 \times 10^{-8} = 1.4 \times 10^{-6}$. Treating the case in terms of the interferences of thin plates and two wave-lengths, $\lambda$ and $\lambda + d\lambda$,

$$n\lambda = \text{constant}, \quad \text{or} \quad \frac{\Delta\lambda}{\lambda} = \frac{\Delta n}{n} = \frac{1}{n} \text{ for each period}$$

while

$$n\lambda = \frac{\lambda^2}{\Delta\lambda} = 2\Delta N \cos\theta \quad \text{or} \quad \Delta N = \lambda^2/2\Delta\lambda \cos\theta$$

since ($\theta = 45°$) approximately,

$\lambda = 60 \times 10^{-6}$ cm., $\quad \Delta\lambda = 6 \times 10^{-8}$ cm., $\quad \cos\theta = 0.71$, $\quad \Delta N = 0.041$ cm.

agreeing as nearly as may be expected with the experimental datum. The apparatus thus serves incidentally for investigating such properties of spectrum lines as Michelson in particular has detected. Finally, with the sodium arc the data of figure 81 were found, where black dots denote fringes, open circles a clear yellow field. The mean trend is about $\Delta N = 0.043$ cm. per period or wave-length gained. White fringes coincided with $n = 2$.

With white light the interference grid does not usually reappear rhythmically, nor does it correspond to the zero period of figure 80—i.e., to the ovals for sodium light. It was exactly of the size of the fourth period, in yellow light; it always coincides with the central ellipses of the spectroscope as stated, but does not require sharp horizontal and virtual coincidence of the superposed images. The reappearance of the achromatic fringes obviously depends on conditions different from the case of sodium light.

In a flash of the arc, showing many sharp spectrum lines in all colors, each of the lines gives evidence of the phenomenon—i.e., if the residual fringes are oblique, each such line is strongly helical in appearance.

If a single compensator (i.e., a glass plate in one interfering beam) is used and the path-difference annulled, the fringes are visible again, but very rapidly grow smaller with the increase of glass-path. If compensators of nearly like thickness and glass are used in both beams, they nearly neutralize each other if at the proper angle one to the other. But there is almost always an outstanding micrometeric difference in thickness (if ordinary glass plate is used) of great importance in modifying the residual phenomenon. The following experiments, for instance, were made with a compensator 0.944 cm. thick in the rear and 0.958 cm. thick in the front beam, both of the same glass. The half-silver mirrors were 0.7 cm. thick. The wide-slit experiments are supposed to start after the spectrum ellipses first to be found (fine slit) have been centered. The fringes are always clear and very sharp when the white slit images accurately coincide.

With the compensators $A$, $B$ at the proper angle and rotating in the same direction (fig. 82), fringes of very slight enlargement were seen with the lines nearly vertical. If the compensators $A$, $B$ were rotated at a proper pace in the opposite direction to each other, $A$, $B$, figure 83, the fringes $f'$ and $f''$ grew rapidly smaller and turned toward the horizontal. Since the fringes are large circles and the beams here rise and fall, respectively, while a greater

glass thickness is introduced, this result is to be expected. It shows the importance of the differential glass-path.

The preceding thick half-silver mirrors (0.7 cm.) were now replaced by thinner half-silvers, the glass plates being each about 0.3 cm. thick. The fringes after being found had not appreciably changed. Another pair of half-silvers of the same thickness was then installed with like results. But now, on adding the compensators (0.944 and 0.958 cm.) as above, a marked enlargement of fringes resulted. Small differential thicknesses must here have been accidentally compensated. Opposite rotations, as in figure 83, rapidly produced very fine, nearly horizontal fringes $f'f''$. Rotation as in figure 82 left the vertical fringes nearly intact, but on passing from the position $AB$ to $A'B'$ very marked enlargement occurred, as follows:

| Mean angle of glass plates. | —45° | 0° | +45° |
|---|---|---|---|
| Mean angle subtended by one fringe in the telescope. | 0.0015 rad. | 0.008 rad. | 0.0005 rad. |

The compensator plates were now exchanged and the fringes found after centering. They proved to be very much smaller, the angle subtended in the same telescope being only about 0.0002 radian. The preceding accidental compensator has therefore been destroyed by exchange.

On passing through the normal position of one plate in figure 82, the fringes usually incline toward one side or the other. Thus there can be little doubt that the fringes in question are due to slight difference of glass-path or extremely sharp glass-wedge excess in one or the other component beam. In fact, I found eventually that fringes could be enlarged by rotating the proper compensator around a vertical axis. Large fringes (up to 0.002 radian in the given telescope) are usually colored and curved and not so available as smaller fringes highly magnified. It is in this way (double rotation) that it was possible to make the white fringes coincide in order with the ovals of the fringes for homogeneous light ($n=0$), the orders met with above being the $n=2$ and $n=4$. The fringes resemble those of Fresnel's biprism; but as they are seen with a wide slit or in the absence of a slit only, as they coincide with the centered spectrum ellipses of a fine slit and as they are a definite order (second, for instance) of the fringes seen with a flame of homogeneous light, they are necessarily referable to the colors of thin plates.

Hence the equation for these fringes may be assumed to be (as may be seen from figure 84, where $A$ and $B$ are the compensators)

$$n\lambda = (e - e')\ (\mu \cos (r - a) - \cos i)$$

when $e$ and $e'$ are the thicknesses of the two half-silver plates, $\mu$ their index of refraction, $i$ the angle of incidence, $r$ the angle of refraction of an incident ray, and where $a$ is the outstanding angle between the faces of the differential
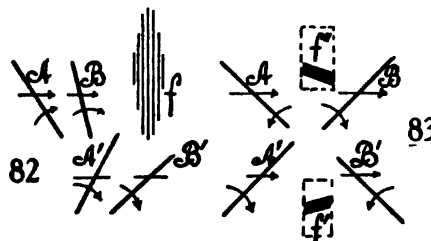
glass wedge, $e-e'$ thick at the ray in question. The possibility of throwing these fringes into any order of size, their small extent, sharpness, and great abundance of light constitute their value for measurement.

Thus it is furthermore obvious that the achromatic fringes must also be obtainable in Michelson's interferometer, in any order of size and in a field of white light. Tests were made with this object, beginning with the fine slit and the centered ellipses of the spectrum interferences. Removing the spectroscope and enlarging the slit indefinitely, the residual fringes appeared. They were never so strong and clear, however, in any order, as was the case with the Jamin interferometer, although many trials with different compensators were made. They would not be useful for measurement. Removing white light and replacing it by sodium light, the white fringes were found to be of exceedingly high order, more than 0.7 cm. of micrometer-screw being needed before the circles of the yellow field were approached. The latter were very vague and usually not seen in the principal focal plane of the telescope. Since the rays retrace their path in the Michelson interferometer, the raising and lowering of the spectrum ellipses is not possible; but the residual fringes may be put in any order by changing the differential glass-path of the rays. They appear but once, not rhythmically like the sodium fringes.

The equation for this phenomenon would thus be (since the rays retrace their paths)

$$n\lambda = 2e\mu \cos (r - \alpha)$$

where $e$ is the thickness of the single half-silver and $\alpha$ its effective wedge angle, positive or negative.
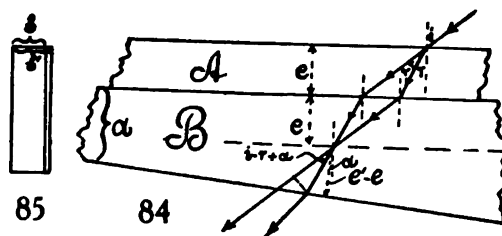


To obtain the circular fringes in Michelson's interferometer with a wide slit and homogeneous light, the rays must rigorously retrace their path—i.e., all reflection must take place at the same spot on the half-silver plate. When this is the case the fringes, even though obtained with common plate-glass and a sodium flame, are beautifully circular and sharp. This is due to the fact that so small a part of the plate is used. They are stationary and exhibit the Fizean periods due to the doublet $D_1D_2$, admirably. With white light the fringes are faint and useless. When the rays do not accurately retrace their paths—i.e., when there are two spots of light on the half-silver one or more centimeters apart—the fringes are soon linear and very small, as above.

With regard to the last equation, if $N$ is the *difference* of normal distances to the two opaque mirrors $(M, N)$ of the Michelson interferometer, from the

two respective extremities of the normal to the half-silver, at the point where the incident ray impinges on it, the equation may be more completely written

(1) $$n\lambda = 2e\mu \cos R - 2N$$

if $\alpha$ is temporarily disregarded. $N$ is independent of color $\lambda$, but otherwise represents the difference of air-paths of the two interfering rays. From this equation

(2) $$\frac{d\lambda}{dn} = \frac{\lambda^2}{2e(\mu \cos R - (\lambda/\cos R)(d\mu/d\lambda)) - 2N}$$

so that the center of ellipses is at $\lambda$ in the spectrum when

(3) $$N = N_e = e\left(\mu \cos R - \frac{\lambda}{\cos R}\frac{d\mu}{d\lambda}\right)$$

Furthermore,

(4) $$\frac{d\lambda}{dN} = \frac{\lambda}{N - N_e}$$

and $$n = \frac{2e}{\cos R}\frac{d\mu}{d\lambda} \text{ depends essentially on } \frac{d\mu}{d\lambda}$$

On the other hand, in case of homogeneous light of wave-length $\lambda$,

(5) $$\frac{di}{dn} = \frac{\lambda}{2\mu \cos R.(de/di) - 2e \tan R \cos i} = \frac{\lambda}{n\lambda(de/e)/di - 2e \tan R \cos i}$$

where $de/di$ may be either positive or negative.

Centers occur when

(6) $$\frac{de}{di} = \frac{e \tan R \cos i}{\mu \cos R} \quad \text{or} \quad \frac{de}{dR} = e \tan R$$

Thus $di/dn$ is never independent of $\lambda$ and the centers of equation (6) are, as a rule, quite different from those of equation (3). If the angle $\alpha$ is admitted, equation (6) takes the form

(7) $$\frac{de}{dr} = e \tan R (1 - 2\alpha/\sin 2R)$$

The occurrence of the residual fringes for the same adjustment of the micrometer as the centered spectrum fringes is thus incidental. To obtain the latter the two superimposed spectra of a fine slit must coincide horizontally and vertically throughout their extent—*i.e.*, the two linear white slit images must coincide. If now the slit is indefinitely widened, there are two vertical lines in the superposed broad white images which are completely in coincidence. In case of ordinary plate-glass the remainder of the images will not be mutually in coincidence or generally there can not be coincidence in every color. The residual or achromatic fringes are found at and near the line of coincidence in question. Hence if either opaque mirror is slightly rotated on a vertical axis the residual fringes pass from edge to edge of the broad white slit images, $S$ and $S'$, figure 85, of slightly unequal width. Thus if the mean breadth is $S$ and the difference of breadth $\Delta S = S' - S$, the very small

angle corresponding to $\Delta S$ is measured by the motion of the fringes over the relatively large angle $S$. Hence this is a sensitive method for measuring angles which will be utilized below.

Finally, the cause of displacement is to be given. If the fringes were homogeneous in light, they would fill the whole field and simply wander indistinguishably to or from the center of homogeneous circles when the micrometer is moved. But when white light is used the phenomenon is narrowed to a few fringes systematically grouped about two sharply distinguishable achromatic vertical fringes in the middle. The displacement of these is thus accurately measurable and they may always be brought back to the field of the telescope. Moreover, the distance apart of two black fringes must correspond to the mean wave-length of light—$i.e.$, if $\Delta N$ is the displacement of the micrometer mirror corresponding to a fringe-breadth for the angle of incidence $i$ (here $45°$),

$$2\Delta N \cos i = \lambda$$

or

$$\Delta N = \lambda/2 \cos i = 60 \times 10^{-6}/2 \times 0.707 = 43 \times 10^{-6} \text{ cm.}$$

agreeing reasonably closely with the above rough estimate of $\Delta N = 5 \times 10^{-6}$ cm.

If we take the equation for the residual fringes in the Jamin apparatus as

$$n\lambda = \epsilon(\mu \cos R - \cos i)$$

where $\epsilon = e - e'$ is the differential thickness of the compensators and the residual angle $\alpha$ is neglected (fig. 84),

$$\frac{di}{dn} = \frac{\lambda}{(\mu \cos R - \cos i) \, (d\epsilon/di + \epsilon \sin R/\mu \cos R)}$$

so that for large fringes the compensators must be so chosen that both $\epsilon$ and $d\epsilon/di$ may be small, where $d\epsilon/di$ may be either positive or negative.

The last equation may be written

$$\frac{di}{dn} = \frac{1}{\left(\dfrac{d\epsilon/\epsilon}{di} + \dfrac{\sin R}{\mu \cos R}\right) n}$$

and accounts for the rapid decrease of size of fringes with the differential thickness of the plate compensators.

**65. Vertical displacement.**—In conclusion, the rise and fall of spectrum fringes ($i.e.$, the transverse motion observed and utilized when a compensator of the form figure 77 rotates on a horizontal axis) must be considered. This method was used above for centering the spectrum fringes. Naturally the actual motion of centers is obliquely upward or downward, unless the increase of glass-path is compensated by the micrometer at the opaque mirror. The rays leaving the collimator are parallel in a horizontal plane only. They are not collimated in a vertical plane. Hence these rays intersect at the

conjugate focus of the objective of the collimator, usually somewhere between the mirrors $M M'$ and $N N'$ in figure 73. This intersection is nearly in a horizontal line, owing to the horizontal width of the collimated beam. Hence as in figure 86 there are two virtual linear sources of light, $a$ and $b$, normal to the plane of the diagram, the rays from which may be treated for practical purposes as capable of interfering, since they come originally from the identical slit of the collimator. The effect of rotating the compensator (fig. 77) on a horizontal axis is thus to move these linear sources, $a$ and $b$, through each other vertically, and hence their distance apart may be called $h$, where if $d$ is the compensator thickness, $i, r$ angles of incidence and refraction at the compensator, $\mu$ its index of refraction,

$$h = d \, (\sin i - \cos i \tan R) = di \frac{\mu - 1}{\mu} \text{ nearly}$$

The fringes will thus be larger as $h$ is smaller (fig. 86), in accordance with the equation

$$\frac{\lambda}{h} = \frac{x}{r} = \theta$$

where $x$ is the distance apart for the distance $r$ and $\theta$ the angle between two fringes observed in the telescope, for instance.

Experiments were made to test the last equation by attaching an ocular micrometer to the telescope, so that if $x$ is the distance and $r$ the length of the telescope, $\theta$ is given. The distance between fringes in the same part of the field was then measured from different angles of incidence $i$ at the compensator. The results were, if $\lambda = 6 \times 10^{-5}$ cm., $r = 19.5$ cm. (table 34).

TABLE 34.

| $i$ | $h \times 10^3$ | $(\lambda/h) \times 10^3$ | $x$ | $(x/r) \times 10^3$ |
|---|---|---|---|---|
| 0° | 0 cm. | 0.0 | (0.2) cm. | .... |
| 3.6° | 22 | 2.8 | .05 | 2.6 |
| 6.6° | 40 | 1.5 | .03 | 1.5 |
| 8.6° | 51 | 1.2 | .025 | 1.3 |

These results for $\theta = \lambda/h$ and $\theta = x/r$ may therefore be considered as identical, since the fringes vary in size within the field of the telescope.

Finally, a displacement $\Delta N$ at the opaque mirror will move the virtual sources $a$ and $b$ in a horizontal plane, $2\Delta N \cos I$ in the direction of rays and $2\Delta N \sin I$ transverse to that direction if $I$ is the angle of incidence. Hence $b$ is usually found at some point $c$ and moves into $c'$ by the rotation of the compensator in question about a horizontal axis. The fringes do not therefore necessarily pass through infinite size unless $c$ is at $b$, which would then pass through $a$. The condition of maximum sensitiveness in transverse displacement is therefore a large fringe-angle $\theta$, a condition which requires use of optic plate. Fringes subtending 1° would admit of $\Delta h = 3.5 \times 10^{-3}$ cm.

per fringe, and that is about the mean value obtained in table 33 and elsewhere. In the present mode of treatment merely practical conveniences are aimed at. A more uniform method will be given in the next chapter.

**66. Angular displacement of fringes.**—Having for other purposes installed an ocular micrometer in connection with the telescope, it seemed worth while to make a direct test of the equations given elsewhere.* These are apart from signs

$$\frac{d\lambda}{dN_e} = \frac{\lambda e}{\cos R}\left\{\frac{\tan^2 R}{\mu}\left(\frac{d\mu}{d\lambda}\right)^2 + \frac{d^2\mu}{d\lambda}\right\}$$

When $\mu = A + B/\lambda^2$, $\lambda = D$ (sin $i$ — sin $\theta$), and when two plates, the half-silver of thickness $e$ and angles of incidence $i$ (constant) and of refraction $R$, and a compensator of thickness $E$ and at normal incidence are included, these may be changed to

$$\frac{d\theta}{dN_e} = \frac{\lambda}{(2B/\lambda^2) D \cos^2 \theta}\left\{\frac{1}{\frac{e}{\cos R}\left(3 + \frac{2B}{\lambda^2}\frac{\tan^2 R}{\mu}\right)} + \frac{1}{3E}\right\}$$

Here $d\theta/dN_e$ is the displacement of the center of ellipses per centimeter of displacement of the normal micrometer at one opaque mirror of the Michelson device, for the wave-length $\lambda$. $D$ is the grating constant and $\theta$ the angle of diffraction. In the apparatus used $D = 167 \times 10^{-6}$ cm., $\theta = 20°40'$ at $D$ line, $i = 30°$, $R = 19° 5'$ in case of glass and $17° 52'$ in case of carbon-bisulphide plates; $\lambda = 58.93 \times 10^{-6}$ cm.; $B = 4.6 \times 10^{-11}$ or $2B/\lambda^2 = 0.0265$, $\mu = 1.53$ (glass). Under these circumstances the term

$$2B \tan^2 R/\lambda^2\mu = 0.0021$$

and may be neglected in comparison with 3. Thus the equation takes the simpler form

$$\frac{d\theta}{dN_e} = \frac{\lambda}{(6B/\lambda^2) D \cos \theta}\frac{1}{E + e/\cos R}$$

The values of $E$ and $e$ are given in table 35. The data marked $d\theta/dN_e$ (computed) in the table were found from the last equation.

TABLE 35.—Reduction of sensitiveness by glass thickness. $D = d/\cos r$. Incidence at $i = 30°$, $R = 19° 5'$ (glass), $17° 52'$ (CS$_2$), compensators normal. Glass: $\mu = 1.53$; CS$_2$, $\mu = 1.63$. Telescope 19.5 cm. long. $2B/\lambda^2 = 0.0265$. $D = 167 \times 10^{-6}$ cm. $\theta_D = 20° 40'$.

| Detail. | $e$ | $E$ | Glass. $ed/\cos R$ | CS$_2$ $E/\cos R$ | Total $E' \pm E$ $+e/\cos R$ | $\frac{dx}{dN_e}$ | $\frac{d\theta}{dN_e}$ observed. | $\frac{d\theta}{dN_e}$ computed. |
|---|---|---|---|---|---|---|---|---|
| | cm. | cm. | cm. | cm. | cm. | | | |
| Glass+CS$_2$... | +0.27 to 0.27 | 0.60 | .0 | 0.63 | 0.63 | 33 | 1.70 | .... |
| Glass+glass | 0.695 | .562 | .735 | .562 | 1.297 | 63 | 3.2 | 3.7 |
| Glass........ | .695 | .0 | .735 | .0 | .735 | 126 | 6.5 | 6.5 |
| Glass—glass | .695 | .247 | .735 | .247 | .488 | 182 | 9.3 | 9.7 |
| Glass—glass | .695 | .562 | .735 | .562 | .173 | 500 | 25.64 | 27.6 |

* Carnegie Inst. Wash. Pub. No. 229, 1915, p. 74 et seq., §§ 40, 41. In equations (13) and (18) $d\lambda/dN_e$ and $d\theta/dN_e$ should be inverted and $D \cos \theta$ in the latter put in the numerator.

If $x$ is the displacement in centimeters in the ocular, $\theta = x/19.5$, the denominator being the length of the telescope. The successive values of $x$ in terms of $N$, the mirror displacement, are given graphically in figure 87 for the different values of $E' = E + e/\cos R$ in question, and from them $d\theta/dN_e$ was taken graphically. All the curves are appreciably straight, except the one for $E' = 1.3$ cm., which is definitely curved.
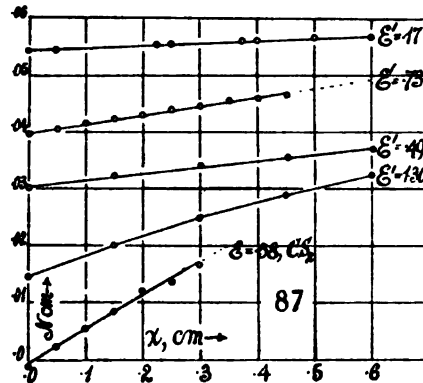


The values of $d\theta/dN_e$ observed and computed obviously agree as closely as may be expected for mean conditions of the spectrum between green and red and of the mode of procedure. The small coefficient for carbon bisulphide is, moreover, in keeping with its large value of $B$ or high dispersion. In a sensitive displacement interferometer $B$ like $E'D$ should all be small; but unfortunately this implies large ellipses. The beautiful small ellipses obtained with the carbon-bisulphide plate are of little avail because of their sluggish motion. In fact, the small thickness of the carbon bisulphide layer and the reduced coefficient observed are quite striking in comparison with glass. Moreover, since for an order $n$

$$\frac{d\theta}{dn} = \frac{1}{2} \frac{\lambda^2}{D \cos \theta \, (\cos R + 2B/\lambda^2 \cos R) - N}$$

the effect of a large $B$, though it reduces the general size of ellipses, does so but slightly, since the term in $B$ can not be more than a few per cent (3 to 6) of the other term in the binomial.

# CHAPTER VI.

## THE DISPLACEMENT INTERFEROMETRY OF SMALL ANGLES AND OF LONG DISTANCES. COMPLEMENTARY FRINGES.

**67. Parallel rays retracing their path.**—The following method was devised with a view to the micrometric measurement of angles. It will be used elsewhere in connection with an electrometer for reading microvolts. An interference method of a different kind for measuring small angles was developed some time since and used at length in connection with the deviation of the horizontal pendulum.[*] Again, the electrometer was treated in different ways[†] by the aid of the interferometer. The present method, however, will differ from all of these. In figure 88, $L$ is a horizontal beam of white light from a collimator after passing through the auxiliary clear plate $P$ (to be used preliminarily for parallelizing the mirrors of the system in a way presently to be shown),



88

the beam is reflected at $a$ and $b$ by the half-silver plates $H_1$ and $H_2$ respectively, to the wide opaque mirror $m$. The rays now retrace their paths or nearly so, to be in turn transmitted at $a$ and $b$ by the half-silvers $H_1$ and $H_2$. These transmitted pencils similarly impinge on the opaque mirror $M$ and the half-silver $H_3$ at $c$ and $d$ respectively, and pass thence (the ray from $c$ being transmitted) into the telescope at $T$. The direct-vision grating prism $g$ may be swiveled in place or removed at pleasure.
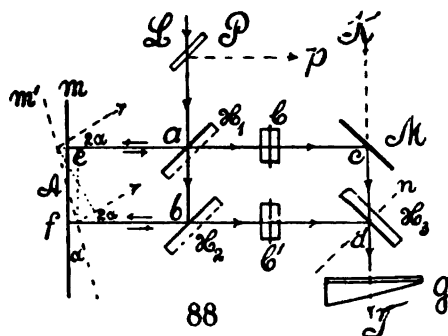
To bring the system of four mirrors into complete parallelism is here of considerable importance if the spectrum fringes or the achromatic phenomenon are to be adequately large for measurement. The presence of the common mirror $m$, however, suggests the procedure. When the clear plate $P$ is in place, the rays $ae$ and $bf$ on returning are also again reflected at $a$ and $b$ toward $L$ and may be clearly seen in a telescope at $p$. Hence if $m$ is the standard plane and nearly vertical, the mirrors $H_1$ and $H_2$ will be parallel when the slit images seen at $p$ coincide horizontally and vertically, while $H_1$, $H_2$, and $m$ will have their common normal plane in the diagram. In the same way the mirrors $M$ and $H_3$ may be parallelized with their common normal plane in the diagram. Again, the return rays $aL$ and $bL$ may be projected on the objective of the collimator, or on a small screen near it, by correspondingly focusing the collimator. The two sharp slit images are put in coincidence

130

horizontally and vertically. This is usually more convenient and as a rule adequate. Other methods are given below.

If the distances $ac$ and $bd$, $ab$ and $cd$ have previously been made nearly equal and the angles approximately $90°$, the fringes will usually be found on moving the micrometer-screw normal to $H_2$.

As the mirrors are thick glass plates, it is preferable that the half-silvered sides of $H_1$ and $H_2$ be toward $L$ and the half-silvered side of $H_3$ toward $T$. In this case each ray passes the plates twice, as indicated in figure 88. With ordinary plate-glass the fringes when found are still apt to be small. They are then to be enlarged and centered, by compensator of clear glass $C$ and $C'$, in the two rays respectively, rotated in opposite directions around a horizontal axis until the center of ellipses is in the field of the spectroscope. It may be necessary to actuate the micrometer-screw at $d$ to complete the adjustment. If $m$ is adjustable on two axes, the compensators $C$, $C'$ are superfluous, as will presently appear.

When the ellipses are centered, the direct-vision spectroscope $g$ removed, and the slit widened or removed, the residual or achromatic fringes appear in sight and are ready for use. These are always strong. The spectrum fringes are apt to be less so, since the parts of the ray $L$ pass through two half-silvered surfaces, $H_1 H_2$ or $H_1 H_3$, in succession. The spectrum fringes are only sharp when the slit is fine. If the white residual fringes are too dazzling, a single or two half-silvers may be placed before the objective of the telescope with advantage. Two plates with their half-silvered sides in contact and held so by a steel clip are excellent for this purpose, while they are at the same time protected from sulphur corrosion. This, in fact, is the best method of preserving silver mirrors (in pairs) when not in use.

If $\alpha$ is the fraction of light transmitted and $1 - \alpha$ reflected, the fraction of the original light $L$ reaching the telescope $T$ will be $2\alpha^2(1 - \alpha)^2$. This is a maximum if $\alpha = \frac{1}{2}$. Thus the illumination is reduced to $\frac{1}{8}$.

When the spectra are in coincidence and the fringes sharp, the mirror $m$ may be rotated around a vertical axis at $A$ into some position, $m'$. In such a case the two spectra will move through the field of the telescope at $T$, but their coincidence will not be destroyed. The $D$ lines, for instance, will continue to be superposed throughout. Considerable path-difference is, however, introduced in this way, and hence the fringes will march through the spectrum at an *enormously* more rapid rate. The following data may be given, where $\alpha$ is the angle of rotation of the mirror $m$ and $N$ the reading of the micrometer at $H_2$ (screw in the normal $dn$) necessary to bring the center of ellipses back to the sodium lines. In both cases the centers were out of the field above or below, so that horizontal fringes were made the criterion for adjustment. This method is somewhat rough, but adequate for the present purposes.

(1) Fine thin fringes. Relatively large glass-path. Distance $ab$, figure 88, $2R = 21$ cm. Thickness of glass plates (half-silvers), $e = 0.70$ cm.

| $\alpha$ | $=0°$ | $0.05°$ | $0.20°$ | $0.30°$ | $0.40°$ | $0.50°$ | $0.60°$ |
|---|---|---|---|---|---|---|---|
| $N \times 10^3 =$ | 23 | 30 | 128 | 162 | 215 | 258 | 299 cm. |

This is curve $a$ in figure 89. From it the mean rate

$$\frac{\Delta N}{\Delta \alpha} = 0.47 \text{ cm./degree, or } 27 \text{ cm./radian}$$
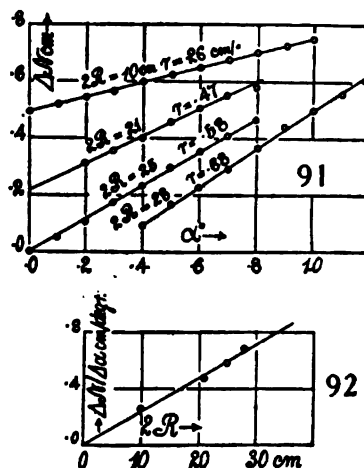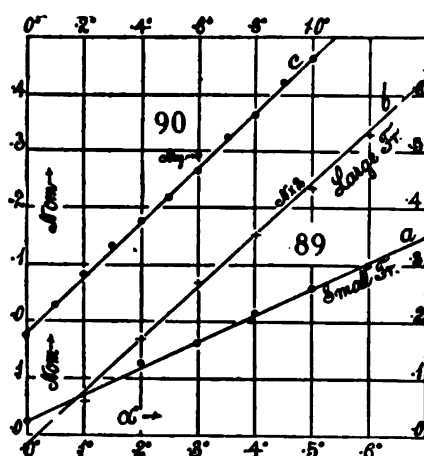
may be found.

(2) Coarse large fringes. Smaller differential glass-path.

| $\alpha =$ | 0° | 0.1° | 0.2° | 0.3° | 0.4° | 0.5° | 0.6° | 0.7° | 0.8° | 0.9° | 1.0° |
|---|---|---|---|---|---|---|---|---|---|---|---|
| $N \times 10^4 =$ | $-25$ | $+29$ | 84 | 134 | 176 | 217 | 265 | 323 | 365 | 420 | 467 cm. |

This is the curve given (with double ordinates for distinction) in curve $b$, figure 89, and in figure 90. Besides this the datum $\alpha = -0.6°$, $N = -0.320$ cm. was obtained. In figure 90 the mean rate is

$$\frac{\Delta N}{\Delta \alpha} = 0.465 \text{ cm./degree, or } 26.6 \text{ cm./radian}$$

agreeing with the preceding as closely as may be expected. We may thus estimate $\Delta N = 27 \times 10^{-6}$ of displacement at the micrometer at $H_2$ per micro-radian of turn $\alpha$ at the mirror $m$, which amounts to a little less than one interference ring per micro-radian (about 0.2 second of arc) of turn. Moreover, turns of $\alpha$ less than a few degrees are certainly measurable. Through-



out all this work the achromatic fringes are also available for precision in $N$, but for this reason are more difficult to manipulate if individual fringes are treated. They may, moreover, be much enlarged by rotating the mirror $m$ and advancing the micrometer at $H_2$ in small steps in such a way as to produce contrary effects and thus keep the achromatic fringes in the field. If the fringes leave the principal focus, the micrometer at $H_2$ and its adjustment screws may be actuated together in the same way. This is the most available method for eliminating the glass-path, so that enormous spectrum ellipses are obtainable. Finally, three groups of achromatic fringes (on each side of the strong central group) were noticed, the distance apart of groups corresponding to about $\Delta N = 0.0014$ cm.

It is obvious that $2\Delta N \cos i$ will increase with $2R$, the distance apart of the parallel rays $ae$ and $bf$, figure 88, as well as with the rotation $\alpha$. But the relations are not obvious, and experiments were therefore made for the relation of $\Delta N$ and $\alpha$ in case of different distances apart ($2R = 10, 21, 25, 28$ cm.) of the rays in question. The results are given in figure 91, where the abbreviation $r = \Delta N/\Delta \alpha$. In figure 92 and table 35, furthermore, this value, as obtained from figure 91 graphically, is compared with $2R$. The results are not quite smooth; but as $2R$ is the distance apart of two spots of light, it can not be specified sharply. Moreover, a variety of other discrepancies of adjustment enter which need not be detailed here. From figure 92 it appears that on the average $r/2R = 0.024$ in terms of degrees or $= 1.35$ in terms of radian. Hence we may consider an equation of the form

$$2R\Delta\alpha = \Delta N \cos i$$

So computed $\cos i$ would be $0.73$ instead of $0.71$, but the difference is referable to the outstanding glass-path and outstanding air-paths which have not been included.

**68. Groups of achromatic fringes.**—With the good adjustment stated, a number of further experimental measurements of the mean position ($\Delta N$) of the fringe patterns on the micrometer at $H_2$ were made, with results as follows: The size of the individual fringes was about $0.0225/35 = 0.00064$ radian in the telescope at $T$—i.e., about $0.034°$ of arc. The fringe patterns will be designated primary, secondary, etc. The data are $10^3 \Delta N$ cm.

| | | | | |
|---|---|---|---|---|
| Tertiary......... +2.6 | 2.7 | ... | ... | 2.7 cm. $\times 10^{-3}$ |
| Secondary....... +1.3 | 1.2 | 1.3 | 1.4 | 1.4 |
| Primary......... ±0.0 | 0.0 | 0.0 | 0.0 | 0.0 |
| Secondary....... −1.3 | 1.1 | ... | 1.2 | 1.2 |

One group was visible on one side and two on the other and one or more frequently escaped capture by the micrometer. The wave-length difference of these positions is exceedingly small. Using the above expression, $\Delta\lambda = \lambda^2/2\Delta N \cos \theta$,

$$\Delta\lambda = \frac{36 \times 10^{-10}}{2 \times 1.3 \times 10^{-3} \times 0.71} = 1.9 \times 10^{-6} \text{ cm. nearly}$$

But there is no suggestion in this datum. The displacement $\Delta N$ is equivalent to a glass thickness $e$, where $\Delta N = e(\mu - 1)$, roughly. Hence $e = 1.3 \times 10^{-3}/53 = 0.0025$ cm. This precludes the possibility of reflections from the two sides of the half-silver film, since this is about 1,000 times thinner, apart from its index of refraction.

Some experiments were also made with the primary achromatic fringes (treated as a single group and not individually, as the angle of measurement of $\alpha$ was not correspondingly delicate) to determine $\Delta N/\Delta\alpha$. Two series with different adjustments showed results as given in table 35 ($2R = 21$ cm.).

TABLE 36.

| Fringes— | Series I. | | Series II. | |
|---|---|---|---|---|
| | $\alpha$ | $N \times 10^3$ | $\alpha$ | $N \times 10^3$ |
| Smaller....... | −0.2 | 112 | −0.2 | 114 |
| Smaller....... | − .1 | 47 | − .1 | 63 |
| Very large..... | ± .0 | 0 | ± .0 | 0 |
| Smaller....... | + .1 | 56 | ..... | ... |
| Smaller....... | + .2 | 111 | ..... | ... |
| Smallest....... | + .3 | 170 | ..... | ... |

These data contain the new result that the achromatic fringes decrease in size with great rapidity in both directions of the increments from the central position ($\alpha = 0$). Two sets were usually present. The rate of growth as well as the ratio $\Delta N / \Delta \alpha$ is not the same on both sides of the position of maximum size ($\alpha = 0$). The mean coefficient may be found graphically as

$$\frac{\Delta N}{\Delta \alpha} = 0.56 \text{ cm./degree or } 32 \text{ cm./radian}$$

which is larger than the preceding estimate for spectrum fringes.

This experiment bears directly on the nature of the achromatic fringes. It shows, moreover, that the compensators $C$ and $C'$ in figure 88 are not essential and that ellipses may be centered by rotating the mirror $m$ on a horizontal and vertical axis. It is, in fact, possible to increase the achromatic fringes indefinitely in size in this way; but with ordinary glass they eventually become sinuous and no longer useful. When the slit is fine and the ocular out of focus, well-marked



hyperbolic patterns may be recognized; but these become straight on returning to the wide slit in focus.
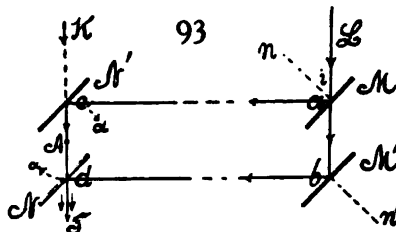
**69. Measurement of small angles without auxiliary mirror.**—This method makes use of the original apparatus, figure 73, but the two mirrors $M$ and $M'$ or $N$ and $N'$, figure 93, are rotated together as a rigid system around a vertical axis, at $A$, for instance. In view of the absence of auxiliary reflection, the method will be but half as sensitive as the preceding one, so that the equation

$$R\Delta \alpha = \Delta N \cos i$$

is sufficient to express the results. But on the other hand, if spectrum fringes are to be observed, there is greater abundance of light, since the half-silver film is penetrated but once by each component, $ac$ or $bd$. When the achromatic fringes are used the light is always superabundant and must be reduced in intensity. To try this method the mirrors $N$ and $N'$ were mounted on a good divided circle so as to rotate together on a rigid arm over a small angle $\alpha$. The achromatic fringes displaced in this way were restored by advancing

the mirror $M'$ over the distance $\Delta N$ along the normal micrometer-screw at $n'$. The following is an example of the results of corresponding values of $\Delta N$ and $\Delta \alpha$, when the distance apart of the rays $ac$ and $bd$ was $2R = 7$ cm.:

| $\alpha$ | $=0.0°$ | $0.1°$ | $0.2°$ | $0.3°$ | $0.4°$ | $0.5°$ | $0.6°$ | $0.7°$ | $0.8°$ | $0.9°$ | $1.0°$ |
|---|---|---|---|---|---|---|---|---|---|---|---|
| $\Delta N \times 10^3 =$ | $0.0$ | $8.0$ | $16.6$ | $25.6$ | $34.9$ | $42.7$ | $50.7$ | $61.7$ | $70.5$ | $78.5$ | $90.6$ cm. |

These results as a whole are much smoother than above, for incidental reasons. From a graphic construction the mean rate $\Delta N/\Delta \alpha = 0.088$ cm./degree or $5.0$ cm./radian may be obtained. Hence, since $2R = 7$ cm. $(\Delta N/\Delta \alpha)/2R$ $= 0.013$ in terms of degrees or $0.72$ in terms of radians (table 37). This result is roughly half the preceding, if incidental errors be disregarded. From the above equation, since $I = 45°$ nearly,

$$\frac{\Delta N}{\Delta \alpha} = \frac{2R}{2 \cos i} = \frac{7.0}{1.41} = 5.0 \text{ cm./radian}$$

agrees closely with the experimental result.

TABLE 37.—Values of $r = \Delta N/\Delta \alpha$ micrometer displacement per degree of mirror rotation.

| A. Case of auxiliary mirror, fig. 88. | | | | |
|---|---|---|---|---|
| Series No. | $\dfrac{\Delta N}{\Delta \alpha}$ | $\dfrac{\Delta N}{\Delta \alpha}$ | $2R$ | $\dfrac{\Delta N}{\Delta \alpha} \Big/ 2R$ |
| | *cm./°* | *cm./rad.* | *cm.* | *mean.* |
| 6, 7; 1, 2 | 0.47 | 27 | 21 | $0.024^1/$ degree |
| 8 | .58 | 33 | 25 | $1.35^1/$ radian |
| 9 | .68 | 39 | 28 | |
| 10, 11 | .26 | 15 | 10 | |
| B. Case of rotating pairs of mirrors, fig. 93. | | | | |
| 1 | 0.088 | 5.0 | 7 | $0.0126^1/$degree .$72^1/$radian |

**70. Complementary fringes.**—Some additional attention was now given to the hyperbolic fringes of a fine slit and white light observed when the ocular is drawn outward or to the rear of the position for the principal focus and the spectroscope is removed. They appear and widen with the washed image of the slit. They are quite strong, sharp throughout, and gorgeously colored, the fields and shades, figure 94, $a$, being nearly complementary in color. The spectrum fringes must be centered if the others are to occur. The former, figure 94, $b$, are usually long ellipses or hyperbolic with their major axes horizontal, while the corresponding new fringes are hyperbolic with the major axes vertical. They are extremely sensitive to rotation of the micrometer mirror about a horizontal axis, rising or falling, but they soon vanish. When the micrometer mirror is rotated around a vertical axis, an operation which separates the white slit images if originally coincident, the new fringes move bodily by displacement from left to right, or the reverse, depending on the sign of the rotation, while they continually change their color-scheme. When the design is thus displaced as a whole the individual fringes move as shown

in figure 94, a. As a group the fringes closely resemble the lemniscates of a binaxial crystal in polarized light. The variation of the color-scheme is probably the same, since with sodium homogeneous light the design is in yellow and black. The pattern is not quite dichroic, but appears so, red-green, blue-yellow combinations with an intermediate violet-yellowish succeeding each other. In polarized light the figures are sharpened as a whole, but there is no discrimination. The pattern gradually vanishes with a wide slit, where-upon the achromatic fringes may be seen when the ocular is restored to the principal focal plane.

If the white slit images pass through each other (in consequence of the vertical rotation specified) the direction of fringes twice changes sign in rapid succession, and this probably occurs when the white slit images are coin-cident. Barring this inversion, the march is regularly proportional to the rotation.

With the displacement ($\Delta N$) of the mirror on the micrometer-screw nor-mal to its face, the fringes pass through a continuous succession of color-schemes, but soon vanish, for they coincide in adjustment with the centered spectrum fringes. Similarly, if a pair of mirrors ($M M'$ or $N N'$, fig. 93) rotates about a vertical axis as a rigid system, the same continuous change of color-scheme and evanescence is apparent.

These interferences differ, naturally, from the spectrum interferences; they also differ from the achromatic interferences, which are much finer fringes, partaking of the regular fringe pattern seen with biprisms. They are a separate phenomenon, quite sharp and definite, occurring under like con-ditions of adjustment, but under different conditions of observation (ocular out of focus and fine slit). In the principal focus the two sharp, extremely bright slit images are alone present. They are absolutely identical in struct-ure, however, and their spectra when superposed would interfere symmetri-ally throughout their extent. Under these circumstances the rays intersect-ing in the white slit images also interfere before and behind the principal focal plane of the telescopic images specified, and this interference is not destroyed when the slit images are separated (rotation of opaque mirror about vertical axis), or when the slit images are passed through each other. What is not easily seen, however, is the reason of the occurrence of large, sharp, definite hyperbolic forms instead of the usual Young or Fresnel fringes of two slits or slit images.

On the Michelson interferometer these fringes, like the achromatic fringes, are extremely faint and can hardly be detected except by putting them in slow motion. The spectrum fringes are equally strong in all cases. It appears, therefore, that the two half-silvers are favorable to evolving both the hyper-bolic and the achromatic sets of fringes. The Michelson design is thus not useful here, nor for the measurement of small angles of rotation by the meth-ods described, as the mirrors would have to be rotated in opposite directions.

Further work with the complementary fringes on different interferometers of the Jamin type showed that to produce the hyperbolics the fine slit images

must coincide horizontally and vertically. They do not in this case probably coincide in the fore-and-aft direction, for the plates, etc., are not optically flat. When the slit images are separated at the same horizontal level into two fine parallel lines, the complementary fringes in fact become Fresnellian fringes, finer as the slit images are more separated and as the ocular is more rearward or forward. This is precisely what should occur. We may conclude, therefore, that the complementary fringes are Fresnellian interferences of two slit images and that the central hyperbolic forms are due to outstanding front and rear positions of the two slit images, which seem to coincide in the field of the telescope. Differentiated from these, the achromatic fringes are referable to the colors of thin plates. I have, in fact, also succeeded in obtaining the complementary fringes in the shape of broad, straight, gorgeously colored vertical bars, without suggestion of hyperbolic contour.



94                    95
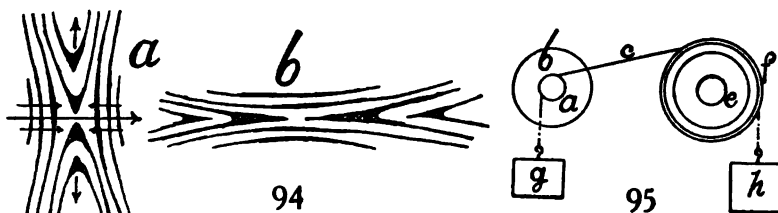
An attempt was made to get quantitative estimates of the passage of fringes on rotating the paired mirrors over an angle $\alpha$. To control the small angles the device, figure 95, was improvised and did good service. Here $e$ is the tangent screw of a divided circle 6 inches in diameter. It is surrounded by a snug annulus of cork and holds the brass ring $f$, on whose surface a coarse screw-thread has been cut. Near this and with its axis in parallel is a quarter-inch screw $a$ and socket (not shown) controlled by the disk $b$. A strong linen thread $c$ is looped once around $f$ in the grooves of the screw and once or twice around $a$, the string being normal to the cylinders and kept taut by two small weights, $g$ about a half ounce and $h$ about an ounce. The head $b$ may be turned either way and the angle read off in minutes on the head of the tangent screw $e$.

The theoretical value, apart from glass-paths and other corrections, should be, per fringe vanishing,

$$2R\Delta\alpha = \lambda$$

where $R$ is the radius of rotation corresponding to the angle $\Delta\alpha$ and $\lambda$ the mean wave-length of light. In the given adjustment, $2R = 10$ cm. was the normal distance apart of the two interfering beams. Hence

$$\Delta\alpha = \frac{\lambda}{2R} = \frac{60 \times 10^{-6}}{10} = 6 \times 10^{-6} \text{ radians or } 1.2''$$

per vanishing fringe. As the change of glass-path of one beam would have to be deducted from $2R$, a somewhat larger value would be anticipated. Testing the complementary fringes (white light), the passage of about 25

fringes completed the phenomenon, after which it paled to whiteness. These 25 fringes passed within $\Delta\alpha = 0.75'$, or per fringe about $0.03'$ or $1.8''$ of arc. Of course, this is merely an estimate from the small angles of turn involved.

The complementary fringes with sodium light are available indefinitely. I counted about 100 fringes for an angle of $2.7'$—*i.e.*, $1.6''$ per fringe.

Finally, using the spectrum fringes of the spectroscope, about 120 fringes were counted within $3'$—*i.e.*, $1.5''$ per fringe. All of these values are larger than the computed value $\lambda/2R$ without correction, but in view of the large number of fringes within exceedingly small angles $\Delta\alpha$, sharp agreement is not to be expected.

**71. Equations.**—To completely trace out the air- and glass-paths in the present apparatus would lead to complicated equations of no further interest here. I have, therefore, contented myself with the preceding experimental result, which is probably more accurate than it appears. To the first order of small quantities one may assert that the rotation of the mirror *m* (fig. 88) over an angle $\alpha$ (here to be called $\Delta\alpha$) cuts off the path $2R\Delta\alpha$ from the *b* ray and adds the same path to the *a* ray. Hence the total change of path is $4R\Delta\alpha$.

Again, though the additional glass-paths at $H_1$ and $H_2$ (being equally incremented for both the *a* and *b* rays) compensate each other, this is not true at $H_1$ and $H_2$ for the *b* and *a* rays. Since the *b* ray at $H_2$ receives no increment, the total glass-path increment at $H_2$ is effective. The glass-path *s* at $H_2$ may be written as heretofore,

$$2e\left(\sin^2\frac{i}{2} - \mu\sin^2\frac{r}{2}\right)$$

and hence if $\Delta i = -2\Delta\alpha$, since *i* is decreased by $2\alpha$ at $H_2$, the glass-path incremented $(ds/di)$, $\Delta i$ may be found by differentiation to be

$$-2\frac{e\sin(i-r)}{\cos r}\Delta\alpha$$

Finally, the compensation at the micrometer-screw at *d* is $2\Delta N\cos i$. Hence when the center of ellipses is restored to the fiducial line,

$$\frac{\Delta N}{\Delta\alpha} = \frac{4R - 2e\sin(i-r)/\cos r}{2\cos i}$$

Here $2R$ is the normal distance between the *a* and *b* rays, *e* the thickness of the glass-plate $H_2$, and *i*, *r* the angles of incidence and refraction.

In the apparatus $2i$ was not measured, but made nearly $90°$ by eye adjustment. $2R$ was measured. Hence, in the first set of experiments,

$$i = 45°, \quad \mu = 1.53, \quad r = 27.5°, \quad 2R = 21 \text{ cm.}, \quad e = 0.70 \text{ cm.}$$

and

$$r = \frac{\Delta N}{\Delta\alpha} = \frac{42 - 2\times0.70\times0.30/0.89}{2\times0.707} = 29.5\frac{\text{cm.}}{\text{radian}}$$

This is larger than the corresponding experimental value 27 cm./radian, but

no more so than the estimated data imply. In fact, the particular adjustment for achromatic fringes gave a larger result $r = 32$ cm./radian, for reasons not apparent. One may note that the correction for glass-path is small.

With regard to the application to the electrometer, we may come to the following conclusion: A good instrument of the quadrant or similar type should give about a radian of deflection per volt, or a microradian per microvolt. In the present interferometer the microradian is about equivalent to the passage of one interference fringe. Hence one fringe per microvolt is about the order of sensitiveness obtainable.

**72. Separated rigid vertical system.**—The method used above, of attaching the deflecting mirrors at $45°$ to the U-tubes, is faulty in design and difficult to adjust. It was, therefore, subsequently discarded in favor of the rigid deflecting system, figure 96, consisting of a wide mirror at $45°$, $m$, and
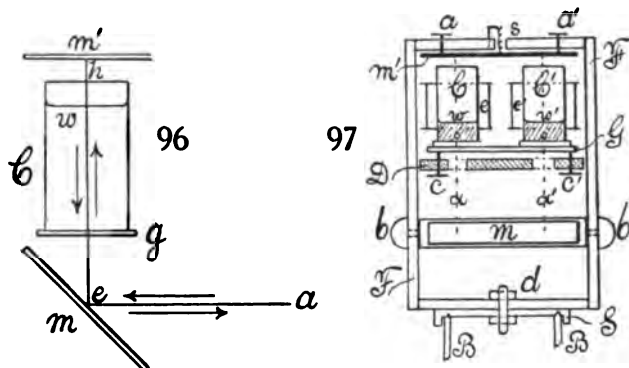


a horizontal mirror $m'$. Both must be provided with adjusting screws for axes respectively parallel to the traces $m$ and $m'$ and normal to the diagram, if the fringes when found are to be centered and enlarged. It is particularly essential that the framework supporting $m$ and $m'$ be rigid, otherwise the quiver introduced here is superposed on and accentuates the corresponding tendency of the very mobile liquid column. This is contained in the brass tube $C$ (with glass window at $g$) which is supported on an independent standard, rigidly. There are two of these tubes ($C$, $C'$, fig. 97), side by side, parallel, and at the same level, one for each component beam. As the rays $aeh$ are to retrace their path, the apparatus, figure 88, should be used, with the mirror $m$ of that figure tilted up as in figure 96. Hence the two component beams $ae$ and $bf$, figure 88, prolonged as at $eh$, figure 96, each penetrate a column $C$ and are returned by the normal mirror $m'$. Thus one reflection of the old method is obviated and adjustment is facilitated, since both beams are reflected from the common mirrors $m$ and $m'$. To assist in the preliminary adjustment, the rigid system $m$, $m'$ should be capable of revolving roughly about a vertical axis. With a wide beam the rays may then be guided by the eye to retrace their path. Fine adjustment is made by the triple screws on $m$ and $m'$ already mentioned.

The fringes in coincident spectra should first be sought. When found they will usually be very small. They may then be centered by rotating the mirror *m* about the horizontal axis, cautiously. They may be enlarged by rotating *m* with the same caution around the axis parallel to its trace in the diagram. The latter operation (or both) succeeds best with the achromatic fringes of a wide slit (no spectroscope). The horizontal axis is employed for erecting them, the axis parallel to the diagram for enlarging them, use being also made of the micrometer-screw at *d* on $H_2$, figure 88, if the fringes escape. In fact, the achromatic fringes are so sharp and luminous that in a quivering system the fringes are distinctly seen at the two elongations, doubled by the quiver.

To adequately support the mirrors *m* and *m'* reasonably free from vibration, a rectangular wooden yoke *F F*, figure 97, is best, so long as the installation is not permanent. This yoke is made of inch boarding about 18 inches high, 15 inches broad, and 3 inches deep. It is bolted below at *d* to the iron carriage *S*, and thus capable of rotation around a vertical axis and of sliding normal to its face on the iron slides *B B'* (about 1.5 meters long) of the base. *S* and *B B'* are arranged like a lath-bed.

The mirror *m'*, which is horizontal, is adjustably attached to the top of the frame *F F*; three adjustment screws (two seen at *a, a'*) and the strong spring *s* (pulling upward) control the position of *m'* with the usual plane dot-slot mechanism and axes of rotation parallel to and normal to the plane of the frame.

The board carrying the mirror *m* may be roughly set at 45° to the vertical by rotation on the strong bolts *b b'* and clamped in position. The mirror *m* is attached to it by three adjustment screws and a rearward-acting spring, as shown in the case of *m'*. The axes of rotation are parallel to the two edges of *m*, and all fine adjustment, together with the final rotation of fringes and changes of their size, are made here.

The columns of the U-tubes *C* and *C'* must be supported from an independent bracket, suitably braced from the wall or from a separate pier, if liquid surfaces are in question. A part of this free support, the table, also of wood, appears at *D*, and holes are cut in it sufficiently large for the passage of the two beams of light *α, α'*, which retrace their paths between *m* and *m'*, passing through *C* and *C'*. The table *D* is provided with three leveling screws (two shown at *c* and *c'*) on which a plate of thick glass *G* may be mounted and made accurately horizontal by aid of a spirit-level. The two columns *C* and *C'*, joined by a flexible rubber pipe and provided at the bottom with glass windows, are placed on *G*, so that the beams of light pass through their axes. The magnetizing helix of each is shown at *e* and *e'*.

It is obvious, therefore, that the two columns of liquid in *C* and *C'* are of the same height and their ends parallel, other things being equal. Hence, if the apparatus is adjusted for the achromatic fringes in the absence of the U-tube *C C'*, it will be nearly in adjustment when the columns are introduced; and this proved to be the case. The rigid system is easily adjusted for strong

vertical achromatic fringes. The fringes are found with a few turns of the micrometer after the liquid $w$ has been poured in.

The fringes as seen through the liquid columns are still strong and clear, with scarcely any deterioration; but unfortunately in this locality they are in incessant and vigorous vibration. It is indeed astonishing that a phenomenon so sensitive can survive such relatively rough treatment.

With this apparatus the endeavor was again made to determine the susceptibility of water. Good fringes were first produced, but for all levels of the water-surfaces the effect of the presence or absence of a magnetic field was quite *nil*, so far as any appreciable displacement of fringes was concerned. They remained in place while the current in the helix was alternately closed and opened. The reason for this completely negative result I am unable to explain.

In a repetition of such experiments tubes much wider than 4 cm. should be used. At this diameter the liquid surfaces still show appreciable curvature, which is an annoyance.

The yoke, figures 96 and 97, is finally a considerable convenience in the measurement of vertical angles near the zenith. The rotation of the mirror $m'$ around its two axes is here available. Horizontal achromatic fringes in all these cases may often be produced and used to advantage. In such a case the two adjustment screws of the mirror $m'$ change their function, and the fringes travel up and down the wide slit image with changes of $\Delta N$. As this image is more extended vertically than horizontally, the fringes are much longer in sight. Fringes are largest when the planes of symmetry of pencils of rays accurately retrace their paths. But as large fringes are apt to be irregular, a small angle of reflection at the mirror $m'$ is preferable.

**73. The displacement interferometry of long distances.**—In the preceding paragraphs I suggested two methods for the measurement of small angles. The first (fig. 88) used an auxiliary mirror, and, apart from corrections, the angle $\Delta\alpha$ over which the auxiliary mirror $m$ turns is

(1) $$\Delta\alpha = \Delta N \cos i / 2R$$

where $\Delta N$ is the displacement of one of the plane mirrors parallel to itself necessary to restore the achromatic fringes to their former position in the field of the telescope, $i$ the angle of incidence (conveniently 45°), $2R$ the normal distance apart ($ab$ or $cd$) of the (parallel) interfering pencils in the fore-and-aft direction of the incident beam. In the second method (fig. 93) the auxiliary mirror is dispensed with and the rotation of a rigid system of paired mirrors is used. The sensitiveness is half the preceding.

Suppose that the paired mirrors near the telescope (figs. 88, 93) confront but a part of the area of the objective and that the telescope can therefore look over the mirrors directly into the region * beyond, as shown at $K$. The

* A series of small mirrors or reflecting prisms may be employed to the same purpose; or the mirrors may both be half-silvered and transparent.

telescope now contains two images, the first due to rays ($K$) entering it directly, the second due to rays ($L$) reflected into it by the mirrors of the interferometer. Suppose the object seen lies at infinity like a star, that its two images are made to coincide by adjusting the angle $\alpha$, and that the achromatic fringes have been brought into the field by adjusting the micrometer displacement $N$.

Now let the angle $\alpha$ be changed by $\Delta\alpha$ until the two images of an object $M$ at a measurable distance $d$ coincide. Displace the micrometer mirror by $\Delta N$ until the achromatic fringes are restored to their former position. Let $b$ be the effective distance apart ($ac$ or $bd$) of the paired mirrors in the direction right and left to the observer or transverse to the impinging rays ($L$), and finally $s$ the angle at the apex of the triangle of sight on the base $b$—*i.e.*, the small angle between the present rays $KL$. Then

(2)                $d = b \cot g\ s = b \cot g\ 2\Delta\alpha = b/2\Delta\alpha$

(nearly) by the laws of reflection. Hence from equation (1)

(3)                          $d = bR/\Delta N \cos i$

Here $2bR$ is the area of the *ray parallelogram* of the interferometer ($abdc$, fig. 88). Using the constants of my apparatus, let $i = 45°$, $R = 10$ cm., $b = 200$ cm., $\Delta N = 10^{-4}$ cm., the latter being the smallest division on the micrometer. Hence

$d = 200 \times 10/10^{-4} \times 0.71 = 2.8 \times 10^7$ cm. $= 280$ kilometers

or about 170 miles, is the limit of measurement of the apparatus.

Again, from equation (3) the sensitiveness $\delta(\Delta N)/\delta d$, since

(4)                    $\delta d = (d^2 \cos i/bR)\delta(\Delta N)$

is inversely proportional to the square of the long distance $d$ and the area of the ray parallelogram $2bR$. Thus with the above constants, if $d$ is 2 kilometers, $\delta(\Delta N) = 10^{-4}$ cm.,

$\delta d = (d^2 \cos i/bR)\delta(\Delta N)$

Thus an object at about a mile should be located to about 30 feet. Per fringe of mean wave-length $\lambda$, moreover, since $\delta d = \lambda d^2/2bR$, the placement should be about 6 meters at 2 kilometers. I have stated the case, of course, merely for the interferometer, not for subsidiary optical appurtenances, nor for measurement by angular fringe displacement.

74. Theory.—To account for these phenomena theoretically the equations of displacement interferometry are available; for the center of ellipses of these and the central member of the achromatic fringes correspond to the same position, $\Delta N$, of the micrometer mirror. In fact, the fine white slit image which produces the spectrum when observed through the spectroscope is the central achromatic fringe when the spectroscope is removed. We have, there-

fore, for the centers of ellipses in the spectrum fringes the equation heretofore deduced,

$$2\Delta N \cos i = e\left\{(\mu-1)\cos R - \frac{\lambda}{\cos R}\frac{d\mu}{d\lambda}\right\}$$

where $\Delta N$ is the displacement of the micrometer to restore the center of fringes to their original position in wave-length $\lambda$, when the angle of incidence at the mirror is $i$, after a glass plate of thickness $e$ and index of refraction $\mu$ is introduced in one component beam, at an angle of incidence corresponding to the angle of refraction $R$ in the plate. This is equivalent to an equation in terms of the coördinates $N$, if $\mu = A + B/\lambda^2$ is assumed,

$$2N \cos i = e\mu \cos R + 2eB/\lambda^2 \cos R$$

But for the colors of thin plates we may write

$$n\lambda = 2e\mu \cos R$$

where $n$ is the order of the fringe. If the rays, as in the present experiment, do not retrace their paths, the factor 2 is omitted, whence

$$2N \cos i = n\lambda + 2eB/\lambda^2 \cos R$$

Let $N$ and $n$ vary together, $i$, $R$, $\lambda$, $e$, $B$, $\mu$ remaining constant. Then

$$2 \cos i \cdot \Delta N = \lambda \cdot \Delta n$$

Now let $\Delta\varphi$ be the angular breadth of a fringe in the telescope, so that

$$n \cdot \Delta\varphi = \Delta\theta$$

In other words, the displacement $\Delta\theta$ of the group of fringes is due to the displacement of the individual fringes as usual; but as only those achromatic fringes which coincide in micrometer value $\Delta N$ with the centers of the elliptic spectrum fringes are visible, the displacement of the group is actually seen and thus determinable. It would not be so in case of sudden displacement and homogeneous light.

Finally, the relative sensitiveness of the measurement of the angle $\Delta\alpha$, directly in terms of $\Delta N$ and indirectly in terms of the displacement of achromatic fringes, must be presented. The given rough data in table 38 are as close as they could be obtained from the small displacements entering. The quantities to be compared are: $\Delta N$, the displacement of the micrometer; $\Delta\alpha$, the corresponding rotation of the auxiliary mirror in the first method; $\Delta\varphi$, the angle subtended by a single fringe in the telescope, and $\Delta\theta$, the corresponding angle of the displacement of the fringes in the telescope. $\Delta\theta$ was constant throughout and measured about 3 mm. in the ocular of a telescope 33 cm. long.

TABLE 38.—Values of $\Delta N$, $\Delta\theta$, $\Delta\varphi$, $\Delta\alpha$. All angles in radians, $\Delta N$ in cm.

| $\Delta\theta \times 10^6$ | $\Delta\varphi \times 10^6$ | $\Delta N \times 10^6$ | $\Delta\alpha \times 10^6$ | $\Delta\theta/\Delta N$ | $\Delta\theta/\Delta\alpha$ | $\Delta\varphi\Delta N \times 10^6$ | $\Delta\varphi\Delta\alpha \times 10^6$ |
|---|---|---|---|---|---|---|---|
| 9000 | 500 | 730 | 52 | 12.3 | 170 | 0.365 | 0.026 |
| 9000 | 1500 | 250 | 18 | 36.0 | 500 | .375 | .027 |

Here $\Delta\alpha$ is computed from equation (1), where $i=45°$ and $2R=10$ cm., about. The fringes of width $100''$ and $300''$ were both brilliant and capable of high magnification.

Thus it appears that the fringes travel faster in proportion to their width, or if $\Delta\varphi$ increases $n$ times, $\Delta N$ (for the same telescopic excursion $\Delta\theta$) will decrease $n$ times. Again, the fringes travel as a body over hundreds of times the angle described by the auxiliary mirror ($\Delta\alpha$), when both are observed in the telescope. In the table $\Delta\theta/\Delta\alpha$ is 170 to 500 and could be increased indefinitely for larger fringes. The rotation $\Delta\alpha$ seen in the telescope would be but $2\Delta\alpha$. This is the gist of the present method of measuring small angles— *i.e., the fringe index moves through the telescopic field many hundred times faster than the image of the slit which measures the change of $\Delta\alpha$ directly.*

Finally, for the same $\Delta\theta$ or displacement of the fringe group, $\Delta\alpha\Delta\varphi$ is a constant, say $C$, or

$$\Delta\theta = C\Delta\varphi \cdot \Delta\alpha = C'\Delta\varphi \cdot \Delta N$$

where

$$C = \frac{9000}{0.0265} = 340,000 \qquad C' = \frac{9000}{0.370} = 24,500$$

It is not necessary to obtain sharper data, because these constants can be found theoretically. It will presently be shown that

$$C = 4R/\lambda, \quad C' = \frac{2\cos i}{\lambda}$$

where $R$ is the radius of rotation measuring $\alpha$. Thus

$$\frac{\Delta\theta}{\Delta N} = \frac{\Delta n\Delta\varphi}{\Delta N} = \frac{2\Delta\varphi\cos i}{\lambda}$$

If the $\Delta\varphi$ in the table be used, and $\lambda=60\times10^{-6}$ cm., $i=45°$, the results are

| | $\Delta\varphi = 500\times10^{-6}$ | $1500\times10^{-6}$ | |
|---|---|---|---|
| $\Delta\theta/\Delta N =$ | 11·8 | 35·3 | (computed) |
| $\Delta\theta/\Delta N =$ | 12 | 36 | (observed) |

results which agree with the values of the table as closely as these subtle measurements permit.

A few words may be added relative to the size of fringes so far as the glass-paths are concerned, the air-path conditions having been stated. For this purpose the equation of the phenomenon may be written

$$n\lambda = 2e\mu\cos R - 2N\cos i$$

where $N$ is the coördinate of the mirror at the micrometer. When the center of ellipses (or of achromatic fringes) is at wave-length $\lambda$, $N=N_0$, the value given for centers above. If $n$, $i$, $R$ above vary, while $e$, $\mu$, $\lambda$, $N$ are fixed, since $\sin i = \mu \sin R$,

$$\Delta\varphi = \frac{di}{dn} = \frac{\lambda}{2N\sin i - 2e\tan R\cos i}.$$

so that the size $\Delta\varphi$ is influenced inversely as the effective thickness $e$ (*i.e.*, the difference of thickness) of plates and depends on the position $N$ of the micrometer. If $N = N_e = e\,(\mu\cos R + 2B/\lambda^2\cos R)/\cos i$

$$\Delta\varphi = \frac{di}{dn} = \frac{\lambda}{2e(\mu\cos R\tan i - \cos i\tan R + 2B\tan i/\lambda^2\cos R)}$$

$$= \frac{\lambda\cos R}{2e\tan i\big((\mu^2-1)/\mu + 2B/\lambda^2\big)}$$

Since $i = 45°$, $R = 27° 9'$, $\lambda = 60\times 10^{-6}$ cm.

$$\Delta\varphi = \frac{60\times 10^{-6}}{2e(1.55\times 0.89 - 0.513\times 0.71 + 0.03)}$$

The parenthesis is 1.05. Hence

$$e = \frac{\lambda}{2\Delta\varphi}\ \text{ nearly}$$

which would make the effective glass thickness $e = 0.06$ cm. and 0.02 cm. for $\Delta\varphi = 5\times 10^{-4}$ radian and $15\times 10^{-4}$ radian, as above. Moreover, the rays $K$, figure 93, entering the telescope from the foreground directly and the rays $L$ reflected into it by the plates of the interferometer, will not be parallel when the fringes are of maximum size unless the plates $M$ and $N$ are equally thick. Finally, the size of fringes in general (apart from wedge-shape of plates) will be inversely as the effective differential thickness $e$ of the plates used.

If we collect the above equations* we may write roughly (since $e = \dfrac{\lambda}{2\Delta\varphi}$ nearly),

$$\Delta\theta = \frac{4R}{\lambda}\Delta\varphi\Delta\alpha = 2R\Delta\alpha/e \qquad \Delta\theta = \frac{2\cos i}{\lambda}\Delta\varphi\Delta N = \frac{\cos i}{e}\Delta N \qquad d = \frac{bR}{\Delta N\cos i} = \frac{bR}{e\Delta\theta}$$

so that the measurement of the long distance $d$ depends ultimately on the area of the ray parallelogram $2bR$, the differential thickness $e$ of the corresponding half-silvers, and the (relatively to $\Delta\alpha$) enormous displacement $\Delta\theta$ of the achromatic fringes.

Finally, if optic plate-glass were used for the half-silvered mirrors, the parallelism of rays $KL$ would coincide with the occurrence of centered or circular achromatic fringes; while the whole preliminary adjustment of mirrors for parallelism would consist in bringing the image from $LMN'T$, figure 93, and from $LM'NT$, successively into coincidence with the direct image from $K$, in case of a very distant source of light.

The remarkable sensitiveness which accrues to the method, if the angular displacement of fringes is measured in the ocular of a long telescope, comes

---

* The text unduly accentuates the glass-paths, whereas the air-paths are more important. I shall give a rigorous deduction of all the path-differences in my next Report to the Institution, where they will be sustained in detail by experiments.

out clearly if the last equation for $d$ is used. In case of corresponding incre-
ments $\delta d$ and $\delta(\Delta\theta)$, this equation is equivalent to

$$-\delta d = \frac{d^2 e}{bR}\ \delta(\Delta\theta)$$

But if $L$ is the length of the telescope and $\delta n$ the micrometric displacement of
fringes in the ocular corresponding to $\delta d$,

$$\delta(\Delta\theta) = \frac{\delta n}{L}$$

whence

$$\delta d = \frac{d^2 e}{bRL}\delta n$$

Thus if $e$, the difference in thickness of the corresponding half-silver mirrors,
and $\delta n$ be each even as large as 0.1 mm., and $d$ a kilometer,

$$d = 10^5 \text{ cm.}, \quad e = 10^{-2} \text{ cm.}, \quad b = 200 \text{ cm.}, \quad R = 10 \text{ cm.}, \quad L = 50 \text{ cm.}, \quad \delta n = 10^{-2} \text{ cm.}$$

$$\delta d = \frac{10^{10} \times 10^{-2} \times 10^{-2}}{200 \times 10 \times 50} = 10 \text{ cm.}$$

With these very moderate estimates a distance of 1 kilometer should be
measurable to 10 cm., so far as the glass-paths of the interferometer are
concerned.